

SCIENCE  
Applications  
INCORPORATED

MECHANICAL PROPERTIES

OF

DEVONIAN SHALES

FROM THE

APPALACHIAN BASIN

by

Thomas L. Blanton

Steven A. Dischler

Nancy C. Patti

FINAL REPORT

September 30, 1981

Prepared For

Eastern Gas Shales Project  
Morgantown Energy Technology Center  
Collins Ferry Road  
Morgantown, West Virginia 26505

Contract No. DE-AM21-78MC08216  
Year III, Mod 7, Activity 3

Prepared by

Science Applications, Inc.  
P.O. Box 880010  
Steamboat Springs, Colorado 80488

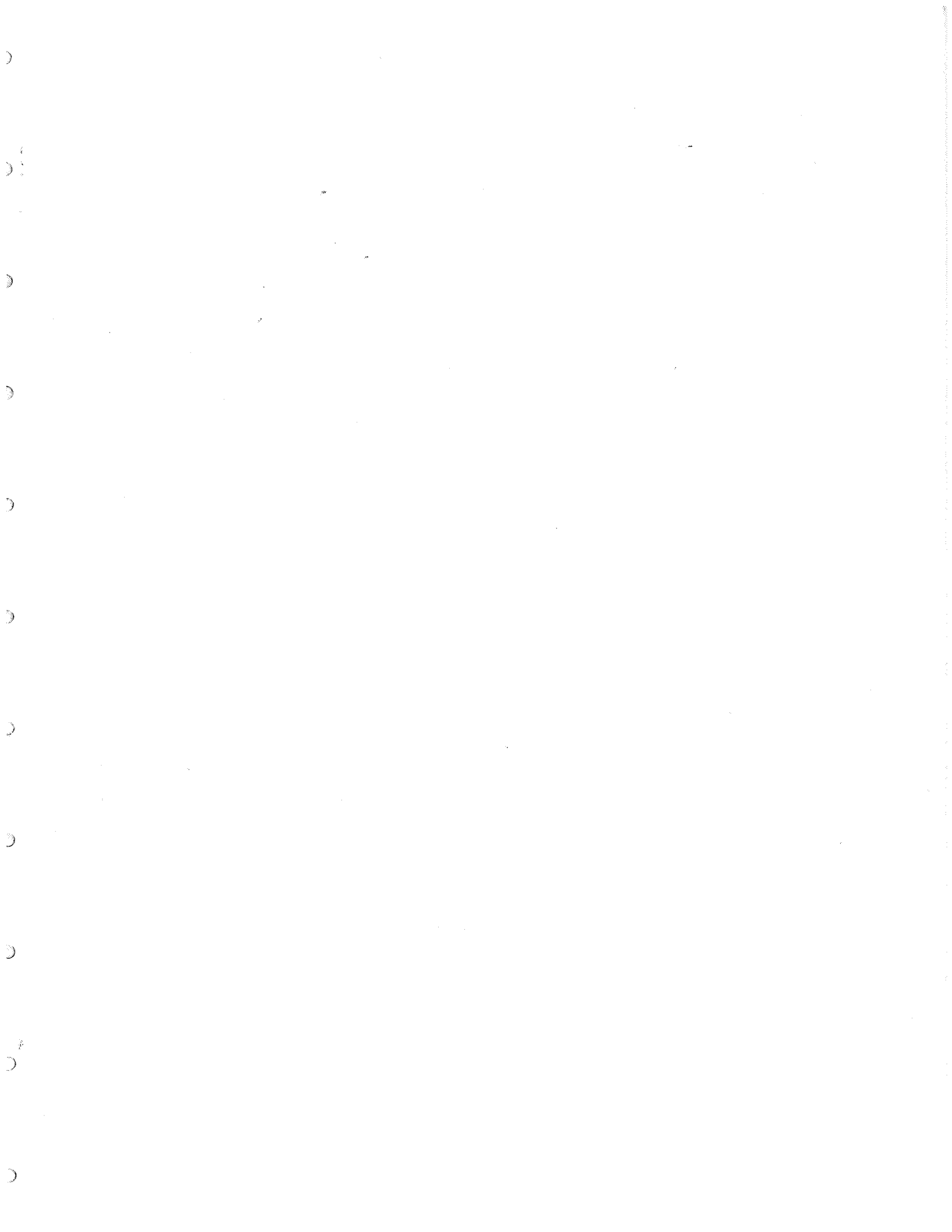


TABLE OF CONTENTS

EXECUTIVE SUMMARY . . . . . 1

SECTION 1. INTRODUCTION

    1.1. Purpose and Scope of Study . . . . . 3

    1.2. Character and Setting of Devonian Shales . . . . . 5

    1.3. Choice of Core for Testing . . . . . 13

SECTION 2. RESULTS OF MECHANICAL PROPERTIES TESTS

    2.1. Compression Tests: Elasticity and Strength . . . . . 16

    2.2. Tensile Tests . . . . . 50

    2.3. Fracture Energy Tests . . . . . 50

SECTION 3. CONCLUSION

    3.1. Trends In Mechanical Properties of Devonian Shales . . . 61

    3.2. Future Work . . . . . 63

REFERENCES . . . . . 64

APPENDIX A: Stress-Strain Curves for Compression Tests . . . . 67

APPENDIX B: Load-Displacement Curves for Fracture Energy Tests . . 120

## LIST OF FIGURES

|                    |  |     |
|--------------------|--|-----|
| Figure 1.          | Devonian shale gas production in the Appalachian Basin .                                 | 6   |
| Figure 2.          | Nomenclature of Devonian shales and their bounding units . . . . .                       | 7   |
| Figure 3.          | Stress trajectories for the maximum principal stress in the Appalachian Basin . . . . .  | 9   |
| Figure 4.          | Location of wells from which core was obtained for mechanical property testing . . . . . | .14 |
| Figure 5.          | Stratigraphic and depth relations for sampled zones .                                    | .15 |
| Figure 6.          | Example of a stress-strain curve exhibiting failure without yielding . . . . .           | .17 |
| Figure 7.          | Example of a stress-strain curve showing the yield point . . . . .                       | .18 |
| Figures 8A - 8I.   | Young's modulus as a function of confining pressure for each zone tested . . . . .       | .23 |
| Figures 9A - 9D.   | Young's modulus as a function of depth for each confining pressure . . . . .             | .32 |
| Figures 10A - 10I. | Strength as a function of confining pressure for each zone tested . . . . .              | .38 |
| Figure 11.         | Average ultimate strengths of black and gray shales .                                    | .47 |
| Figure 12.         | Strength of Devonian shales from WV3 loaded perpendicular to bedding . . . . .           | .48 |
| Figure 13.         | Strength of Devonian shales from WV3 loaded parallel to bedding . . . . .                | .49 |
| Figure 14.         | Brittle-ductile transition for Devonian shales from WV3 . . . . .                        | .51 |
| Figure 15.         | Average tensile strengths as a function of depth . .                                     | .54 |
| Figure 16.         | Average fracture energies as a function of depth . .                                     | .59 |

LIST OF TABLES

Table 1. Results of Compression Tests for Black Shales . . . . 19

Table 2. Results of Compression Tests for Gray Shales . . . . 20

Table 3. Elastic Constants for Devonian Shale from WV3,  
Lincoln County, West Virginia . . . . . 36

Table 4. Results of Direct-Pull Tensile Tests for  
Black Shales . . . . . 52

Table 5. Results of Direct-Pull Tensile Tests for  
Gray Shales . . . . . 53

Table 6. Tensile Strengths for Devonian Shale from WV3,  
Lincoln County, West Virginia. . . . . 55

Table 7. Tensile Strength of New Albany Shale,  
Christian County, Kentucky . . . . . 56

Table 8. Results of Fracture Energy Tests for Black Shales . . . 57

Table 9. Results of Fracture Energy Tests for Gray Shales . . . 58

## EXECUTIVE SUMMARY

This report is intended to be a reference on the mechanical properties of Devonian shales for people conducting stimulation research as part of the Eastern Gas Shales Project. The research involves development of novel stimulation techniques, such as tailored-pulse-loading, achieved by using combinations of explosives and/or propellants, as well as refinement of conventional stimulation techniques by varying treating materials and procedures. Evaluation of these techniques is being accomplished through a combination of numerical simulations, laboratory experiments, and full-scale field tests. Each of these approaches requires that the mechanical behavior of Devonian shales be characterized. Thus, numerical data on mechanical properties is presented herein, along with specific information on the tectonic setting so that mechanical behavior can be interpreted in the appropriate context.

Prior to this study, mechanical property data existed only for a few specific localities. Attempts to develop and refine stimulation techniques for more general use in Devonian shales were hampered by a lack of generic mechanical property data. Thus, a prime objective of the current study has been to establish wherever possible regional or stratigraphic trends in the various properties required by stimulation research. Lithologically Devonian shales tend to fall into two categories: gray shales and organic-rich black shales. Two black/gray pairs, Huron/Hanover and Marcellus/Mahantango, were selected from four localities in Pennsylvania and Ohio for comprehensive testing. Over 130 experiments were run on these zones to determine elasticity, fracture properties, yield and ultimate strength, and ductility. The results of these tests and previous tests run on core from West Virginia and Kentucky provide a basis for the following conclusions about Devonian shale mechanical properties and their applications in stimulation research:

- Elasticity of Devonian shale matrix material showed no strong trends with respect to either lithology, locality, or confining pressure. Gray shales tended to have a slightly higher Young's modulus than black shales, but

the difference between the averages was less than the standard deviation of each average. More important in determining the contrast in elasticity between black and gray shales may be the tendency of the black shales to be more highly fractured, which would tend to lower the modulus of black shales as a rock mass.

- Ultimate strength, yield strength, and ductility all increase with increasing confining pressure, which is typical for most rocks. Ultimate strength and yield strength tend to be higher for gray shales, whereas black shales tend to be more ductile. In developing dynamic stimulation techniques so that the peak compressive stress stays below the yield strength, one should use a true yield envelope and not an envelope for ultimate strength which may be higher at higher confining pressures.
- Tensile strength showed no particular trends either regionally or lithologically, whereas fracture energy seemed to have the most consistent trends of any material property measured. Black shales tended to have a higher fracture energy, and fracture energy for both black and gray shales tended to increase with depth of burial. In performing calculations for stimulation research, formulations employing fracture energy as a measure of strength rather than tensile strength may be more desirable.
- Two promising topics for continued study are the effect of confining pressure on fracture energy and the effect of deformation rate on material properties.

## SECTION 1. INTRODUCTION

### 1.1. Purpose and Scope of Study

The objective of this study has been to determine whether some generic trends, either regional or stratigraphic, could be established for mechanical properties of Devonian shales, or if Devonian shales were so heterogeneous mechanically that site-specific measurements would have to be made each time mechanical property data was required. In fact some trends have been found and are presented in SECTION 2 and discussed in SECTION 3 of this report.

The present study was undertaken partly as a result of conclusions made in an SAI report entitled "Material Properties of Devonian Shale for Stimulation Technology Development", (Blanton et al., 1980). The latter report presents new data on dynamic mechanical properties needed for the development of novel stimulation techniques, and also contains a survey of existing material properties, including physical properties such as density, porosity and permeability, and mechanical properties such as static and dynamic measurements of elasticity and strength. From the survey it was found that, while the several labs working on various aspects of Devonian shale material properties had generated a large volume of data, with the exception of density measurements most of it was so site-specific that regional or generic trends could not be established.

The one exception, density, was what gave some indication that in fact trends could be established. Samples for density measurements had been taken from enough localities to allow correlation between density and lithology on a regional basis. Black and brown organic-rich shales were found to have lower densities than gray shales on the average. This was an important correlation because it suggested a relation between something measurable from logs, i.e. density, and the thing ultimately being sought, hydrocarbons. This has been a definite aid in locating potential producers, but getting the organic-rich zones to actually produce often requires stimulation and this is where mechanical properties begin to play an important role.

In selecting and designing stimulation treatments for Devonian shales, one is currently faced with the choice of making site-specific

measurements of the properties required by the design equations, or relying on past experience, or simply guessing. If a set of mechanical properties could be established for black and gray shales at various down-hole conditions, this would eliminate the need for making measurements for each treatment design. Mechanical properties are also important to research and development of novel stimulation techniques. In order to optimize these techniques they must be tailored to a particular set of mechanical properties. If that set of mechanical properties represented the sort of generic trend discussed above then the novel techniques would have regional application.

This report is intended to be a self-contained reference on mechanical properties of Devonian shales and therefore parts of the previous report on material properties must be repeated here for purposes of completeness and comparison. However, the main focus of this report is mechanical properties, and thus physical properties such as density, porosity and permeability will be mentioned only in so far as they concern mechanical properties.

To provide a statistical base for establishing trends, a certain number of tests are required. If one considers how this number is increased by the various permutations of lithology, environmental parameters, regional variations, and different mechanical properties, then one quickly realizes that some limitations and exclusions must be made if the project is to be completed in a reasonable time. First the region has been limited to the producing part of the Appalachian Basin. Devonian shales produce gas in the Illinois and Michigan Basin, too, but this study will be limited to the larger Appalachian Basin. Mechanical property measurements have been limited to static measurements. Dynamic measurements are useful to research on explosive stimulation treatments, and some have already been made on Devonian shales, (Carter and Olinger, 1977, and Blanton et al., 1980), but the results proved to be difficult to interpret in the intermediate strain-rate range because of the anisotropic failure of the test specimens. Also, there is some evidence that dynamic behavior can be characterized by properties measured in static tests as long as inertial effects are taken into account (Brace and Jones, 1971, Young and Powell, 1979, and Blanton, 1981). Static tests have a broader

application and so this study has been limited to them. Three types of static mechanical tests have been run: compression tests under confining pressure, direct-pull tensile tests, and fracture energy tests. Limits placed on lithology, environmental parameters and regional distribution are discussed in the following two subsections.

## 1.2. Character and Setting of Devonian Shales

Mechanical properties of rocks vary with both composition and environment, and therefore in interpreting and applying the data presented in this report it is necessary to have an idea of the character and setting of Devonian shales. Gas-bearing Devonian shales underlie a major portion of the Appalachian Basin, as can be seen in Figure 1, and within this region both lithology and tectonics can be quite heterogeneous. Nevertheless, there are regional trends that provide a framework in which to consider mechanical properties, and these trends are the topic of this subsection.

Shales of the Devonian occur primarily in the Middle and Upper series with the Lower Devonian being composed primarily of limestone. The stratigraphic nomenclature of Devonian shales and their bounding units is shown in Figure 2. In general the shale section is composed of gray shales interbedded with organic-rich brown and black shale sequences. These are interbedded with occasional sandy and silty layers and a few thin limestones. Regionally the Middle and Upper Devonian tend to be thicker in the east where sandy deltaic wedges interfinger with the shales. The brown and black shales occur more frequently in the central and western portions and represent an organic mud facies that accumulated on the western side of an epicontinental sea. The location of these organic shales is reflected by the areas of production delineated in Figure 1.

As mentioned earlier, a correlation has already been found between density and organic content, the black shales having a lower density ( $\sim 2.5 \text{ gm/cm}^3$ ) than the gray shales ( $\sim 2.6 \text{ gm/cm}^3$ ), (Kalyoncu et al., 1977, 1979, and Schmoker, 1977). If a similar correlation could be found for mechanical properties, the task of selecting mechanical properties pertinent to shale stimulation would be greatly simplified.

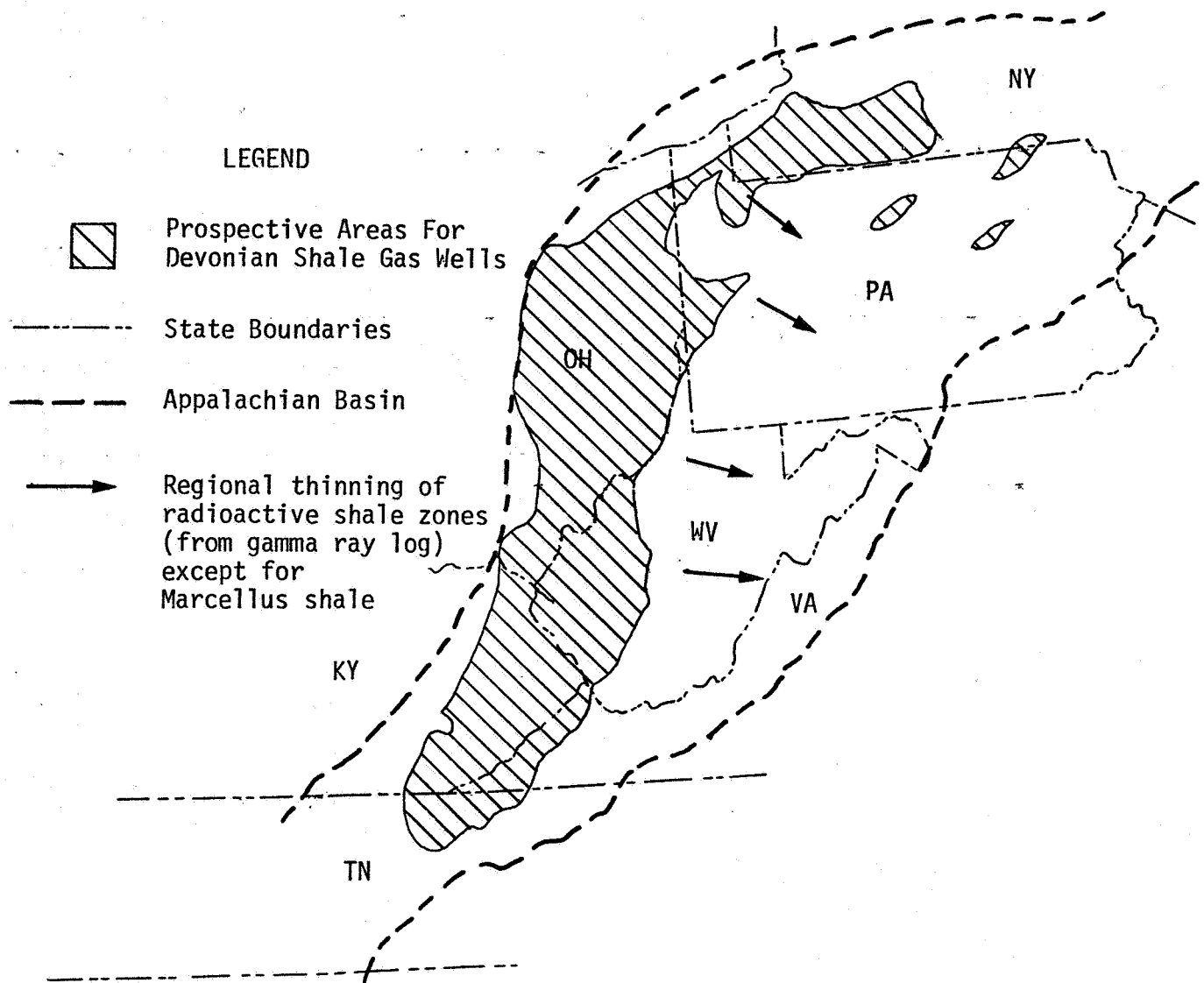


Figure 1. Devonian shale gas production in the Appalachian Basin.

| SERIES                 | OHIO<br>W. WEST VIRGINIA | NORTH OHIO<br>W. PENNSYLVANIA | NEW YORK                 | PENNSYLVANIA<br>E. WEST VIRGINIA |                    |
|------------------------|--------------------------|-------------------------------|--------------------------|----------------------------------|--------------------|
| Lower<br>Mississippian | Berea Sandstone          | Berea Sandstone               |                          | Pocono Formation                 |                    |
|                        | Bedford Shale            |                               |                          |                                  |                    |
| Upper<br>Devonian      | Cleveland Member         | Cleveland Member              | Conewango Group          | Hampshire Formation              |                    |
|                        | Ohio Shale               | Ohio Shale                    | Conneaut Group           | Chemung Formation                |                    |
|                        | Chagrín Shale            | Chagrín Shale                 | Canadaway Group          |                                  |                    |
|                        | Huron Member*            | Huron Member*                 | Undivided Dunkirk Shale* |                                  |                    |
|                        | Upper Olentangy Shale    |                               | Java Formation           | Java Formation                   | Brallier Formation |
|                        |                          |                               | Hanover Shale            | Hanover Shale                    |                    |
|                        |                          |                               | Pipe Creek Shale*        | Wiscoy Member                    |                    |
|                        |                          |                               | Angola Shale             | Hanover Shale                    |                    |
|                        |                          |                               | West Falls Formation     | Angola Shale                     |                    |
|                        |                          |                               | West Falls Formation     | Rhine-Street Shale*              |                    |
|                        |                          | Rhine-Street Shale*           | Sonyea Formation         | Harrell Formation                |                    |
|                        |                          | Tully Limestone               | Genesee Formation*       | Undivided Burkett Shale*         |                    |
| Middle<br>Devonian     | Lower Olentangy Shale    | Hamilton Group                | Tully Limestone          | Tully Limestone                  |                    |
|                        |                          | Mahantango Formation          | Moscow Formation         | Hamilton Group                   |                    |
|                        | Delaware Limestone       | Onandaga Limestone            | Ludlowville Formation    | Ludlowville Formation            | Marcellus Shale*   |
|                        |                          |                               | Skaneateles Formation    | Skaneateles Formation            |                    |
|                        |                          |                               | Marcellus Shale*         | Marcellus Shale*                 | Marcellus Shale*   |
|                        |                          | Onandaga Limestone            | Onandaga Limestone       | Onandaga Limestone               |                    |

\* Organic-Rich Shales

Figure 2. Nomenclature of Devonian shales and their bounding units.

Therefore, rather than attempt to sample all the formations shown in Figure 2, sampling has been done on the basis of organic content, i.e. units have been selected that are distinctly black or gray. The selection process is discussed in more detail in the following subsection.

Another characteristic of Devonian shales that tends to follow the black/gray contrast is the natural fracture system. Evans (1980) found that natural fracture frequencies show a distinct relationship to certain stratigraphic units, specifically the Marcellus Shale, Tully Limestone, Genesso Shale, West Falls Formation and the Lower Huron Member. Except for the Tully Limestone these units tend to be black and brown organic shales. When these units are capped by a sealing unit, they are usually gas producers. The importance of the natural fracture system in providing the permeability necessary for production has been discussed in numerous reports, e.g. Shumaker et al. (1978) and Ford (1979). Natural fractures also effect the strength and elasticity of rocks and should be taken into consideration in applying laboratory generated mechanical properties.

Five environmental parameters considered to have a primary influence on mechanical properties are stress, pore pressure, temperature, strain rate and pore fluid chemistry. For the applications being considered here, only the first three are part of the natural setting and therefore discussion in this subsection will focus on these. The last two are imposed in the process of drilling, completing and producing the well.

Of the first three parameters, stress has the greatest degree of variability in the Appalachian Basin. To specify the state of stress, both orientation and magnitude of the mutually perpendicular principal stresses must be given. The orientation of the principal stresses can vary locally, particularly near faults or in areas of intense folding, but there seems to be fairly good agreement about the regional orientation in the Appalachian Basin (Overbey, 1976, and Sbar and Sykes, 1973). The maximum principal stress trends slightly north of east except in the Rome trough where it trends N 45°E to N 50°E (see Figure 3). The orientation of the intermediate and minimum principal stresses are subperpendicular and subparallel respectively to the surface at shallow

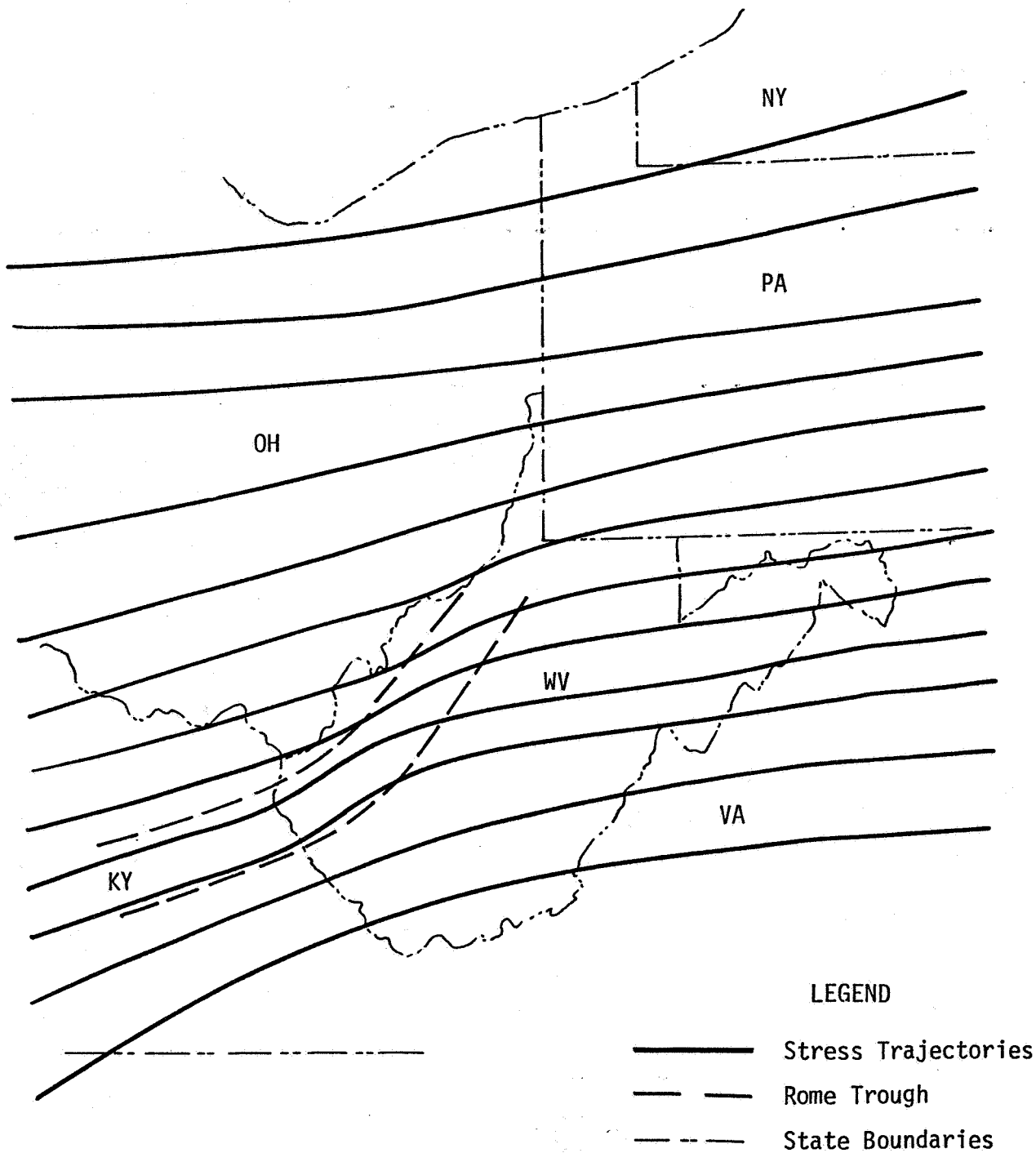


Figure 3. Stress trajectories for the maximum principal stress in the Appalachian Basin.

depths since the surface is a plane of no shear stress. At greater depths they may tend to vary more, especially near faults and folds.

Magnitudes tend to increase with depth due to the increasing weight of the overburden which effects the vertical stress directly and the horizontal stresses indirectly through a Poisson effect. The principal stress magnitudes will thus be given in terms of stress gradients. The simplest stress to determine is the vertical stress which is given by the well known formula for overburden:

$$\sigma_v = \rho gh$$

where

$\rho$  = density

$g$  = acceleration due to gravity

$h$  = depth of burial

Using an average density of 2.6 gm/cm<sup>3</sup> for Devonian shales, one obtains a vertical stress gradient of 25.5 kPa/m (1.13 psi/ft).

Theoretically the horizontal principal stresses can be determined from pressure measurements made during hydraulic fracturing treatments, if the created fracture is vertical. Hydraulic fractures tend to propagate perpendicular to the least principal stress, and it is reasoned that the pressure required to hold the fracture open is equal to the least principal stress. During a treatment as fluid is being pumped the pressure measured at the surface includes pressure due to friction in the pipe, perforations, and fracture. When pumping stops the friction pressure goes to zero. The pressure measured at this time, while the fracture is supposedly still open, is called the instantaneous shut-in pressure (ISIP). When the ISIP is added to the hydraulic head in the wellbore, a bottom-hole pressure is obtained which should be equal to the pressure in the fracture. This bottom hole pressure divided by the depth of the zone being treated is called fracture gradient and is taken as a measure of the minimum horizontal in situ stress, assuming the fracture is vertical. If the fracture gradient is equal to or greater than the overburden gradient, then it is likely that a horizontal fracture has been created. In this case the overburden stress would be the least principal stress.

A wide range of fracture gradients have been reported for Devonian shales. McKetta (1980) collected 67 measurements from Kentucky, West Virginia, and Ohio. The maximum was 23.8 kPa/m (1.05 psi/ft), and the minimum was 5.0 kPa/m (0.22 psi/ft) with an average of about 11 kPa/m (0.5 psi/ft). The lower values are less than a hydrostatic head, which is 9.8 kPa/m (0.433 psi/ft), so that these formations could not support a wellbore full of water. Three fracture gradients measured in the Devonian shales of Gallia, Ohio, are 12.2 kPa/m (0.541 psi/ft), 14.0 kPa/m (0.619 psi/ft), and 17.2 kPa/m (0.760 psi/ft) (Hennington, 1980). A value of 19.5 kPa/m (0.860 psi/ft) was measured by Terra Tek for the upper gray shale of the Huron in Lincoln County, West Virginia (Jones et al., 1977). Calculated in situ horizontal stress gradients for six lower zones in the same well ranged from 10.8 kPa/m (0.475 psi/ft) to 17.9 kPa/m (0.793 psi/ft) with an average of 15.1 kPa/m (0.665 psi/ft). The calculated stresses in the organic rich brown shales were consistently lower than in the gray shale units. The range of all the fracture gradients given above is similar to the range for other regions, but the Devonian shales tend to have more low values than other regions.

The maximum horizontal principal stress is more difficult to determine from hydraulic fracturing because it requires a knowledge of the in situ tensile strength of the rock, which is difficult to measure, and an accurate measure of the breakdown pressure during a fracturing treatment. Uncertainties are introduced in the breakdown pressure by the fact that the pumps are running, and so there is some friction pressure, and also by the fact that the formation may have already been broken down in the process of drilling and completing the well. Nevertheless Terra Tek has attempted to measure the maximum horizontal principal stress from the breakdown pressure in WV3 in Lincoln County, West Virginia (Abou-Sayed et al., 1978). Two methods of calculating the stress from the breakdown pressure were used, one using a simple tensile strength for the rock and the other employing fracture mechanics theory. The first gave a stress of 38.1 MPa, or a gradient of 45.5 kPa/m, and the second gave 30.3 MPa or a gradient of 36.2 kPa/m. This was the maximum principal stress in the case where the overburden was 22.1 MPa and the minimum horizontal principal stress was 16.3 MPa.

In summary, the maximum horizontal principal stress tends east-northeast, and at least in Lincoln County, West Virginia it is approximately 35 to 45 kPa/m (1.5 to 2.0 psi/ft). This magnitude has the most uncertainty associated with it because of the different theories about how it should be calculated and because each theory depends on accurate knowledge of an in situ value of strength (tensile strength or fracture energy) which is difficult to obtain. The other two gradients are based on more direct and more numerous measurements and thus are more reliable. They are 25.5 kPa/m (1.13 psi/ft) for the vertical intermediate stress and 10 to 15 kPa/m (0.5 to 0.7 psi/ft) for the horizontal least principal stress.

Pore fluid pressure also influences mechanical behavior. The properties of many porous rocks have been found to be a function of effective stress as defined by the following equation:

$$\sigma = S - P$$

where  $\sigma$  is the effective stress,  $S$  is the total stress, and  $P$  is the pore fluid pressure. Handin et al. (1963) stated that this effective stress law holds as long as the interstitial fluid is inert at least with respect to the matrix material and that the porosity distribution and permeability are sufficient to allow pervasion of the pore pressure. The dependence of porosity and permeability of Devonian shales on the heterogeneous fracture system is such that the second condition is probably not met in many cases. The magnitude of in situ pore pressure is usually very low in Devonian shales (1.5 to 3.5 MPa or 200 to 300 psi) and thus not quite so important in its influence as total stress. However in situations where the pressure is raised artificially, such as during a fracturing treatment, it should definitely be taken into account.

In order for temperature to have a strong effect on mechanical properties it usually must vary a few hundred degrees centigrade. Bottom-hole temperatures in Devonian shale wells 900 to 1200 m (3,000 to 4,000 ft) deep are on the order of 40°C (100°F), so tests at room temperature are probably adequate to characterize shale behavior.

### 1.3. Choice of Core for Testing

In order to meet the objectives discussed in the first subsection it was necessary to obtain an areal and stratigraphic distribution of core representative of Devonian shales in the Appalachian Basin. Several thousand feet of core were available for sampling. The problem was to select core that would meet the distribution requirements and at the same time be limited enough to allow adequate testing of each zone within the time and budget constraints of the project.

Regionally it was desirable to have core from wells along the trend of the Appalachian Basin as well as across it. Figure 4 shows the location of wells from which core was obtained and one well, WV3, which has been the subject of material property testing in earlier reports (Hanson et al., 1976a, 1976b, Jones et al., 1977). Together these wells form two sections across the basin (OH7-PA2 and OH9-WV3) and one along the basin (OH7-OH8-OH9).

Stratigraphically, the most common target for Devonian shale wells is the Lower Huron Member or its stratigraphic equivalent. It is a black shale with a relatively high organic content and radioactivity as seen on gamma-ray logs. For purposes of comparison, core from an adjacent gray shale was needed. The Huron shale is overlain by the Chagrin shale which is predominantly a gray shale; however, locally it interfingers with black Huron-like shales and cannot be counted on to have a consistently low organic content. The Hanover shale, which underlies the Huron did show a consistently low radioactivity on the gamma-ray logs indicating a low organic content. Thus, the Lower Huron/Hanover was selected as a black/gray pair for mechanical property testing. The Lower Huron pinches out on the eastern side of the basin and was not encountered in PA2. A black shale that was encountered in PA2 in addition to several others, was the Marcellus shale. This is overlain by the gray Mahantango shale, and so the Marcellus/Mahantango was selected as a second black/gray pair for study. Figure 5 shows depth and stratigraphic relationships among the selected wells.

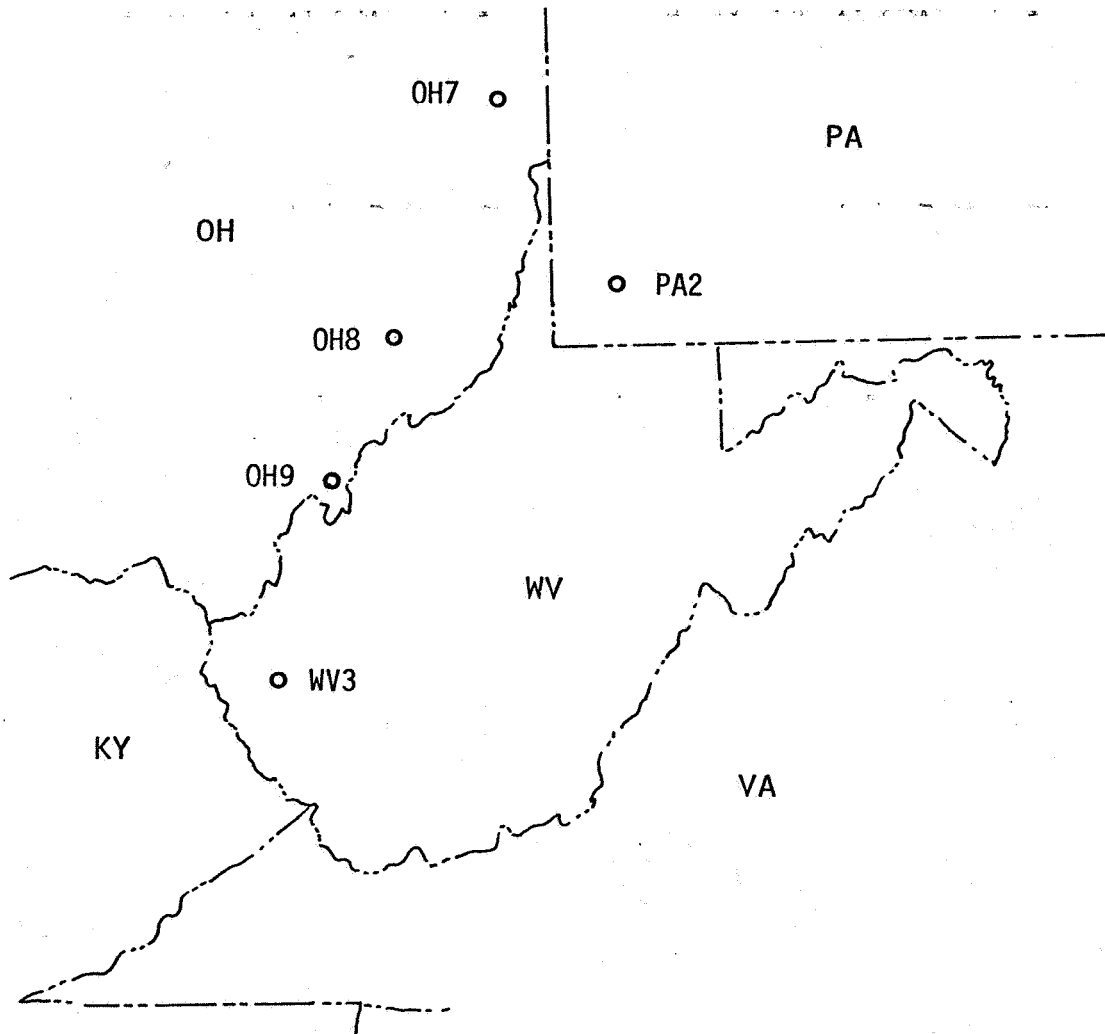


Figure 4. Location of wells from which core was obtained for mechanical property testing.

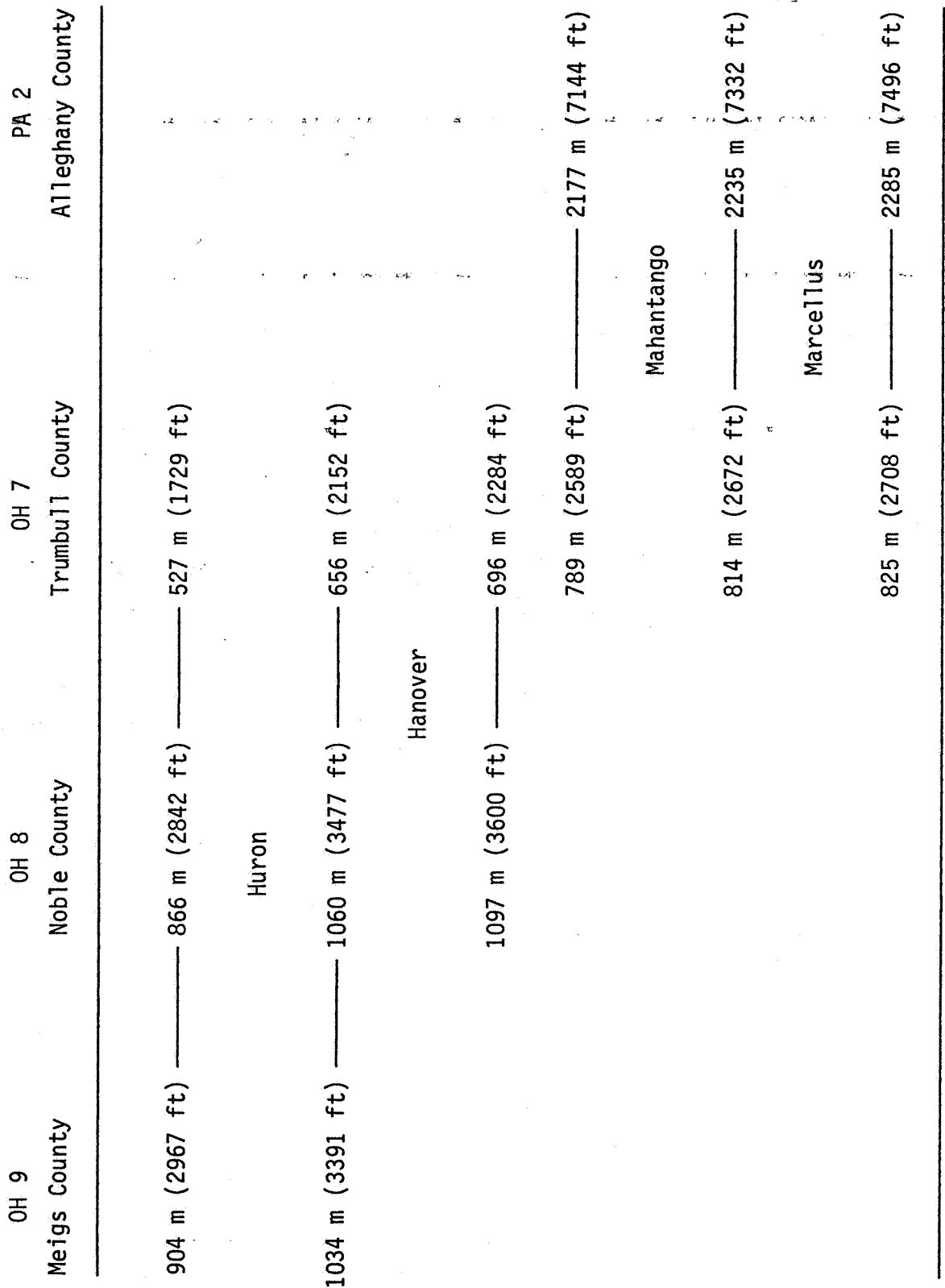


Figure 5. Stratigraphic and depth relations for sampled zones.

## SECTION 2. RESULTS OF MECHANICAL PROPERTIES TESTS

### 2.1 Compression Tests: Elasticity and Strength

The plan for this set of experiments was to run compression tests at confining pressures of 0, 20, 40, and 60 MPa (0, 2900, 5800, and 8700 psi) for each zone in each well shown in Figure 5. In some cases enough core was available to allow replication at some or all confining pressures; however, some of the core was so friable that four test quality specimens could not be prepared. Only three specimens could be prepared from the Marcellus of OH7 and the black Huron of OH9, and no specimens could be prepared from the Mahantango of OH7. Only Huron core was available from OH9, but this contained distinct gray layers in a normally black unit, so test specimens were prepared from both black and gray layers in order to get a comparison.

The test specimens were cylindrical with diameters of 2.54 cm (1 in) and lengths of approximately 6.35 cm (2.5 in). Bedding ran parallel to the axis of the specimens. The ends were lapped to within 0.003 cm (~0.001 in) of parallel. Tests were run by first jacketing a specimen, then placing it under the desired confining pressure in the radial direction, and finally compressing it in the axial direction until failure occurred. Axial load and axial displacement were recorded in analog and digital form. The tests were run by a closed-loop servo-controlled system in which the controlled variable was axial displacement. A ramp-generator was used in the system to produce a constant displacement rate. This rate was adjusted in each test to the specimen length so that the resulting strain rate was always  $10^{-4}\text{s}^{-1}$ .

Examples of typical stress-strain curves are shown in Figures 6 and 7, which also serve to illustrate the data reduction process. The plotted stress is differential stress, which is the axial stress minus the confining pressure. Strain is calculated by dividing axial displacement, corrected for shortening of the loading piston, by specimen length. After plotting differential stress vs. strain from the digital data, a computer calculates, records, and prints Young's modulus, yield strength, and ultimate strength. Stress-strain curves for all the tests are contained in Appendix A. The numerical results are presented in Tables 1 and 2.

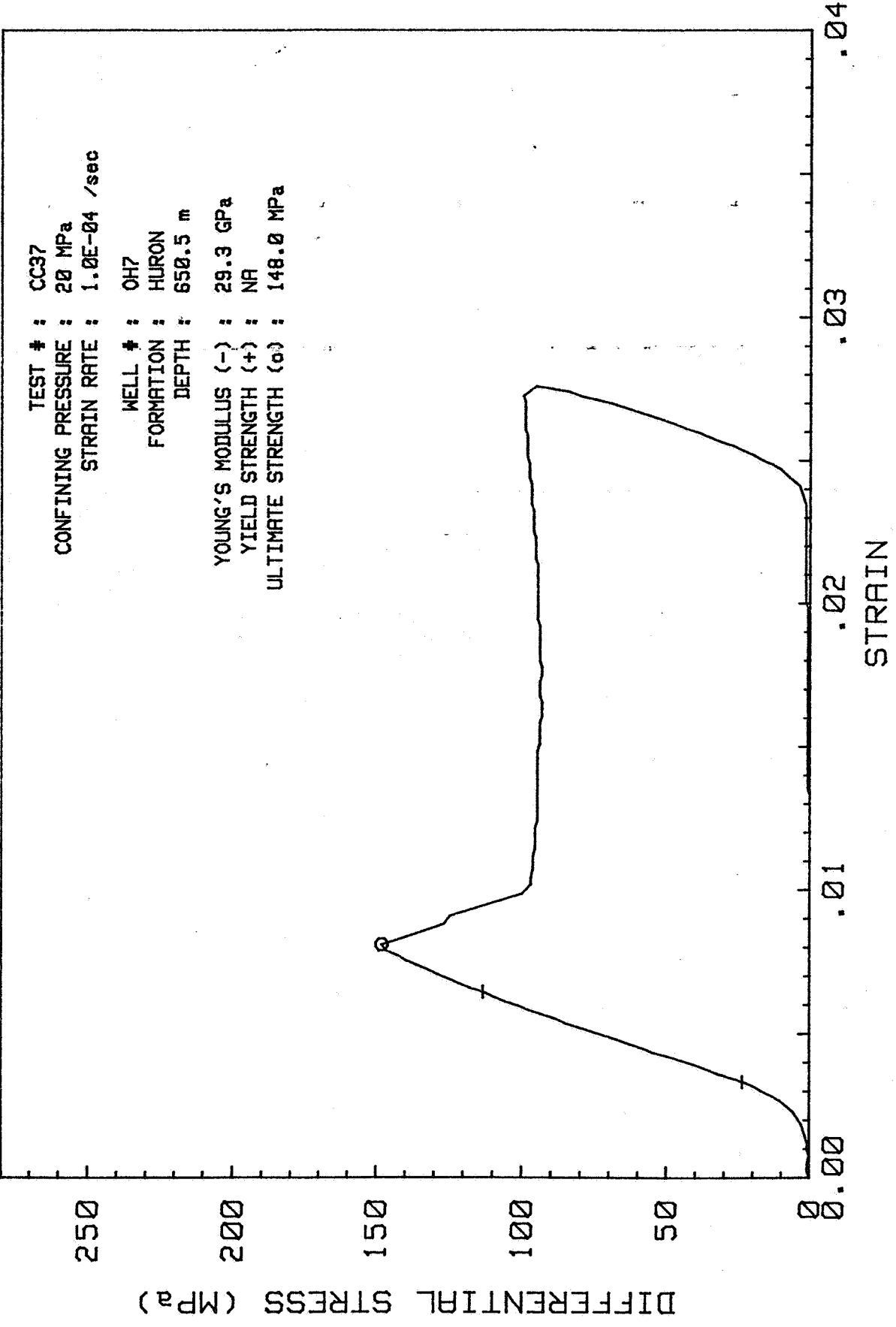


Figure 6. Example of a stress-strain curve exhibiting failure without yielding.

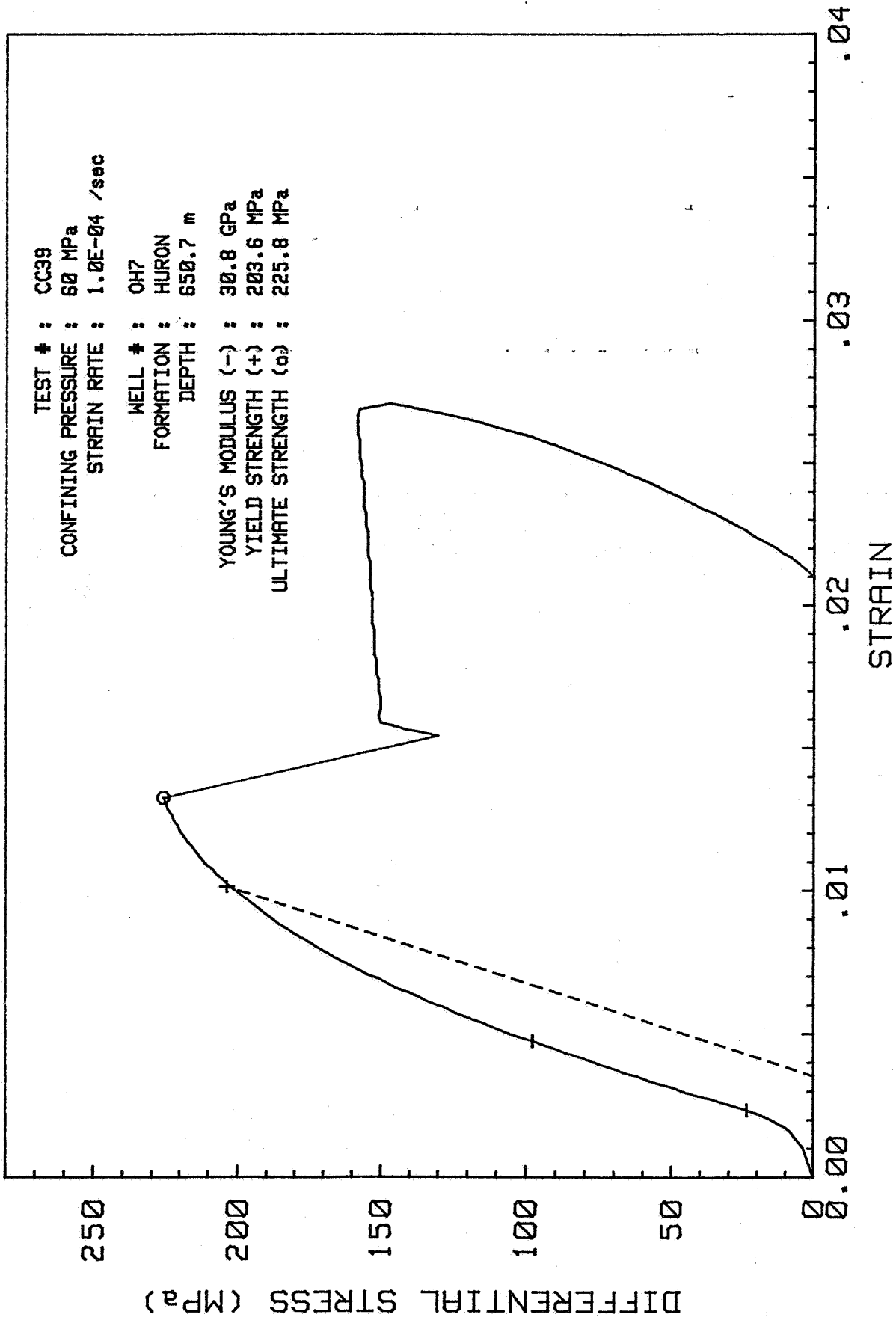


Figure 7. Example of a stress-strain curve showing the yield point.

TABLE 1. RESULTS OF COMPRESSION TESTS FOR BLACK SHALES.

| TEST | WELL | FORMATION | DEPTH (M) | CONFINING PRESSURE (MPa) | YOUNG'S MODULUS (GPa) | YIELD STRENGTH (MPa) | ULTIMATE STRENGTH (MPa) |
|------|------|-----------|-----------|--------------------------|-----------------------|----------------------|-------------------------|
| CU40 | OH7  | HURON     | 652.9     | 0                        | 33.9                  | NA                   | 136.9                   |
| CU43 | OH7  | HURON     | 650.0     | 0                        | 38.0                  | NA                   | 119.9                   |
| CC37 | OH7  | HURON     | 650.5     | 20                       | 29.3                  | NA                   | 148.0                   |
| CC50 | OH7  | HURON     | 650.0     | 20                       | 36.4                  | 187.3                | 191.7                   |
| CC38 | OH7  | HURON     | 650.8     | 40                       | 26.4                  | NA                   | 162.1                   |
| CC46 | OH7  | HURON     | 648.8     | 40                       | 28.7                  | 203.6                | 209.5                   |
| CC47 | OH7  | HURON     | 650.0     | 40                       | 33.0                  | 197.6                | 225.8                   |
| CC49 | OH7  | HURON     | 650.1     | 40                       | 36.7                  | 196.9                | 219.8                   |
| CC39 | OH7  | HURON     | 650.7     | 60                       | 30.8                  | 203.6                | 225.8                   |
| CC48 | OH7  | HURON     | 650.0     | 60                       | 35.2                  | 208.0                | 239.8                   |
| CU49 | OH7  | MARCELLUS | 816.8     | 0                        | 31.2                  | NA                   | 60.0                    |
| CC66 | OH7  | MARCELLUS | 817.3     | 20                       | 34.2                  | NA                   | 113.3                   |
| CC65 | OH7  | MARCELLUS | 817.6     | 60                       | 35.0                  | 185.1                | 200.6                   |
| CU47 | OH9  | HURON     | 1023.8    | 0                        | 27.0                  | NA                   | 76.2                    |
| CC58 | OH9  | HURON     | 1023.5    | 20                       | 27.0                  | 129.5                | 129.5                   |
| CC59 | OH9  | HURON     | 1023.8    | 60                       | 32.4                  | 157.7                | 184.3                   |
| CU46 | OH8  | HURON     | 1052.9    | 0                        | 33.8                  | NA                   | 97.0                    |
| CC35 | OH8  | HURON     | 1052.1    | 20                       | 30.7                  | NA                   | 106.6                   |
| CC56 | OH8  | HURON     | 1052.4    | 40                       | 36.1                  | NA                   | 180.6                   |
| CC57 | OH8  | HURON     | 1052.6    | 60                       | 38.4                  | 201.3                | 209.5                   |
| CU42 | PA2  | MARCELLUS | 2263.1    | 0                        | 18.6                  | NA                   | 32.6                    |
| CC45 | PA2  | MARCELLUS | 2296.8    | 20                       | 21.2                  | NA                   | 96.2                    |
| CC44 | PA2  | MARCELLUS | 2257.3    | 40                       | 25.1                  | NA                   | 128.8                   |
| CC43 | PA2  | MARCELLUS | 2266.9    | 60                       | 23.2                  | 151.7                | 159.9                   |

TABLE 2. RESULTS OF COMPRESSION TESTS FOR GRAY SHALES.

| TEST | WELL | FORMATION    | DEPTH (m) | CONFINING PRESSURE (MPa) | YOUNG'S MODULUS (GPa) | YIELD STRENGTH (MPa) | ULTIMATE STRENGTH (MPa) |
|------|------|--------------|-----------|--------------------------|-----------------------|----------------------|-------------------------|
| CU44 | OH7  | HANOVER      | 657.9     | 0                        | 26.7                  | NA                   | 40.0                    |
| CU45 | OH7  | HANOVER      | 658.1     | 0                        | 30.0                  | NA                   | 69.6                    |
| CC32 | OH7  | HANOVER      | 664.3     | 20                       | 25.5                  | NA                   | 110.3                   |
| CC33 | OH7  | HANOVER      | 663.3     | 20                       | 27.7                  | NA                   | 114.0                   |
| CC51 | OH7  | HANOVER      | 657.9     | 20                       | 29.5                  | NA                   | 156.9                   |
| CC52 | OH7  | HANOVER      | 657.9     | 40                       | 29.5                  | NA                   | 175.4                   |
| CC55 | OH7  | HANOVER      | 658.0     | 40                       | 34.0                  | 191.7                | 199.9                   |
| CC53 | OH7  | HANOVER      | 658.0     | 60                       | 29.9                  | 198.4                | 216.1                   |
| CC54 | OH7  | HANOVER      | 658.0     | 60                       | 35.3                  | 188.8                | 211.7                   |
| CU48 | OH9  | HURON (GRAY) | 1024.5    | 0                        | 35.2                  | NA                   | 119.9                   |
| CC60 | OH9  | HURON (GRAY) | 1024.5    | 20                       | 36.4                  | NA                   | 153.2                   |
| CC63 | OH9  | HURON (GRAY) | 1024.4    | 20                       | 32.6                  | NA                   | 169.5                   |
| CC61 | OH9  | HURON (GRAY) | 1024.5    | 40                       | 38.7                  | 203.6                | 203.6                   |
| CC64 | OH9  | HURON (GRAY) | 1024.6    | 40                       | 27.6                  | NA                   | 149.5                   |
| CC62 | OH9  | HURON (GRAY) | 1024.6    | 60                       | 31.1                  | 213.9                | 235.4                   |
| CU39 | OH8  | HANOVER      | 1061.7    | 0                        | 28.9                  | NA                   | 58.5                    |
| CU50 | OH8  | HANOVER      | 1062.0    | 0                        | 32.8                  | NA                   | 87.3                    |
| CC31 | OH8  | HANOVER      | 1061.3    | 20                       | 34.9                  | NA                   | 132.5                   |
| CC70 | OH8  | HANOVER      | 1062.1    | 20                       | 33.9                  | NA                   | 154.0                   |
| CC29 | OH8  | HANOVER      | 1060.5    | 40                       | 34.0                  | 233.9                | 233.9                   |
| CC69 | OH8  | HANOVER      | 1062.0    | 40                       | 34.2                  | NA                   | 191.7                   |
| CC28 | OH8  | HANOVER      | 1060.3    | 60                       | 39.8                  | 233.2                | 253.2                   |
| CC67 | OH8  | HANOVER      | 1062.0    | 60                       | 34.0                  | 210.2                | 213.2                   |
| CC68 | OH8  | HANOVER      | 1062.0    | 60                       | 37.9                  | 231.7                | 250.9                   |
| CU41 | PA2  | MAHANTANGO   | 2225.6    | 0                        | 25.7                  | NA                   | 38.5                    |
| CC40 | PA2  | MAHANTANGO   | 2225.5    | 20                       | 30.2                  | NA                   | 108.8                   |
| CC41 | PA2  | MAHANTANGO   | 2225.6    | 40                       | 35.3                  | NA                   | 213.2                   |
| CC42 | PA2  | MAHANTANGO   | 2225.4    | 60                       | 36.5                  | NA                   | 239.1                   |

Young's modulus is ideally the slope of the part of the stress-strain curve representing linear elastic behavior. The computer calculates Young's modulus as the slope of a linear least-squares fit to digital points between certain limits marked by a "-" in Figures 6 and 7. These limits are picked by the computer as bounding the maximum positive slope attained before ultimate strength is reached.

Ideally yield stress is the stress at which plastic-strain begins. In rocks, plastic strain usually begins on a microscopic scale around grain boundaries and microcracks, and its onset is difficult to detect. In order to define yield stress for rocks, a somewhat arbitrary definition must be adopted. In the past, (e.g. Handin, 1966) yield has been defined as the stress at some arbitrary small strain like 0.02. This has a defect in that it does not take into account the effect in change of moduli for different rocks. A rock with a low modulus could still be deforming elastically at 0.02 strain. Defining yield at 0.02 strain would give a deceptively low yield stress. Conversely, a rock with a high modulus may have already undergone significant plastic strain by the time 0.02 strain is reached. If work-hardening were occurring, a deceptively high yield stress would be given. To avoid this problem a definition has been borrowed from materials science (McClintock and Argon, 1966), as follows: yield strength is the stress at which a deviation from linear elastic behavior of 0.002 strain occurs. The computer calculates yield strength as the intersection of the stress-strain curve and a straight line representing the least-squares fit used to calculate Young's modulus shifted by a strain of 0.002. If this intersection occurs after the ultimate strength, then NA (not applicable) is printed for yield strength as in Figure 6. If the intersection occurs before the ultimate strength, then the straight line representing a shifted elastic slope is plotted as a dashed line, the intersection is marked by a "+", and the value for yield strength is printed as in Figure 7.

The ultimate strength is defined simply as the maximum stress reached during a test. In some instances, for example when work-hardening is still occurring at the end of a test, this may be an

arbitrary value, but in this study all ultimate strengths were unique. The computer picks these values, marks them with a "o", and prints them as shown in both Figures 6 and 7.

The values obtained for Young's modulus are plotted vs. confining pressure for each of the nine zones tested in Figures 8A through 8I. With the exception of the Huron from OH7 and the Huron (gray) from OH9 there is a tendency for Young's modulus to increase with increasing confining pressure, but only very slightly and by an amount that is of the order of the standard deviation for all the values. There is also a tendency for Young's modulus to be slightly lower for the black shales than for the gray shales. The average  $\pm$  standard deviation (number of values) for the black shales is  $30.9 \pm 5.4$  (24) GPa and for the gray shales is  $32.4 \pm 3.9$  (28) GPa. This trend is not particularly strong and locally can be reversed, as is the case in OH7 where the black Huron averages higher than the gray Hanover.

If there are any regional trends, they are extremely weak. As mentioned in the introduction, the basin deepens to the southeast and the shales tend to become less organic, however this does not appear to have any strong influence on elasticity. When Young's modulus is plotted against depth for each confining pressure, as in Figures 9A through 9D, no apparent trends emerge. What stands out in these figures is that there is a relatively strong grouping independent of depth and lithology at least between 600 and 1100 m (2000 and 3600 ft). Also along the basin there are no apparent trends, although in this direction there is no special reason to expect any. For example consider the Huron from wells OH7, OH8, and OH9, which are in a line along the trend of the basin from northeast to southwest. Average values of Young's modulus first increase from 32.8 GPa to 34.8 GPa then decrease to 28.8 GPa. The standard deviations are 3 to 4 GPa, so the only conclusion seems to be that Young's modulus does not vary much in any direction. This conclusion is supported by tests run in other labs on core from WV3. Table 3 shows values generated by Terra Tek, three of which fall within the values found in our study. The one high value of 55.2 GPa cannot be said to represent any trend. It is simply anomalous. The only other source for

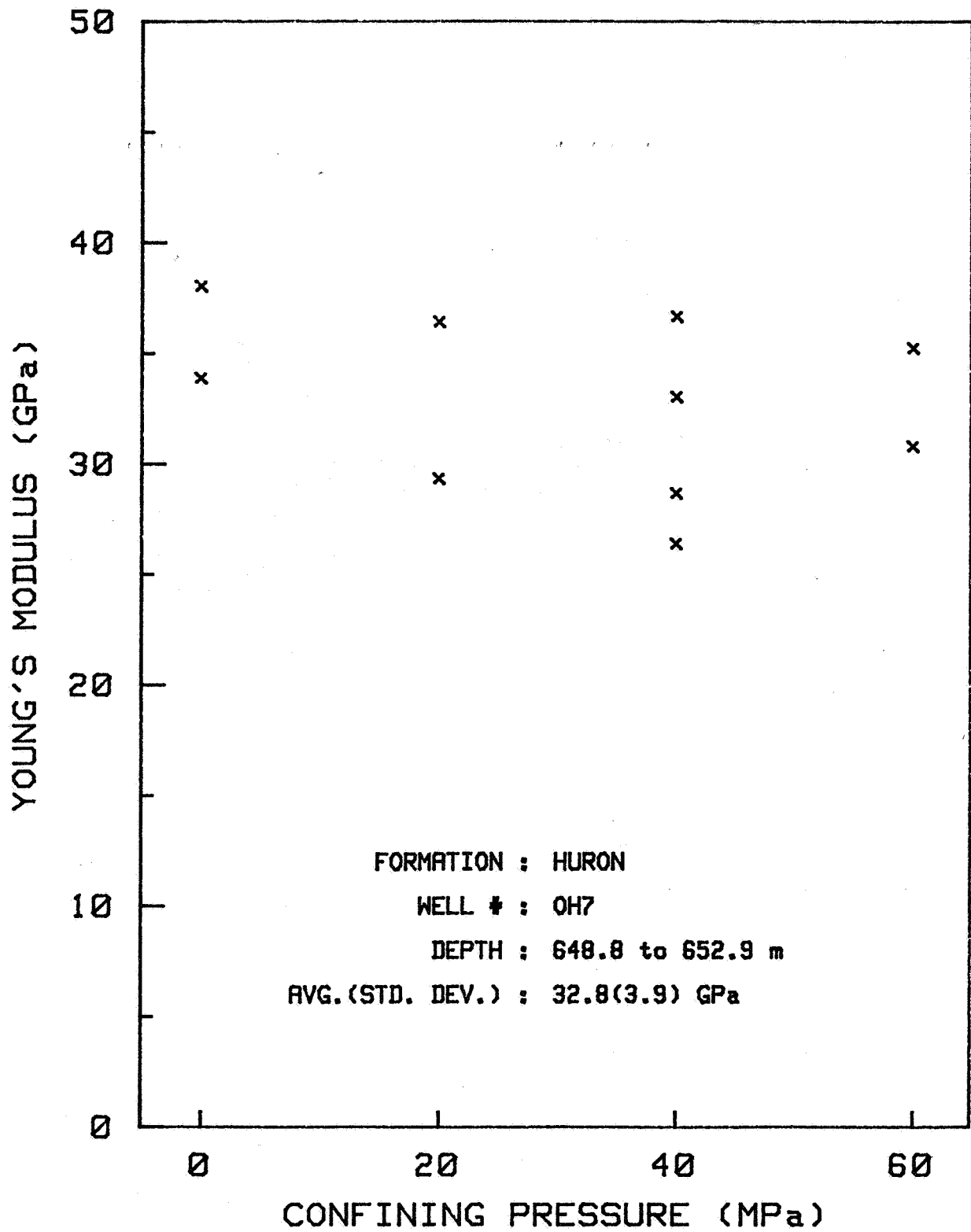


Figure 8A. Young's modulus as a function of confining pressure.

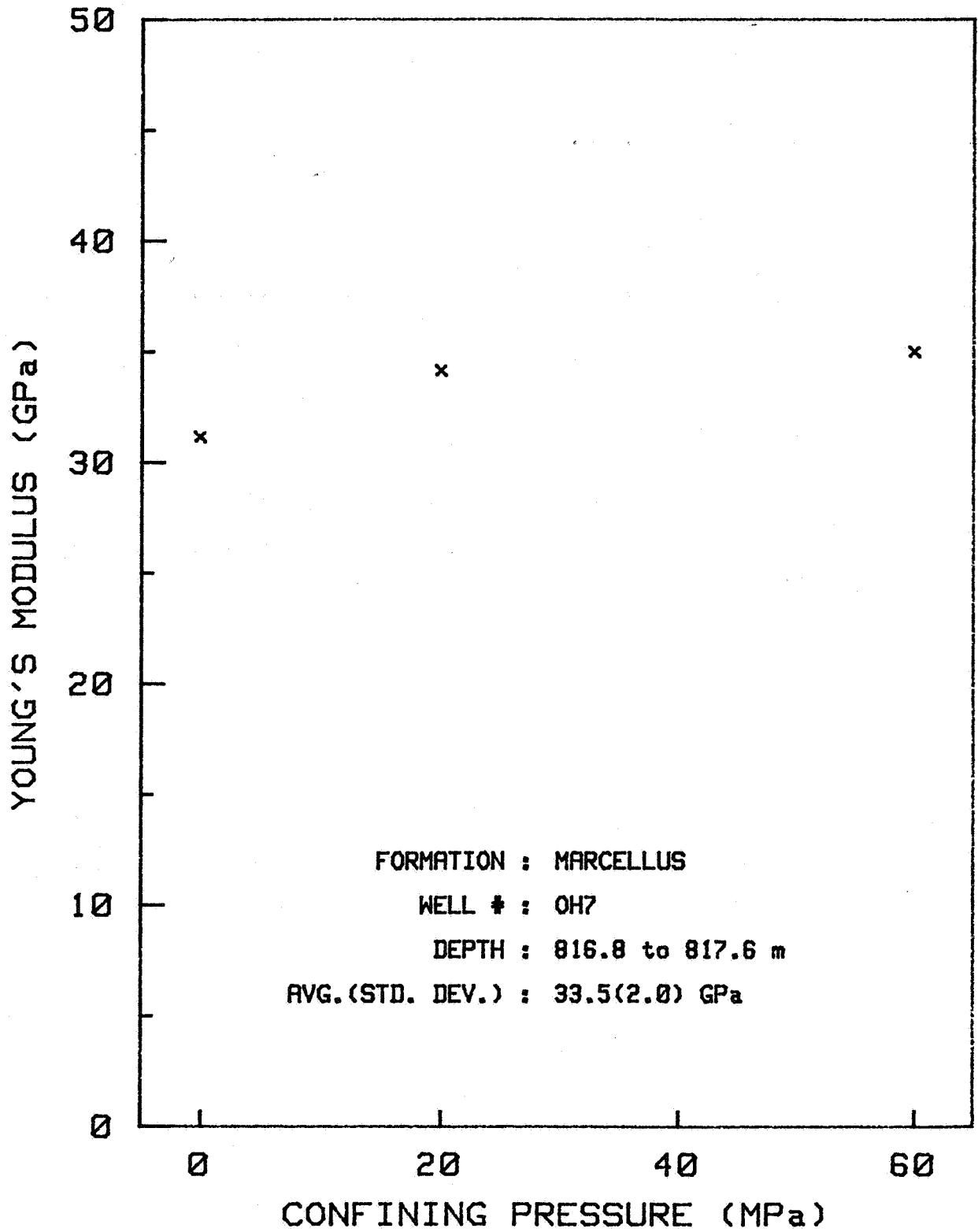


Figure 8B. Young's modulus as a function of confining pressure.

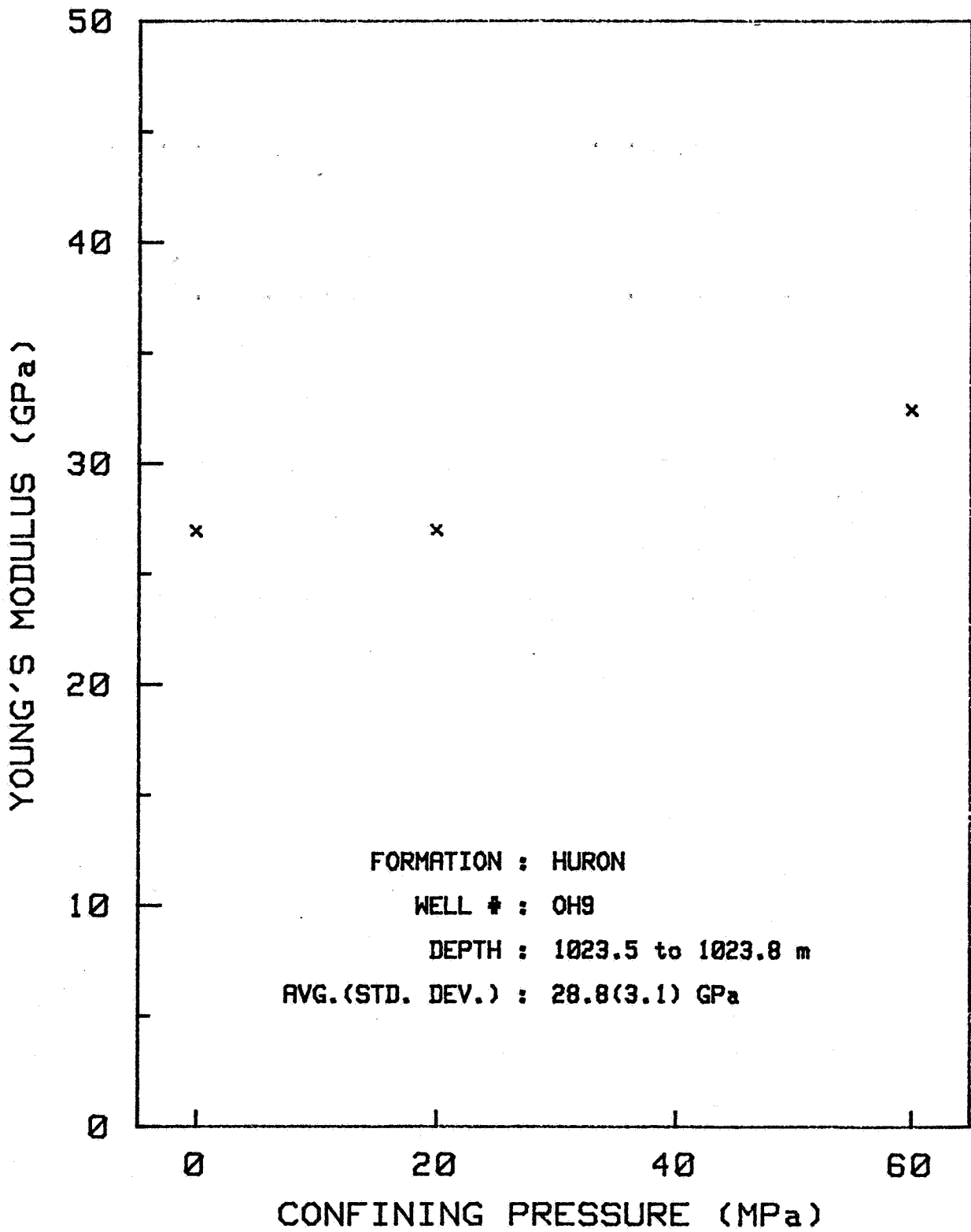


Figure 8C. Young's modulus as a function of confining pressure.

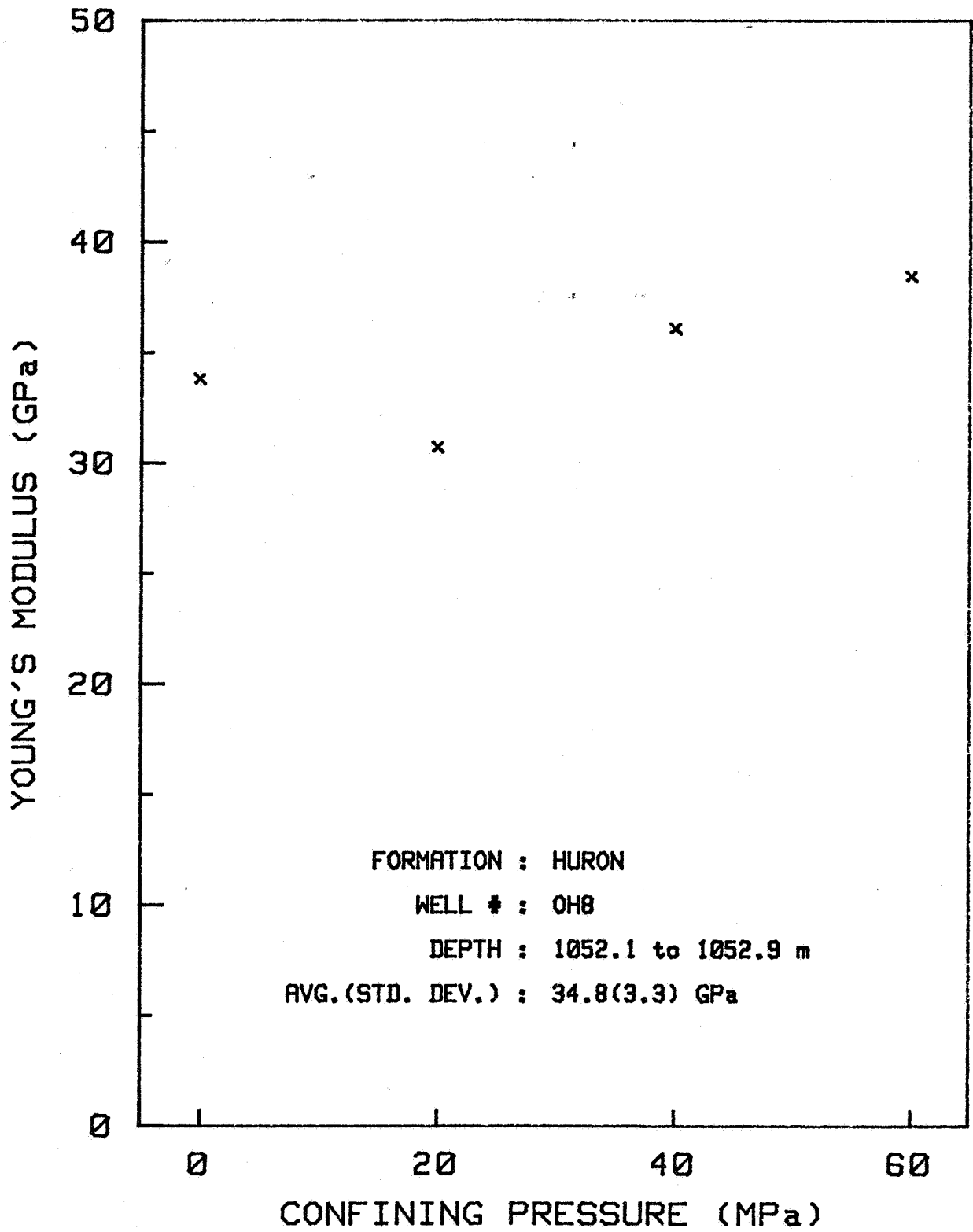


Figure 8D. Young's modulus as a function of confining pressure.

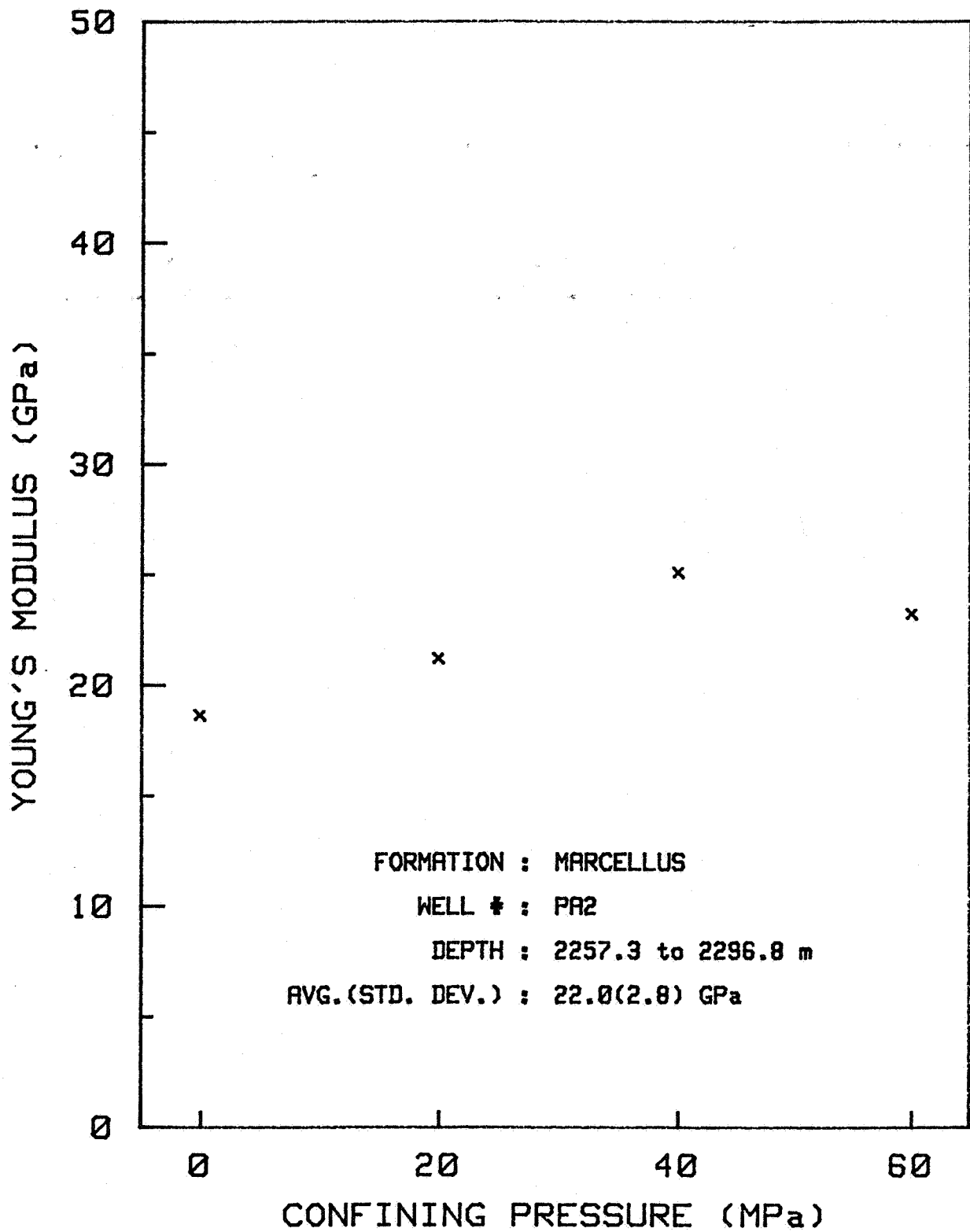


Figure 8E. Young's modulus as a function of confining pressure.

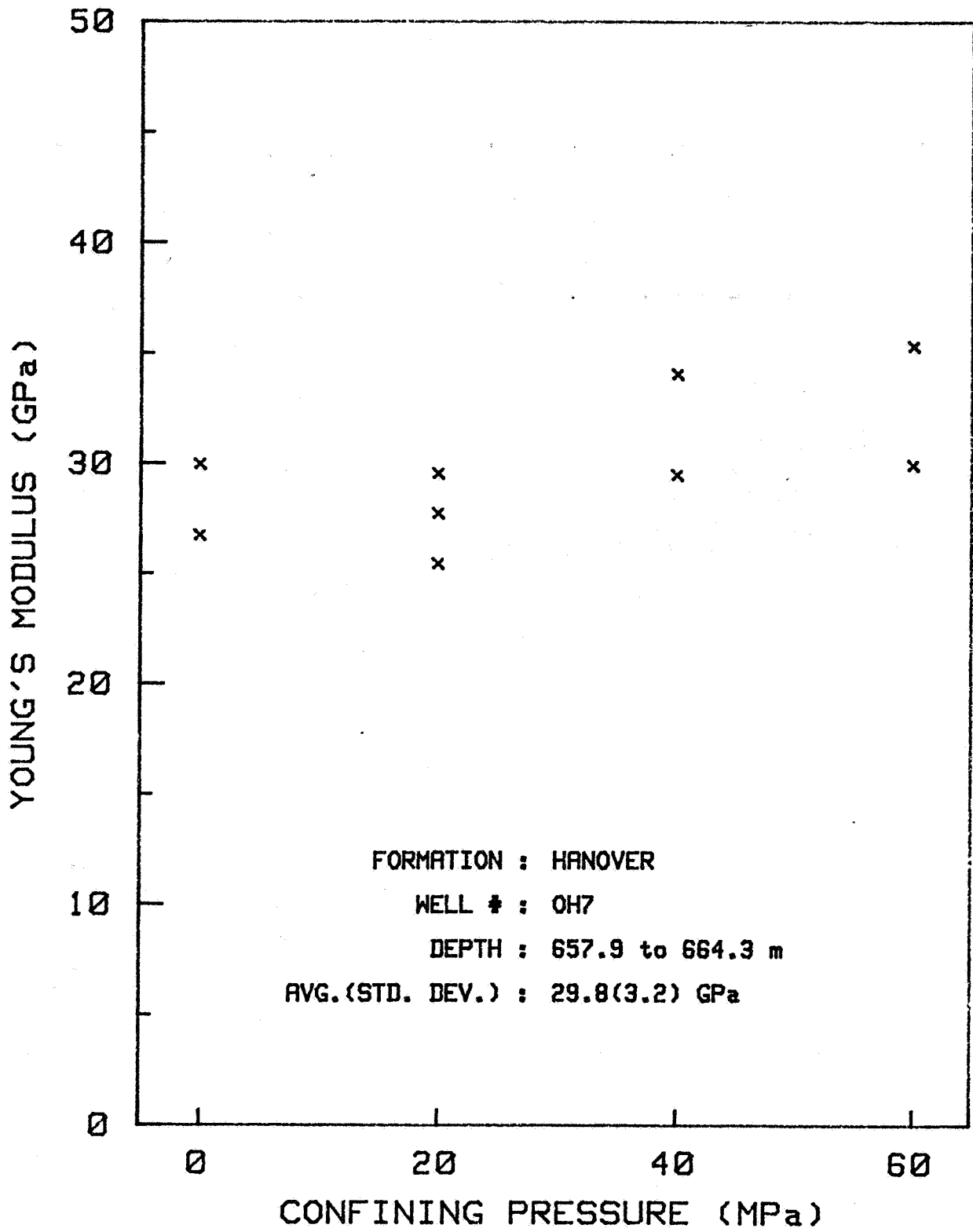


Figure 8F. Young's modulus as a function of confining pressure.

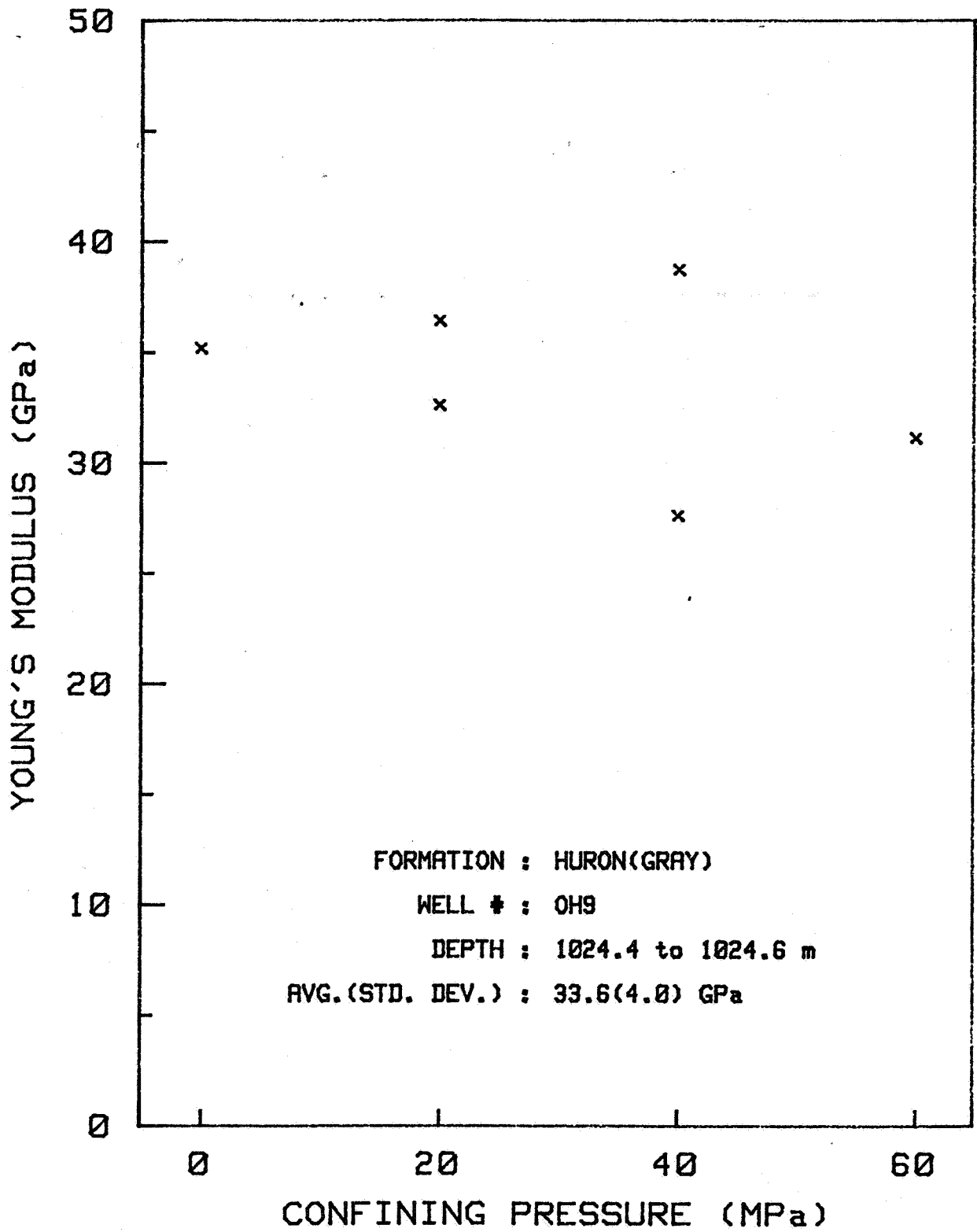


Figure 8G. Young's modulus as a function of confining pressure.

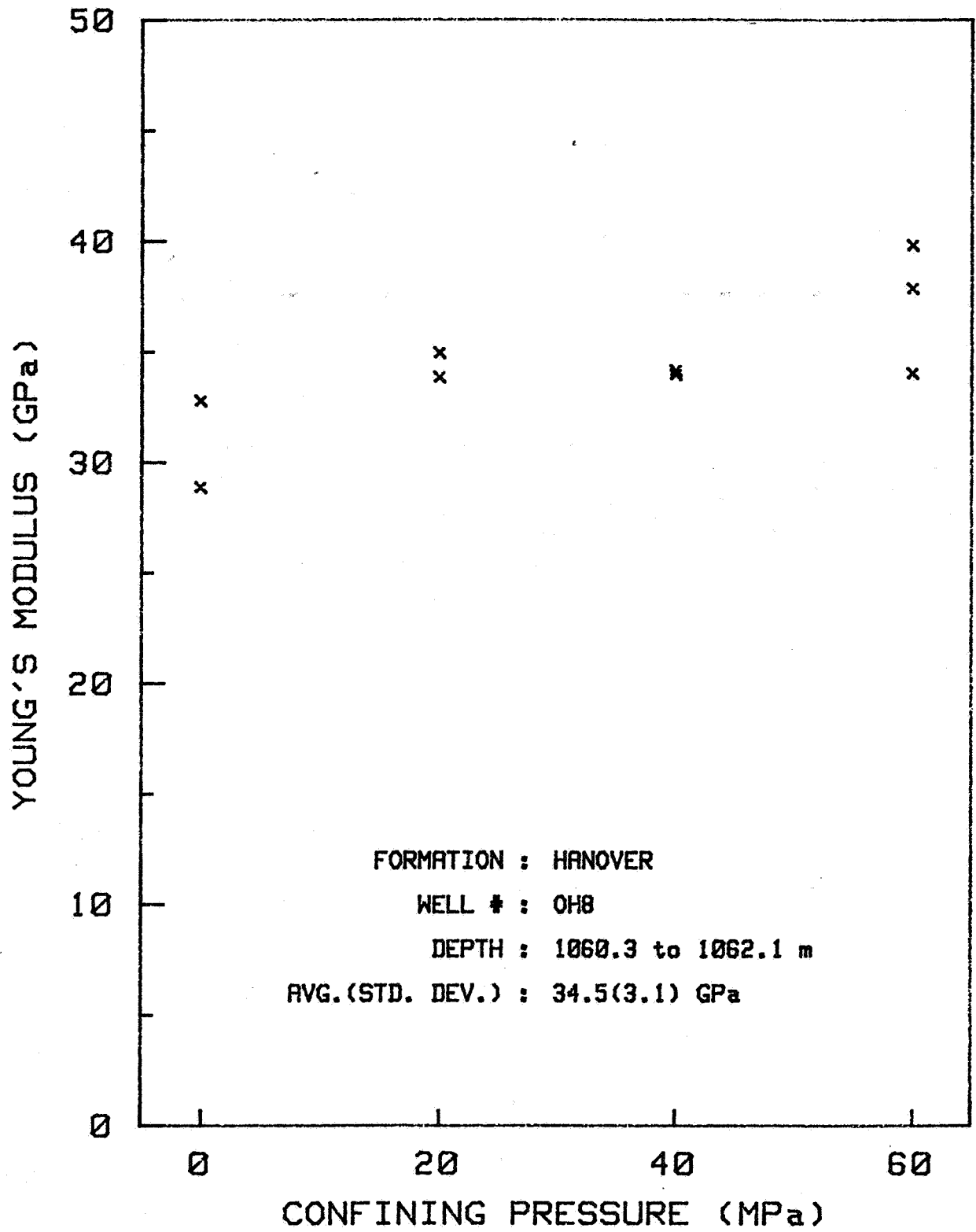


Figure 8H. Young's modulus as a function of confining pressure.

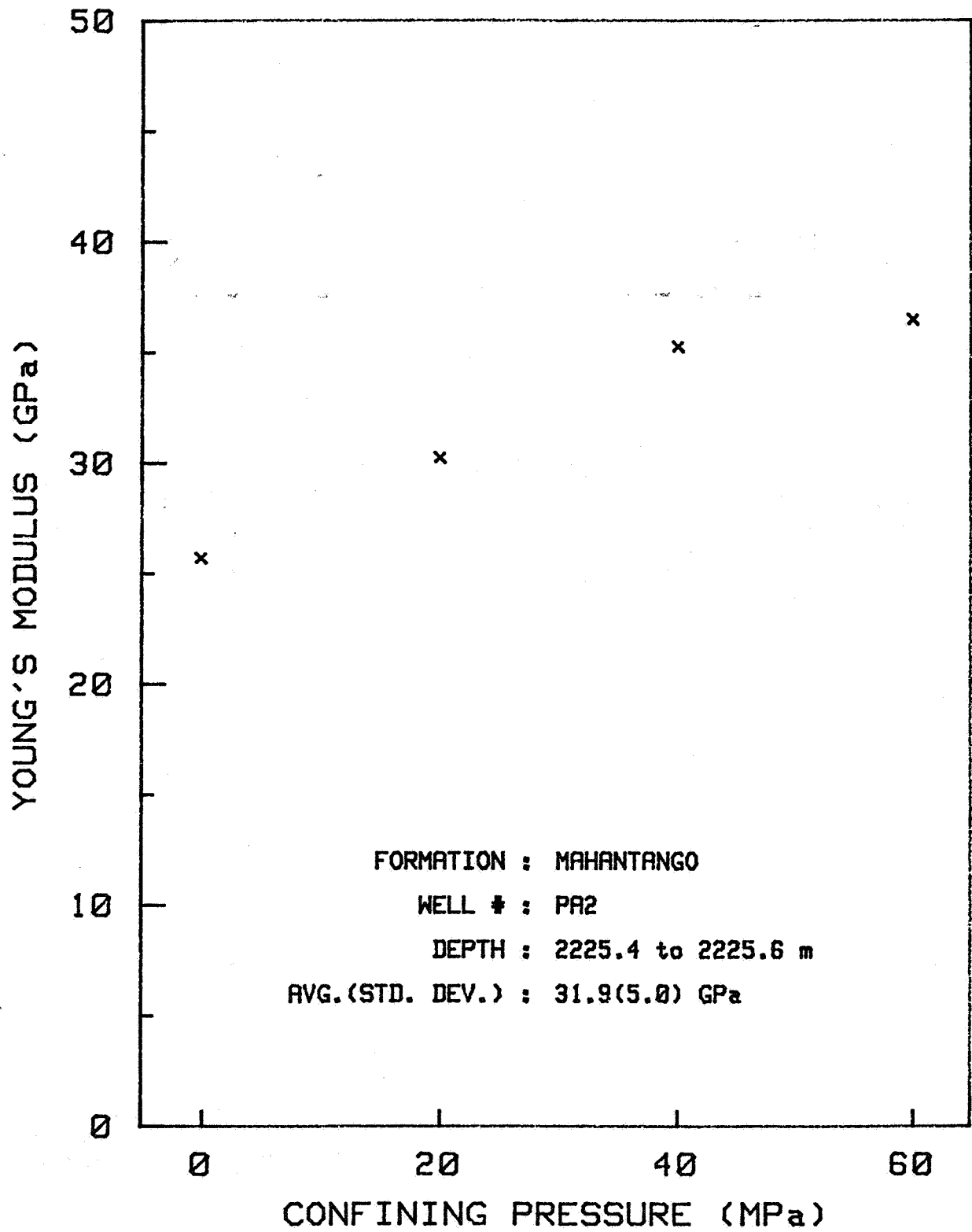


Figure 8I. Young's modulus as a function of confining pressure.

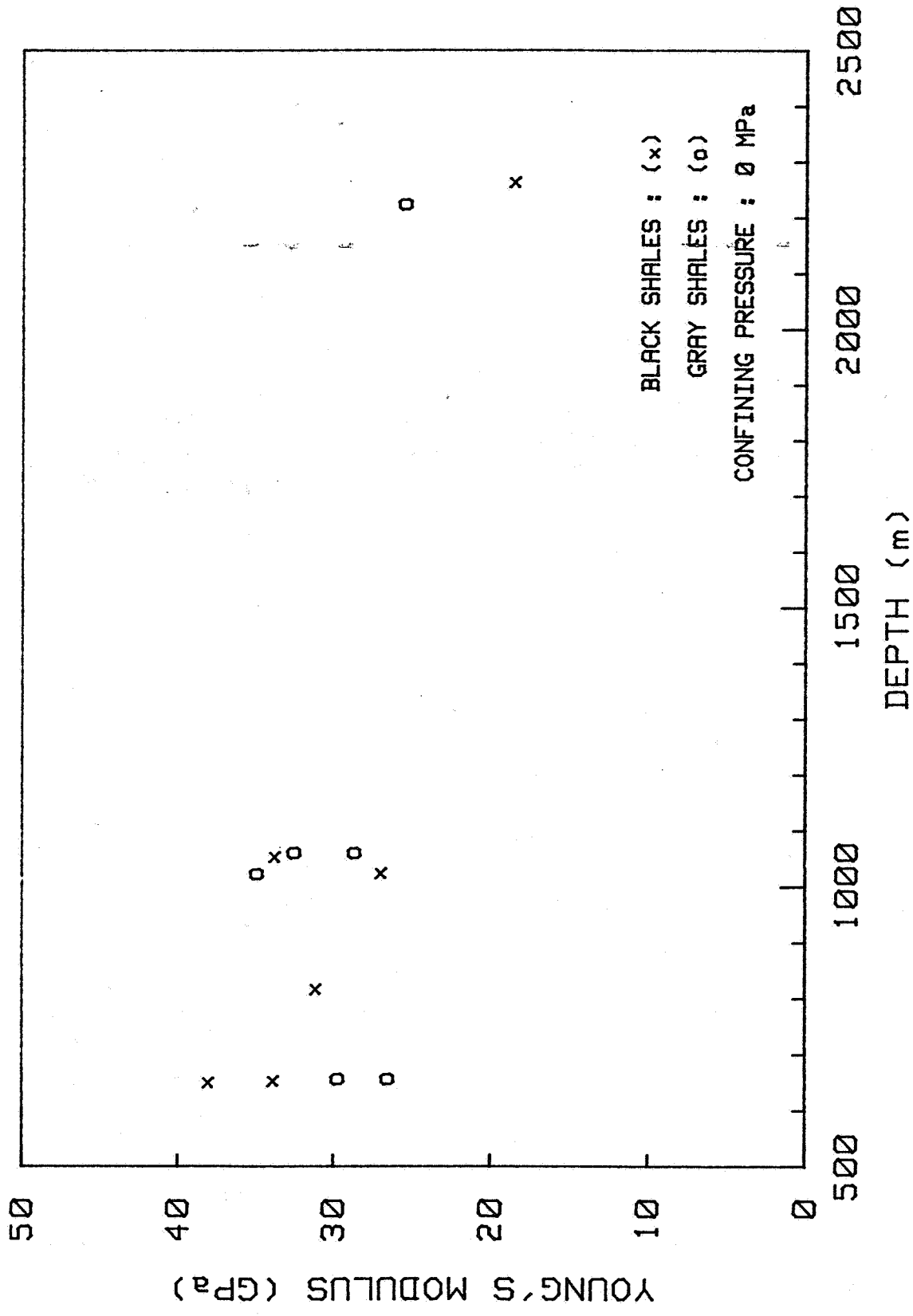


Figure 9A. Young's modulus as a function of depth.

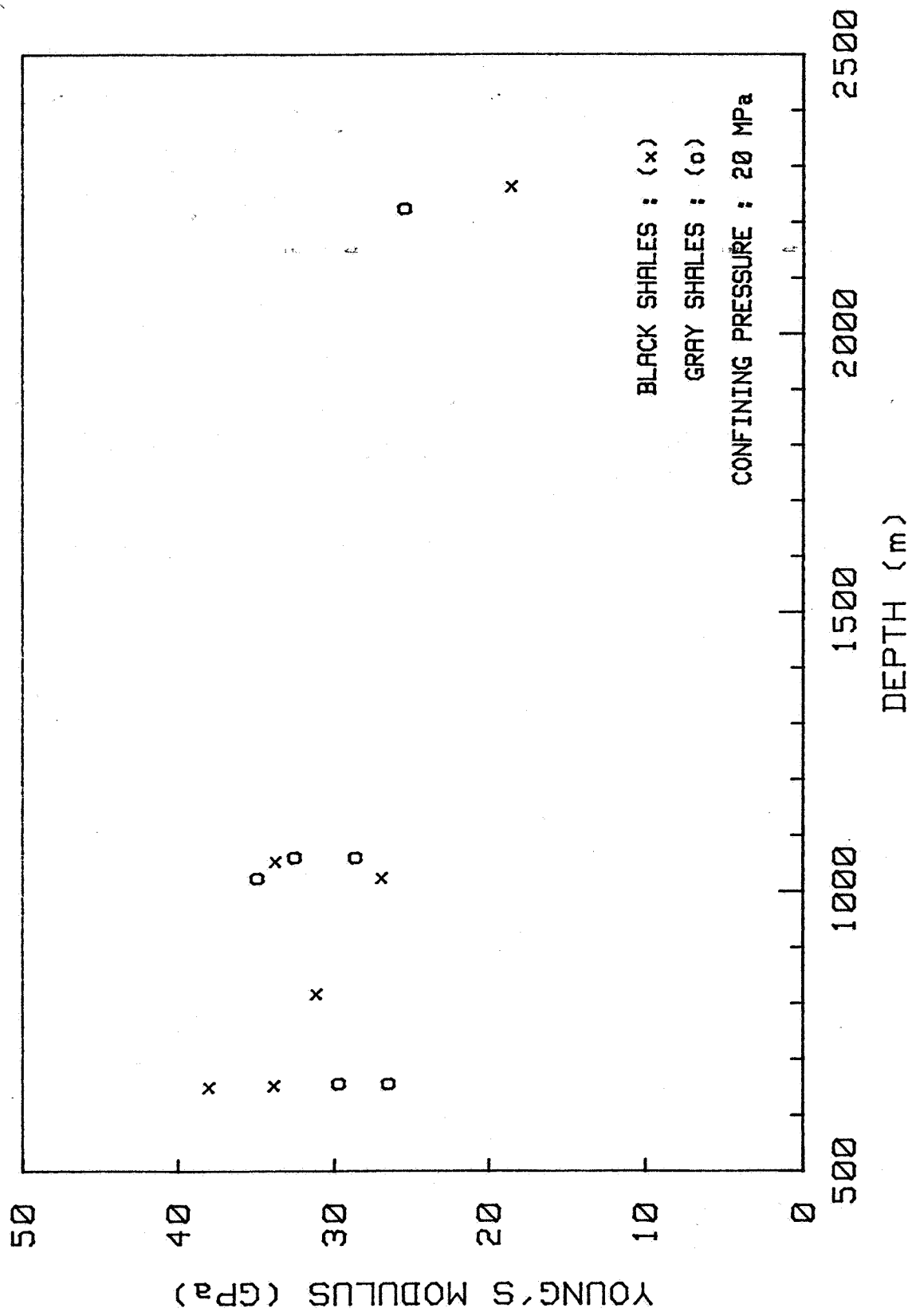


Figure 9B. Young's modulus as a function of depth.

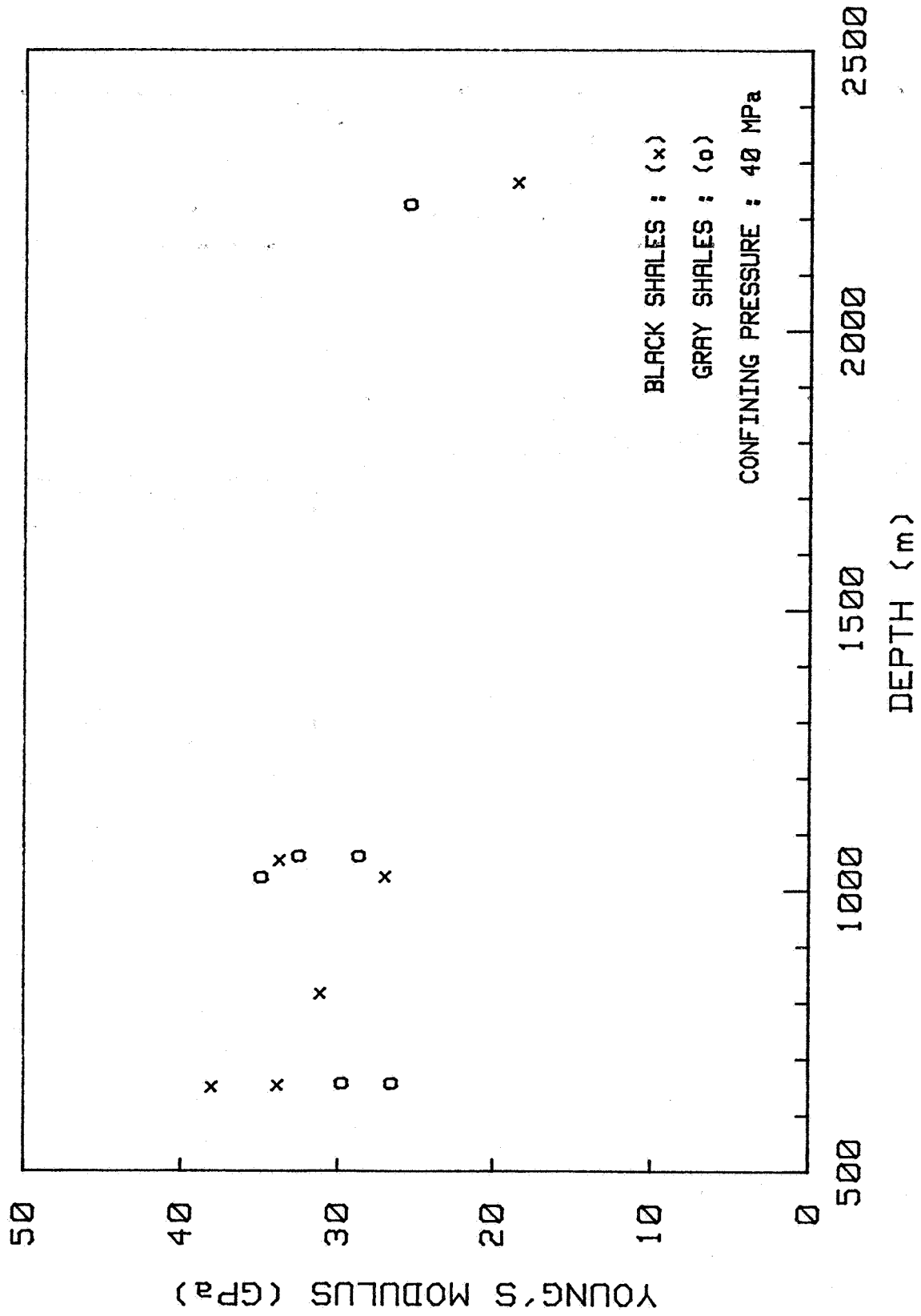


Figure 9C. Young's modulus as a function of depth.

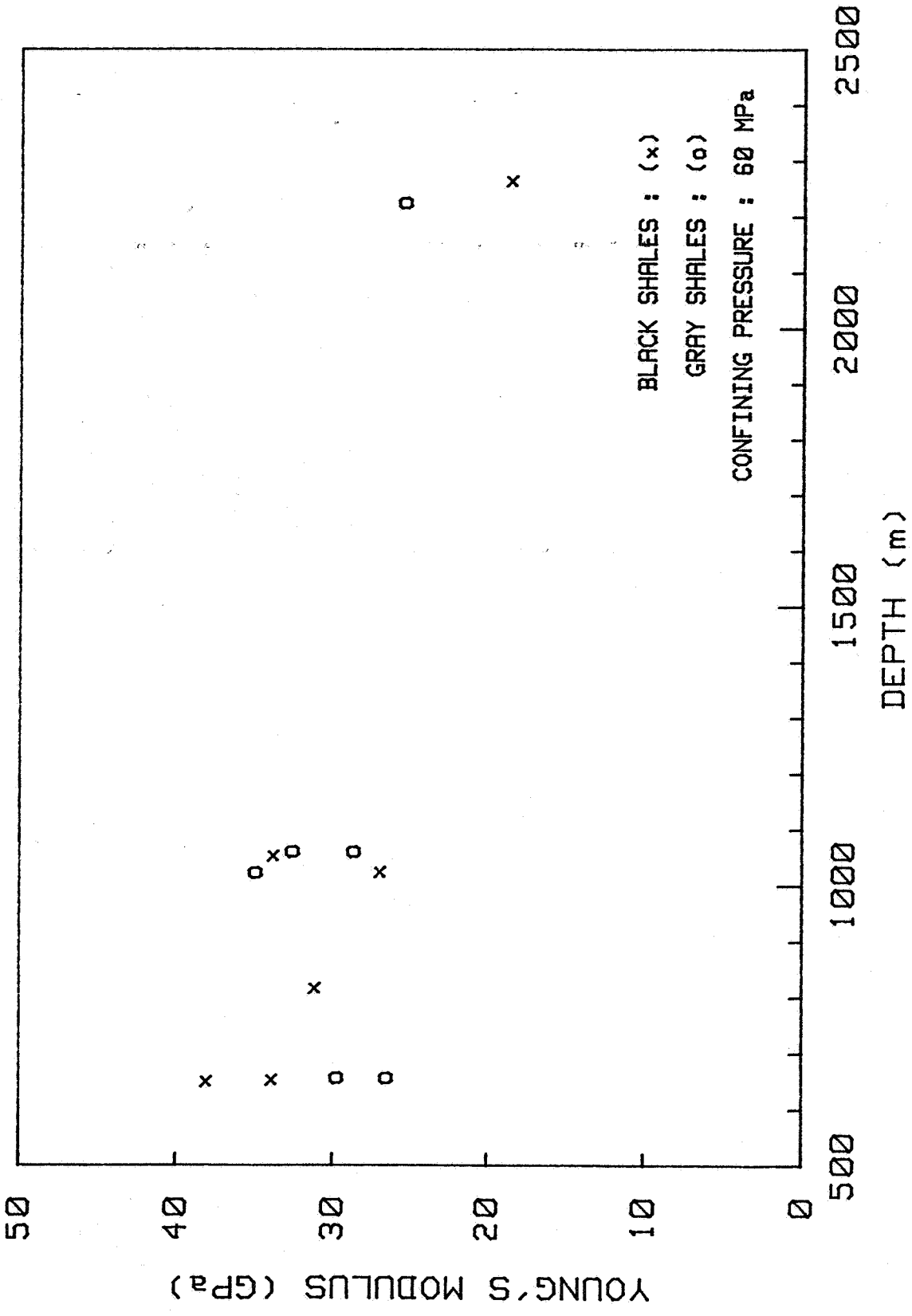


Figure 9D. Young's modulus as a function of depth.

Table 3. Elastic constants for Devonian shale from WV3, Lincoln County, West Virginia.

| Stratigraphic Unit | Depth (m) | Confining Pressure (MPa) | Young's Modulus (GPa) |           | Poisson's Ratio |           |
|--------------------|-----------|--------------------------|-----------------------|-----------|-----------------|-----------|
|                    |           |                          | Compression           | Extension | Compression     | Extension |
| Upper Gray Shale   | 909       | 20.6                     | 29.5                  | 21.7      | 0.21            | 0.17      |
|                    |           |                          | ±3.6                  | ±1.7      | ±0.09           | ±0.09     |
| Middle Brown Shale | 1050      | 23.8                     | 33.0                  | 24.8      | 0.20            | 0.18      |
|                    |           |                          | ±2.8                  | ±2.5      | ±0.03           | ±0.03     |
| Lower Gray Shale   | 1165      | 26.4                     | 33.8                  | 20.7      | 0.25            | 0.20      |
|                    |           |                          | ±11.4                 | ±1.0      | ±0.09           | ±0.03     |
| Lower Brown Shale  | 1218      | 27.6                     | 55.2                  | 24.8      | 0.37            | 0.20      |
|                    |           |                          | ±3.5                  | ±2.8      | ±0.08           | ±0.00     |

elastic constants found is a study by Cremean et al., (1979) of three wells in Lincoln County, West Virginia. The average value of Young's modulus for Devonian shale from these wells is 34.1 GPa, again within the range of values already given.

Compressive strengths show some trends with respect to a contrast in black and gray shale behavior. Both ultimate and yield strengths are plotted as a function of confining pressure in Figures 10A through 10I. With the exception of the last figure, they are arranged in black/gray pairs from each of four wells.

First, for three of the four pairs gray shales tend to be stronger (Figures 10C, 10D, 10E, 10F, 10G, and 10H) with the Hanover/Huron pairs from OH7 being the one exception (Figures 10A and 10B). This is also apparent in the average ultimate strengths plotted in Figure 11. The tendency for gray shales to be stronger than black shales is supported by earlier tests run on core from WV3 (Hanson et al., 1976a, 1976b). As seen in Figures 12 and 13 the one gray zone tested was stronger than the two black zones.

Second, for three of four pairs yielding begins at a lower confining pressure for black shales than for gray shales (Figures 10A, 10B, 10E, 10F, 10G, and 10H). The one exception is the Huron/Hanover pair (Figures 10C and 10D), and even here the Hanover exhibits only very slight yielding at 40 MPa confining pressure in one of two tests (Figure 10D) whereas the Huron shows no yielding at 40 MPa (Figure 10C).

Yielding as defined in this report is an indication of relative ductility because ductility is the ability to undergo permanent deformation without fracture. The more permanent deformation before a rock breaks, the more ductile it is. The fact that yielding tends to occur at lower confining pressures in black shales suggests that the black shales pass through a brittle-ductile transition at a lower mean stress. Ductility also seems to increase with increasing confining pressure. This is reflected by the divergence of ultimate strength, which for these tests is the same as breaking strength, and yield strength at higher confining pressures (e.g., Figure 10A). This trend is again

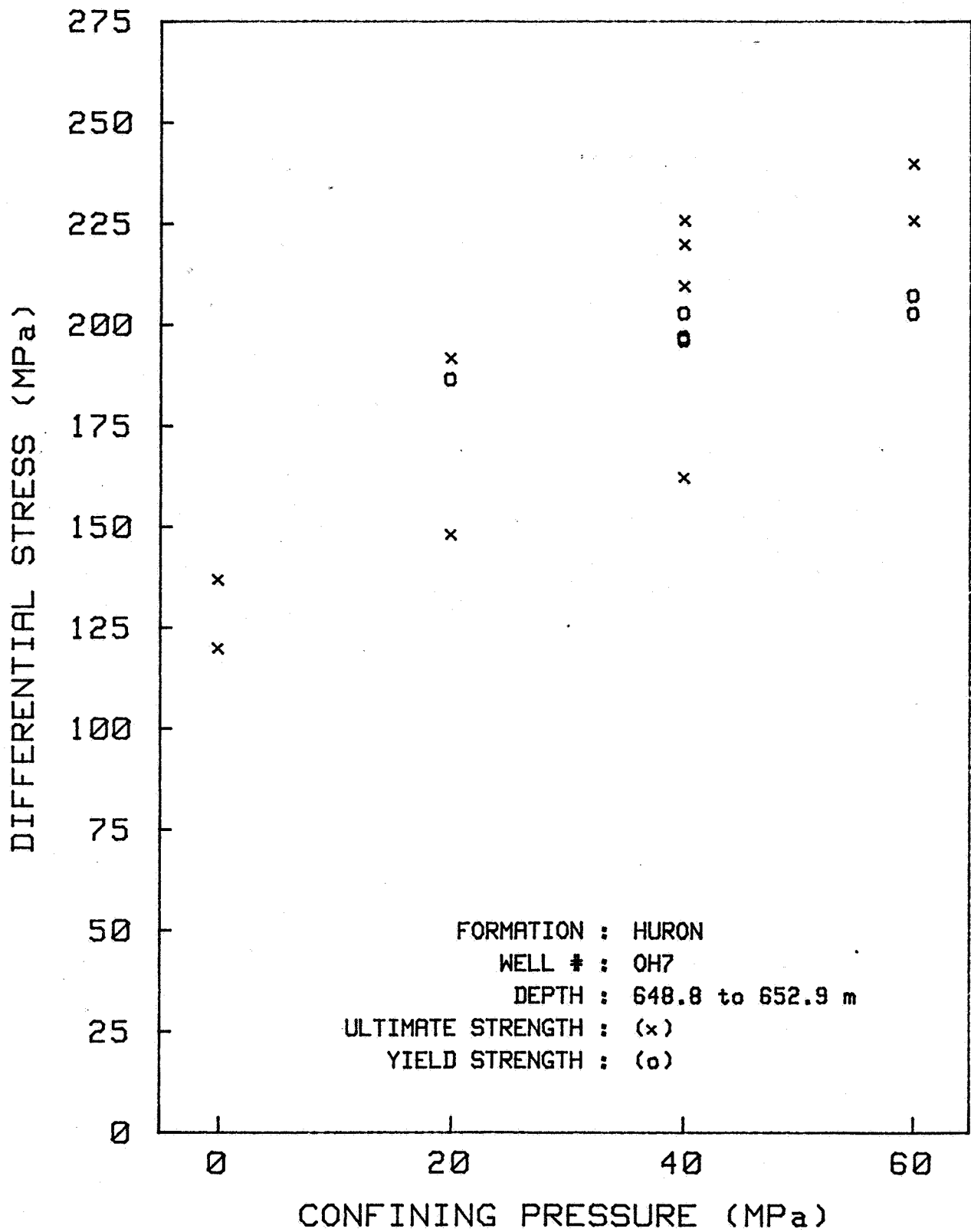


Figure 10A. Strength as a function of confining pressure.

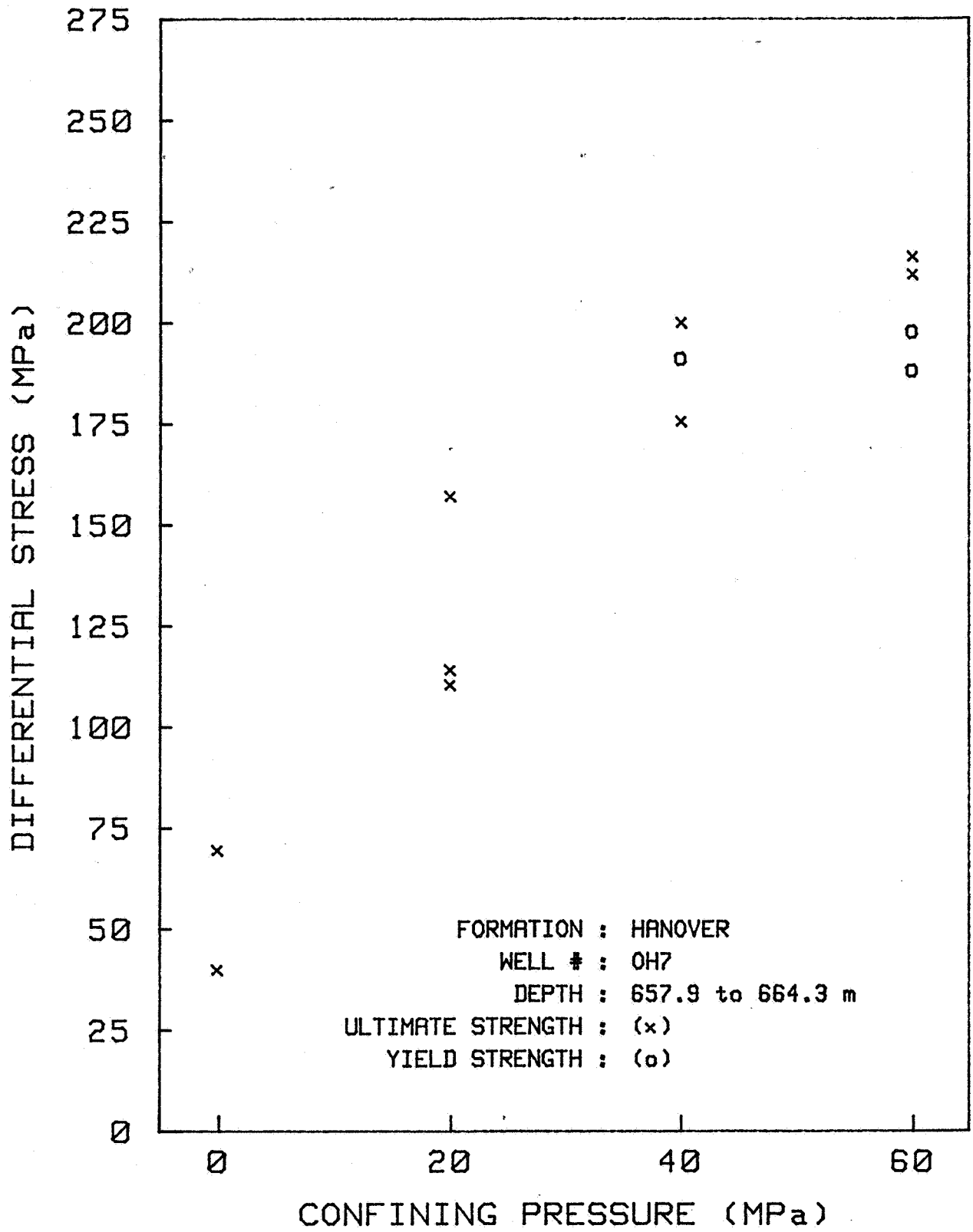


Figure 10B. Strength as a function of confining pressure.

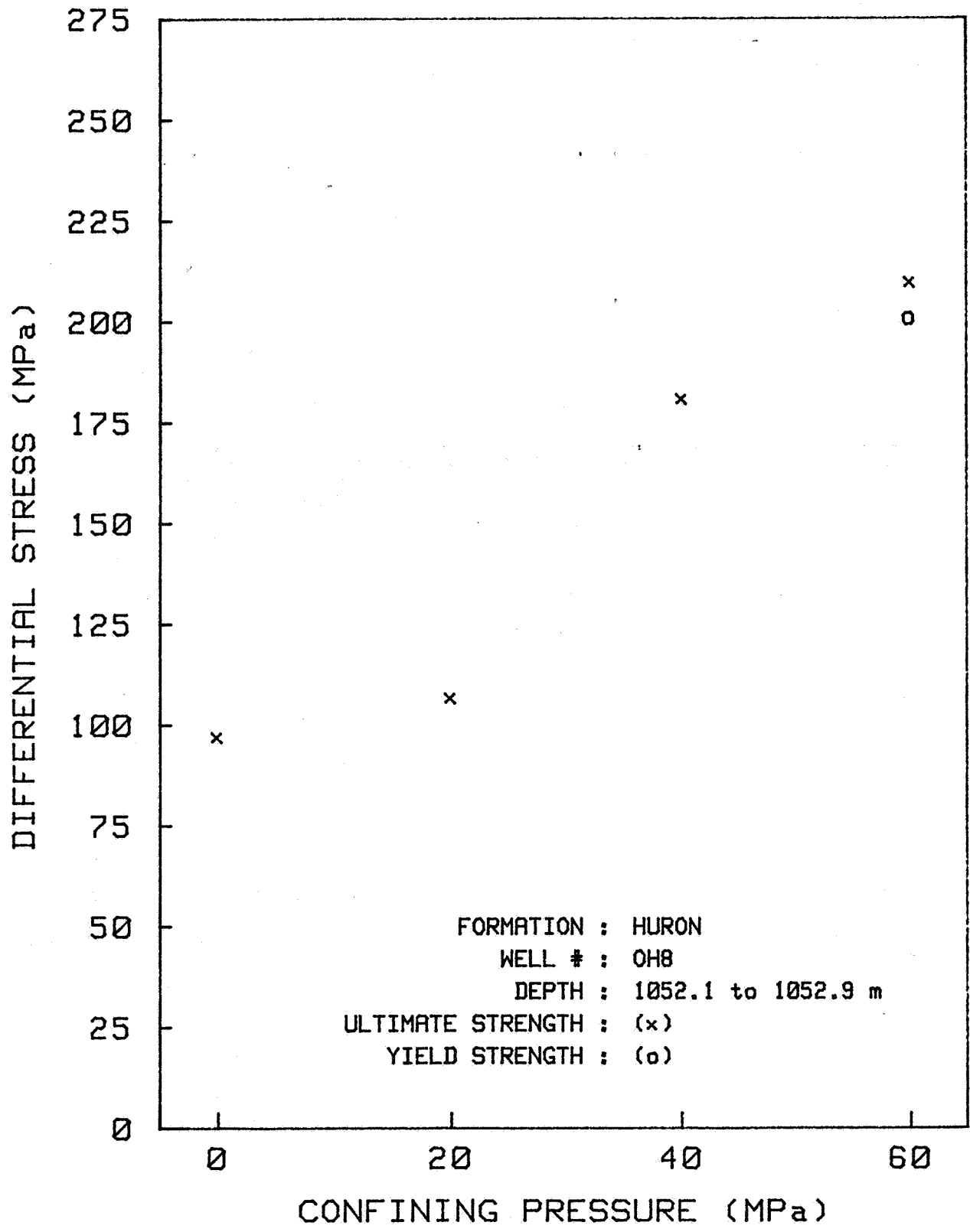


Figure 10C. Strength as a function of confining pressure.

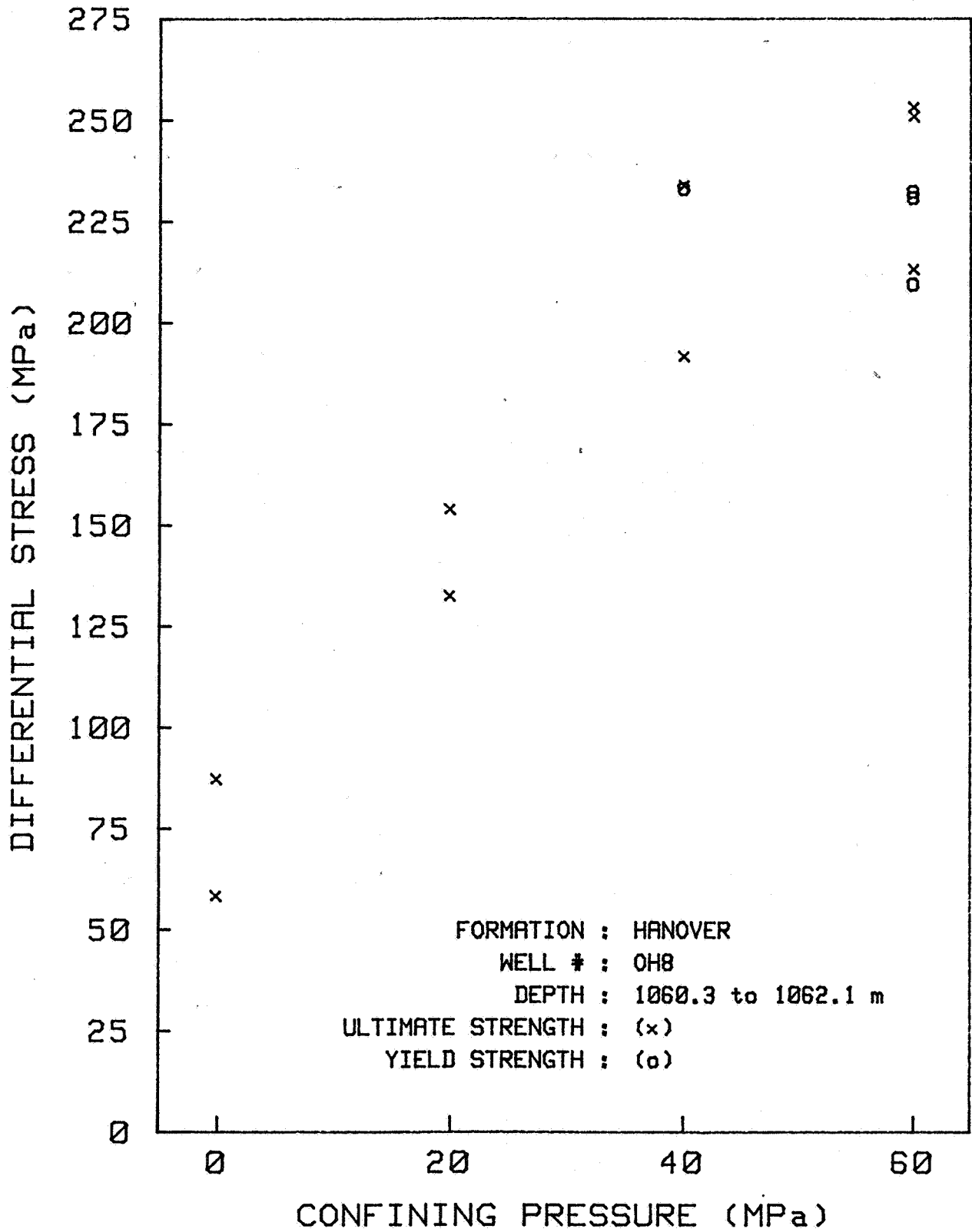


Figure 10D. Strength as a function of confining pressure.

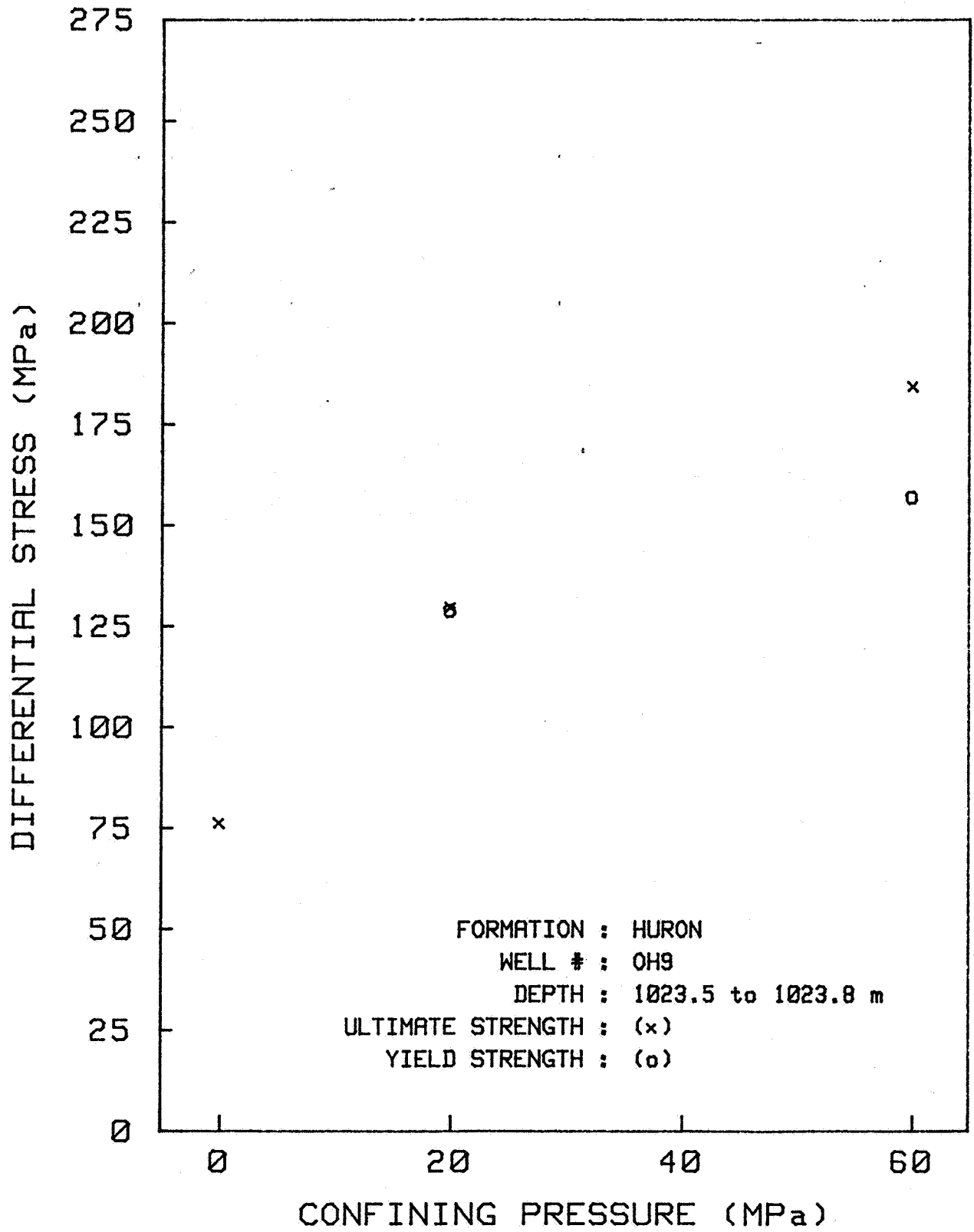


Figure 10E. Strength as a function of confining pressure.

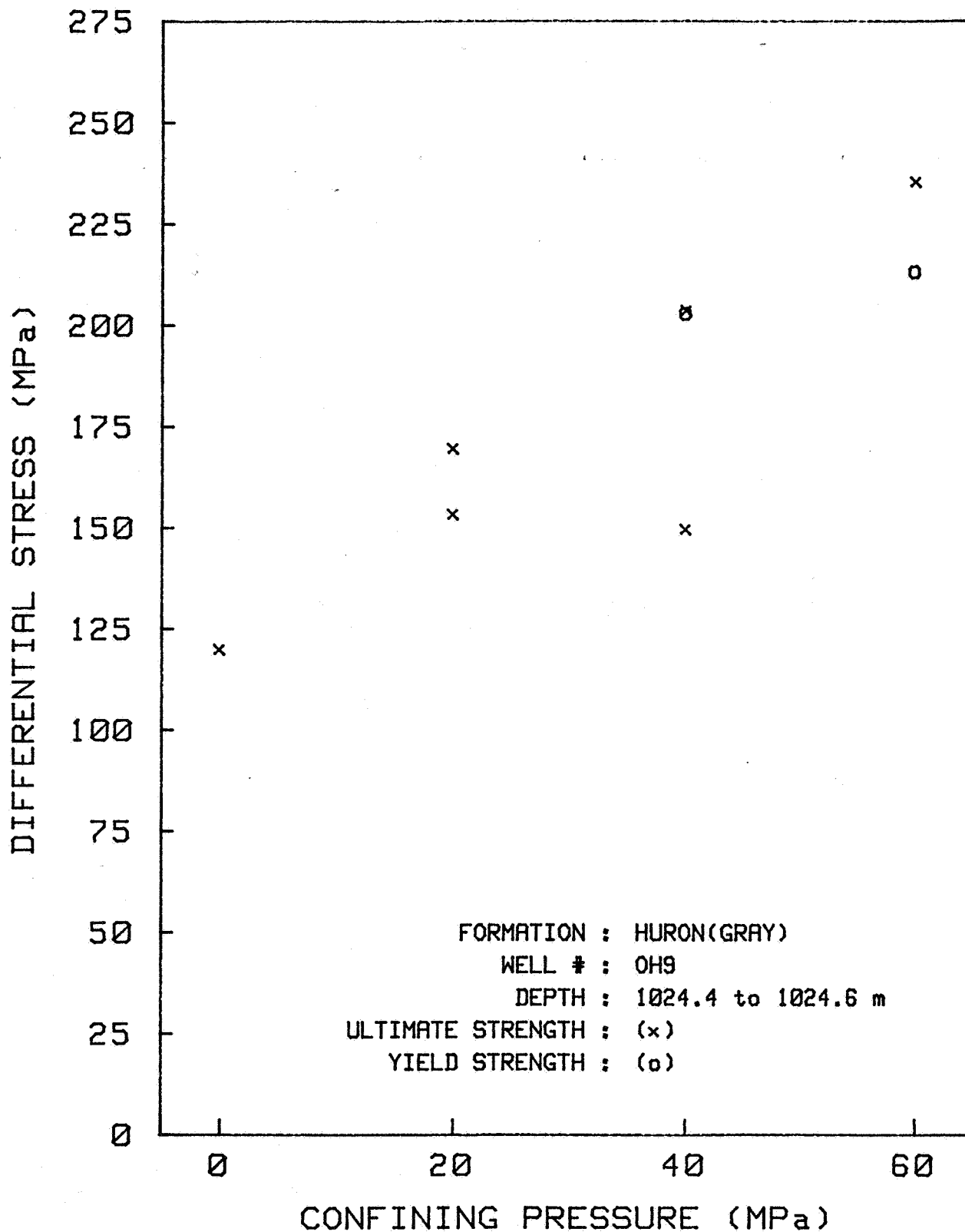


Figure 10F. Strength as a function of confining pressure.

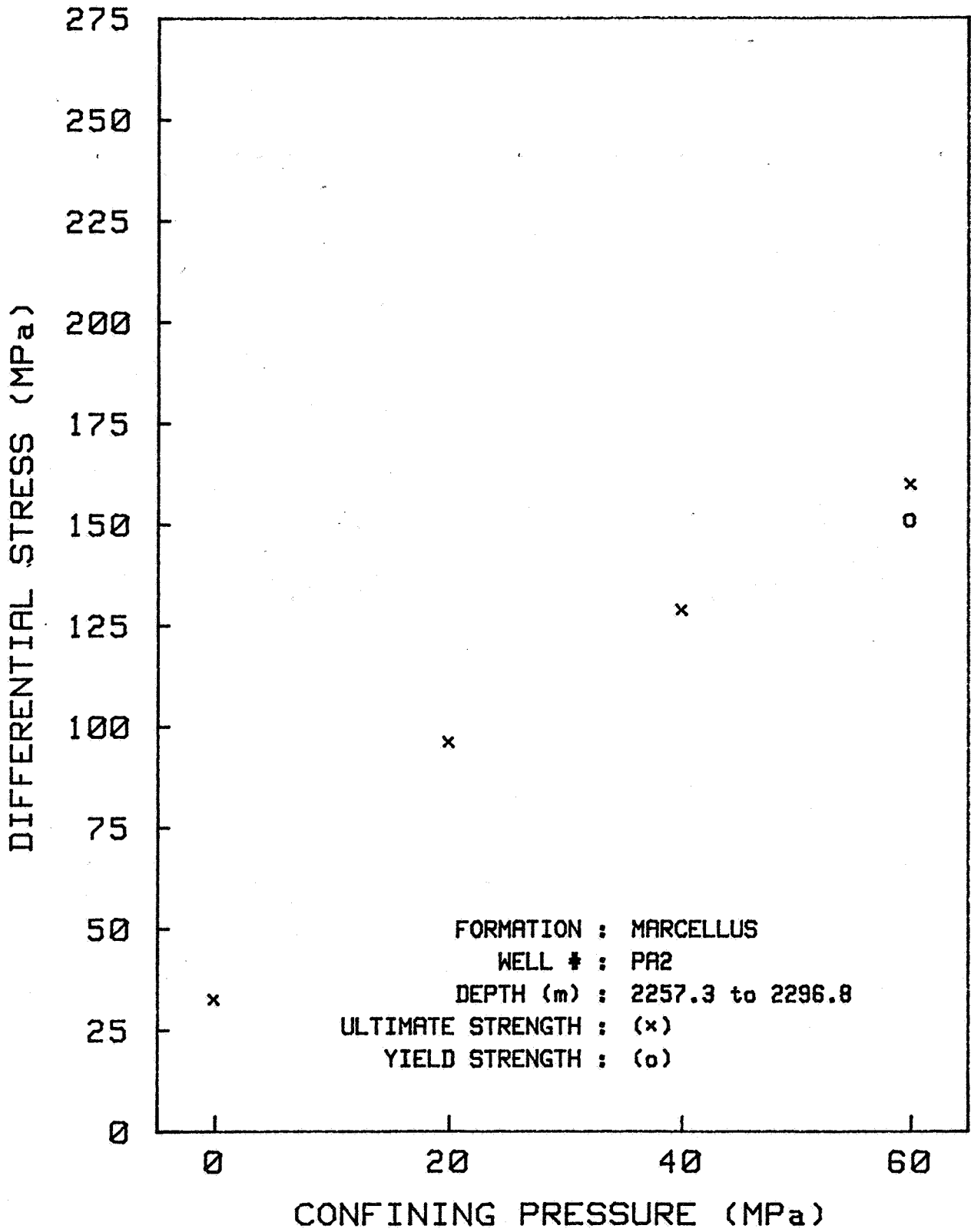


Figure 10G. Strength as a function of confining pressure.

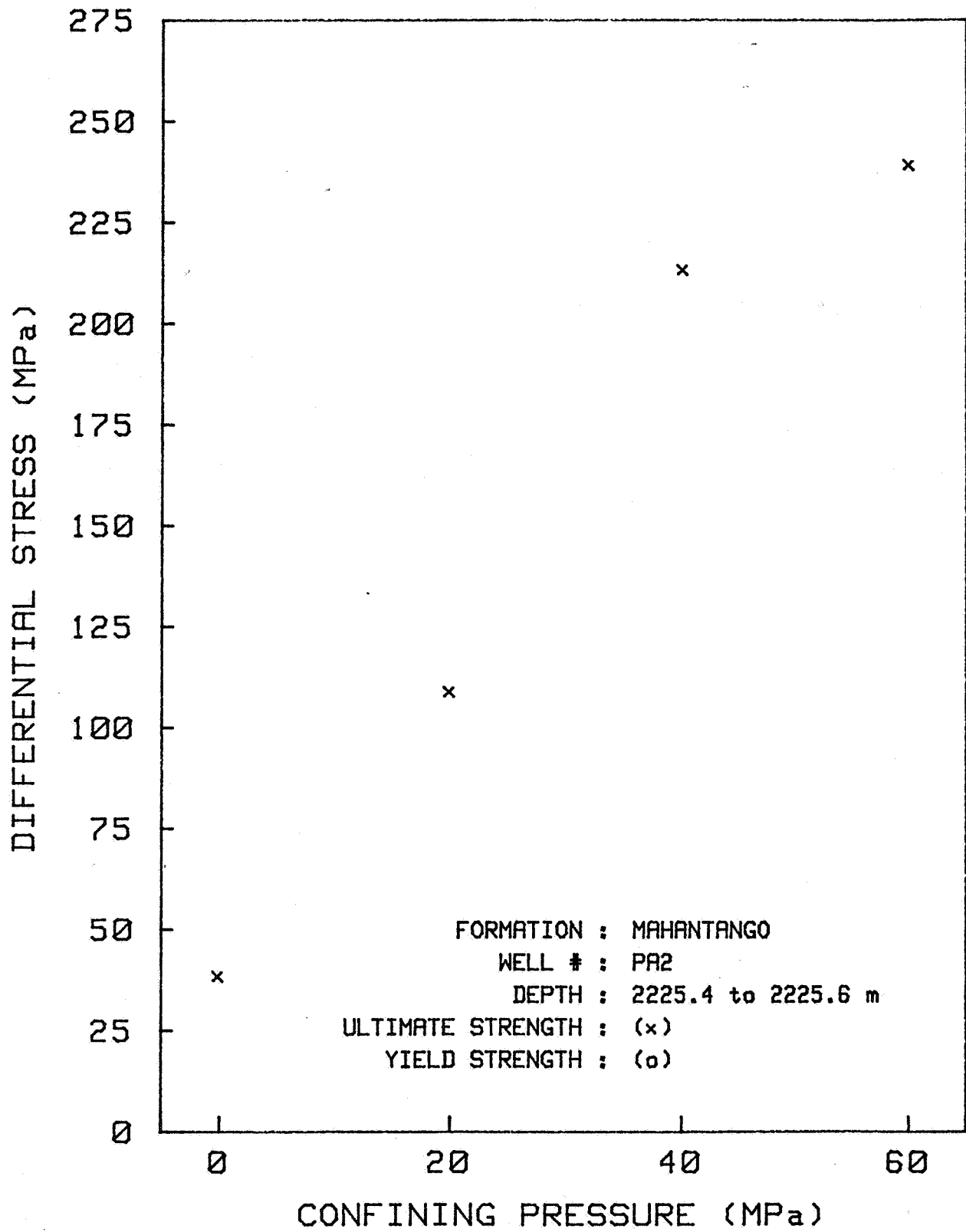


Figure 10H. Strength as a function of confining pressure.

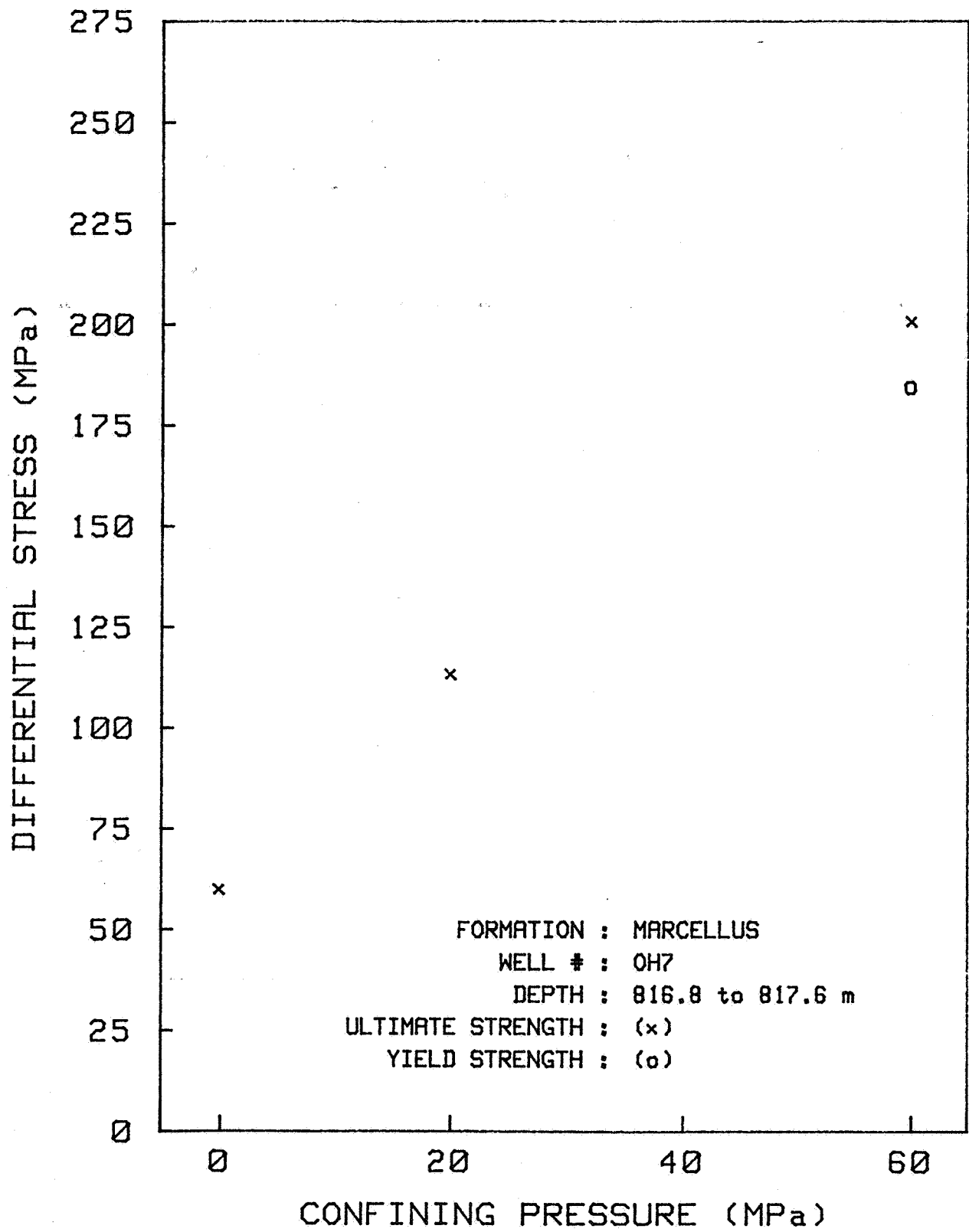


Figure 10I. Strength as a function of confining pressure.

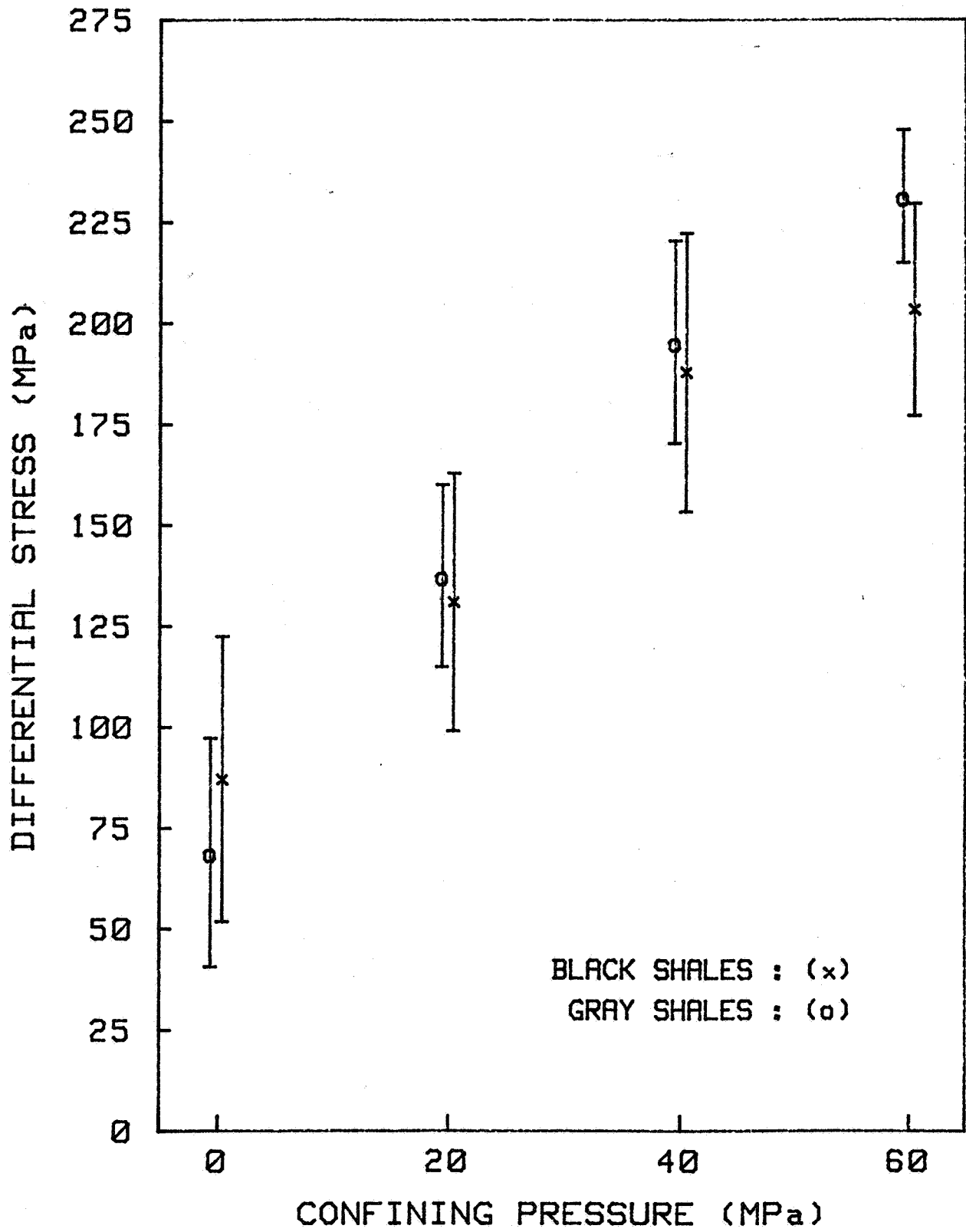


Figure 11. Average ultimate strengths of black and gray shales.

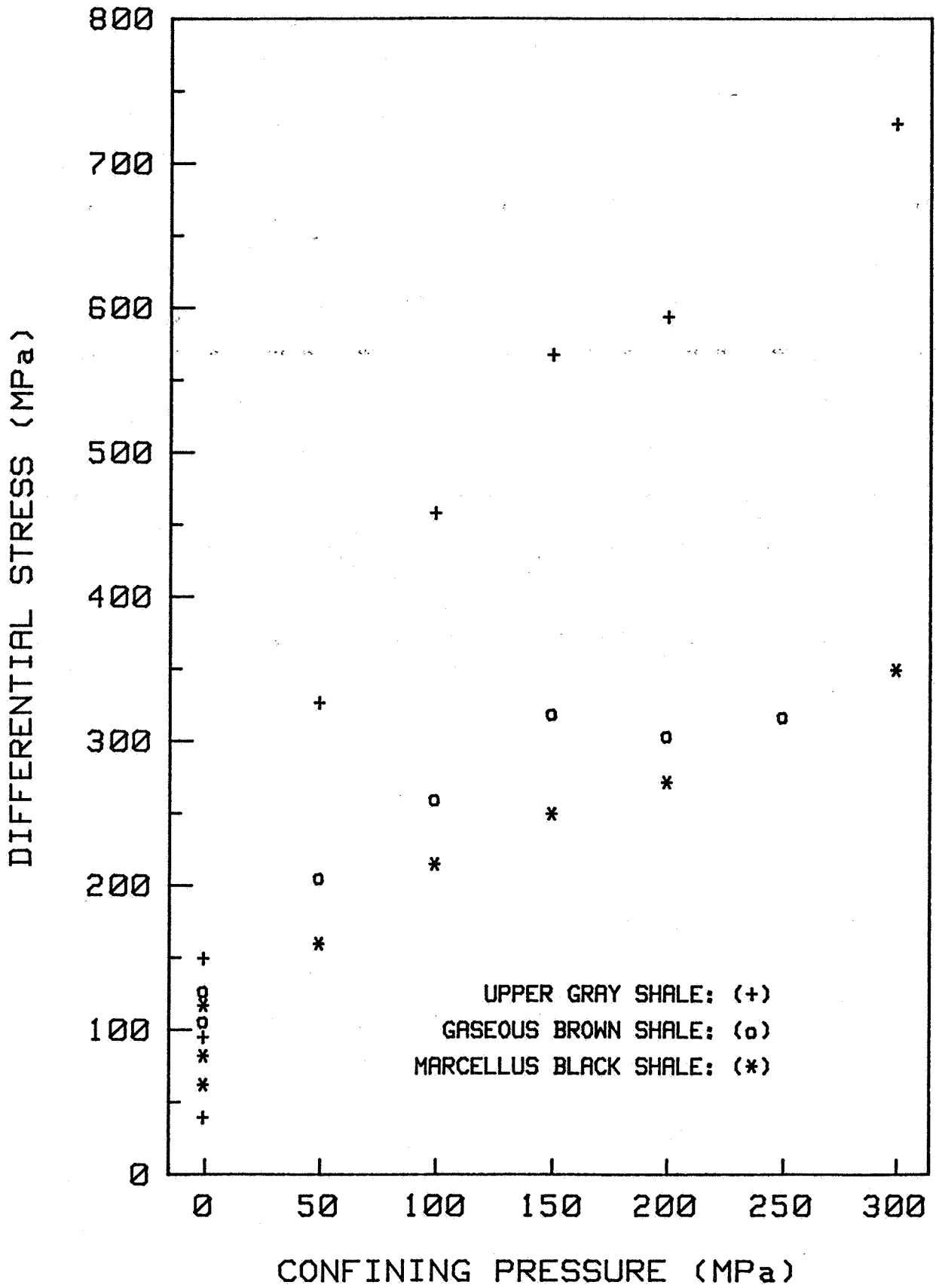


Figure 12. Strength of Devonian shales from WV3 loaded perpendicular to bedding.

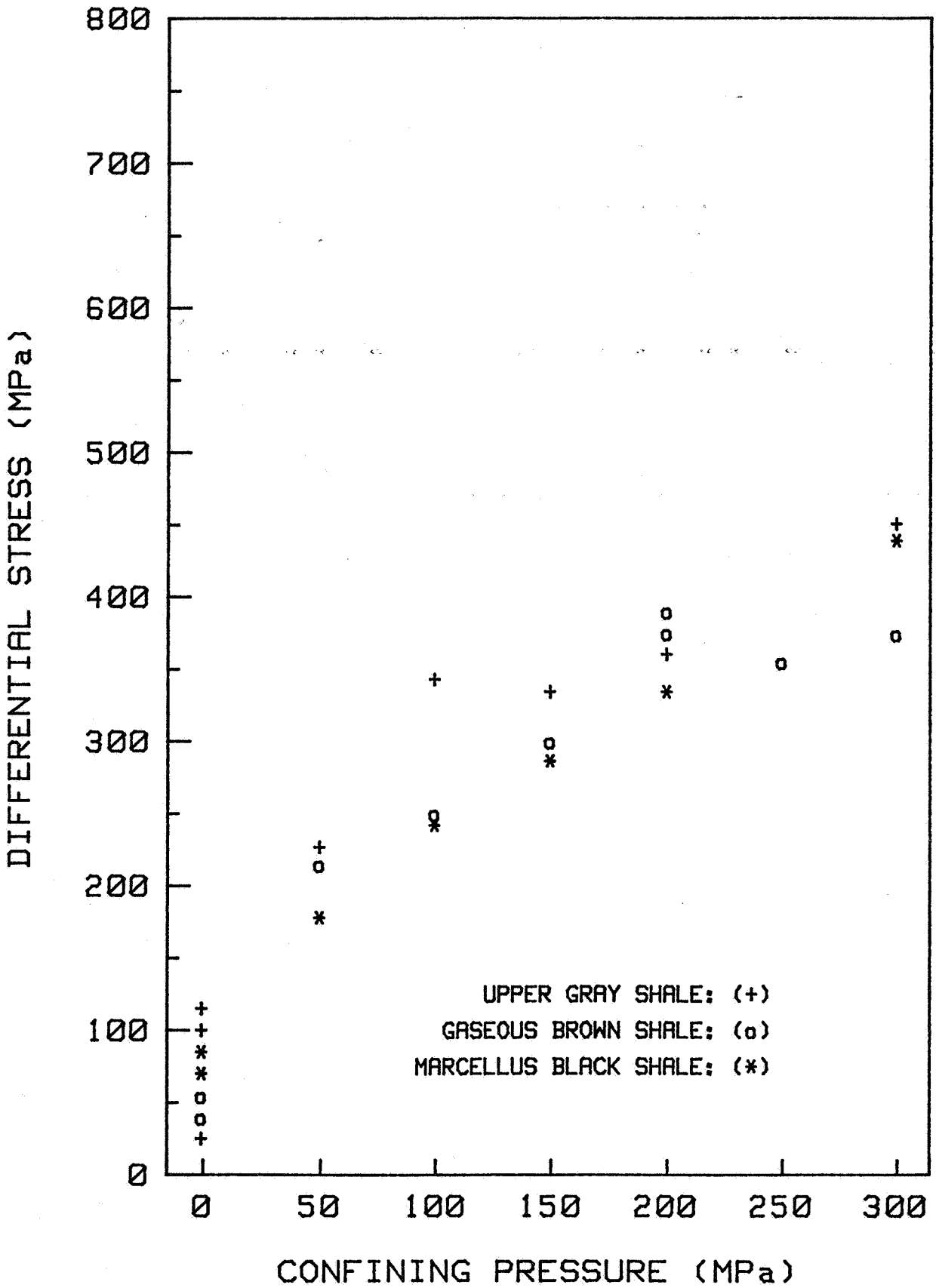


Figure 13. Strength of Devonian shales from WV3 loaded parallel to bedding.

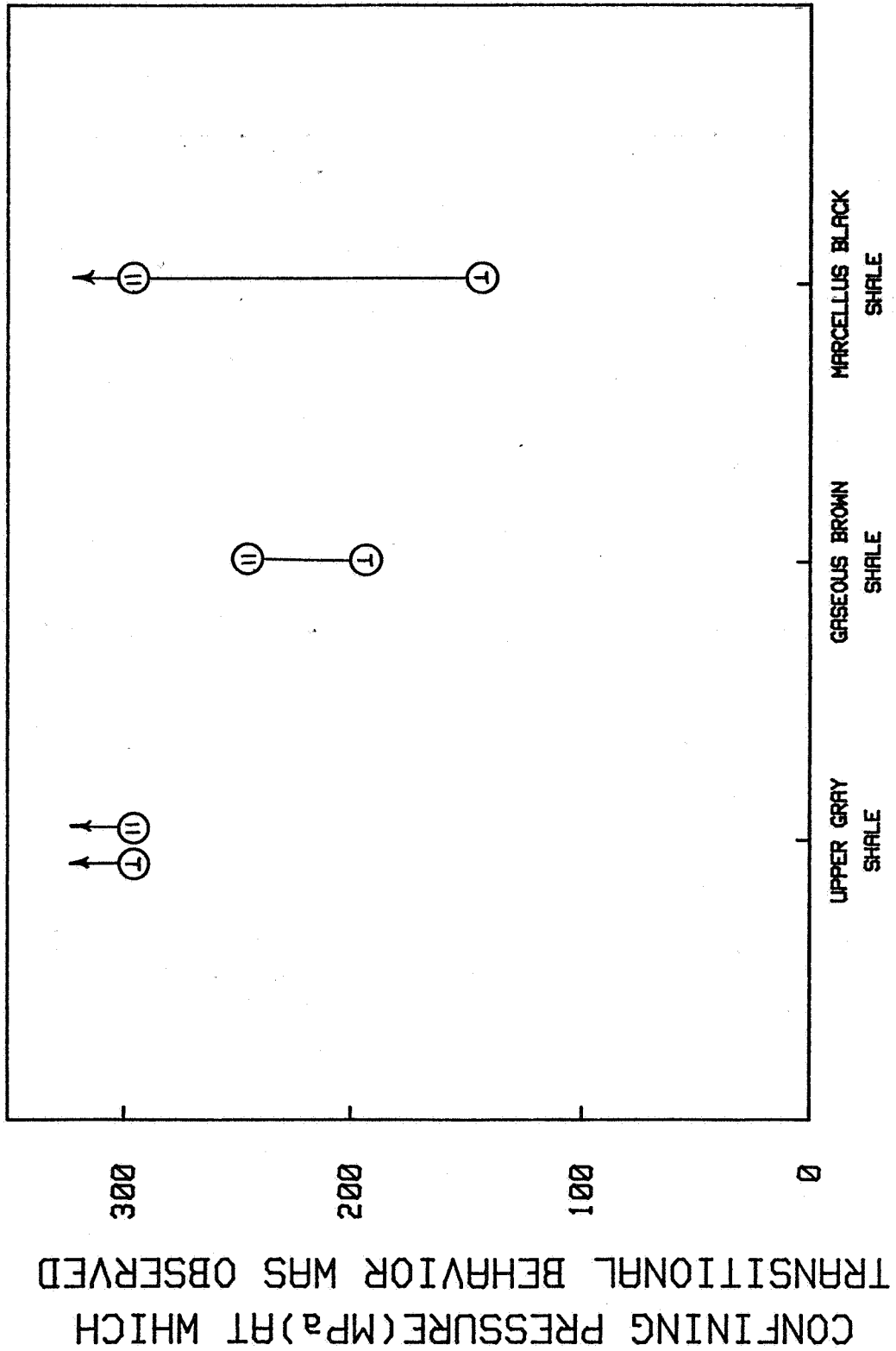
corroborated by tests on core from WV3 as shown in Figure 14 (Hanson et al., 1976a, 1976b).

## 2.2 Tensile Tests

Direct-pull tensile tests were run on specimens 3.8 cm (1.5 in) in diameter and approximately 7.6 cm (3.0 in) long. Loading was parallel to the bedding plane. Peak loads were measured for each test, and tensile strengths were calculated and recorded. The results are presented in Tables 4 and 5 and plotted in Figure 15. There are no obvious trends. One might say that there is a slight tendency for the gray shales to be stronger, but this is reversed for the core from OH7. It is also reversed for measurements made in a previous study (Hanson et al., 1976a, 1976b) on core from WV3, as shown in Table 6 where the gray shales tend to be weaker. Another generalization that can be made from this data is that tensile strength is lower when tension is applied perpendicular to the bedding planes. Additional tensile strength data from a previous study is shown in Table 7 (Miller and Johnson, 1979). Here tensile strength was measured at different orientations in the bedding plane, and there appears to be a slight but consistent variation of strength with orientation.

## 2.3 Fracture Energy Tests

Fracture energy tests were run on rods 1.27 cm (0.5 in) in diameter and 8 cm (~3 in) or more long. Stress to fracture the rock is applied by a four-point bending frame, and the fracture propagates perpendicular to the axis of the rod. To get stable crack growth the rod is cut so that the cross-section where the fracture propagates is wedge shaped. The crack starts at the point of the wedge and stably propagates across it. Stable fracture propagation allows direct correlation between the load-displacement curve for the machine and energy of fracture (Young and Smith, 1979). These curves are contained in Appendix B. The results of the tests are presented in Tables 8 and 9 and plotted in Figure 16.



SHALES IN ORDER OF DECREASING STRENGTH

Figure 14. Brittle-ductile transition for Devonian shales from WV3.

TABLE 4. RESULTS OF DIRECT-PULL TENSILE TESTS FOR BLACK SHALES.

| TEST # | WELL | FORMATION | DEPTH (M) | TENSILE STRENGTH (MPa) | AVG. (STD. DEV.) |
|--------|------|-----------|-----------|------------------------|------------------|
| TP-11  | OH7  | HURON     | 647.2     | 6.3                    | 5.1 ( .8)        |
| TP-26  | OH7  | HURON     | 647.3     | 5.2                    |                  |
| TP-25  | OH7  | HURON     | 647.8     | 5.6                    |                  |
| TP-8   | OH7  | HURON     | 650.4     | 4.3                    |                  |
| TP-13  | OH7  | HURON     | 651.1     | 4.1                    |                  |
| TP-24  | OH7  | MARCELLUS | 819.9     | 5.7                    | 9.0 ( 2.3)       |
| TP-16  | OH7  | MARCELLUS | 821.7     | 8.2                    |                  |
| TP-29  | OH7  | MARCELLUS | 822.0     | 12.4                   |                  |
| TP-9   | OH7  | MARCELLUS | 822.7     | 8.0                    |                  |
| TP-12  | OH7  | MARCELLUS | 821.8     | 10.8                   |                  |
| TP-22  | OH8  | HURON     | 801.0     | 3.0                    | 7.6 ( 3.0)       |
| TP-23  | OH8  | HURON     | 801.0     | 7.7                    |                  |
| TP-36  | OH8  | HURON     | 1051.0    | 5.9                    |                  |
| TP-19  | OH8  | HURON     | 1052.7    | 11.6                   |                  |
| TP-20  | OH8  | HURON     | 1053.1    | 9.9                    |                  |
| TP-34  | PA2  | MARCELLUS | 2258.6    | 2.0                    | 1.0 ( .6)        |
| TP-31  | PA2  | MARCELLUS | 2258.6    | 1.3                    |                  |
| TP-32  | PA2  | MARCELLUS | 2264.7    | .5                     |                  |
| TP-35  | PA2  | MARCELLUS | 2264.8    | .7                     |                  |
| TP-33  | PA2  | MARCELLUS | 2266.0    | .2                     |                  |

TABLE 5. RESULTS OF DIRECT-PULL TENSILE TESTS FOR GRAY SHALES.

| TEST # | WELL | FORMATION  | DEPTH<br>(M) | TENSILE STRENGTH<br>(MPa) | AVG. (STD. DEV.) |
|--------|------|------------|--------------|---------------------------|------------------|
| TP-3   | OH7  | HANOVER    | 661.8        | 4.9                       |                  |
| TP-17  | OH7  | HANOVER    | 662.0        | 4.3                       |                  |
| TP-22  | OH7  | HANOVER    | 664.3        | 3.3                       | 4.2 ( .6)        |
| TP-7   | OH8  | HANOVER    | 1060.4       | 12.6                      |                  |
| TP-10  | OH8  | HANOVER    | 1061.1       | 11.4                      |                  |
| TP-18  | OH8  | HANOVER    | 1061.4       | 7.3                       |                  |
| TP-30  | OH8  | HANOVER    | 1061.8       | 6.3                       |                  |
| TP-5   | PA2  | MAHANTANGO | 2221.6       | 11.7                      | 9.4 ( 2.7)       |
| TP-15  | PA2  | MAHANTANGO | 2221.6       | 8.1                       |                  |
| TP-6   | PA2  | MAHANTANGO | 2227.8       | 5.4                       |                  |
| TP-21  | PA2  | MAHANTANGO | 2228.4       | 7.1                       |                  |
| TP-14  | PA2  | MAHANTANGO | 2228.5       | 4.4                       | 7.3 ( 2.5)       |

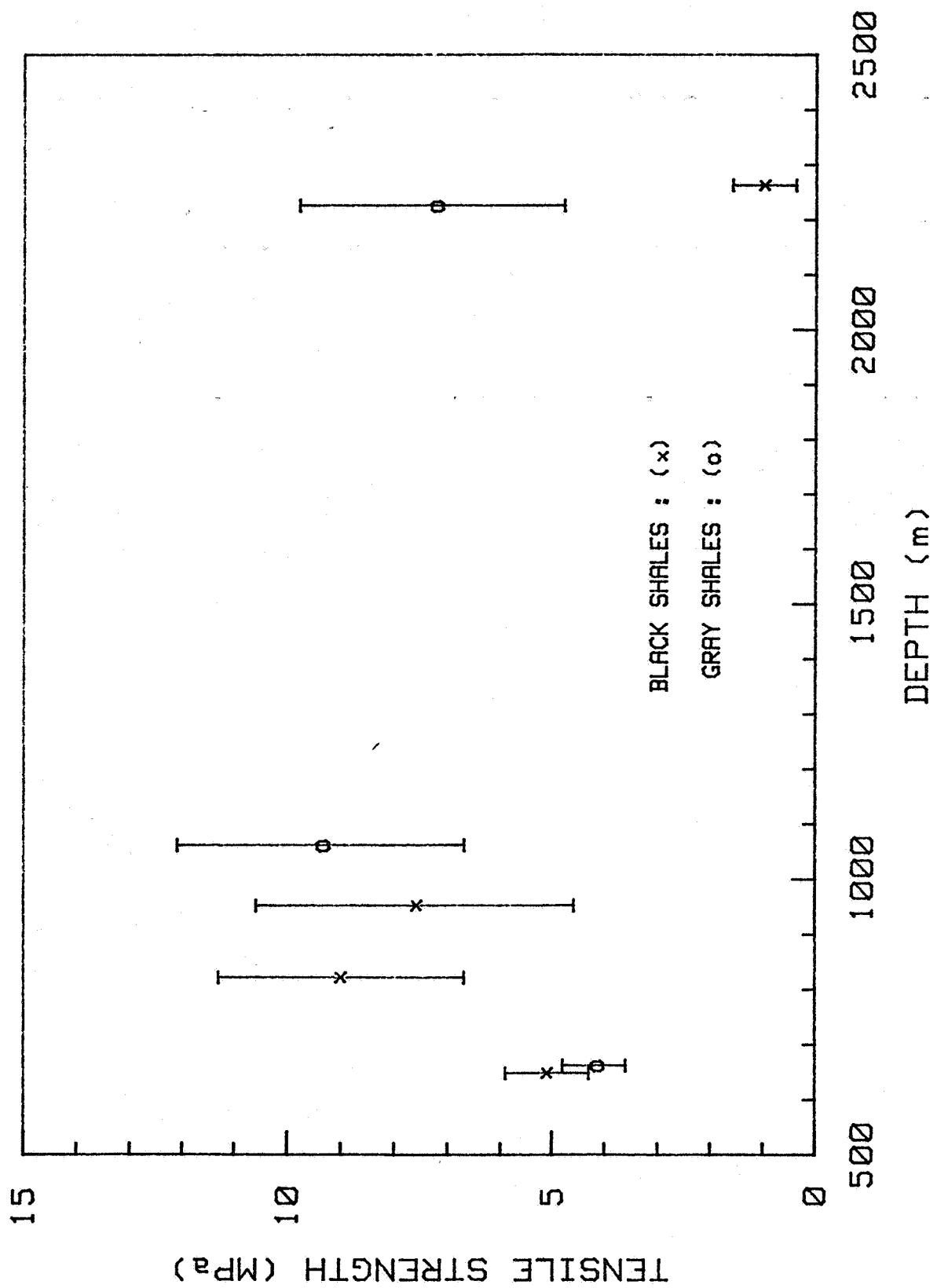


Figure 15. Average tensile strengths as a function of depth.

Table 6. Tensile strength for Devonian shale from WV3,  
Lincoln County, West Virginia.

| <u>Shale</u>       | <u>Depth<br/>(m)</u> | <u>Mean Tensile Strength <math>\pm</math> Std. Dev. (no. tests)<br/>Parallel</u> | <u>Perpendicular</u> |
|--------------------|----------------------|--|----------------------|
| Gray               | 945                  | 2.47 $\pm$ 0.53(10)  |                      |
| Gray               | 856                  | 4.07 $\pm$ 1.30(10)  |                      |
| Gray               | 898                  | 4.65 $\pm$ 1.13 (5)  | 2.52 $\pm$ 0.23 (12) |
| Brown              | 1066, 1089           | 6.24 $\pm$ 0.72 (9)  | 2.78 $\pm$ 0.56 (9)  |
| Black<br>Marcellus | 1212, 1210           | 4.83 $\pm$ 1.83(10)  | 1.91 $\pm$ 0.26 (10) |

---

Table 7. Tensile strength of New Albany Shale, Christian County, Kentucky.

| Orientation      | Number of Samples | Average Tensile Strength (MPa) |
|------------------|-------------------|--------------------------------|
| -60 <sup>o</sup> | 16                | 7.52                           |
| -30 <sup>o</sup> | 12                | 7.28                           |
| 0 <sup>o</sup>   | 14                | 8.04                           |
| 30 <sup>o</sup>  | 9                 | 8.19                           |
| 60 <sup>o</sup>  | 14                | 8.34                           |
| 90 <sup>o</sup>  | 11                | 8.43                           |

TABLE 8. RESULTS OF FRACTURE ENERGY TESTS FOR BLACK SHALES.

| TEST # | WELL | FORMATION | DEPTH (M) | FRACTURE ENERGY (J/M) | AVG. (STD. DEV.) |
|--------|------|-----------|-----------|-----------------------|------------------|
| TF-9   | OH7  | HURON     | 648.9     | 68.2                  | 67.2 (25.8)      |
| TF-10  | OH7  | HURON     | 642.5     | 75.5                  |                  |
| TF-13  | OH7  | HURON     | 648.3     | 118.1                 |                  |
| TF-15  | OH7  | HURON     | 648.3     | 34.5                  |                  |
| TF-16  | OH7  | HURON     | 648.4     | 77.8                  |                  |
| TF-17  | OH7  | HURON     | 648.3     | 49.6                  |                  |
| TF-18  | OH7  | HURON     | 648.4     | 35.1                  |                  |
| TF-19  | OH7  | HURON     | 648.4     | 78.6                  |                  |
| TF-28  | OH7  | MARCELLUS | 822.7     | 68.5                  |                  |
| TF-29  | OH7  | MARCELLUS | 822.7     | 78.2                  |                  |
| TF-55  | OH7  | MARCELLUS | 820.7     | 67.0                  |                  |
| TF-62  | OH9  | HURON     | 1023.9    | 48.5                  | 42.1 (11.6)      |
| TF-63  | OH9  | HURON     | 1023.7    | 58.5                  |                  |
| TF-64  | OH9  | HURON     | 1023.8    | 22.7                  |                  |
| TF-65  | OH9  | HURON     | 1023.8    | 44.8                  |                  |
| TF-66  | OH9  | HURON     | 1023.7    | 33.1                  |                  |
| TF-68  | OH9  | HURON     | 1023.8    | 52.6                  |                  |
| TF-69  | OH9  | HURON     | 1023.8    | 34.6                  |                  |
| TF-44  | OH8  | HURON     | 1052.7    | 108.5                 |                  |
| TF-45  | OH8  | HURON     | 1052.7    | 163.9                 |                  |
| TF-46  | OH8  | HURON     | 1051.9    | 170.0                 |                  |
| TF-47  | OH8  | HURON     | 1051.8    | 39.3                  |                  |
| TF-48  | OH8  | HURON     | 1052.6    | 92.2                  |                  |
| TF-56  | PA2  | MARCELLUS | 2265.0    | 99.1                  | 114.8 (48.4)     |
| TF-57  | PA2  | MARCELLUS | 2264.8    | 121.7                 |                  |
| TF-58  | PA2  | MARCELLUS | 2264.6    | 181.3                 |                  |
| TF-59  | PA2  | MARCELLUS | 2264.6    | 159.5                 |                  |

TABLE 9. RESULTS OF FRACTURE ENERGY TESTS FOR GRAY SHALES.

| TEST # | WELL | FORMATION   | DEPTH (M) | FRACTURE ENERGY (J/M) | AVG. (STD. DEV.) |
|--------|------|-------------|-----------|-----------------------|------------------|
| TF-20  | OH7  | HANOVER     | 668.5     | 41.3                  | 40.1 (14.2)      |
| TF-21  | OH7  | HANOVER     | 662.1     | 37.0                  |                  |
| TF-22  | OH7  | HANOVER     | 661.4     | 24.5                  |                  |
| TF-23  | OH7  | HANOVER     | 662.1     | 33.5                  |                  |
| TF-25  | OH7  | HANOVER     | 661.4     | 34.6                  |                  |
| TF-54  | OH7  | HANOVER     | 668.4     | 69.7                  |                  |
| TF-72  | OH9  | HURON(GRAY) | 1025.0    | 14.1                  | 14.8 (10.7)      |
| TF-73  | OH9  | HURON(GRAY) | 1024.9    | 8.7                   |                  |
| TF-74  | OH9  | HURON(GRAY) | 1024.9    | 6.2                   |                  |
| TF-76  | OH9  | HURON(GRAY) | 1024.9    | 35.5                  |                  |
| TF-77  | OH9  | HURON(GRAY) | 1024.9    | 9.4                   |                  |
| TF-35  | OH8  | HANOVER     | 1061.0    | 49.0                  | 50.9 ( 4.8)      |
| TF-36  | OH8  | HANOVER     | 1061.0    | 50.4                  |                  |
| TF-38  | OH8  | HANOVER     | 1060.8    | 47.6                  |                  |
| TF-39  | OH8  | HANOVER     | 1060.8    | 47.7                  |                  |
| TF-51  | OH8  | HANOVER     | 1060.9    | 49.3                  |                  |
| TF-53  | OH8  | HANOVER     | 1060.9    | 61.4                  |                  |
| TF- 2  | PA2  | MAHANTANGO  | 2228.0    | 76.9                  | 84.9 (33.1)      |
| TF- 4  | PA2  | MAHANTANGO  | 2228.8    | 134.7                 |                  |
| TF- 5  | PA2  | MAHANTANGO  | 2228.8    | 89.0                  |                  |
| TF- 6  | PA2  | MAHANTANGO  | 2225.2    | 50.8                  |                  |
| TF- 7  | PA2  | MAHANTANGO  | 2225.3    | 116.2                 |                  |
| TF- 8  | PA2  | MAHANTANGO  | 2225.3    | 41.6                  |                  |

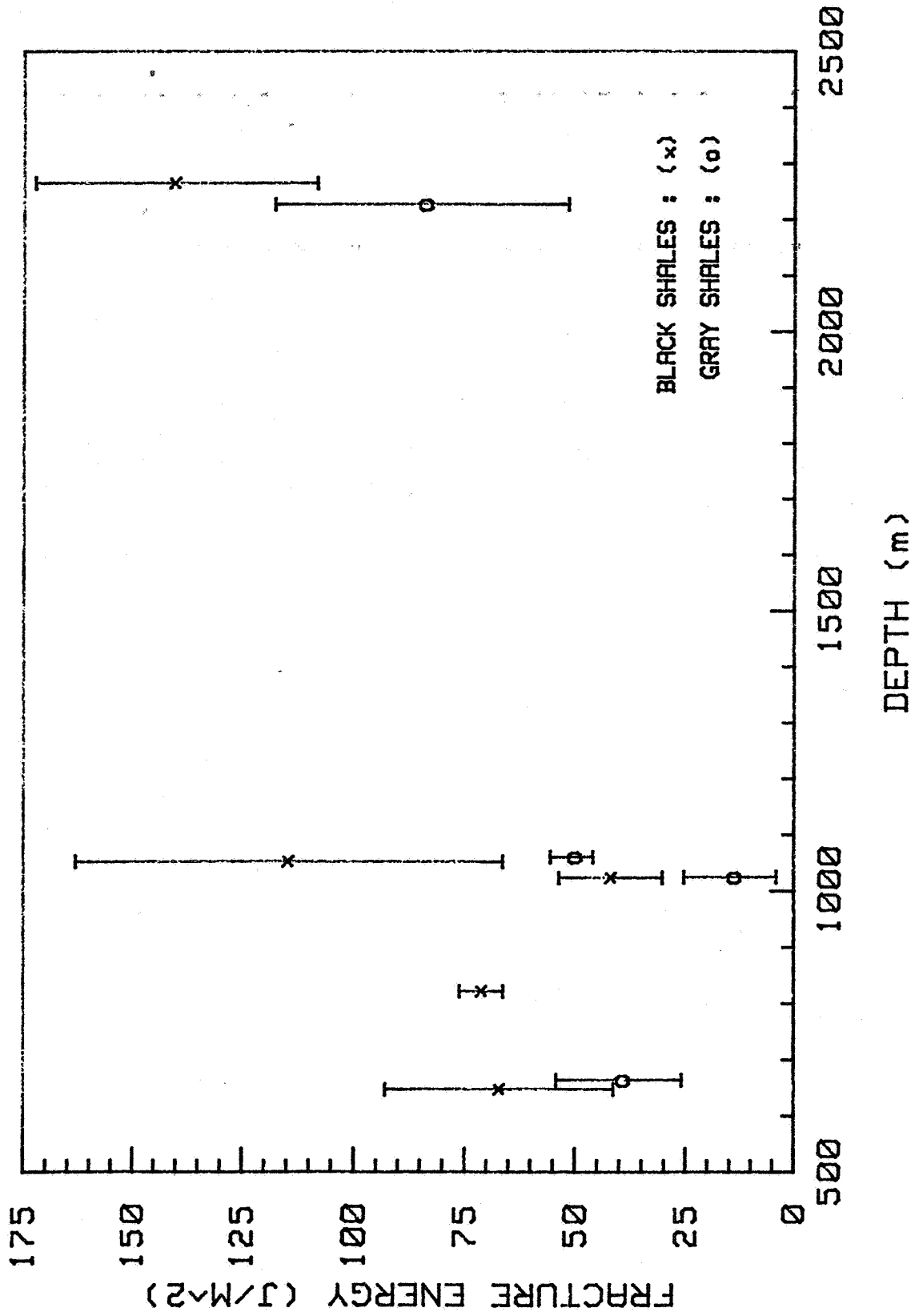


Figure 16. Average fracture energies as a function of depth.

Average values of fracture energy show trends with respect to both lithology and depth. For each black/gray pair from a given well the black shale has a higher fracture energy. Also, with the exception of OH7 there is a trend of increasing fracture energy with depth.

Fracture energy for gray shales has been measured by Terra Tek (Jones et al., 1977). The average value for two tests run on core from 1026 m and 1146 m is 28.7 J/m<sup>2</sup>. This falls between two averages for gray shales at comparable depths shown in Figure 16.

## SECTION 3. CONCLUSION

### 3.1. Trends in Mechanical Properties of Devonian Shales

Elasticity of Devonian shales showed no strong trends with respect to either lithology, locality, or confining pressure. Average values of Young's modulus for gray shales was 32.4 GPa and for black shales was 30.9 GPa. However it cannot be concluded that gray shales are stiffer than black shales in general because the reverse was found in several cases. For modeling purposes and many engineering applications, the average values above may be used, but for situations that require exact information, site-specific measurements should be made. For applications in which one is looking for a contrast in Young's modulus, it may be safe to assume that there is not much since the above values are so close. The difference is only 1.5 GPa whereas the standard deviations are 3.9 GPa and 5.4 GPa respectively.

Some shale units showed a slight tendency to have an increased Young's modulus at higher confining pressures, while others remained relatively unaffected. The lack of a strong confining pressure influence on Young's modulus is probably due to the low porosity (~1%, Blanton et al., 1980) of Devonian shales. In more porous rocks, increases in confining pressure raise Young's modulus. Confining pressure acts to decrease the porosity and increase the contact area of matrix material which stiffens the rock. However, with low initial porosities this effect is not strong.

The effect of natural fractures should be taken into account when attempting to describe bulk behavior. As pointed out in the subsection on Devonian shale character, the black shales tend to be more highly fractured. The presence of natural fractures tends to lower the modulus of a rock mass. Thus, whereas the black shale matrix may be only slightly less stiff than the gray, fractured black shale as a mass may be significantly less stiff. Such a contrast in moduli can affect the design of stimulation treatments (e.g., Jones et al., 1977).

Ultimate strength, yield strength, and ductility all increase with increasing confining pressure, which is typical for most rocks (Handin, 1966). Ultimate strength and yield strength tend to be higher for gray shales, whereas black shales tend to be more ductile. This is a relatively strong trend but may be reversed locally. Knowledge of the behavior of Devonian shales under differential compressive stresses has applications primarily in designing dynamic well stimulation treatments. The initial high compressive stresses produced by a dynamic pulse may exceed the yield strength of the rock and cause plastic deformation. Plastic deformation can reduce permeability in two ways: first by closing fractures and second by causing a residual "stress cage" around the borehole. In designing a dynamic treatment so that the peak compressive stress stays below the yield strength, one would want to be sure to use a true yield envelope and not an envelope for ultimate strengths, which may be somewhat higher especially at the higher confining pressures.

Tensile strength and fracture energy are required by the same types of problems, although the formulation of the problems must be different (e.g., see in situ stress determination in Abou-Sayed et al., 1977). These parameters occur in both dynamic and static stimulation calculations. Tensile strengths, however, have always presented a problem in rock mechanics because they are highly variable and easily influenced by specimen preparation and testing techniques. In this study tensile strengths showed no consistent trends either regionally or lithologically. Fracture energy on the other hand showed the most consistent trends of any mechanical property measured in this study, both with respect to lithology and depth of burial. Black shales tend to have a higher fracture energy, and fracture energy tends to increase with depth of burial. From this point of view formulations employing fracture energy as a measure of the strength of a rock rather than tensile strength may be more desirable. However, when using actual values one may want to be careful that the effects of confining pressure are included as an earlier study (Schmidt and Huddle, 1977) has shown that this effect may be relatively strong.

### 3.2. Future Work

One of the most promising topics for continued study is the effect of confining pressure on fracture energy. Fracture energy data for Devonian shales presented in this and previous reports have been obtained at atmospheric conditions, but a superposed hydrostatic pressure can have a strong effect on fracture toughness of rocks. In Indiana Limestone, Schmidt and Huddle (1977) found that the critical mode-I stress intensity factor,  $K_{IC}$ , was found to increase 4-fold due to an increase in confining pressure from atmospheric pressure to 62 MPa (9000 psi). Fracture energy as a material property enters into several calculations associated with stimulation design, but if these calculations are to be accurate they should take into account the effect of pressures encountered in downhole situations. Compared to the other material properties of Devonian shales, fracture energy seems to have the most consistent trends with respect of lithology and depth of burial. If these generic trends could be extended to include the effect of confining pressure, they would be much more useful in stimulation research and design.

Another area for further study that would have practical applications is the effect of deformation rate. Experimental data on the rate dependency of material properties would be particularly helpful in developing dynamic stimulation techniques. In order for these techniques to be successful the stress pulse (rise time and peak load) must be tailored to the material properties in such a way that maximum radial fracture extension is obtained and damage due to excessive rubblezation is avoided. To be accurate this tailoring process should include the effect of deformation rate on material properties. The most effective way of characterizing rate-dependent behavior is by measuring linear viscoelastic parameters such as creep compliance,  $C(t)$ , or relaxation modulus,  $E(t)$ . Once one or the other of these functions is determined, it can be used to describe stress or strain history dependence of deformation, fracture mechanics (Schapery, 1975), and even plastic flow (Schapery, 1968).

## REFERENCES

- Abou-Sayed, A.A., Brechtel, C.E., and Clifton, R.J., "In Situ Stress Determination by Hydrofracturing: A Fracture Mechanics Approach," J. Geophys. Res. 83, pp. 2851-2862, 1978.
- Blanton, T.L., "Effect of Strain Rates from  $10^{-2}$  to  $10\text{sec}^{-1}$  in Triaxial Compression Tests on Three Rocks," Int. J. Rock Mech. Min. Sci. v. 18, pp. 47-62, 1981.
- Blanton, T.L., Young, C., and Patti, N.C., "Material Properties of Devonian Shale for Stimulation Technology Development," Task No. 21, DOE Contract DE-AM21-78MC08216, October 1980.
- Brace, W.F., and Jones, A.H., "Comparison of Uniaxial Deformation in Shock and Static Loading of Three Rocks," J. Geophys. Res., v. 76, pp. 4913-4921, 1971.
- Carter, W.J., and Olinger, B.W., "Dynamic Properties of Devonian Shales," Proc. 1st EGSP Symposium, 1977, pp. 381-388.
- Cremean, S.P., Forrest, R.M., McKetta, S.F., Morse, M.F., Owens, G.L., and Smith, E.C., "Massive Hydraulic Fracturing Experiments of the Devonian Shale in Lincoln County, West Virginia," METC/CR-79/17, 1979.
- Evans, M.A., "Fractures in Oriented Devonian Shale Cores from the Appalachian Basin, Volume I," Report to DOE under contract DE-AC21-76MC05194, January, 1980.
- Ford, W.K., "The Characterization of the Production Mechanism in the Devonian Shale and its Sensitivity to Changes in Various Reservoir Parameters," Proc. 3rd Eastern Gas Shales Symposium, METC/SP-79/6, Morgantown, West Virginia, October 1979.
- Handin, J., "Strength and Ductility," in Handbook of Physical Constants, ed. by S.P. Clark, Jr., pp. 223-289, 1966.
- Handin, J., Hager, R.V., Friedman, M., and Feather, J.N., "Experimental Deformation of Sedimentary Rocks under Confining Pressure: Pore Pressure Tests," Am. Assoc. Petroleum Geologists Bull., v. 47, pp. 717-755, 1963.
- Hanson, M.E., Emerson, D.O., Heard, H.C., Shaffer, R.J., and Carlson, R.C., "Quarterly Report: The LLL Massive Hydraulic Fracturing Program for Gas Stimulation," July - September, 1976a.
- Hanson, M.E., Heard, H.C., Hearst, J.R., and Shaffer, R.J., "LLL Gas Stimulation Program, Quarterly Progress Report," October - December, 1976b.
- Hennington, W.M., "Unconventional Exploration for Natural Fractures," Unconventional Gas Recovery Symposium, May 1980, pp. 265-274.

Jones, A.H., Abou-Sayed, A.S., Buckholdt, L.M., Lingle, R., and Rogers, L.A., "Rock Mechanics Studies Related to MHF of Eastern United States Devonian Shales: Final Core Analysis Report," 1977, 64 p.

Kalyoncu, R.S., Boyer, J.P., and Snyder, M.J., "Devonian Shales - An In-Depth Analysis of Well EGSP NY No. 1 With Respect to Shale Characterization, Hydrocarbon Gas Content and Wire-Log Data," Proc. 3rd EGSP Symposium, 1979, pp. 115-163.

Kalyoncu, R.S., Coppins, W.G., Hooie, D.T., and Snyder, M.J., "Characterization and Analysis of Devonian Shales: I. Physical Characterization," Proc. 1st EGSP Symposium, 1977, pp. 230-258.

McClintock and Argon, "Mechanical Behavior of Materials," Addison-Wesley, Reading, Massachusetts, p. 7, 1966.

McKetta, S.F., "Earth Stress Relationships in the Appalachian Basin," Unconventional Gas Recovery Symposium, May 1980, pp. 259-264.

Miller, D.D., and Johnson, R.J.E., "Acoustic and Mechanic Analysis of a Transverse Anisotropy in Shale," Proc. Third Eastern Gas Shales Symposium, 1979, pp. 527-542.

Overbey, W.K., "Effect of in situ stress on induced fractures," Proc. 7th Appalachian Petroleum Geology Symposium, 1976, pp. 182-211.

Sbar, M.L., and Sykes, L.R., "Contemporary Compressive Stress and Seismicity in Eastern North America: An Example of Intra-Plate Tectonics," Geol. Soc. Amer. Bull., Vol. 84, 1973, pp. 1861-1882.

Schapery, R.A., "On a Thermodynamic Constitutive Theory and Its Application to Various Nonlinear Materials," Proc. IUTAM Symposium East Kilbride, Springer-Verlag Wien, New York, pp. 259-285, 1968.

Schapery, R.A., "A Theory of Crack Initiation and Growth in Viscoelastic Media, II. Approximate Methods of Analysis," Int. Jour. of Fracture, v. 11, pp. 369-388, 1975.

Schmidt, R.A., and Huddle, C.W., "Effect of Confining Pressure on Fracture Toughness of Indiana Limestone," Int. J. Rock Mech. Min. Sci., v. 14, pp. 289-293, 1977.

Schmoker, J.W., "The Relationship between Density and Gamma-Ray Intensity in the Devonian Shale Sequence, Lincoln County, West Virginia," Proc. 1st EGSP Symposium, 1977, pp. 355-360.

Shumaker, R.C., Kirk, K.G., Nuckols, E.B., and Long, B.R., "Analysis of Structural Geological Parameters that Influence Gas Production from the Devonian Shale of the Appalachian Basin," Proc. 1st EGSP Symposium, 1977, pp. 496-523.

Young, C., and Powell, C.N., "Lateral Inertia Effects on Rock Failure in Split-Hopkinson-Bar Experiments," Proc. 20th U.S. Symposium on Rock Mechanics, 1979, pp. 299-307.

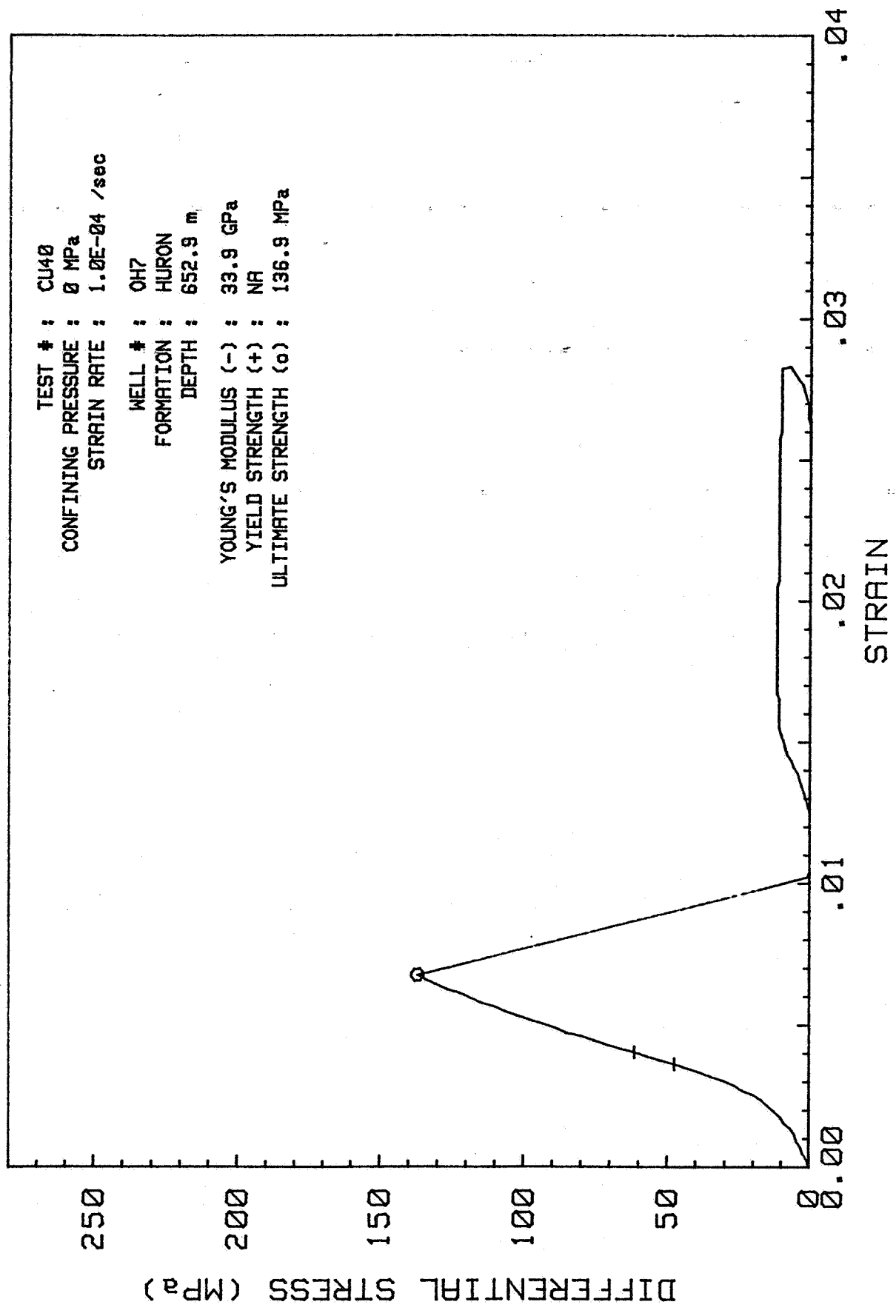
Young, C., and Smith, J.W., "In Situ Variations of Oil Shale Fracture Properties," Department of Civil Engineering Report, Colorado State University, Fort Collins, Colorado, 1979.

**APPENDIX A:**  
**Stress-Strain Curves for Compression Tests**

TEST # : CU40  
CONFINING PRESSURE : 0 MPa  
STRAIN RATE : 1.0E-04 /sec

WELL # : OH7  
FORMATION : HURON  
DEPTH : 652.9 m

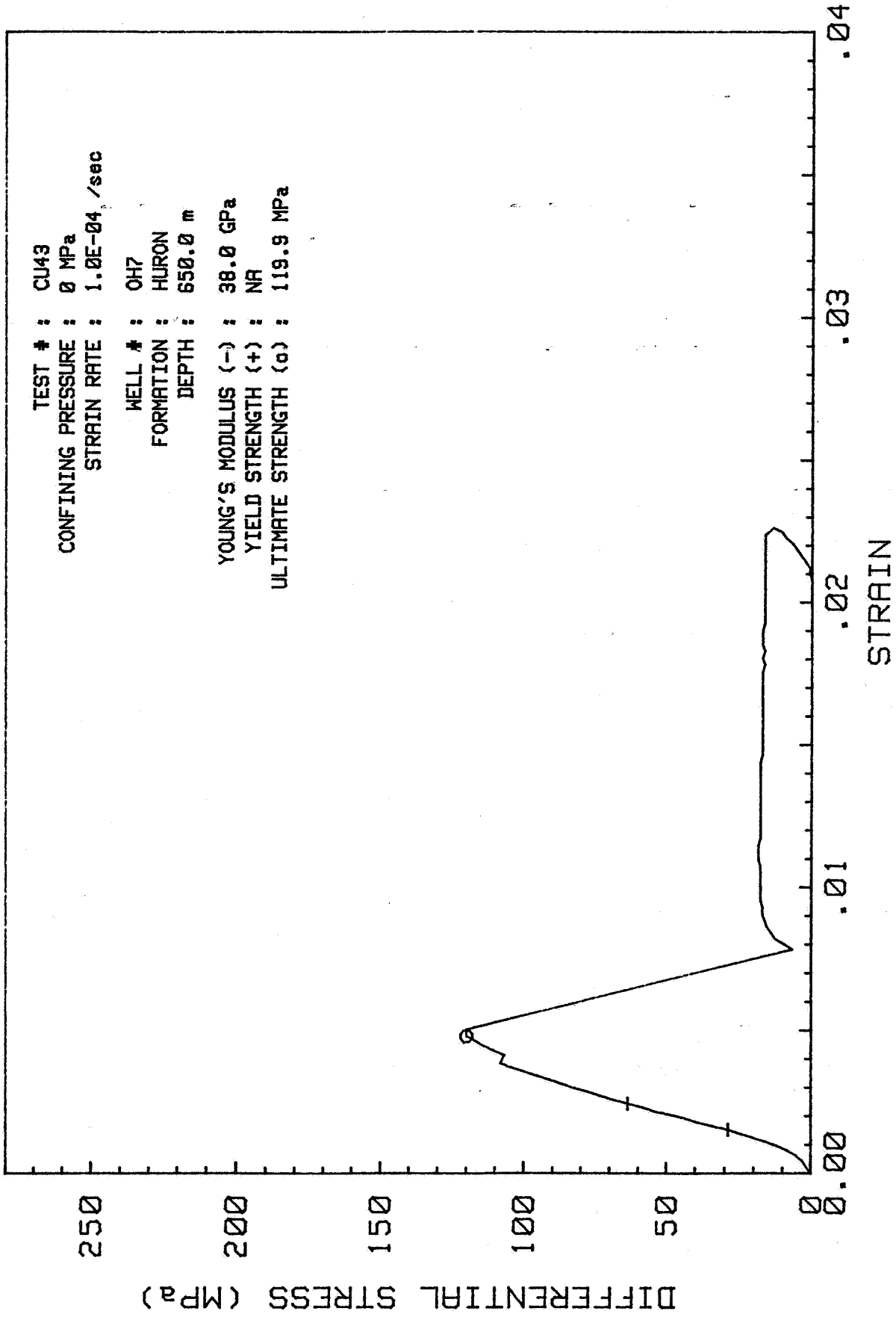
YOUNG'S MODULUS (-) : 33.9 GPa  
YIELD STRENGTH (+) : NA  
ULTIMATE STRENGTH (o) : 136.9 MPa



TEST # : CU43  
CONFINING PRESSURE : 0 MPa  
STRAIN RATE : 1.0E-04 /sec

WELL # : OH7  
FORMATION : HURON  
DEPTH : 650.0 m

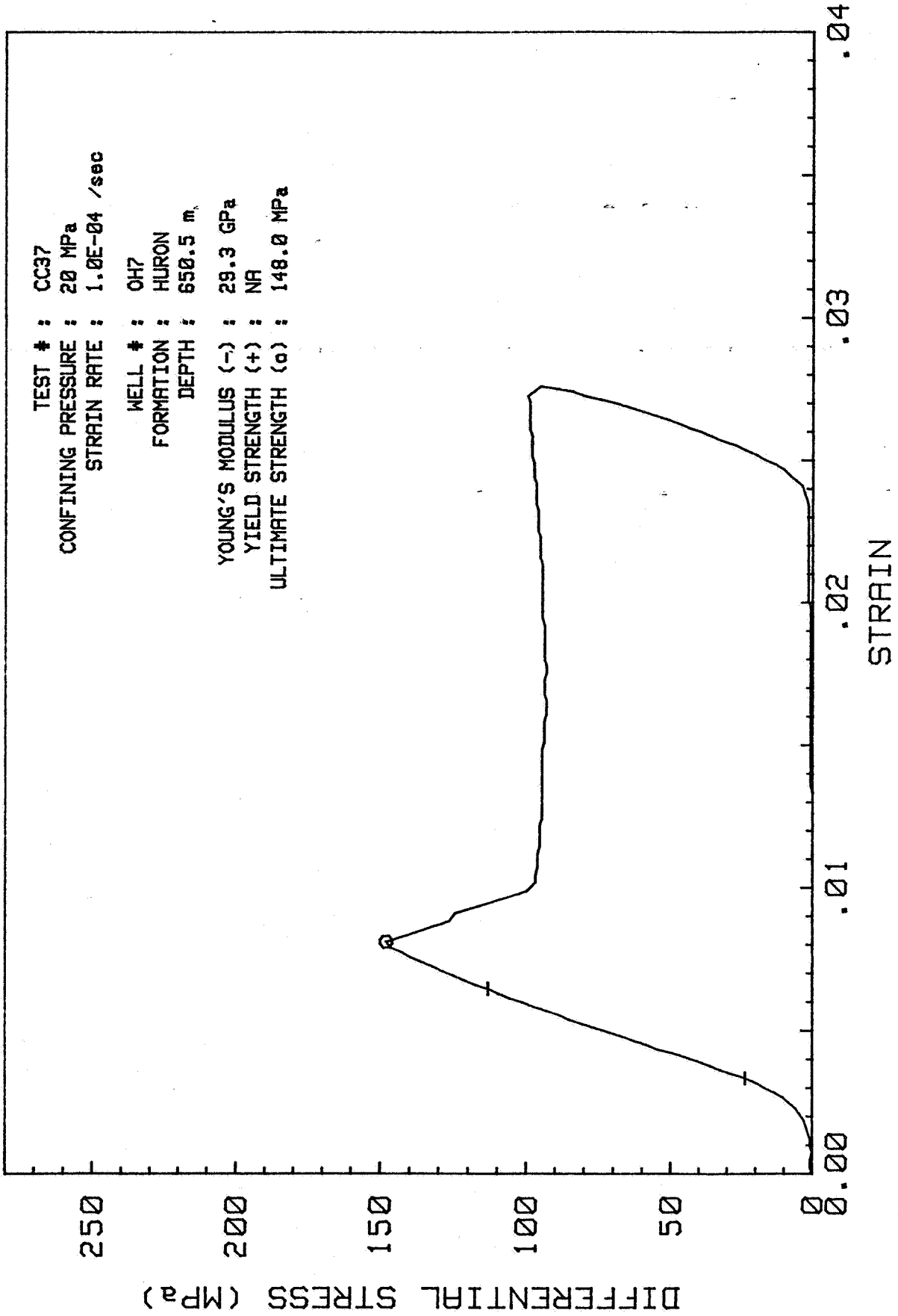
YOUNG'S MODULUS (-) : 38.0 GPa  
YIELD STRENGTH (+) : NA  
ULTIMATE STRENGTH (o) : 119.9 MPa

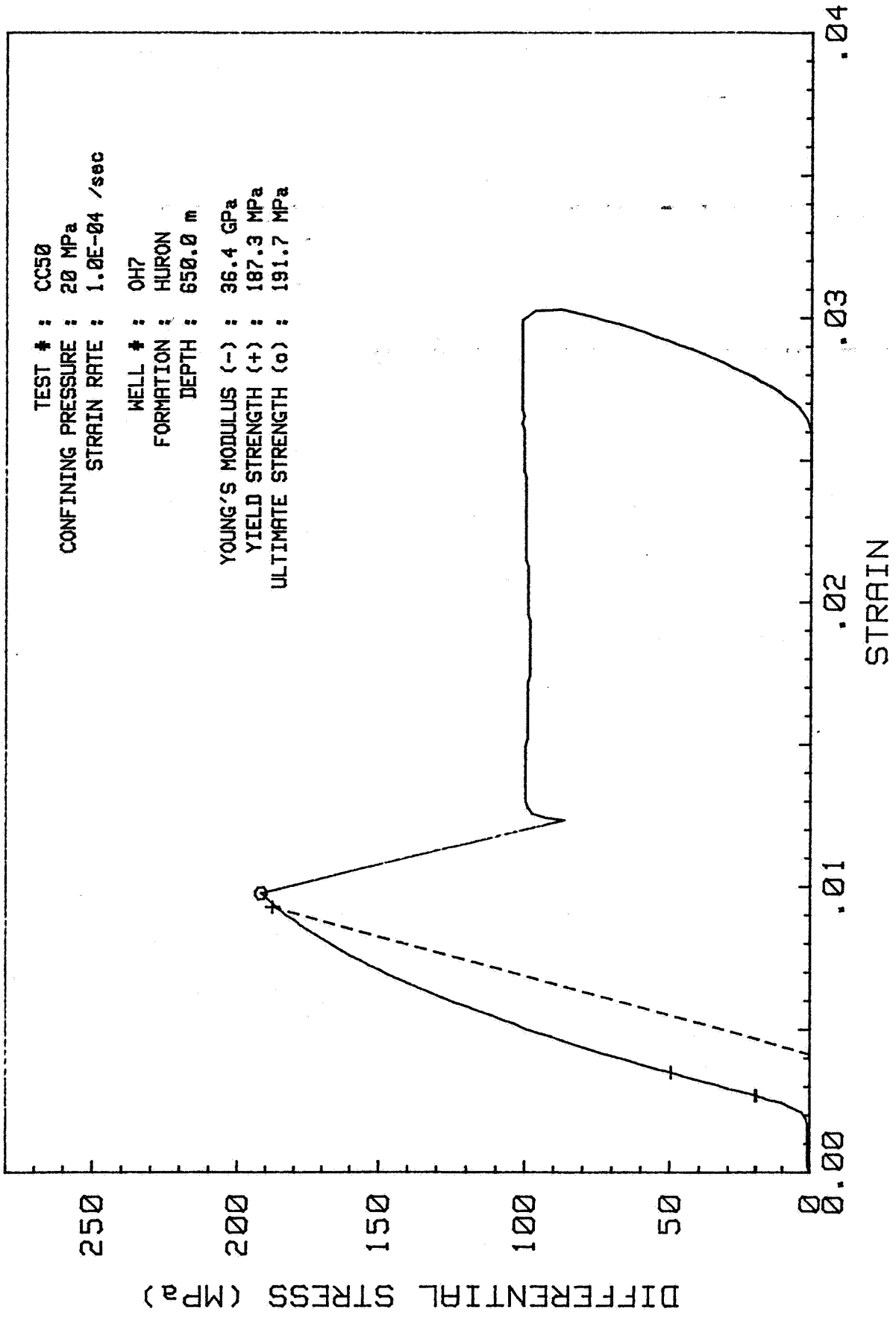


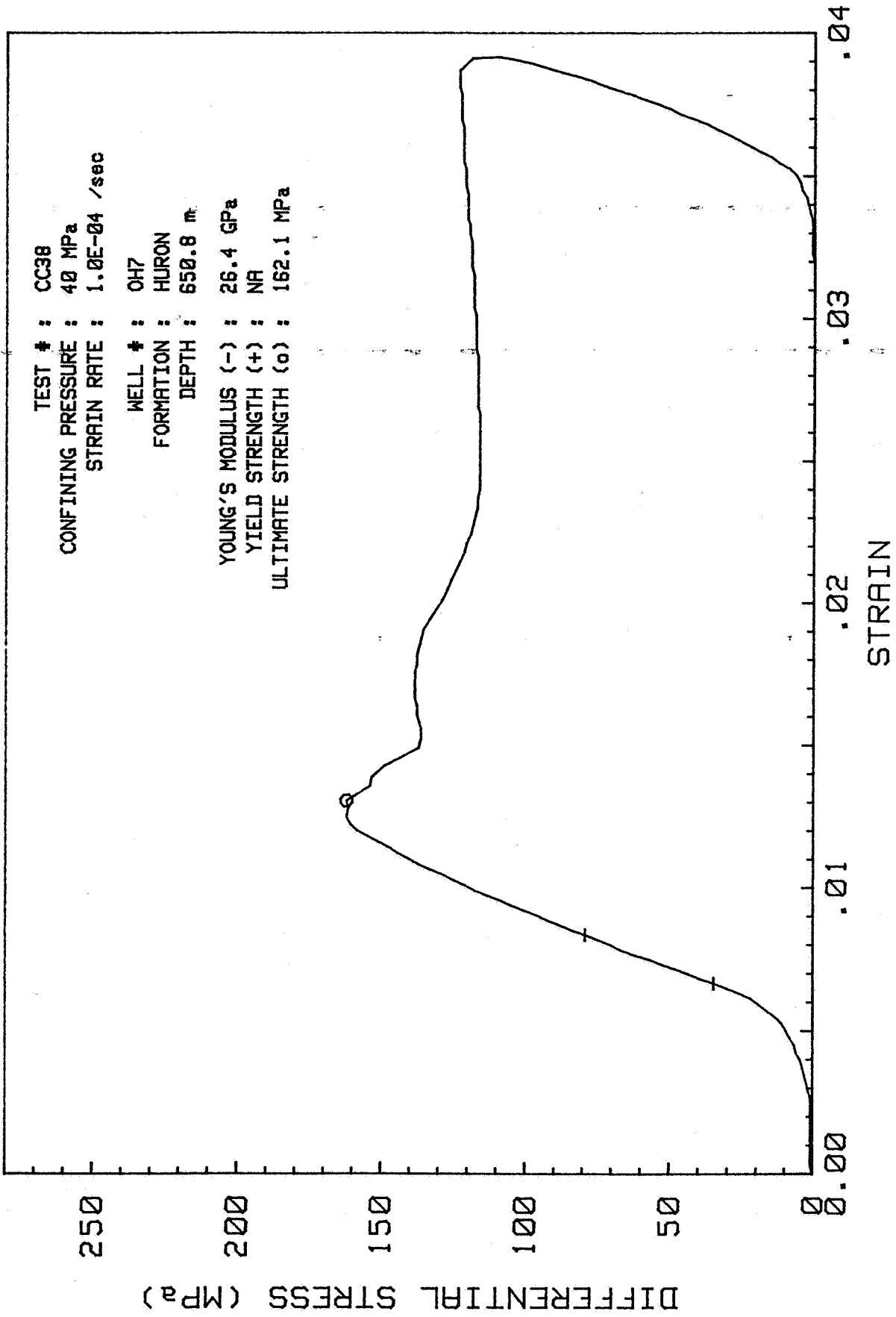
TEST # : CC37  
CONFINING PRESSURE : 20 MPa  
STRAIN RATE : 1.0E-04 /sec

WELL # : OH7  
FORMATION : HURON  
DEPTH : 650.5 m

YOUNG'S MODULUS (-) : 29.3 GPa  
YIELD STRENGTH (+) : NA  
ULTIMATE STRENGTH (o) : 148.0 MPa



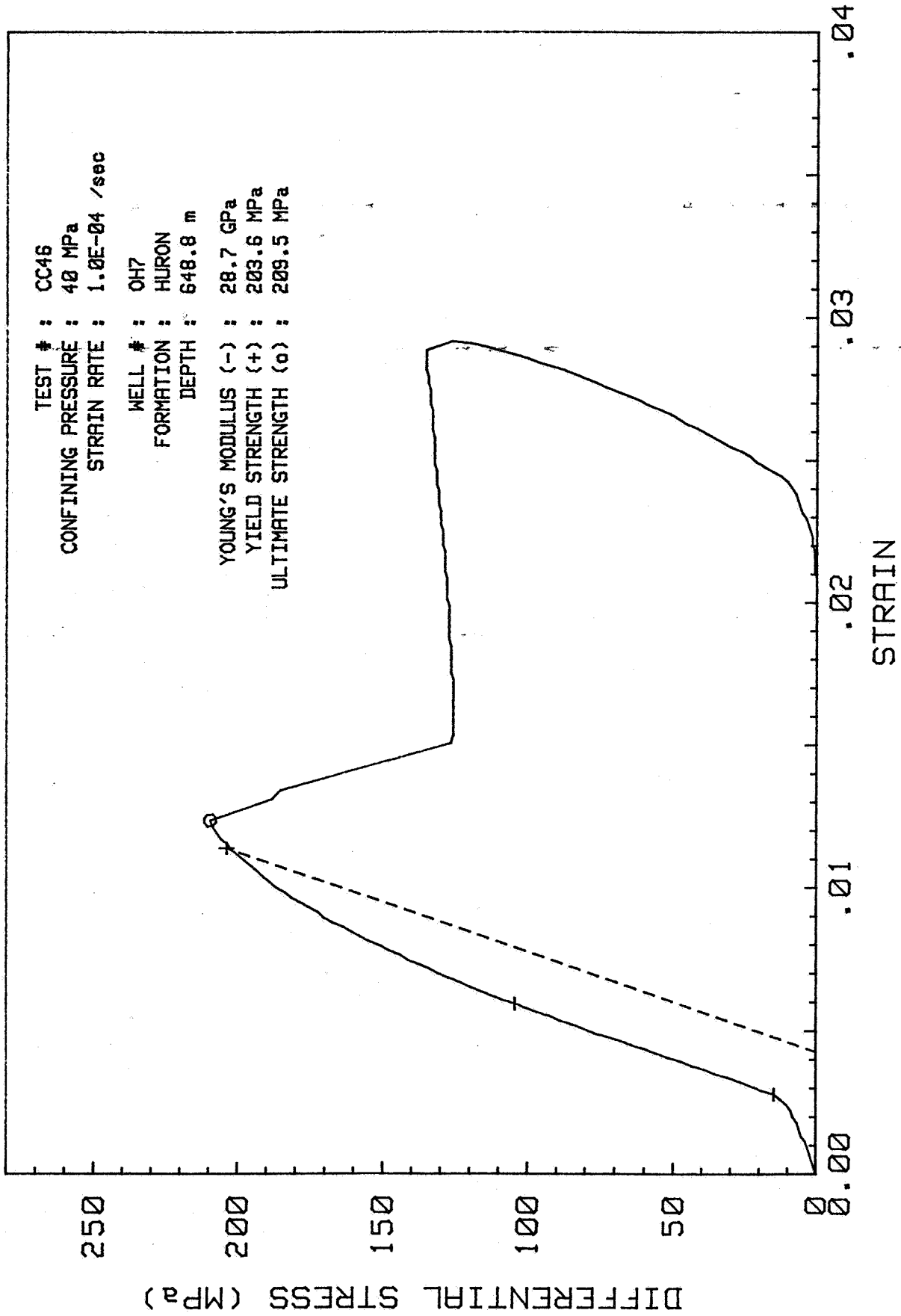


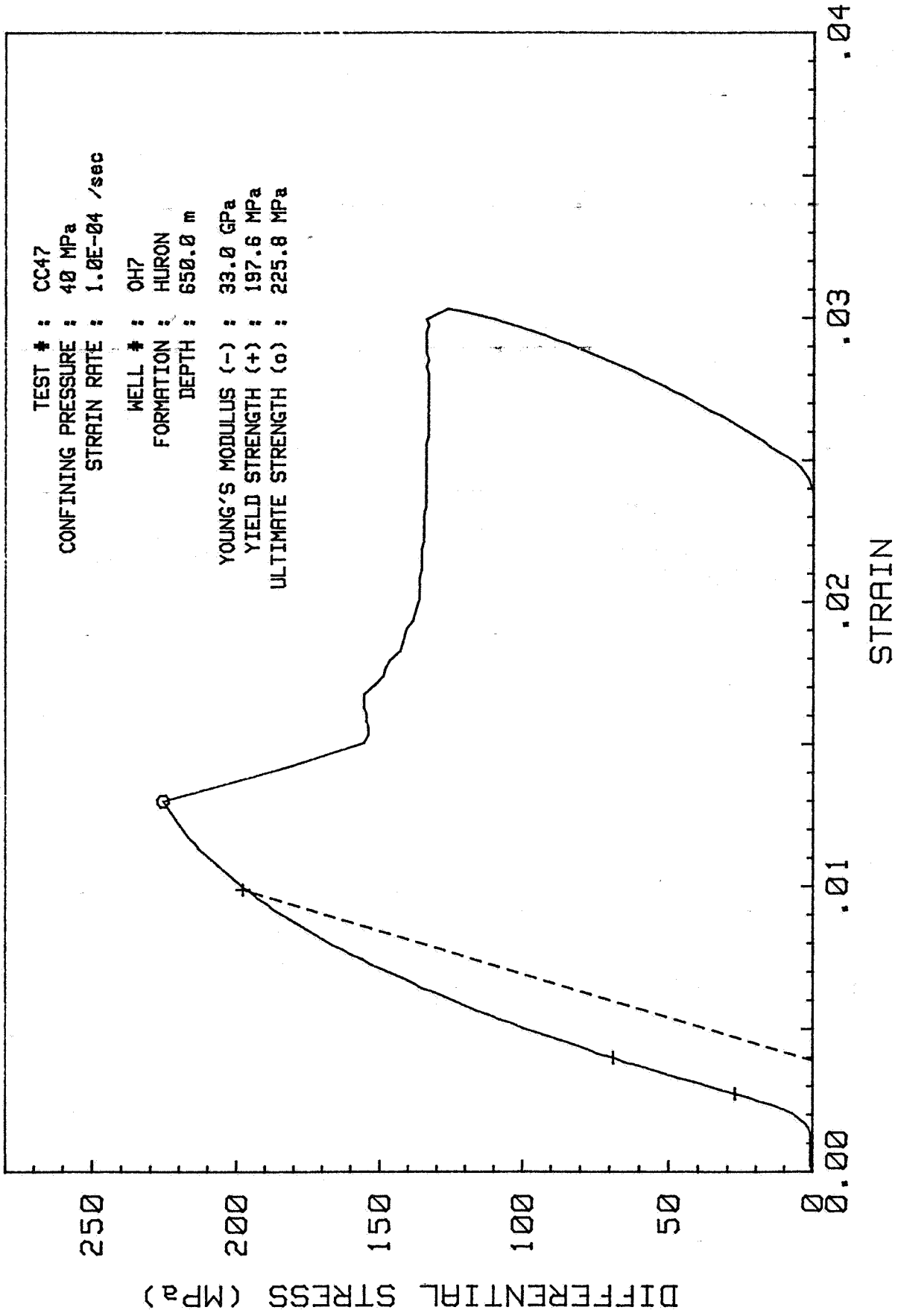


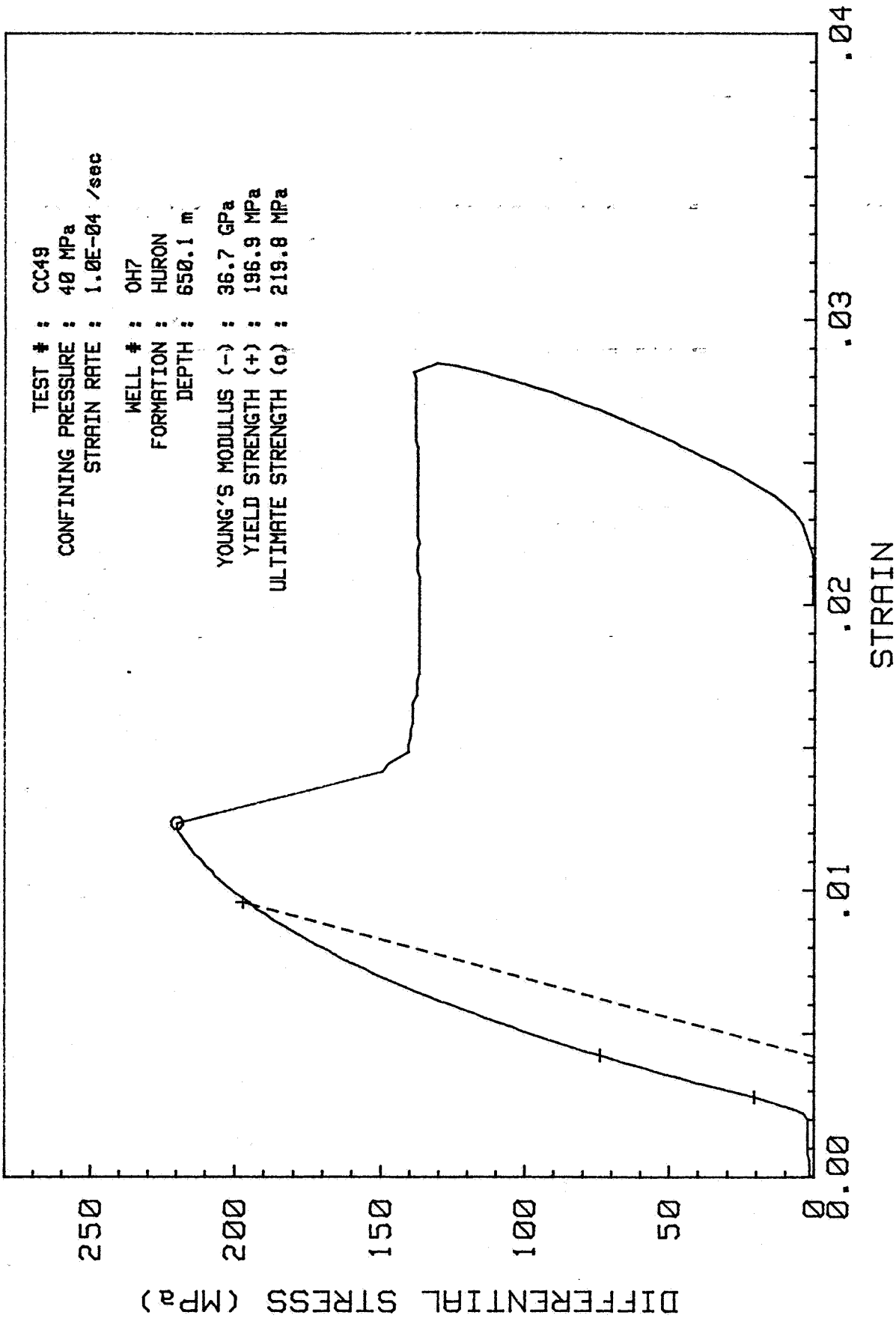
TEST # : CC46  
CONFINING PRESSURE : 40 MPa  
STRAIN RATE : 1.0E-04 /sec

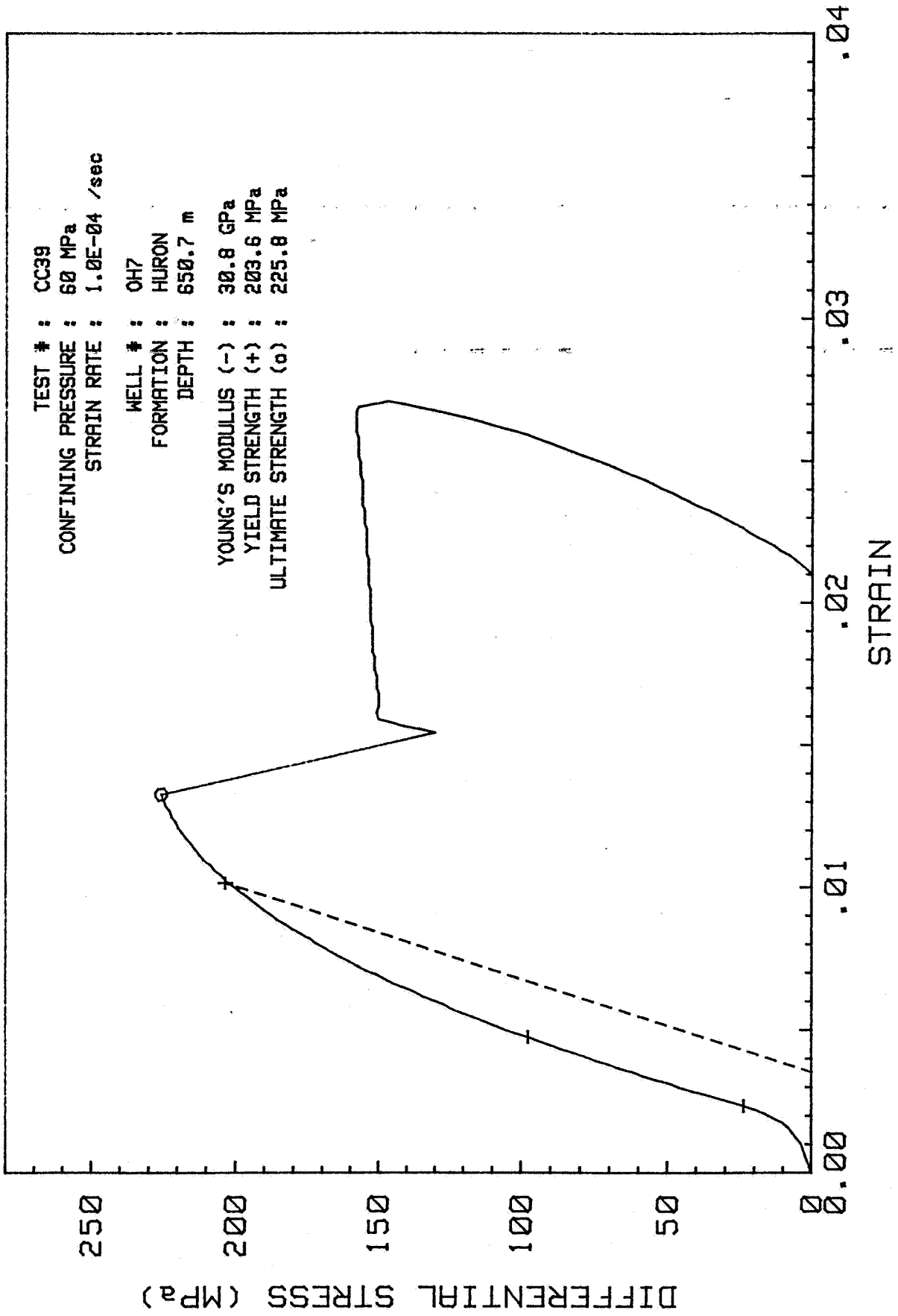
WELL # : OH7  
FORMATION : HURON  
DEPTH : 648.8 m

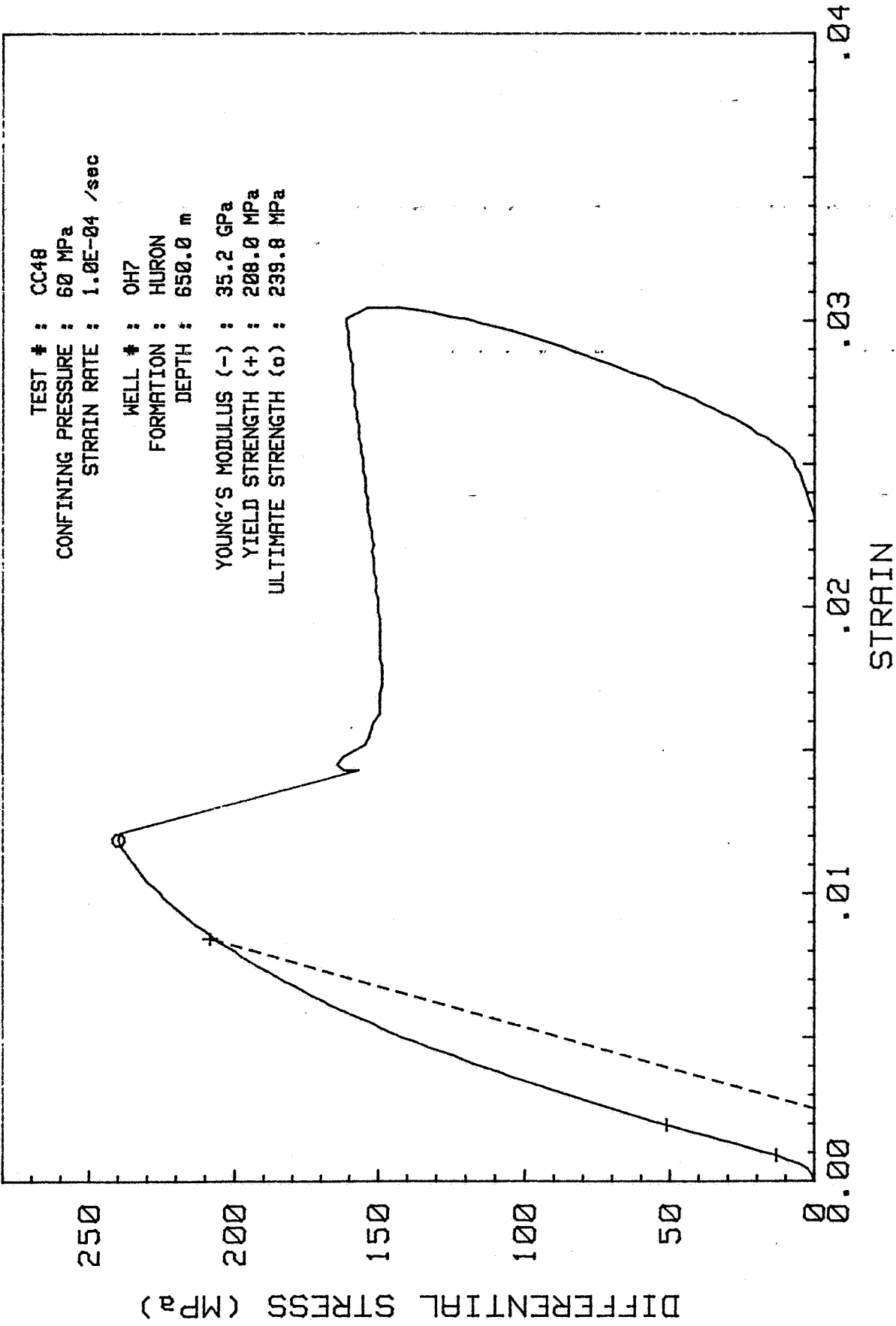
YOUNG'S MODULUS (-) : 28.7 GPa  
YIELD STRENGTH (+) : 203.6 MPa  
ULTIMATE STRENGTH (o) : 209.5 MPa







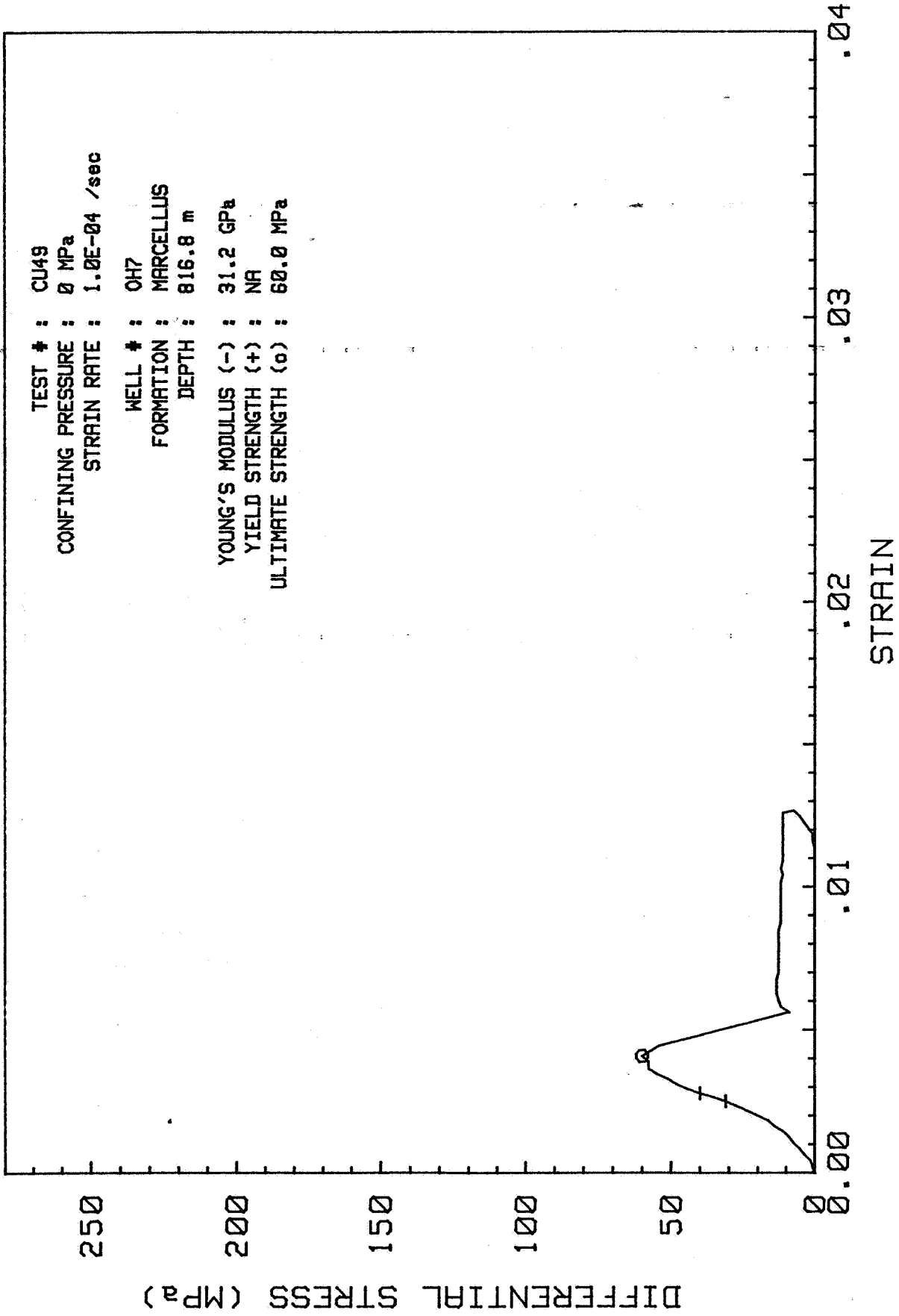


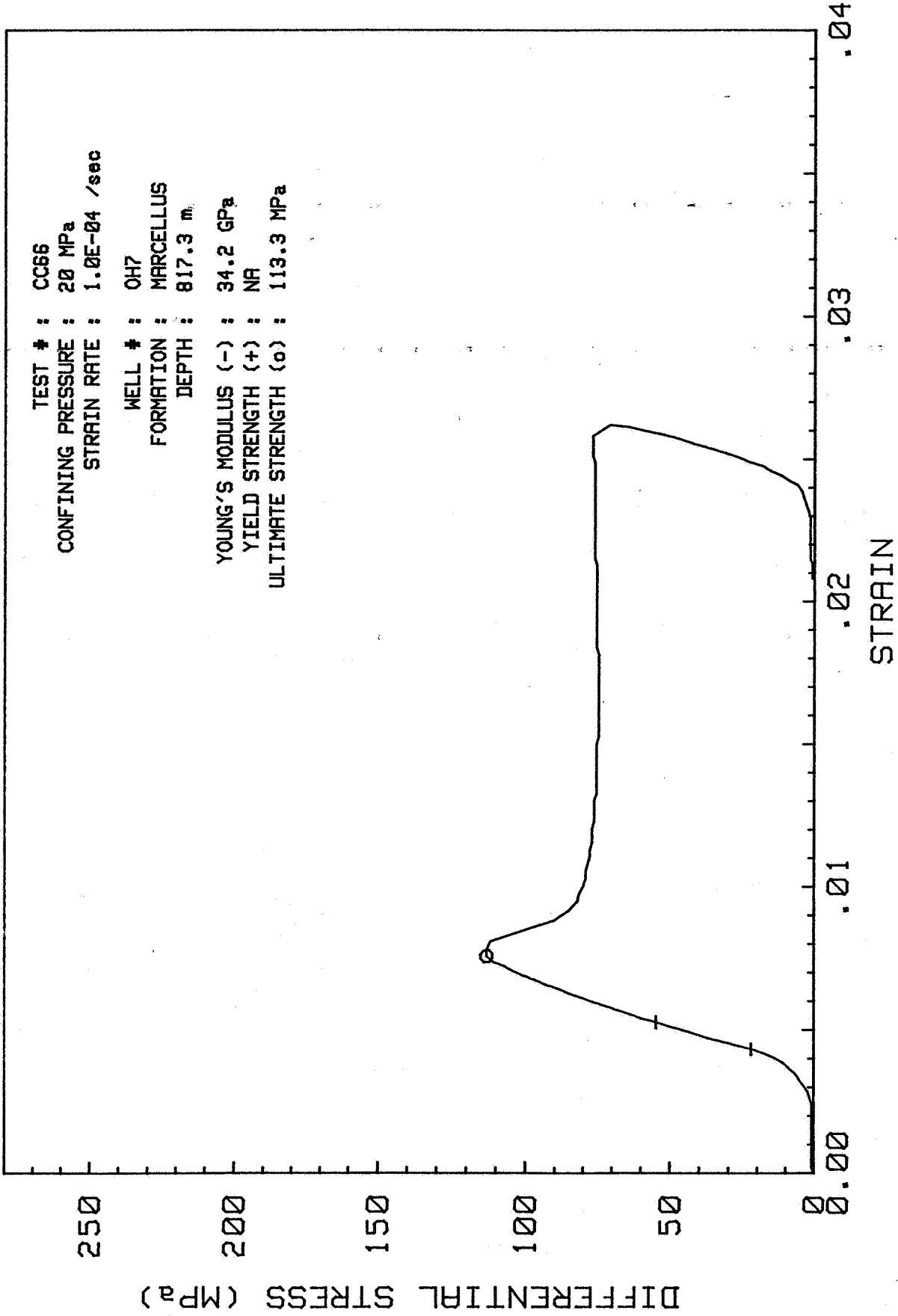


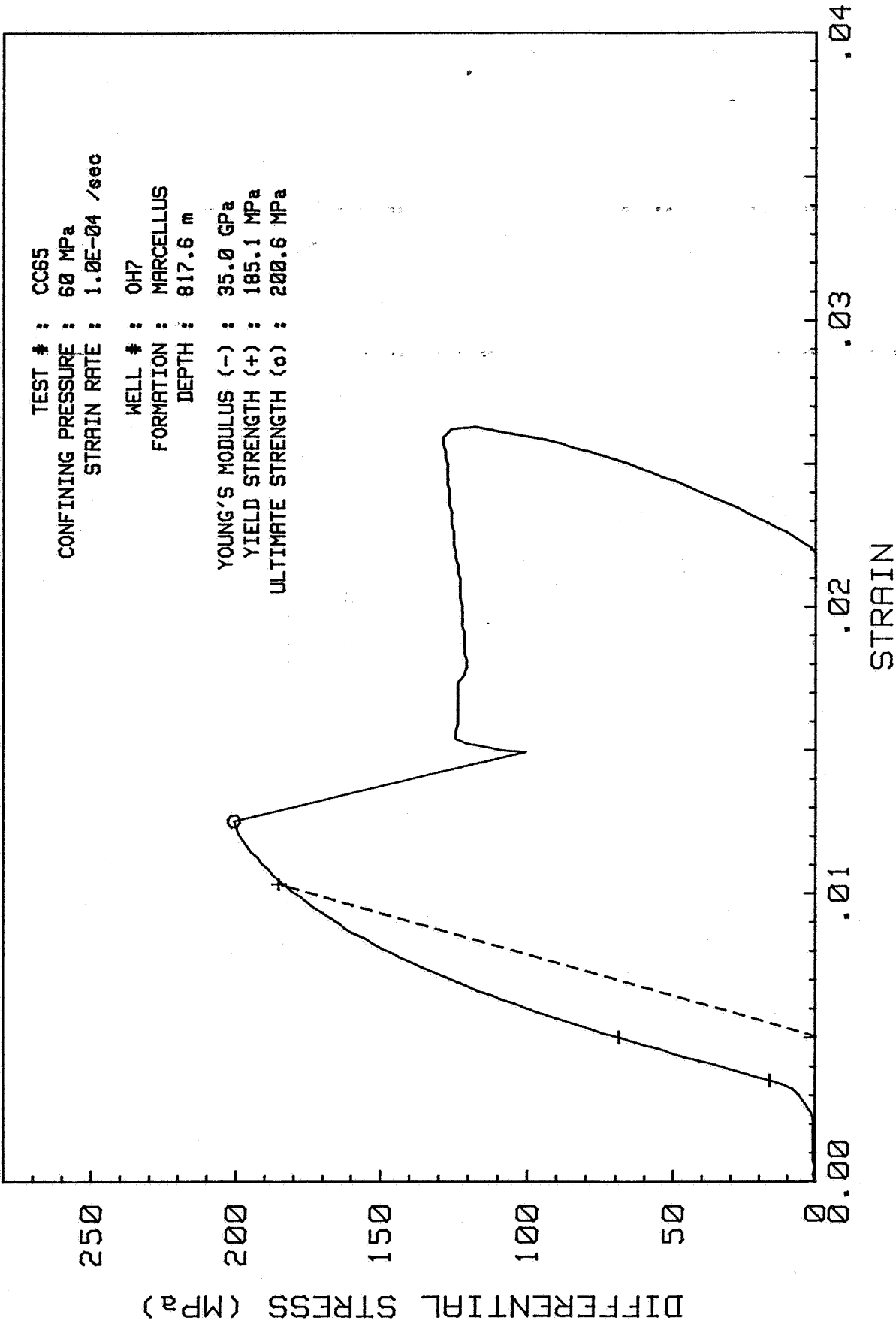
TEST # : CU49  
CONFINING PRESSURE : 0 MPa  
STRAIN RATE : 1.0E-04 /sec

WELL # : OH7  
FORMATION : MARCELLUS  
DEPTH : 816.8 m

YOUNG'S MODULUS (-) : 31.2 GPa  
YIELD STRENGTH (+) : NA  
ULTIMATE STRENGTH (o) : 60.0 MPa



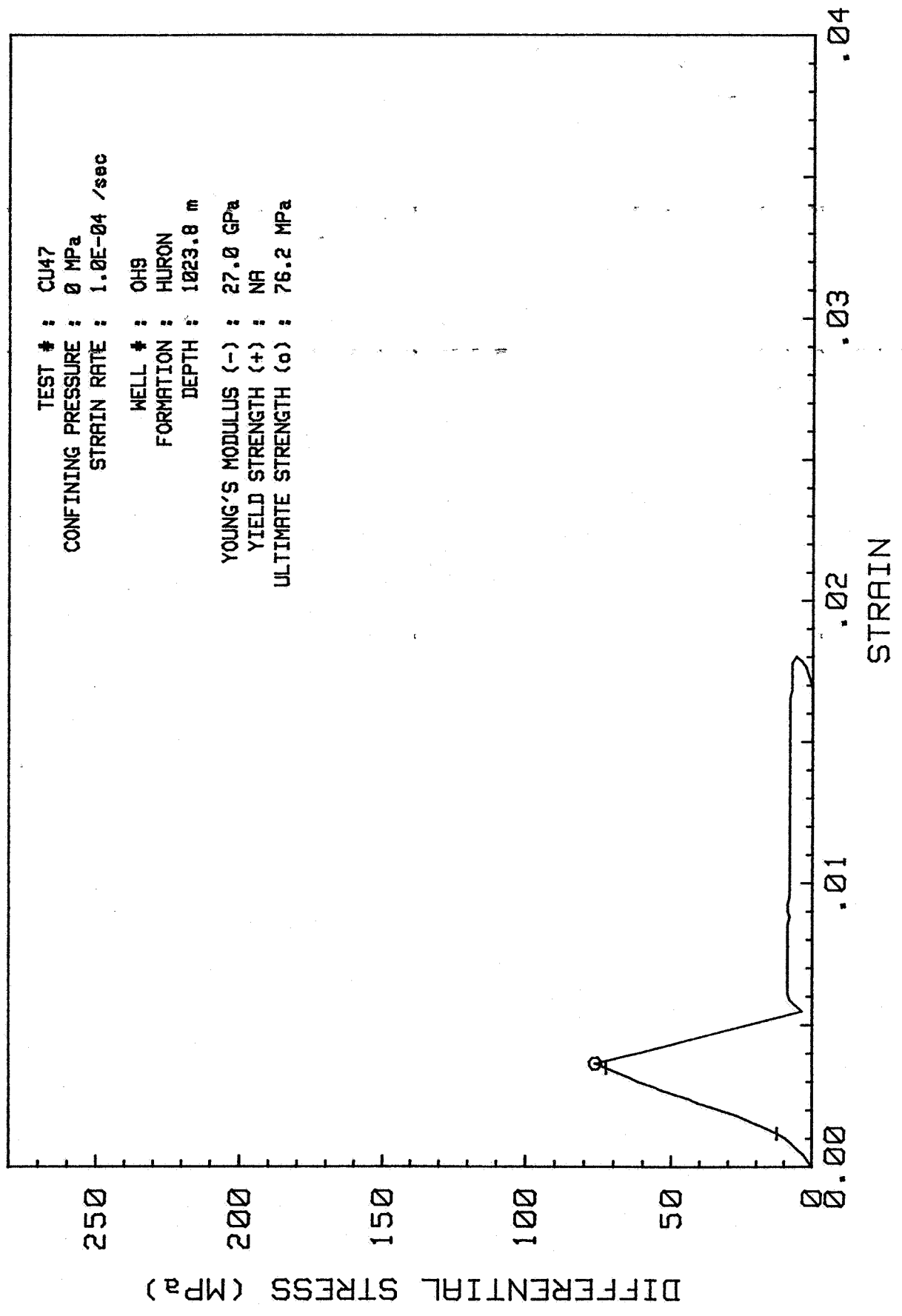




TEST # : CU47  
CONFINING PRESSURE : 0 MPa  
STRAIN RATE : 1.0E-04 /sec

WELL # : OH9  
FORMATION : HURON  
DEPTH : 1023.8 m

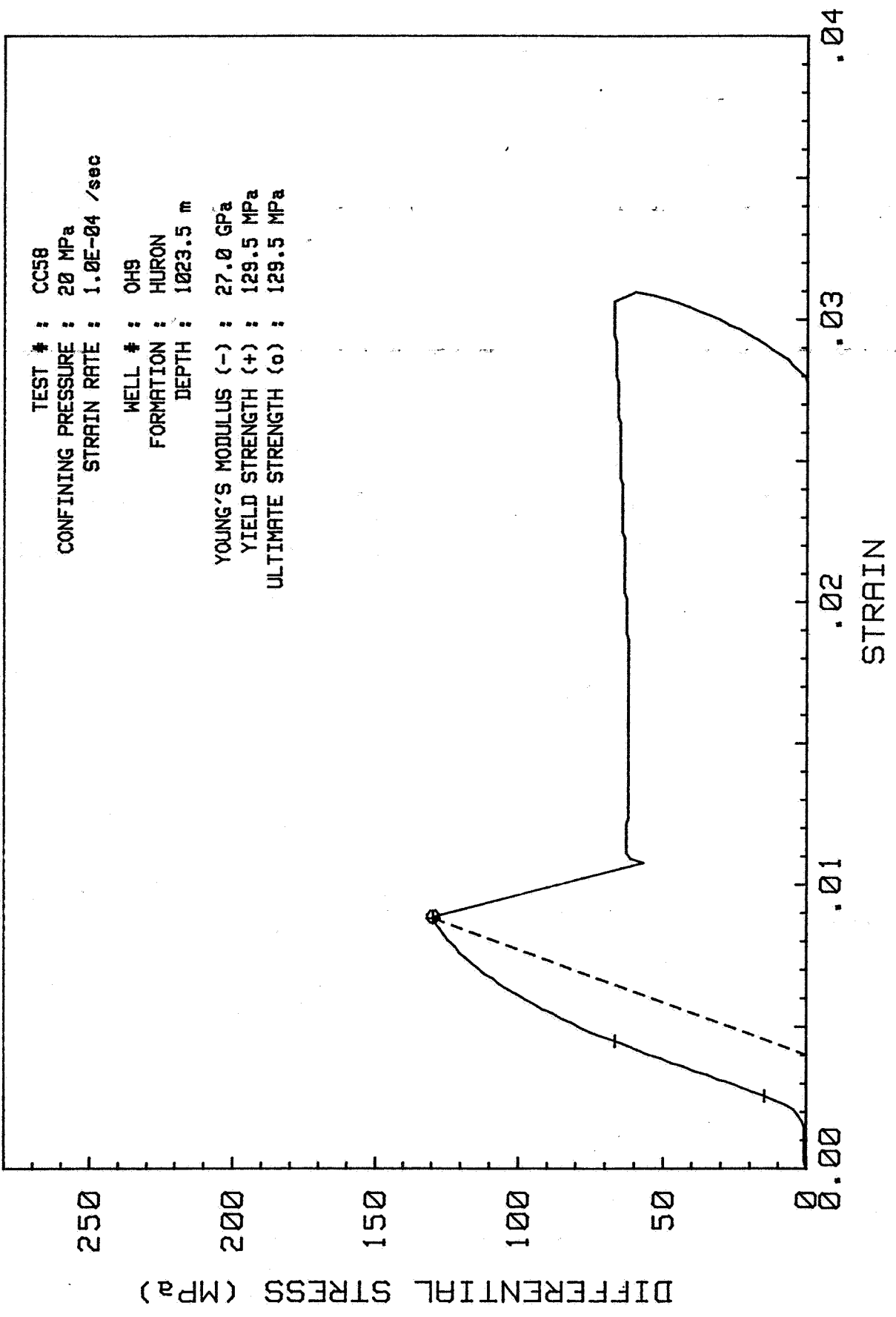
YOUNG'S MODULUS (-) : 27.0 GPa  
YIELD STRENGTH (+) : NA  
ULTIMATE STRENGTH (o) : 76.2 MPa

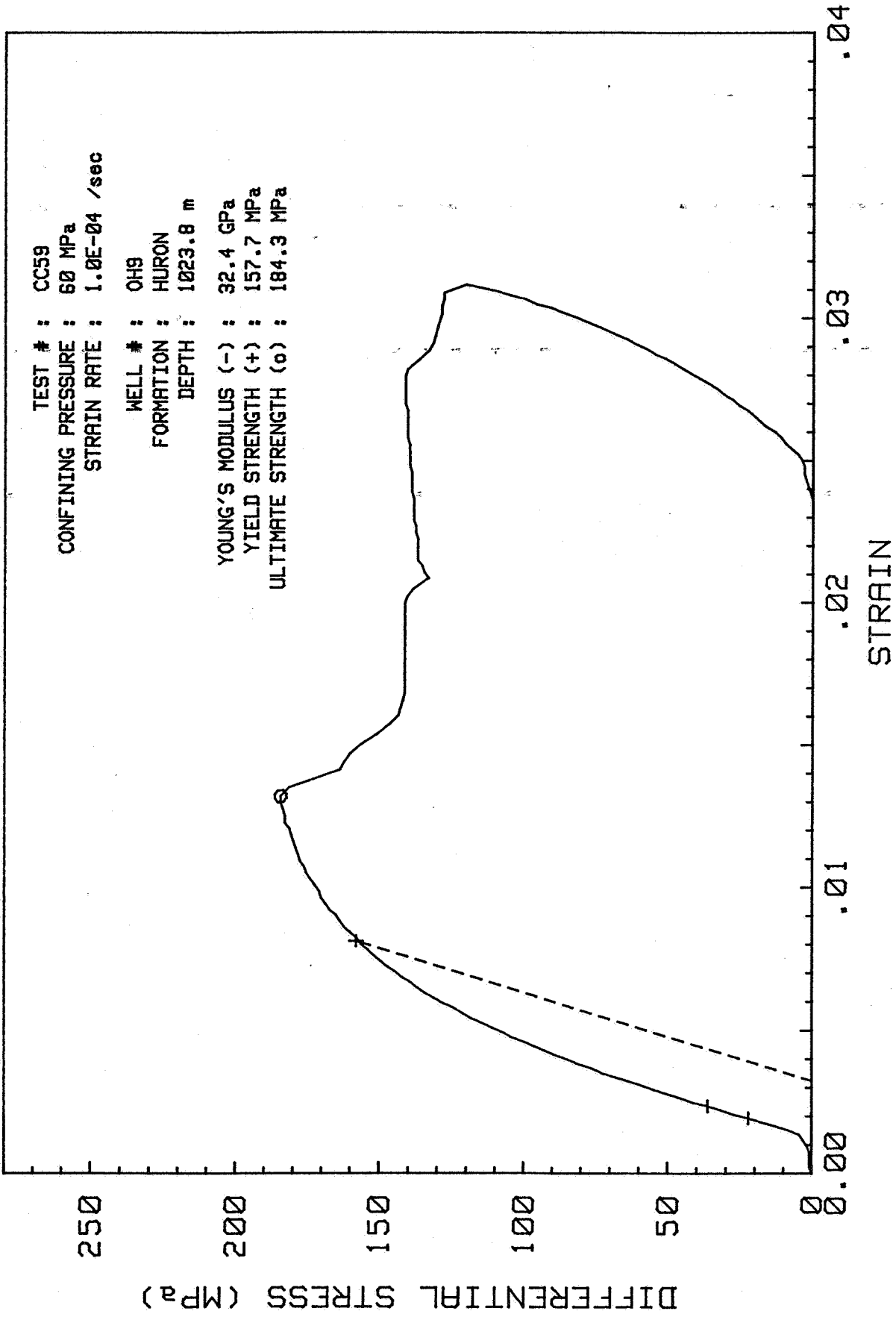


TEST # : CC58  
CONFINING PRESSURE : 20 MPa  
STRAIN RATE : 1.0E-04 /sec

WELL # : OH9  
FORMATION : HURON  
DEPTH : 1023.5 m

YOUNG'S MODULUS (-) : 27.0 GPa  
YIELD STRENGTH (+) : 129.5 MPa  
ULTIMATE STRENGTH (o) : 129.5 MPa

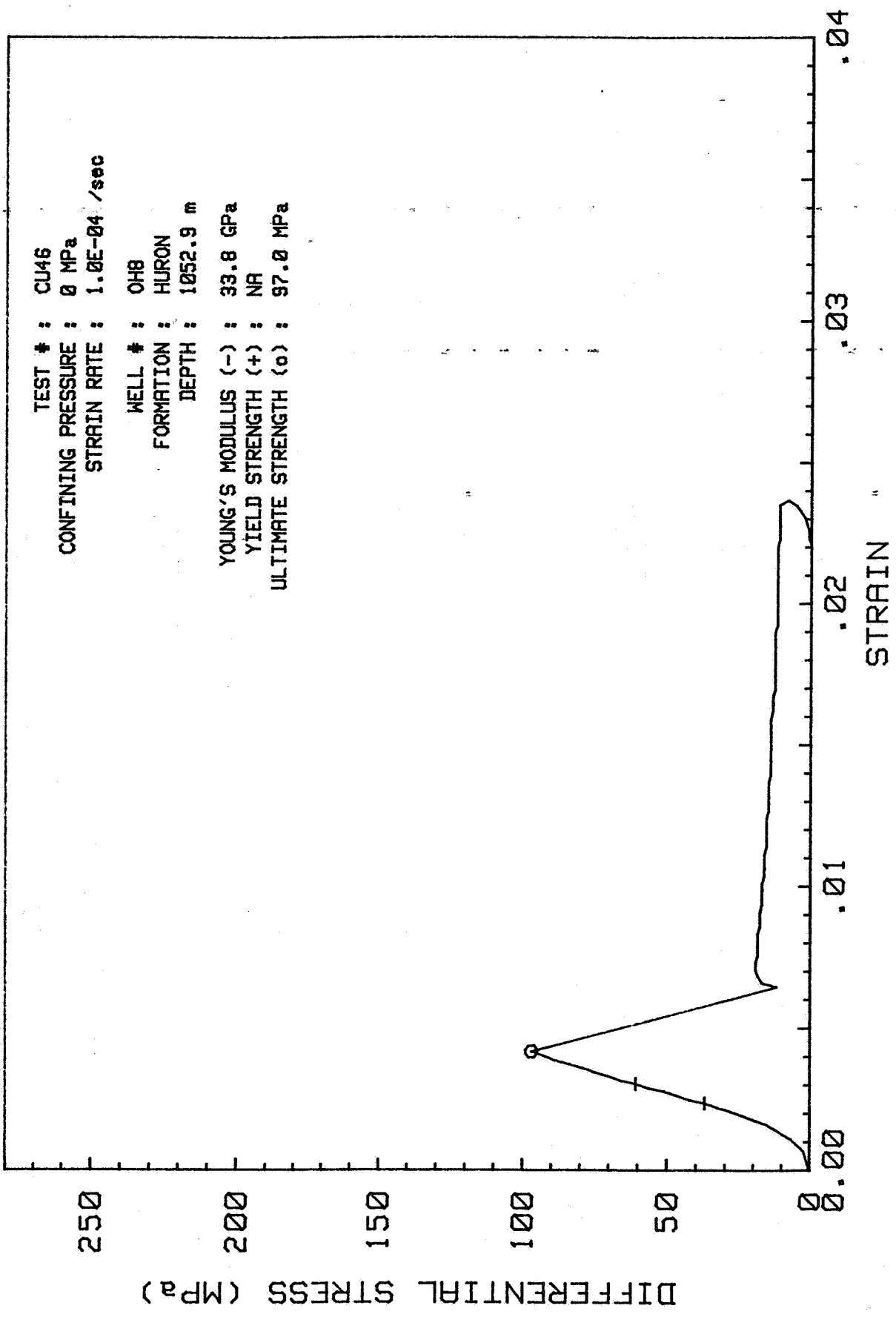


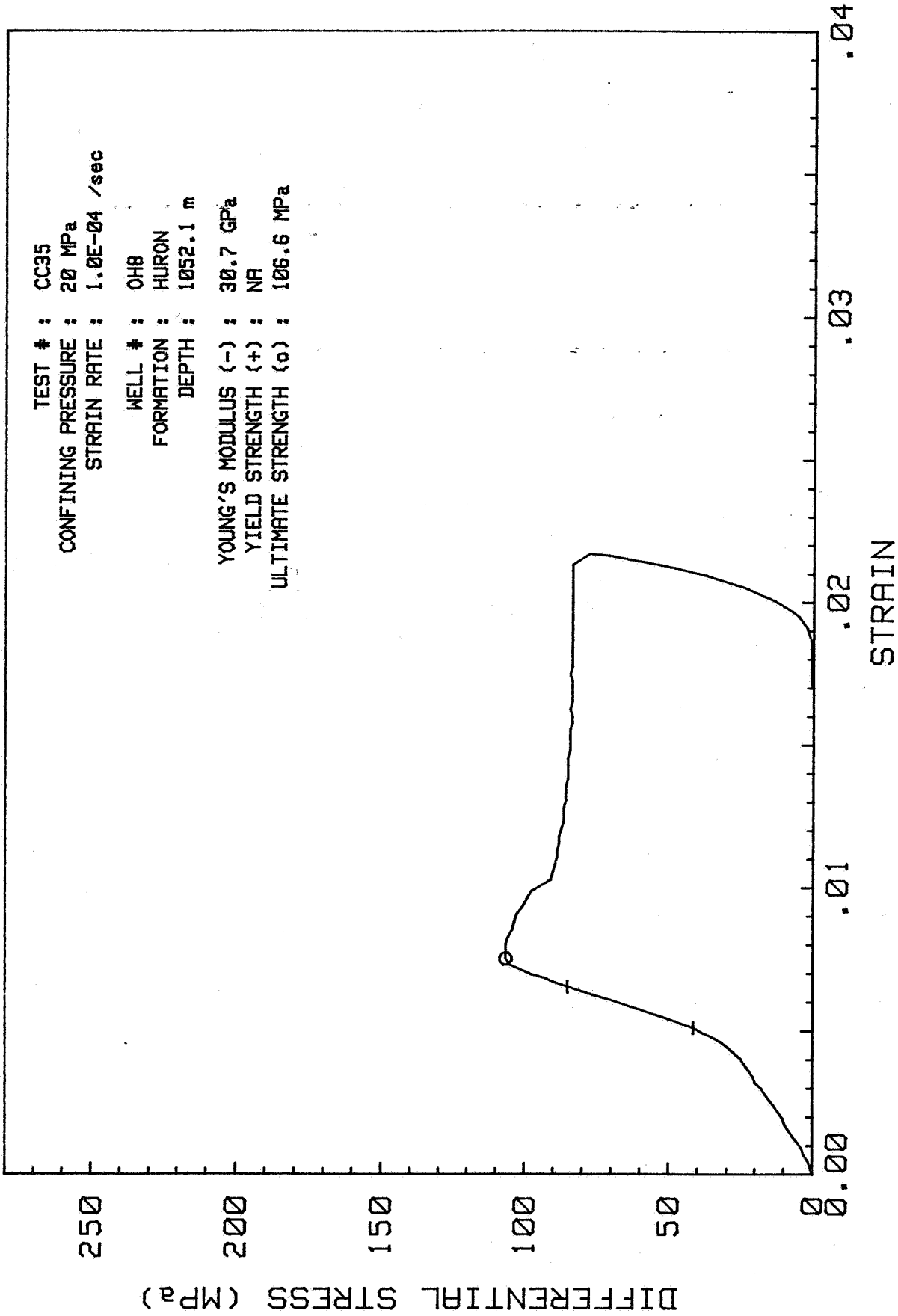


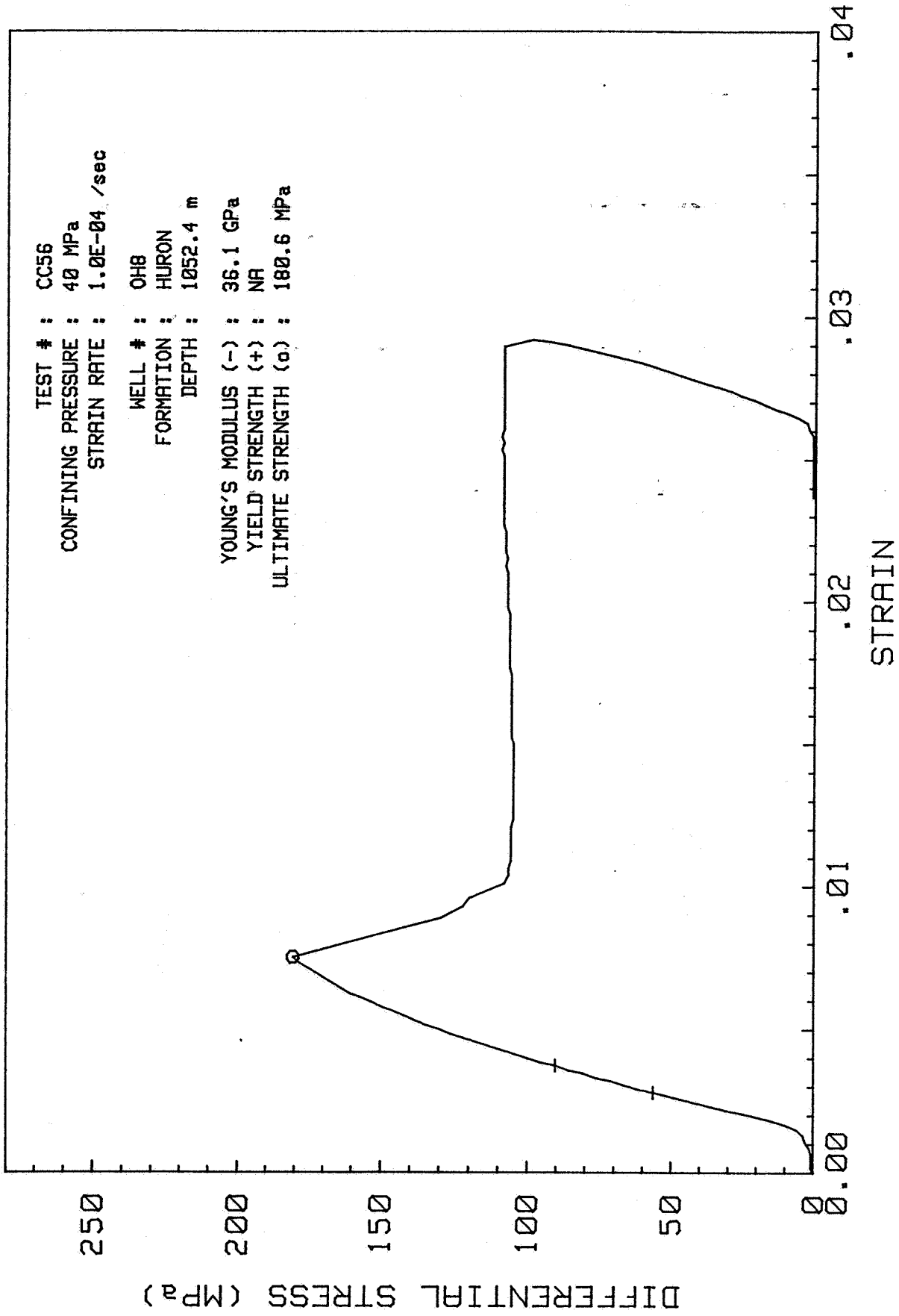
TEST # : CU46  
CONFINING PRESSURE : 0 MPa  
STRAIN RATE : 1.0E-04 /sec

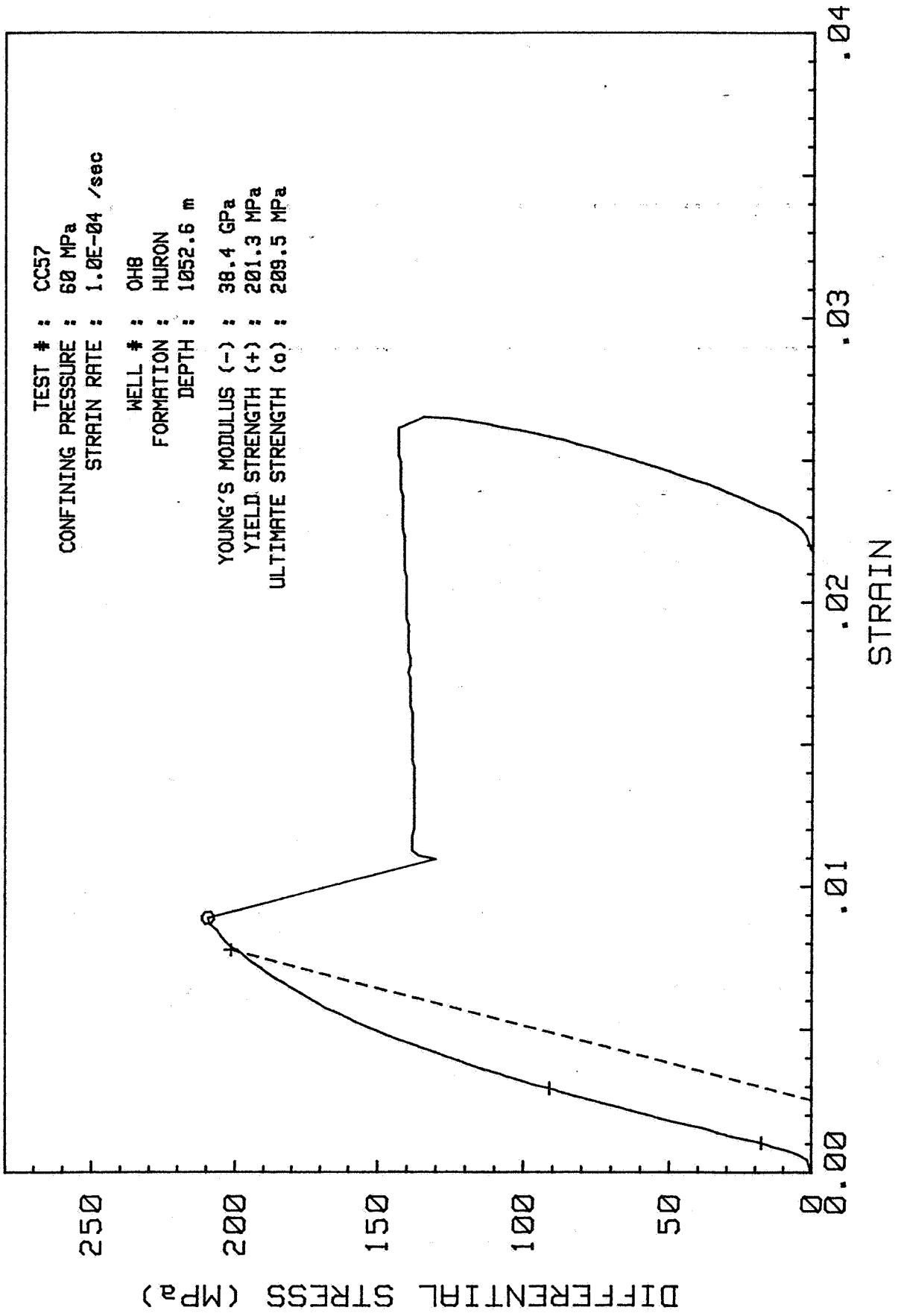
WELL # : OH8  
FORMATION : HURON  
DEPTH : 1052.9 m

YOUNG'S MODULUS (-) : 33.8 GPa  
YIELD STRENGTH (+) : NA  
ULTIMATE STRENGTH (o) : 97.0 MPa





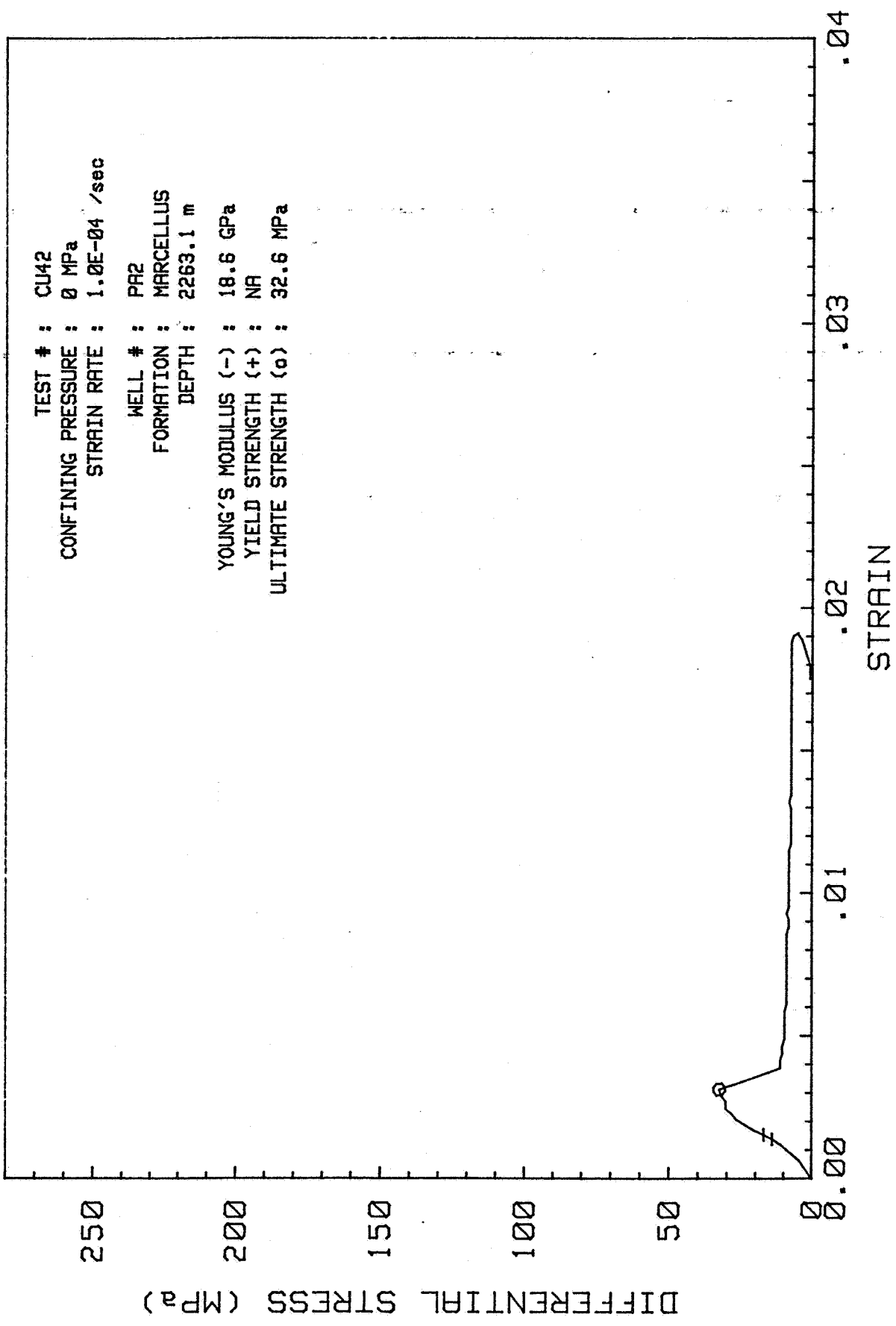


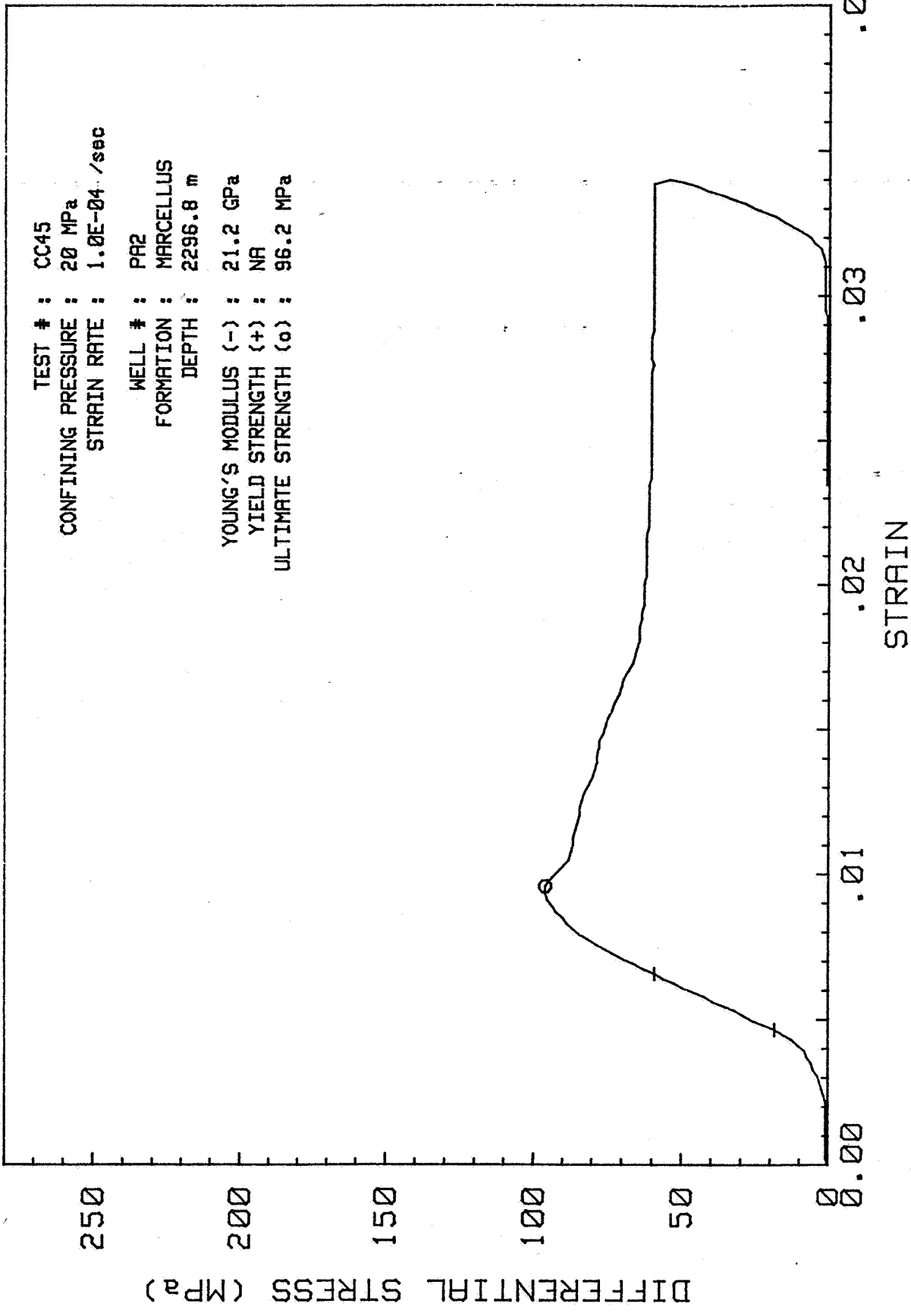


TEST # : CU42  
CONFINING PRESSURE : 0 MPa  
STRAIN RATE : 1.0E-04 /sec

WELL # : PA2  
FORMATION : MARCELLUS  
DEPTH : 2263.1 m

YOUNG'S MODULUS (-) : 18.6 GPa  
YIELD STRENGTH (+) : NA  
ULTIMATE STRENGTH (o) : 32.6 MPa

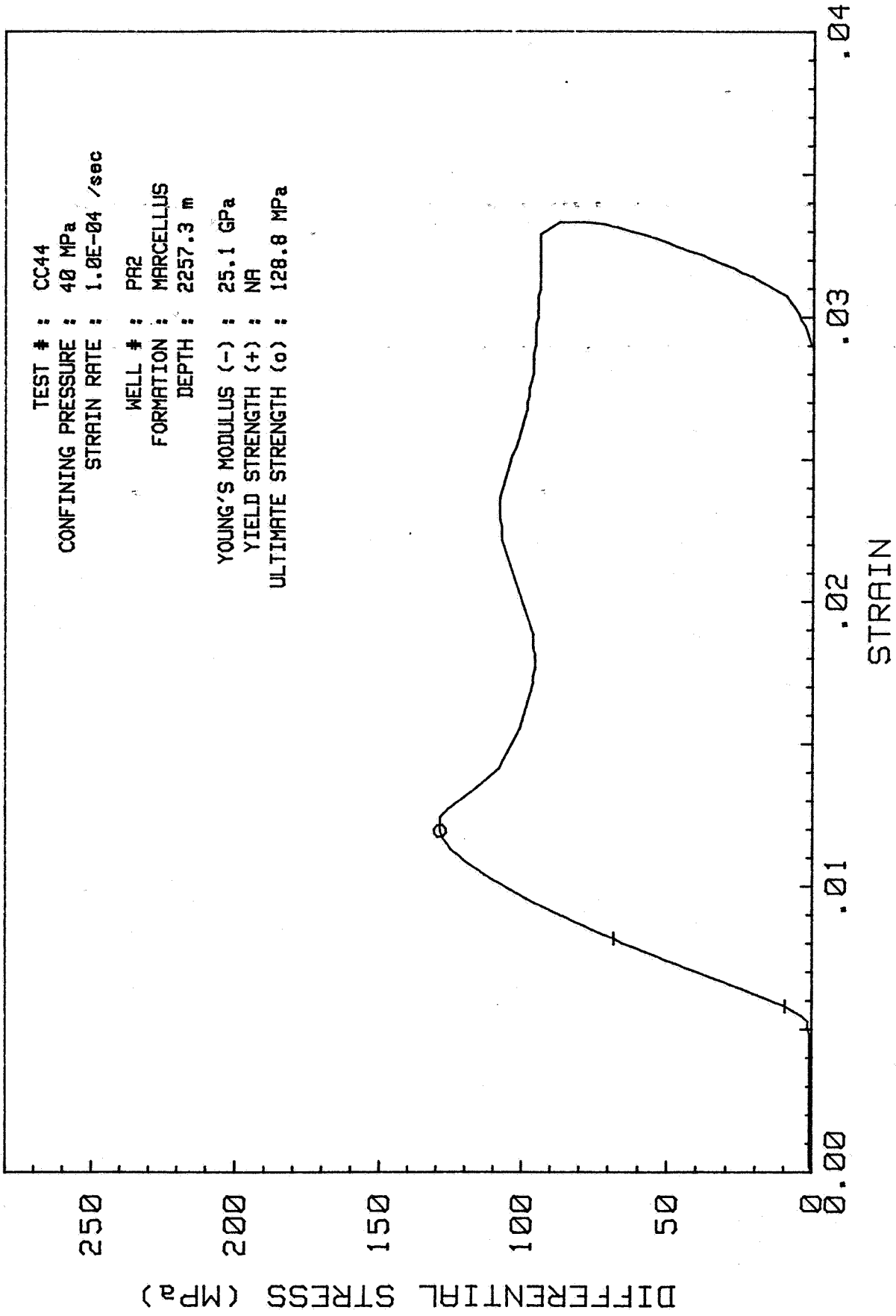


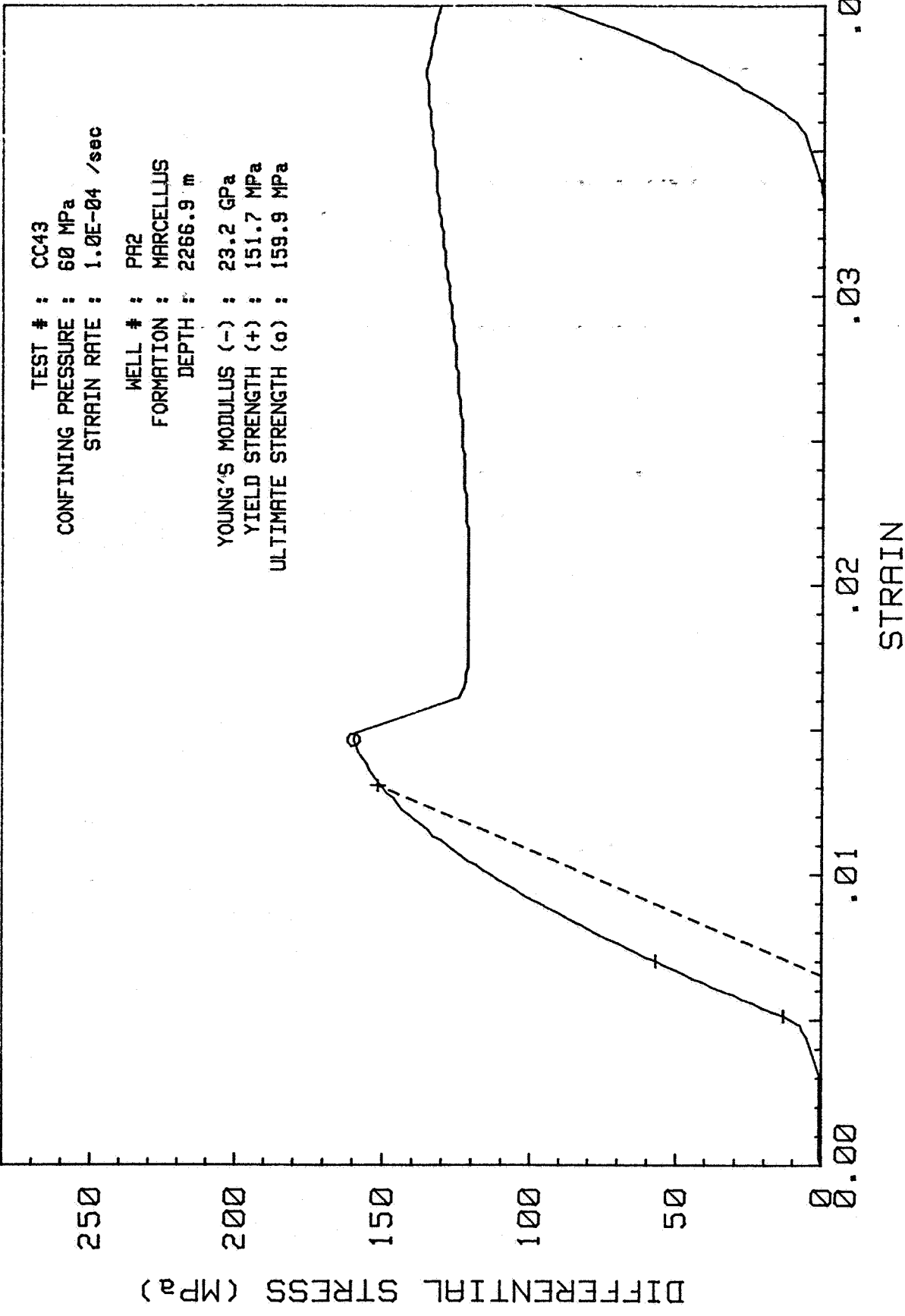


TEST # : CC44  
CONFINING PRESSURE : 40 MPa  
STRAIN RATE : 1.0E-04 /sec

WELL # : PA2  
FORMATION : MARCELLUS  
DEPTH : 2257.3 m

YOUNG'S MODULUS (-) : 25.1 GPa  
YIELD STRENGTH (+) : NA  
ULTIMATE STRENGTH (o) : 128.8 MPa

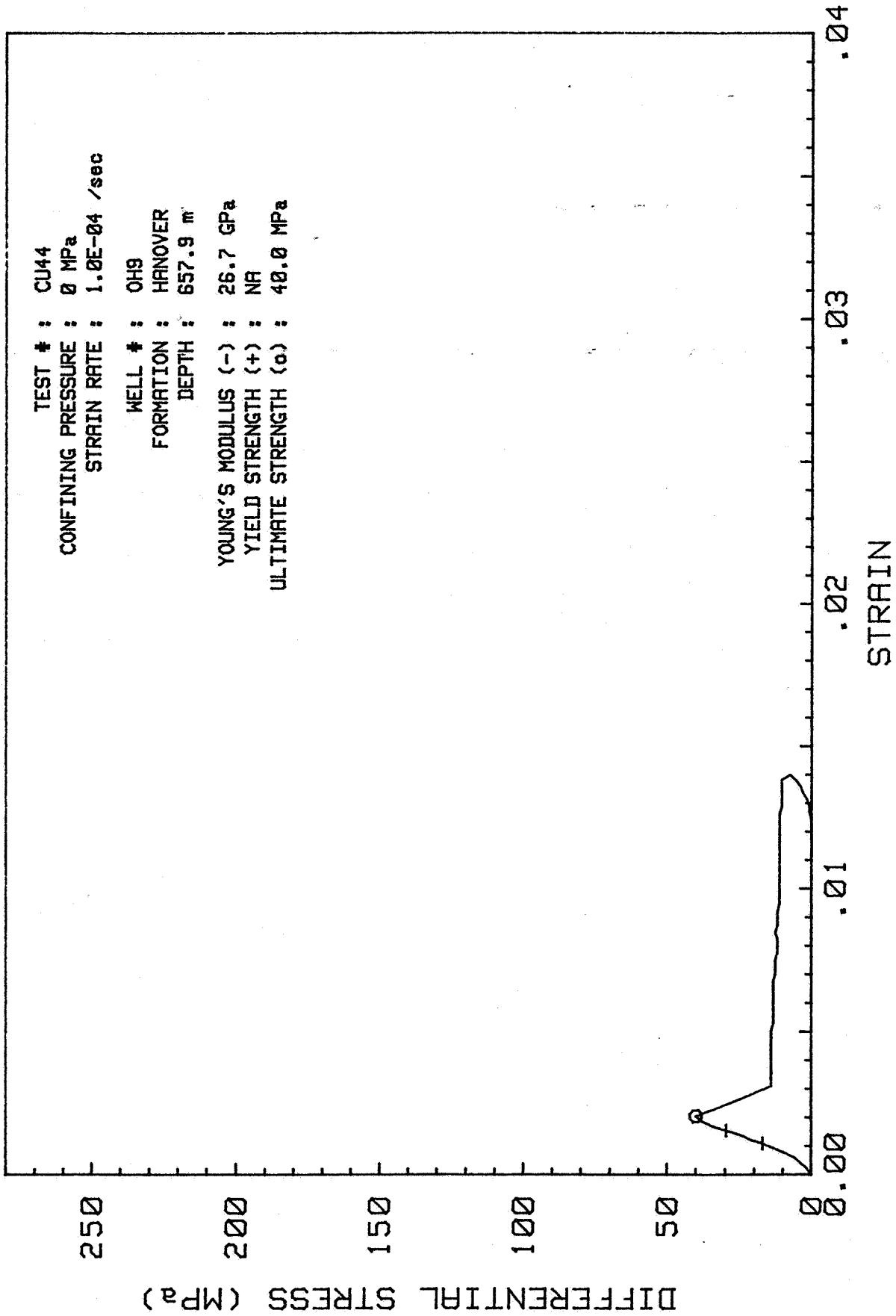




TEST # : CU44  
CONFINING PRESSURE : 0 MPa  
STRAIN RATE : 1.0E-04 /sec

WELL # : OH9  
FORMATION : HANOVER  
DEPTH : 657.9 m

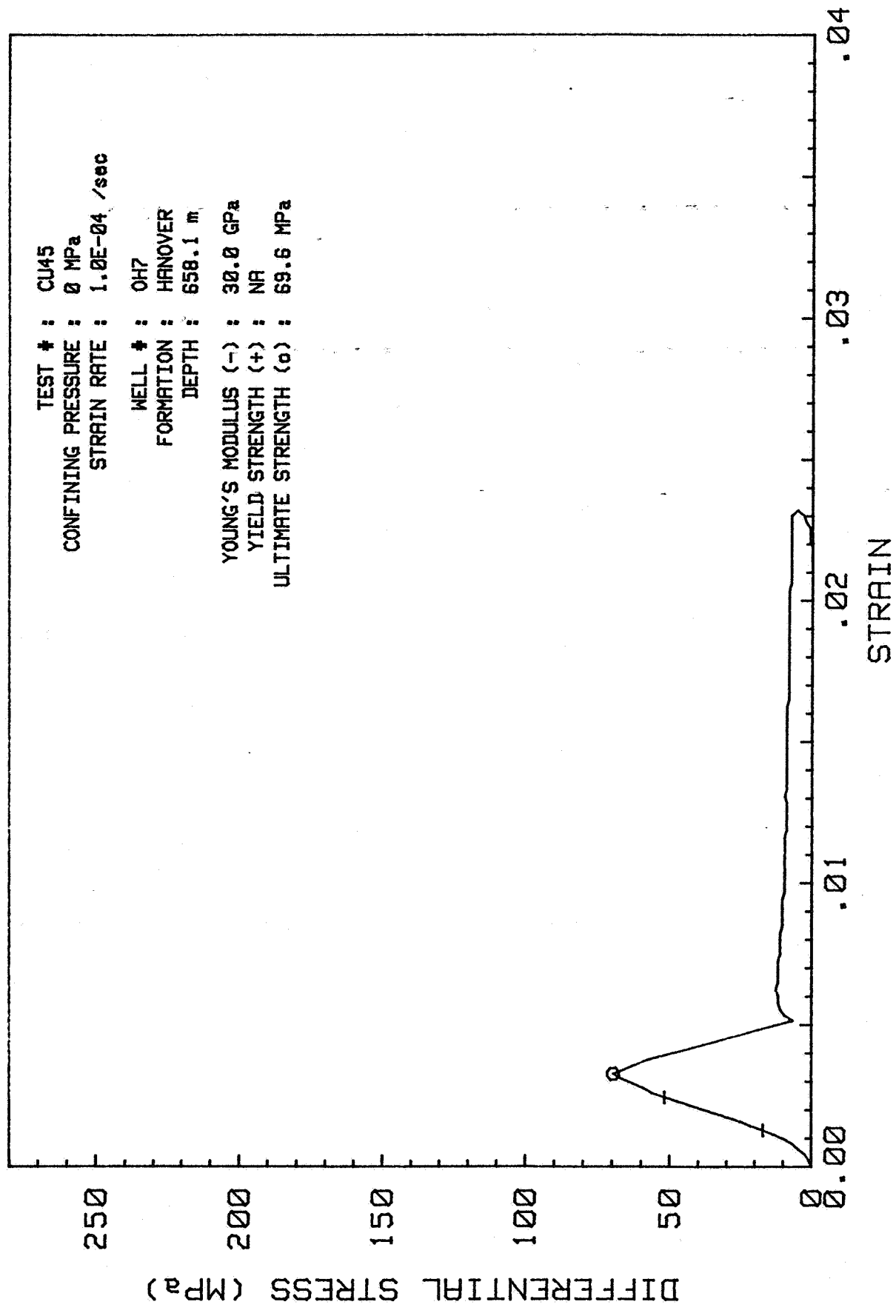
YOUNG'S MODULUS (-) : 26.7 GPa  
YIELD STRENGTH (+) : NA  
ULTIMATE STRENGTH (o) : 40.0 MPa



TEST # : CU45  
CONFINING PRESSURE : 0 MPa  
STRAIN RATE : 1.0E-04 /sec

WELL # : OH7  
FORMATION : HANOVER  
DEPTH : 658.1 m

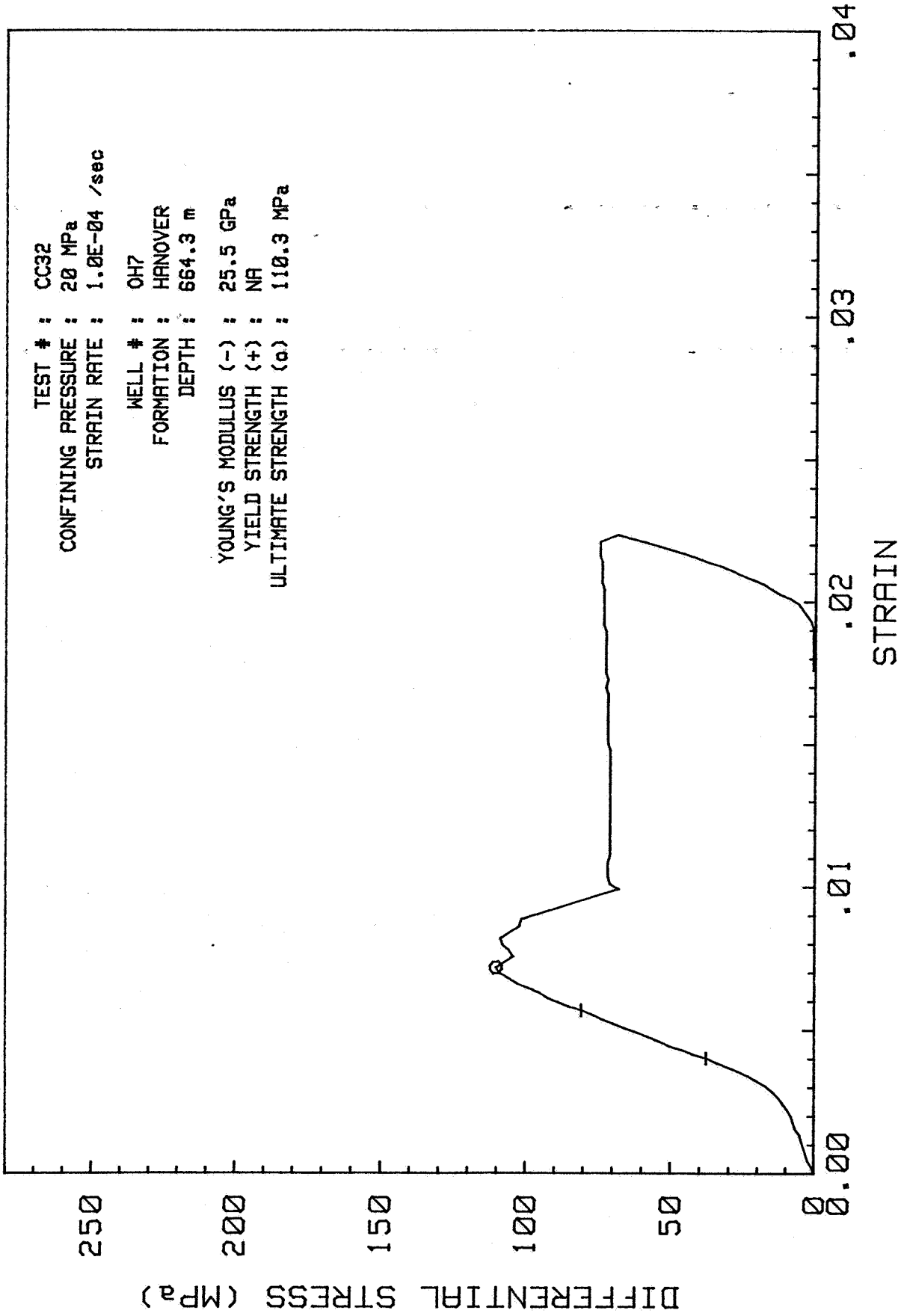
YOUNG'S MODULUS (-) : 30.0 GPa  
YIELD STRENGTH (+) : NA  
ULTIMATE STRENGTH (o) : 69.6 MPa



TEST # : CC32  
CONFINING PRESSURE : 20 MPa  
STRAIN RATE : 1.0E-04 /sec

WELL # : OH7  
FORMATION : HANOVER  
DEPTH : 664.3 m

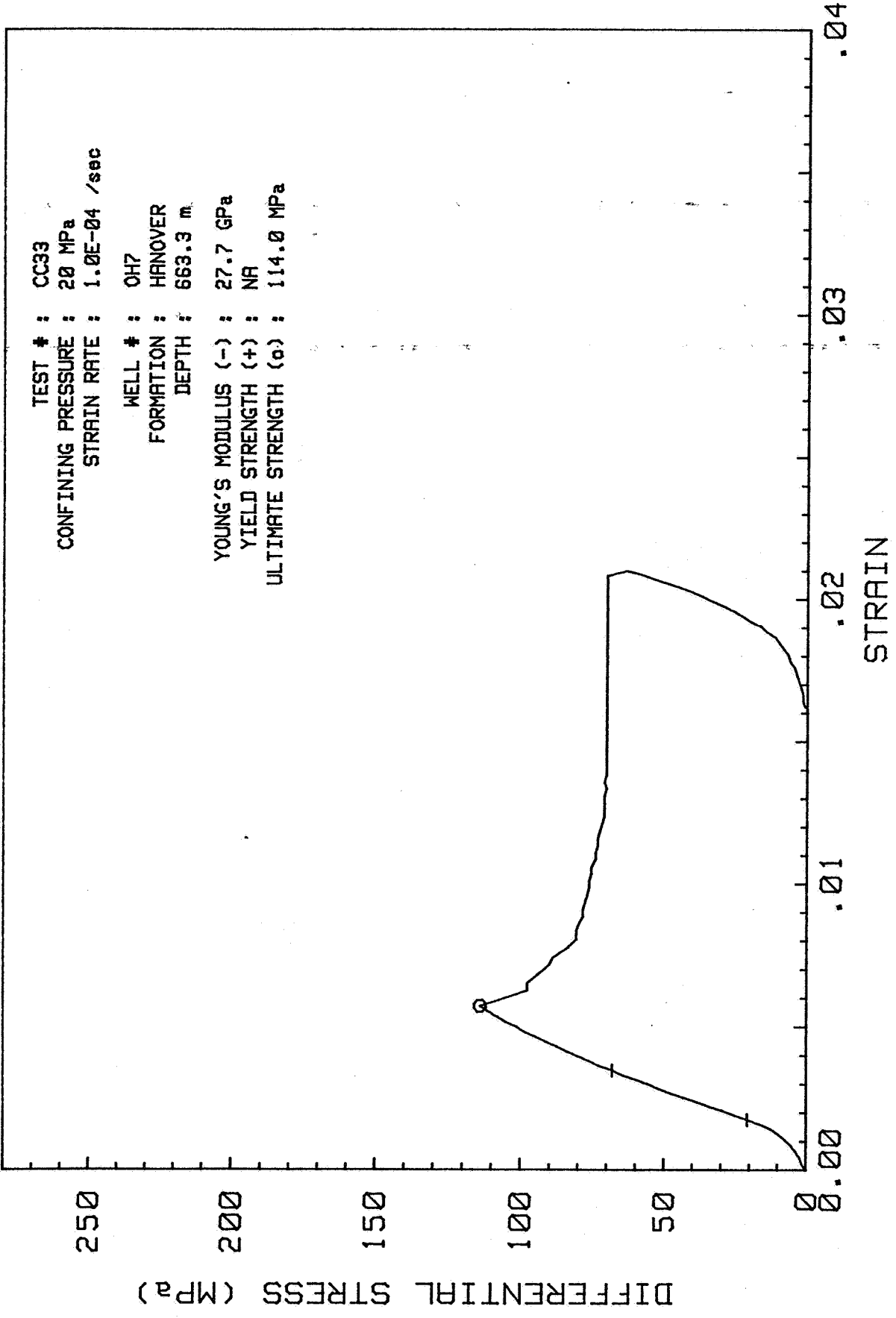
YOUNG'S MODULUS (-) : 25.5 GPa  
YIELD STRENGTH (+) : NA  
ULTIMATE STRENGTH (o) : 110.3 MPa



TEST # : CC33  
CONFINING PRESSURE : 20 MPa  
STRAIN RATE : 1.0E-04 /sec

WELL # : OH7  
FORMATION : HANOVER  
DEPTH : 663.3 m

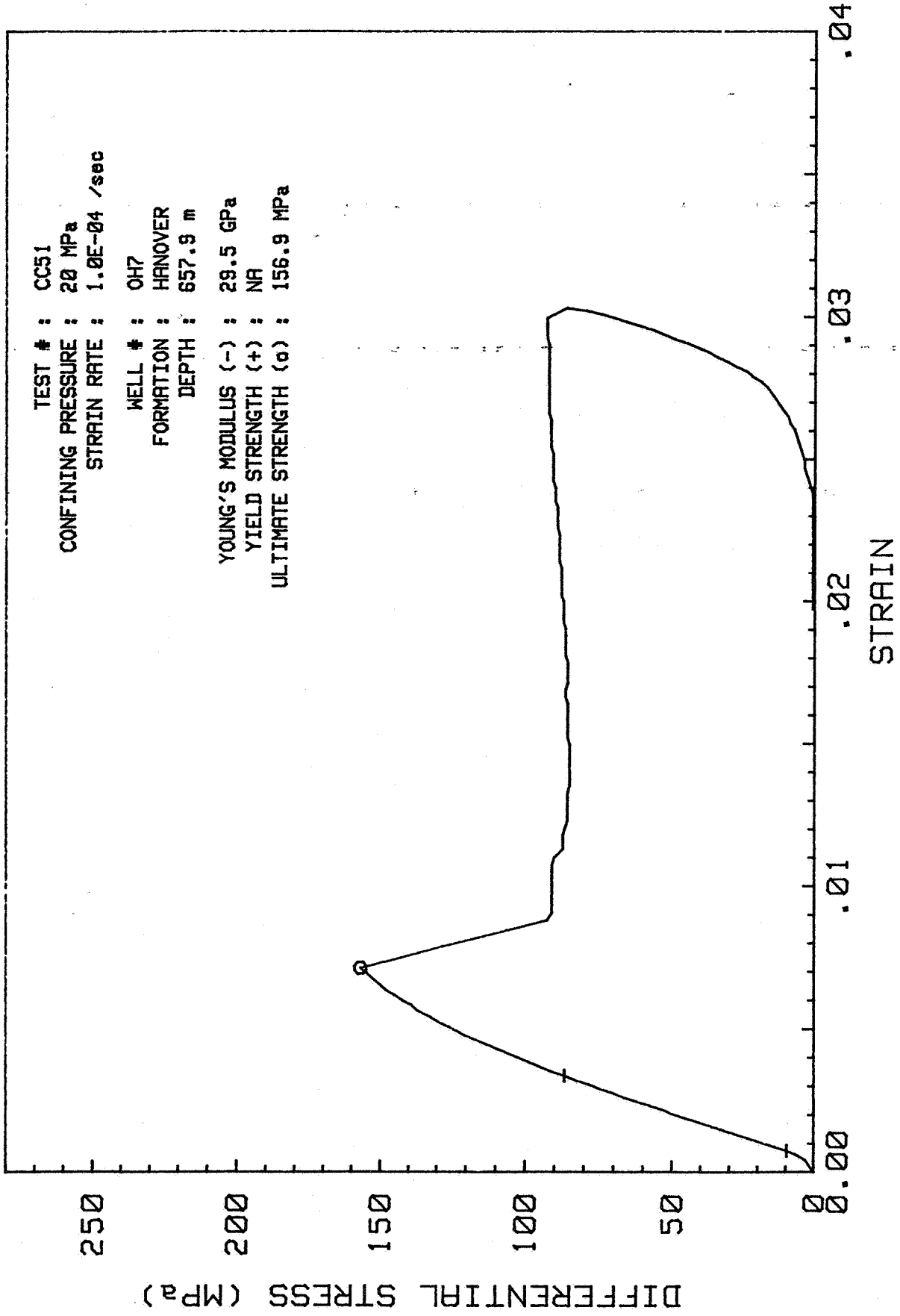
YOUNG'S MODULUS (-) : 27.7 GPa  
YIELD STRENGTH (+) : NA  
ULTIMATE STRENGTH (o) : 114.0 MPa

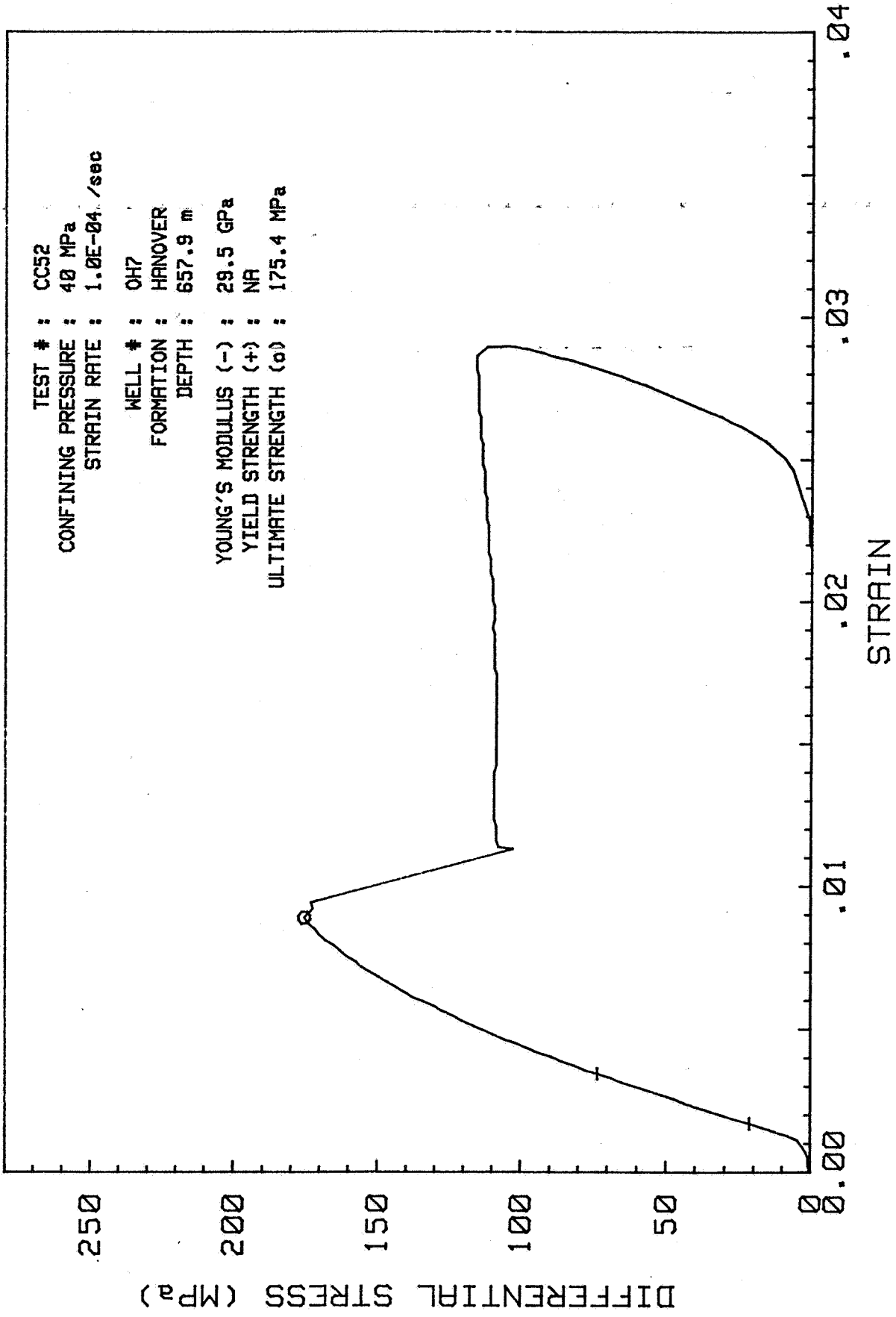


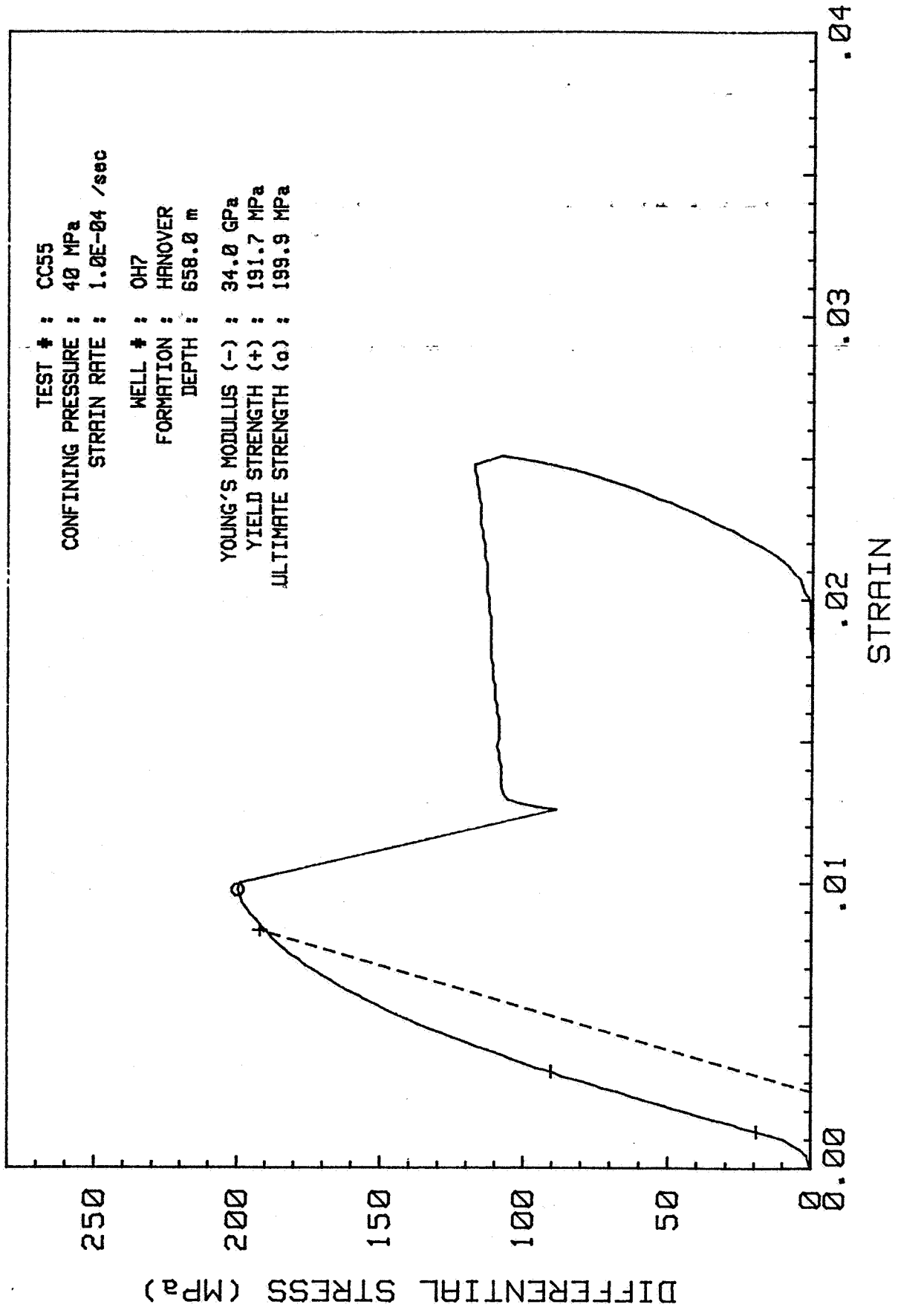
TEST # : CC51  
CONFINING PRESSURE : 20 MPa  
STRAIN RATE : 1.0E-04 /sec

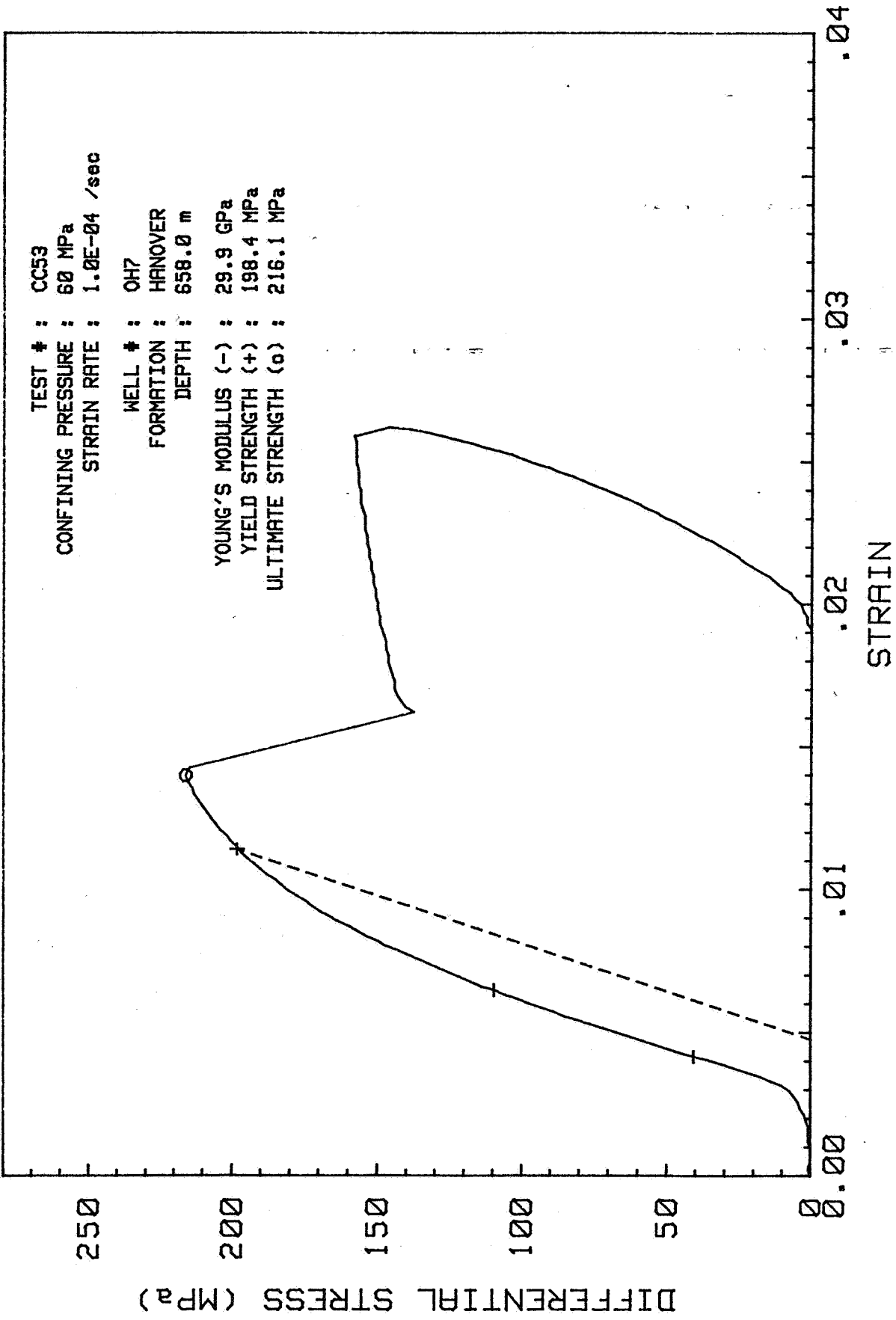
WELL # : OH7  
FORMATION : HANOVER  
DEPTH : 657.9 m

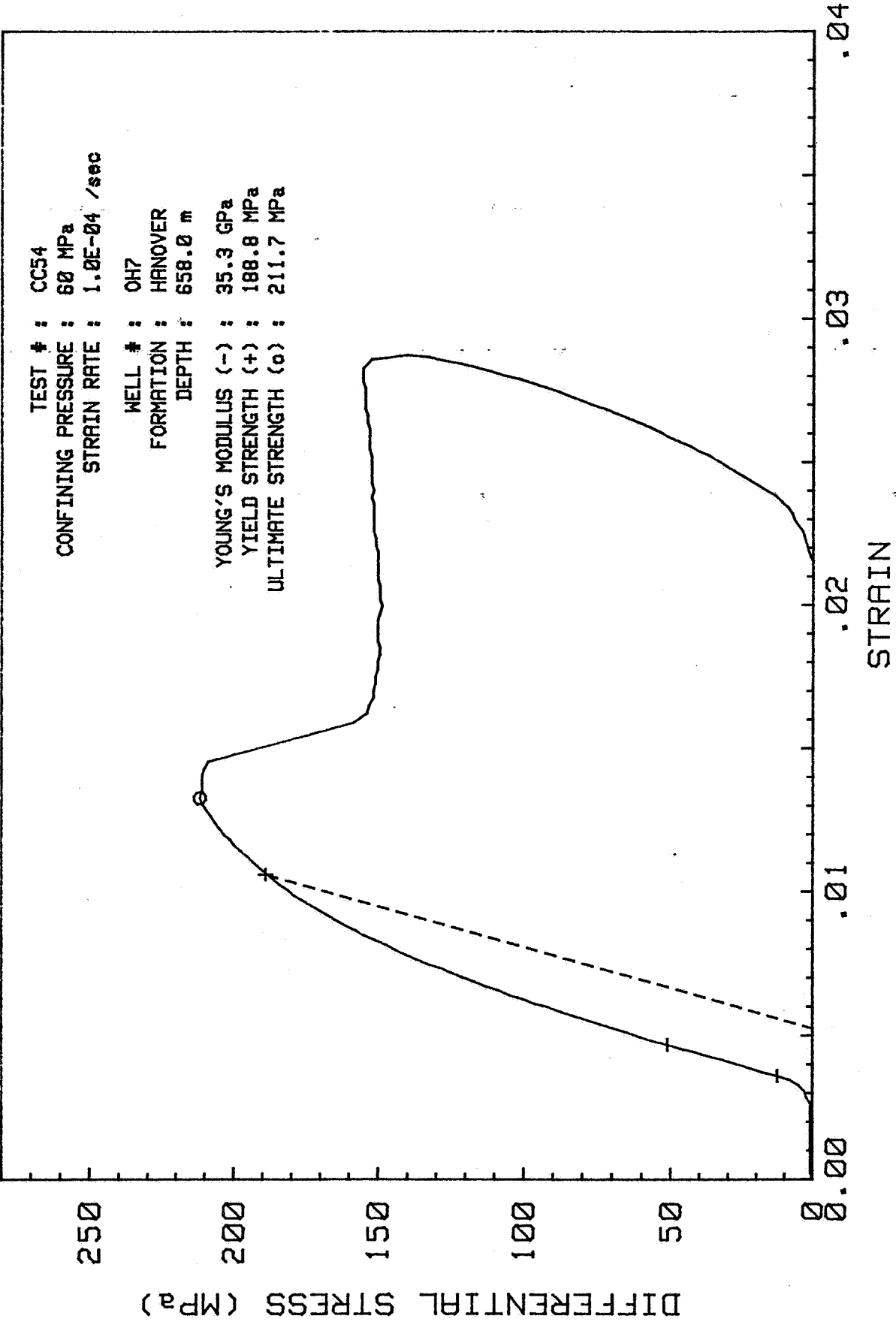
YOUNG'S MODULUS (-) : 29.5 GPa  
YIELD STRENGTH (+) : NA  
ULTIMATE STRENGTH (o) : 156.9 MPa







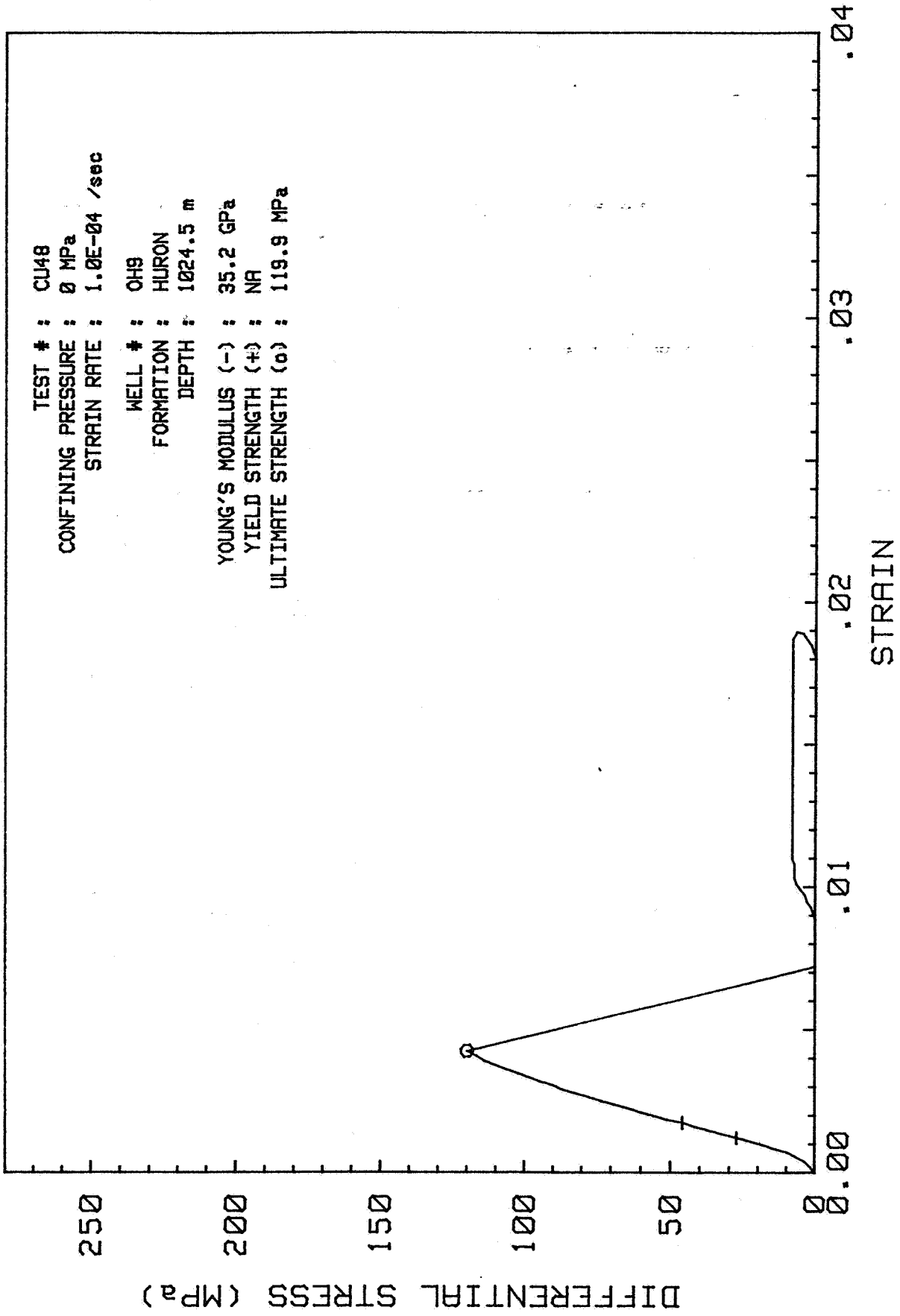


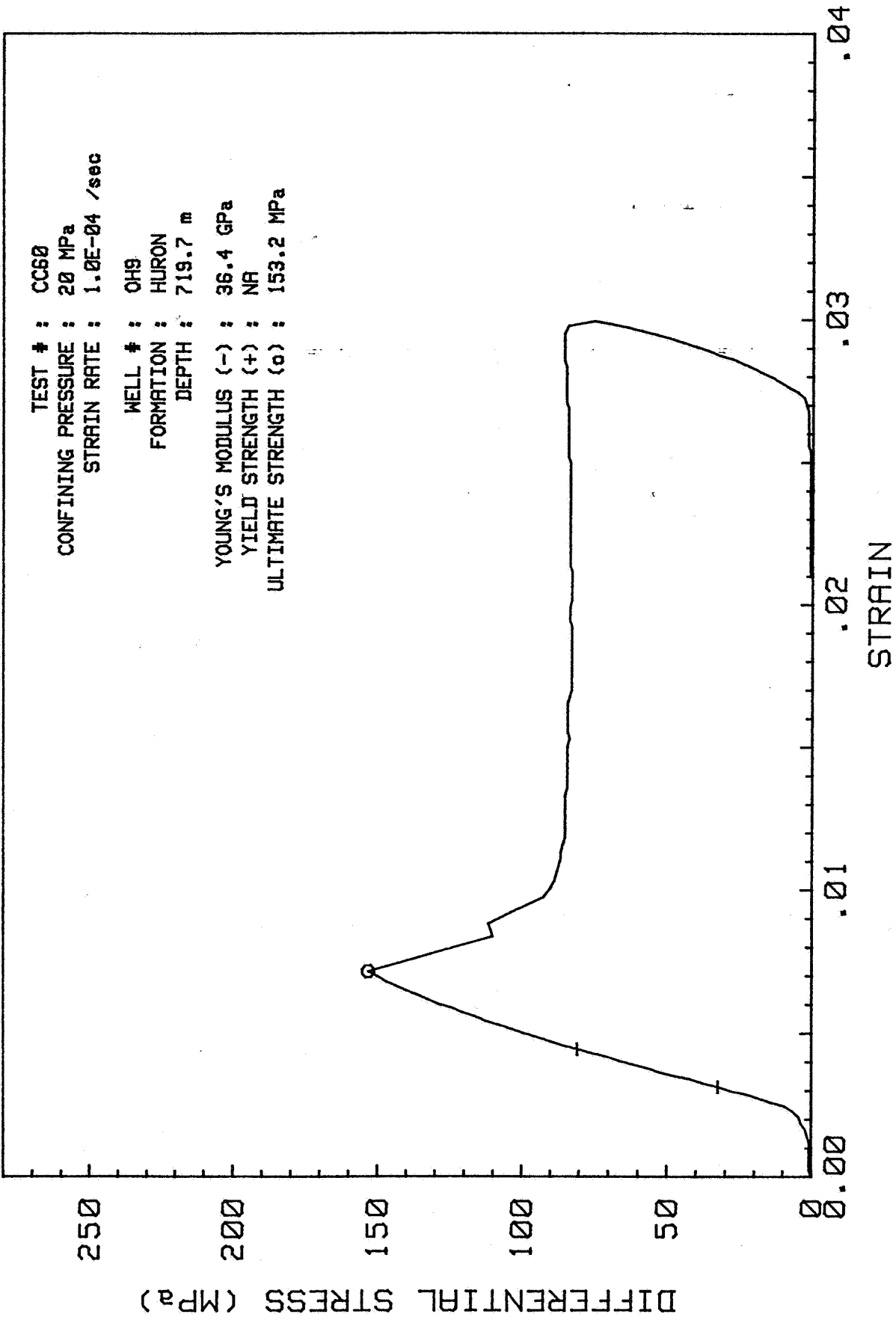


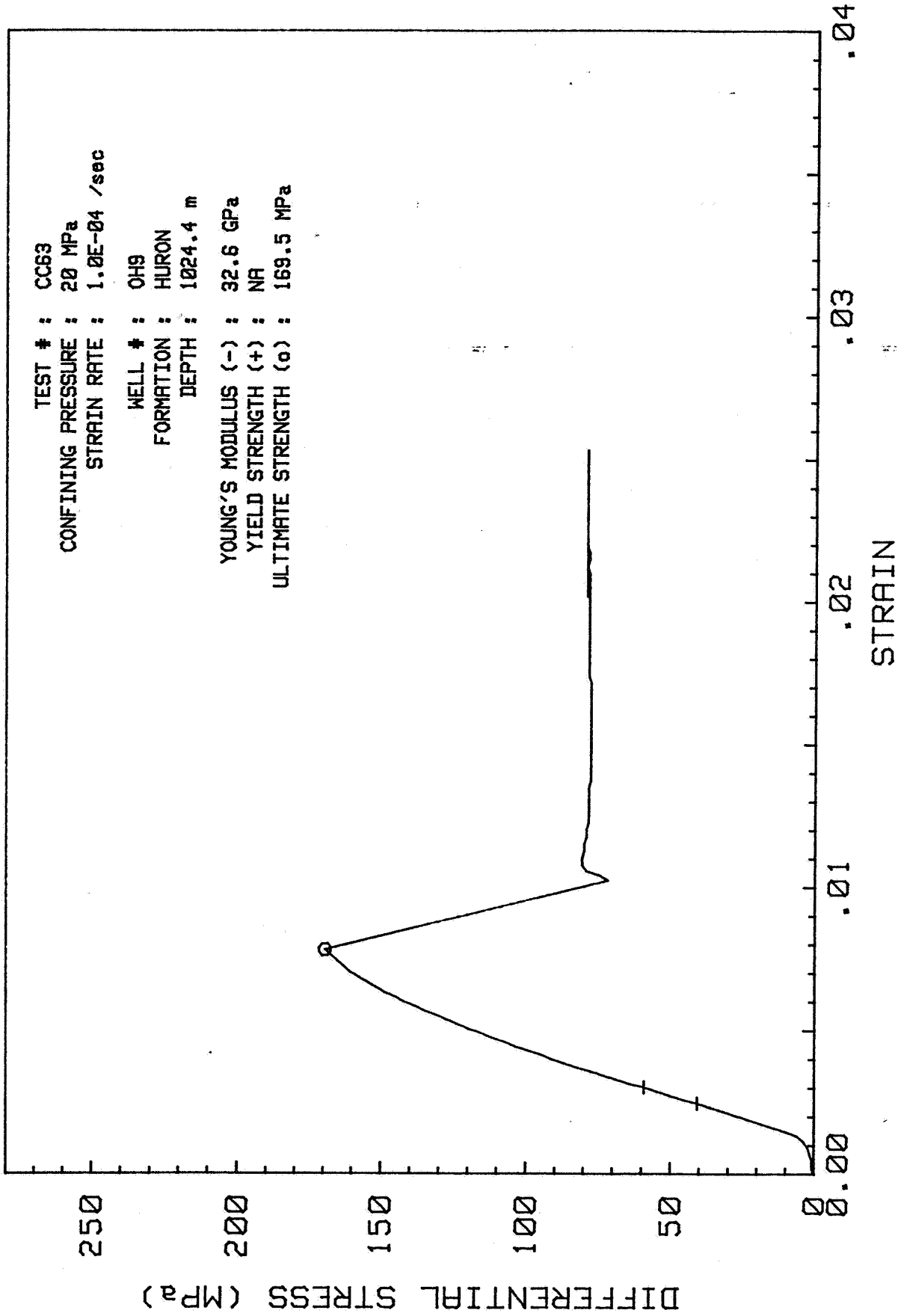
TEST # : CU48  
CONFINING PRESSURE : 0 MPa  
STRAIN RATE : 1.0E-04 /sec

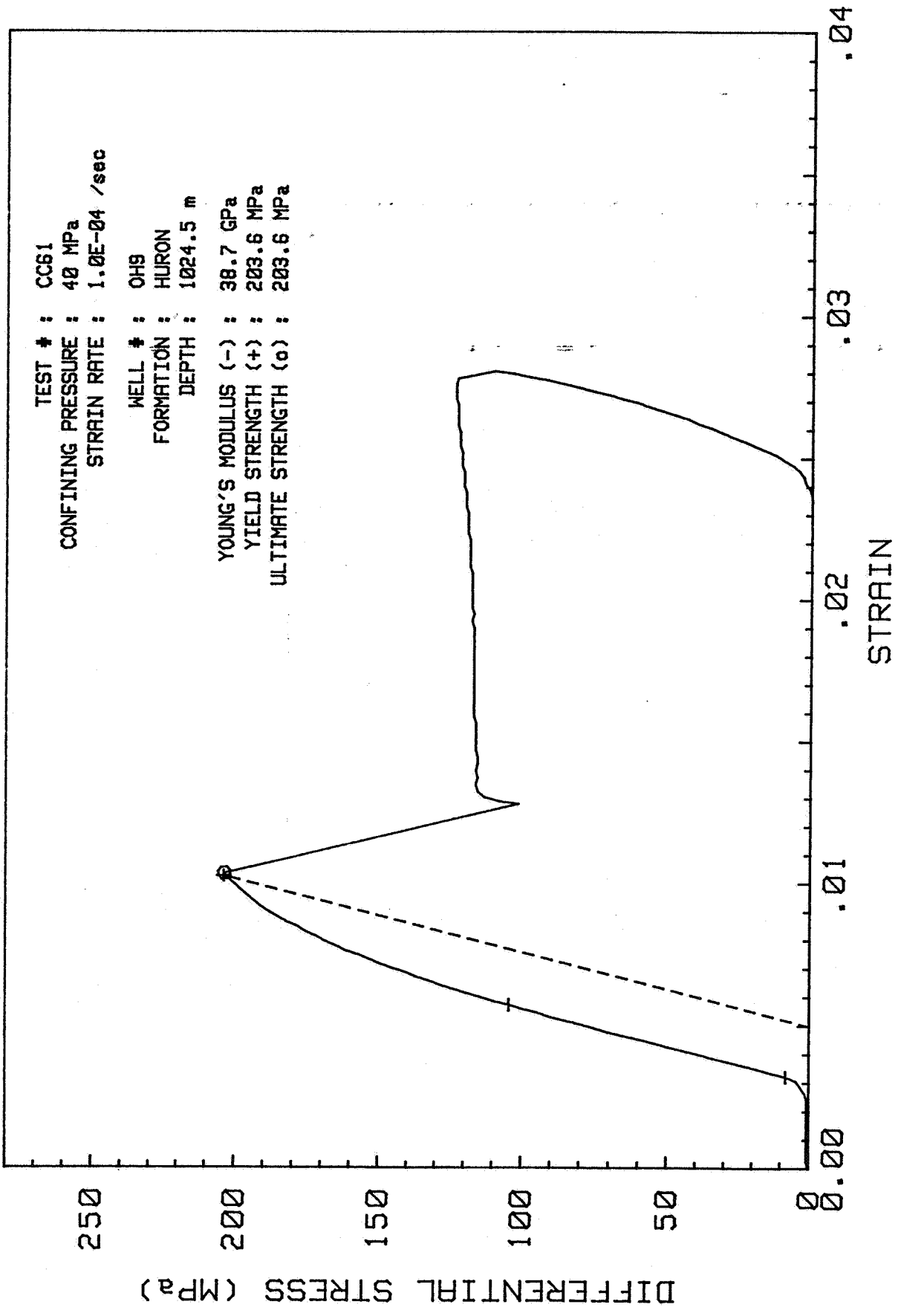
WELL # : OH9  
FORMATION : HURON  
DEPTH : 1024.5 m

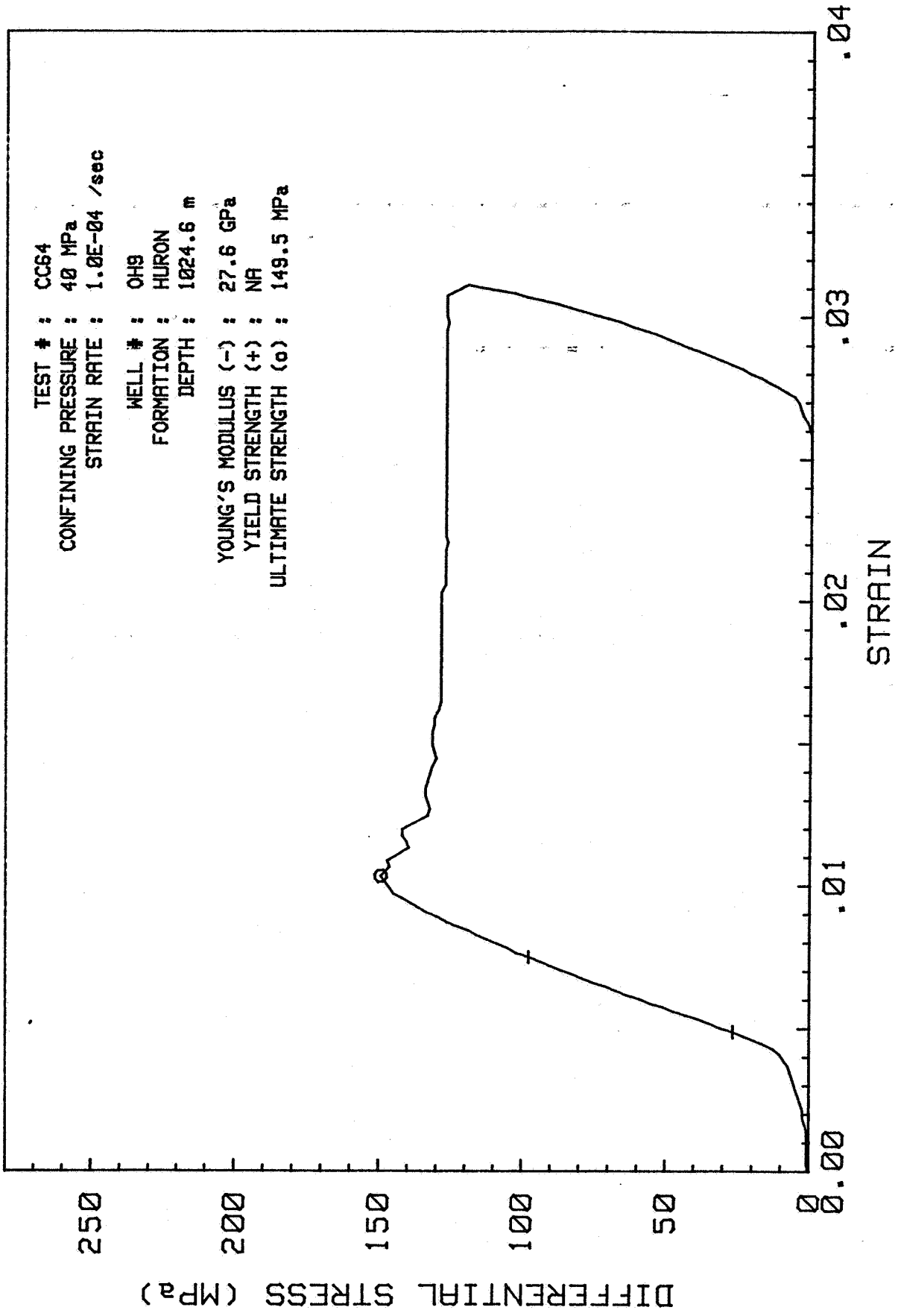
YOUNG'S MODULUS (-) : 35.2 GPa  
YIELD STRENGTH (+) : NA  
ULTIMATE STRENGTH (o) : 119.9 MPa

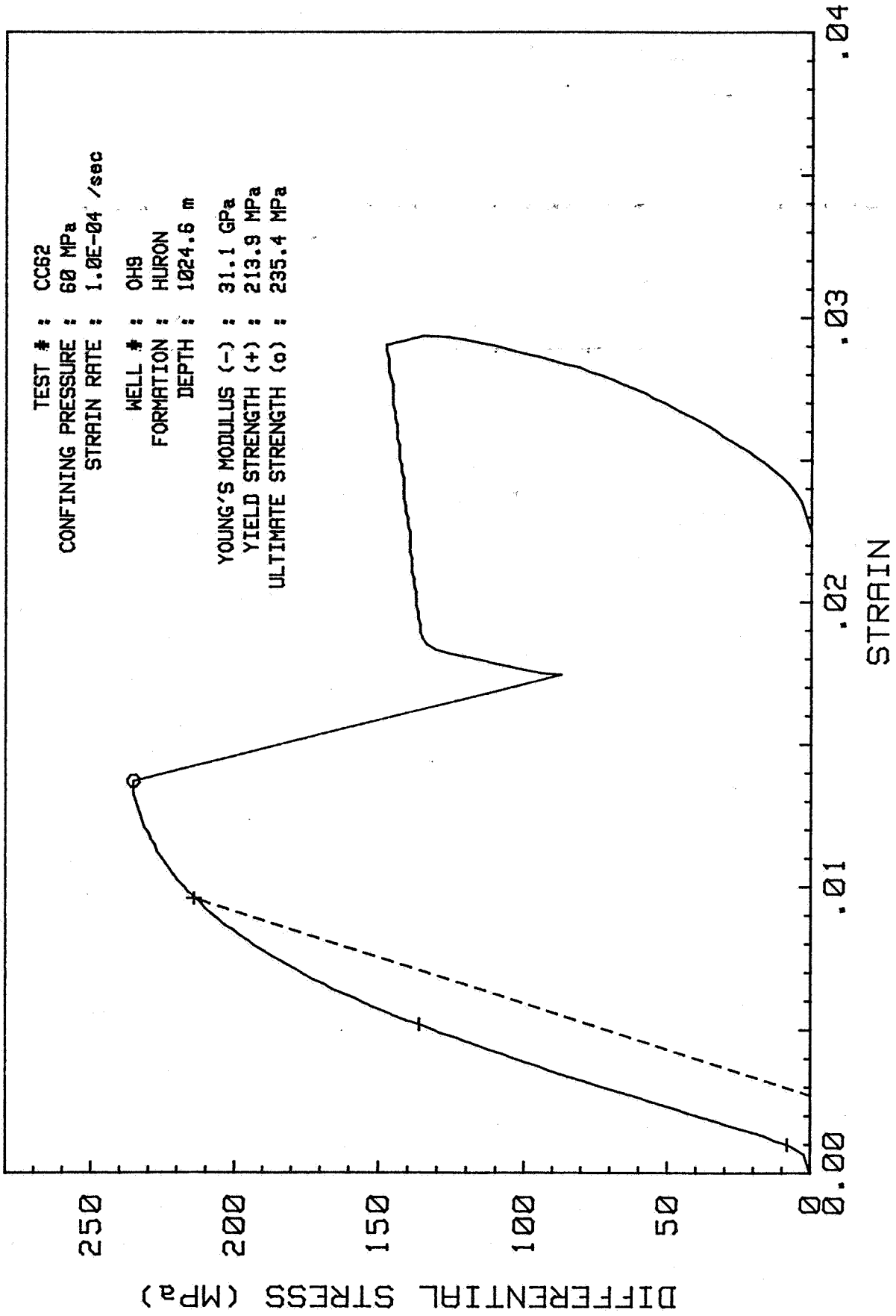








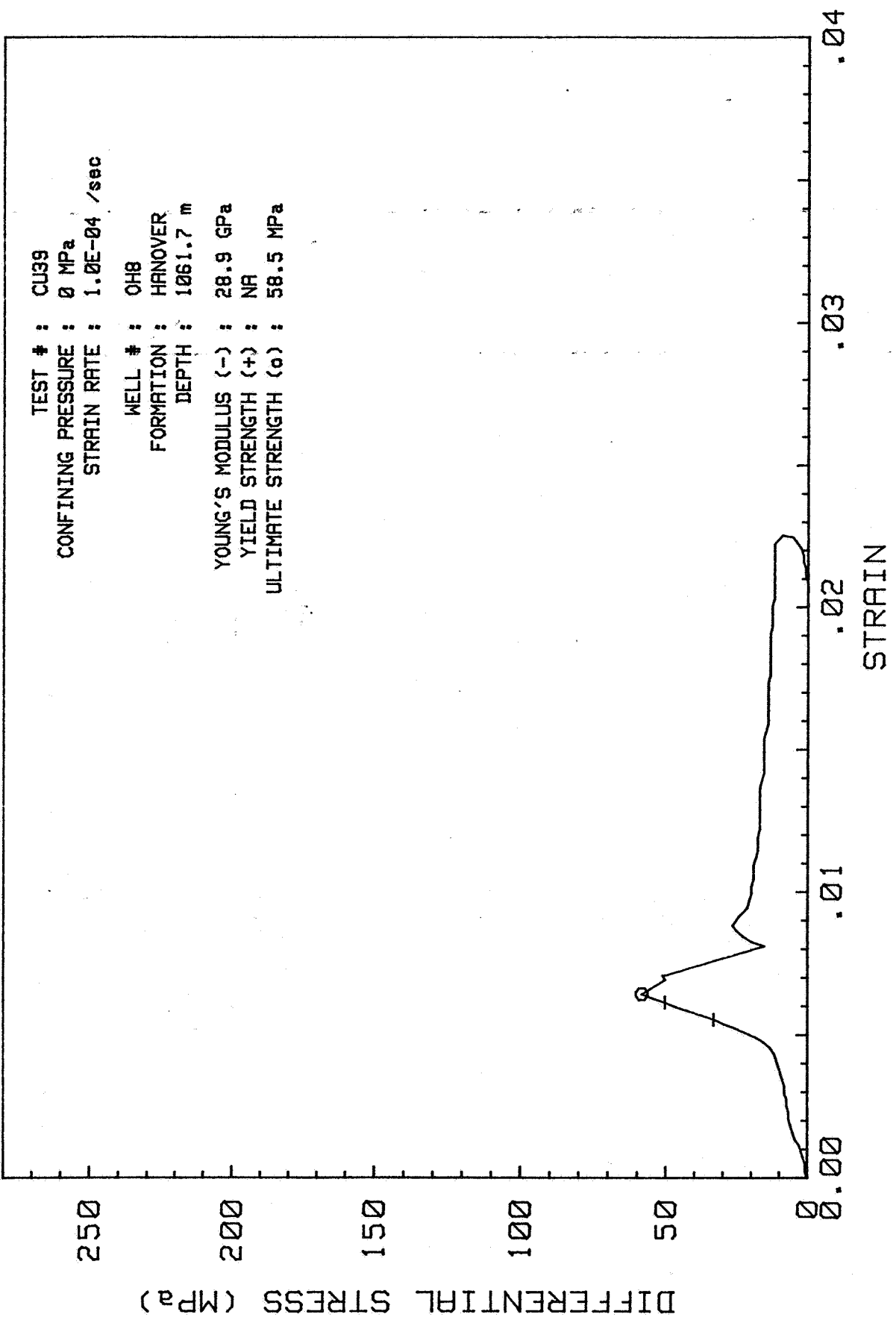


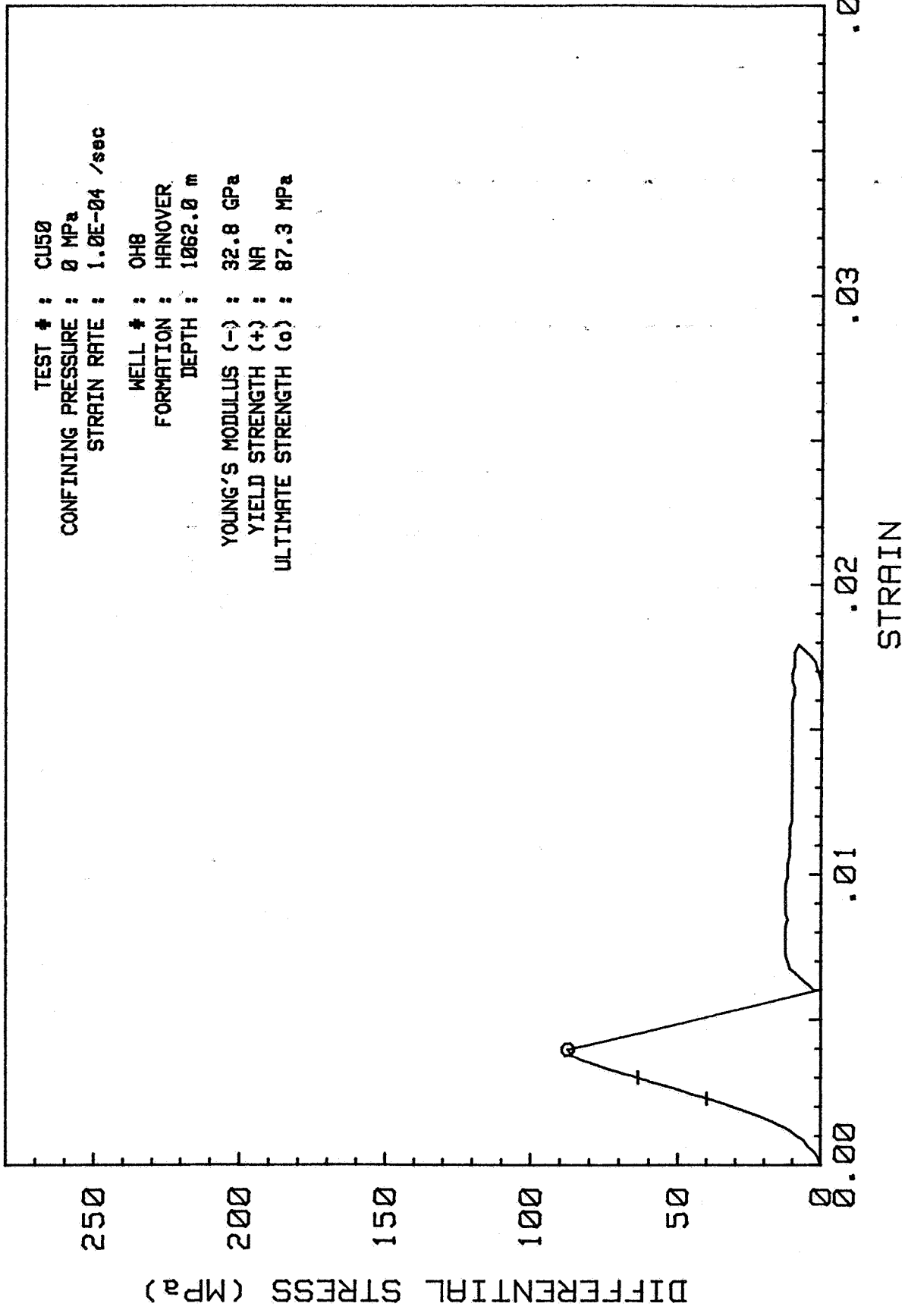


TEST # : CU39  
CONFINING PRESSURE : 0 MPa  
STRAIN RATE : 1.0E-04 /sec

WELL # : OH8  
FORMATION : HANOVER  
DEPTH : 1061.7 m

YOUNG'S MODULUS (-) : 28.9 GPa  
YIELD STRENGTH (+) : NA  
ULTIMATE STRENGTH (o) : 58.5 MPa

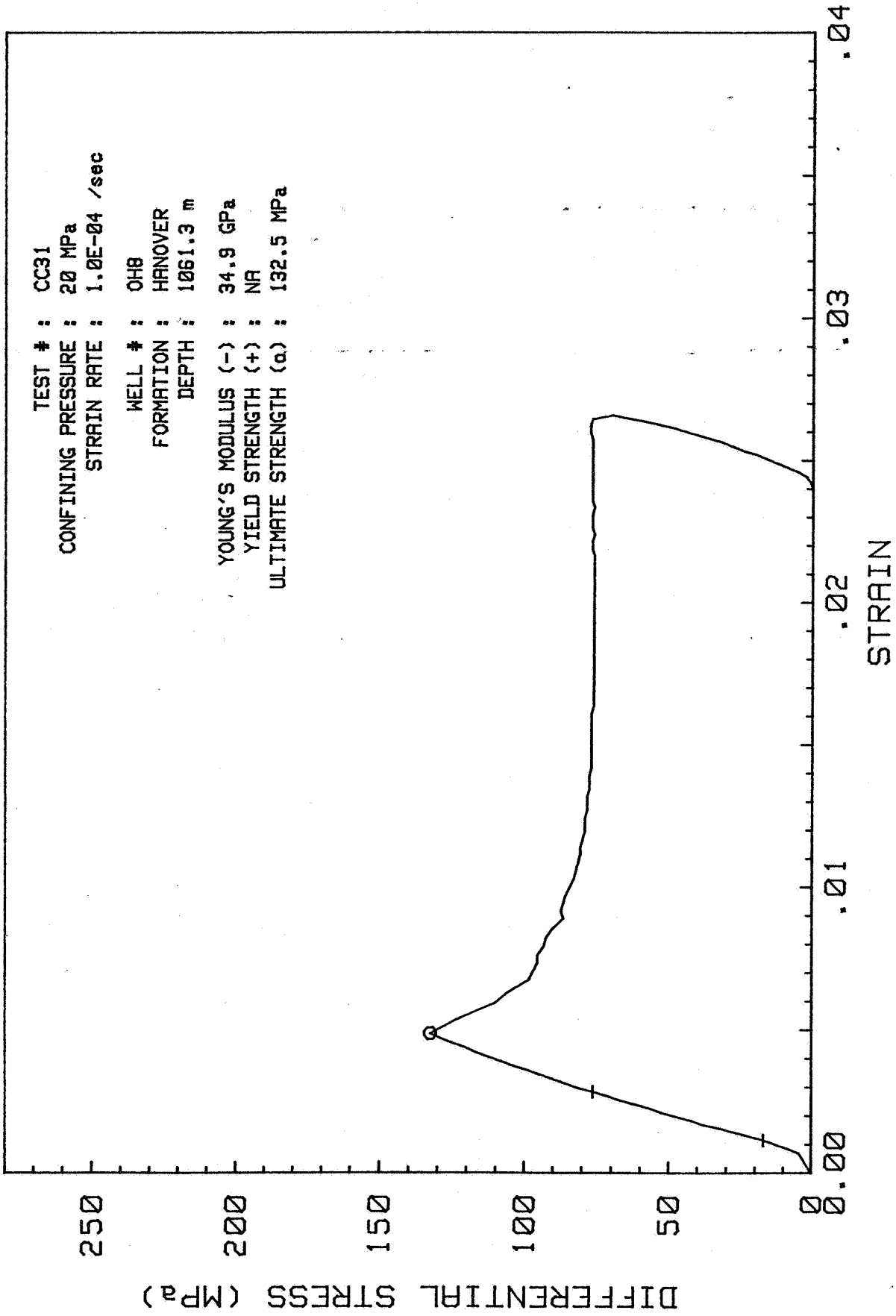




TEST # : CC31  
CONFINING PRESSURE : 20 MPa  
STRAIN RATE : 1.0E-04 /sec

WELL # : OH8  
FORMATION : HANOVER  
DEPTH : 1061.3 m

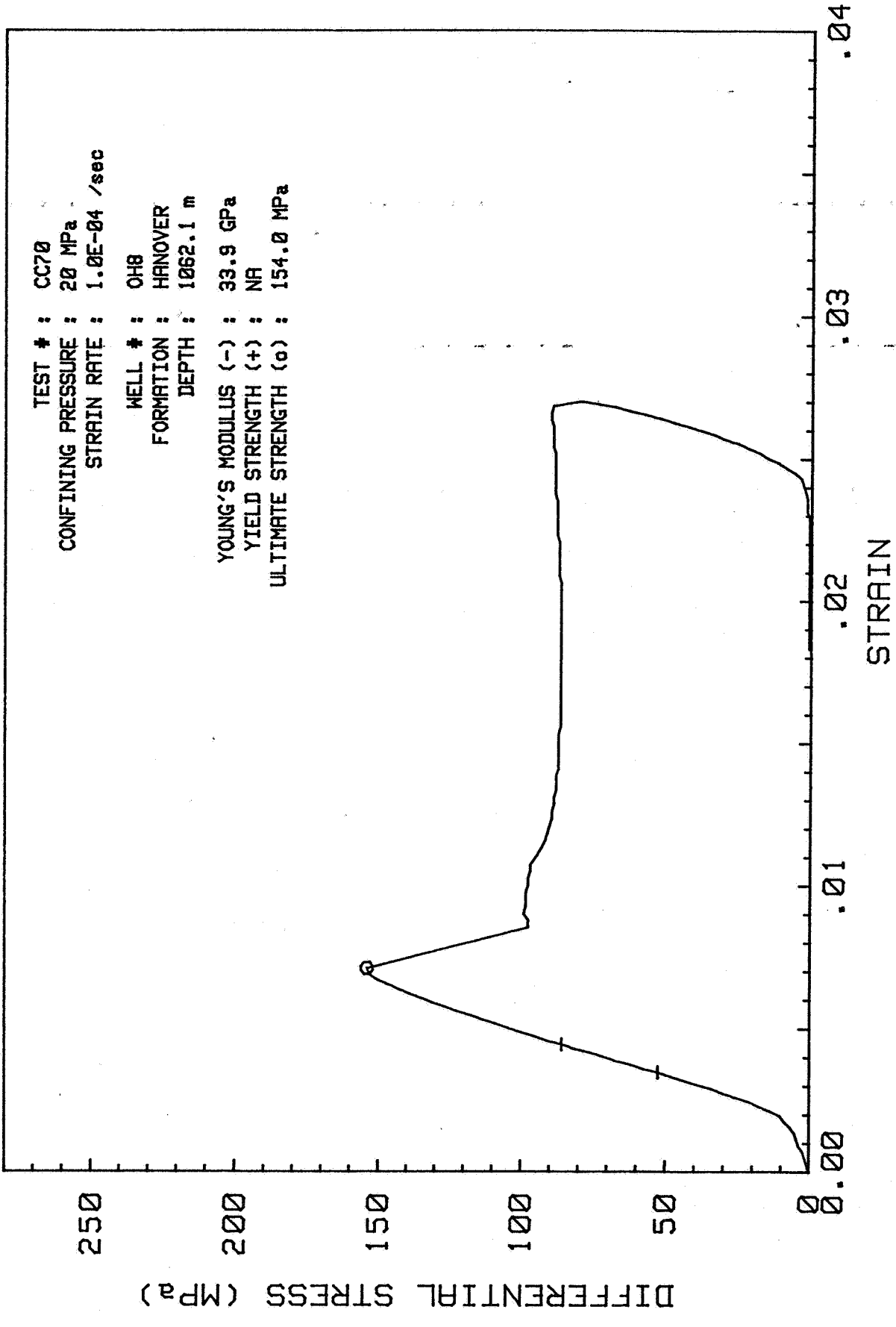
YOUNG'S MODULUS (-) : 34.9 GPa  
YIELD STRENGTH (+) : NA  
ULTIMATE STRENGTH (α) : 132.5 MPa

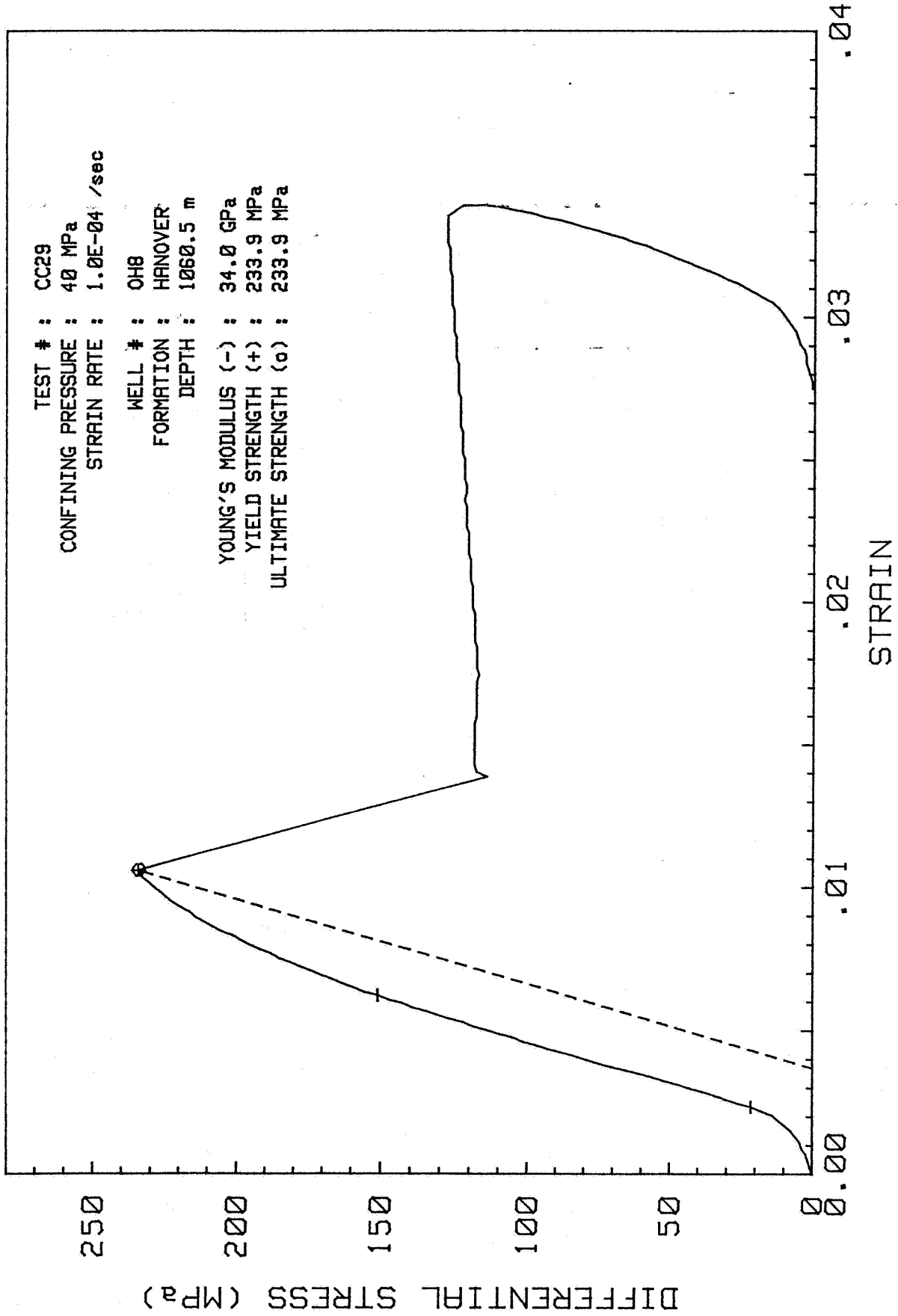


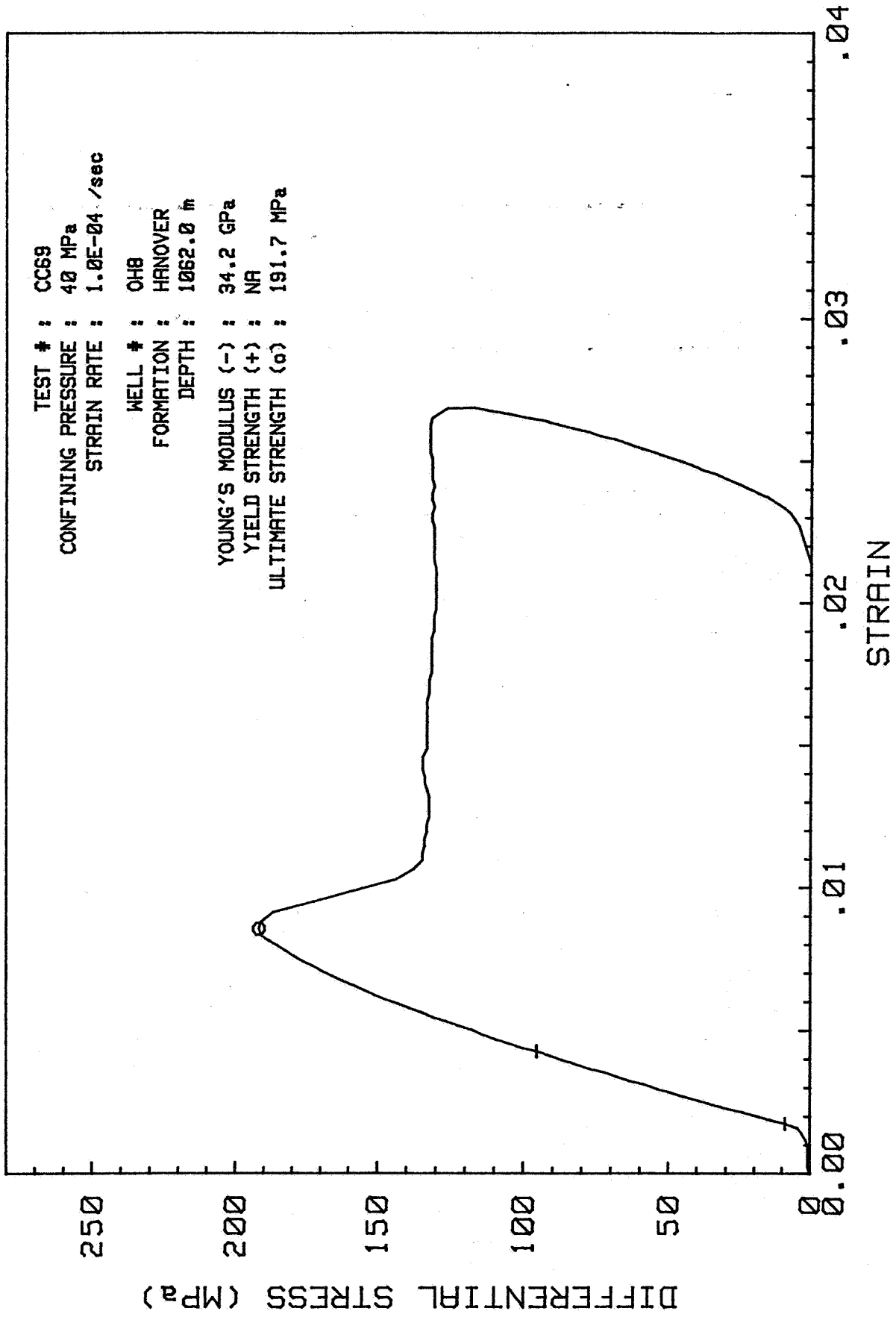
TEST # : CC70  
CONFINING PRESSURE : 20 MPa  
STRAIN RATE : 1.0E-04 /sec

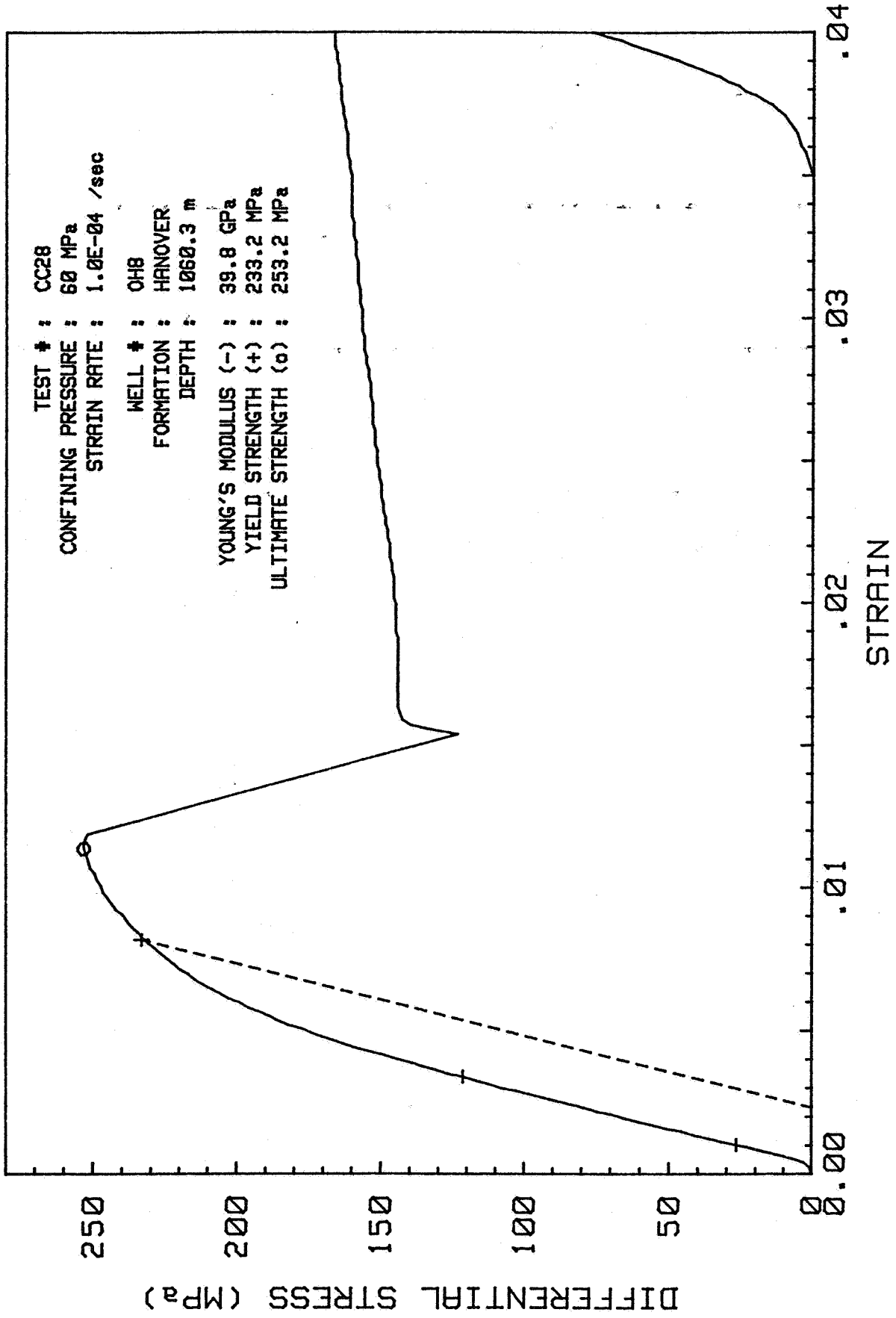
WELL # : OH8  
FORMATION : HANOVER  
DEPTH : 1062.1 m

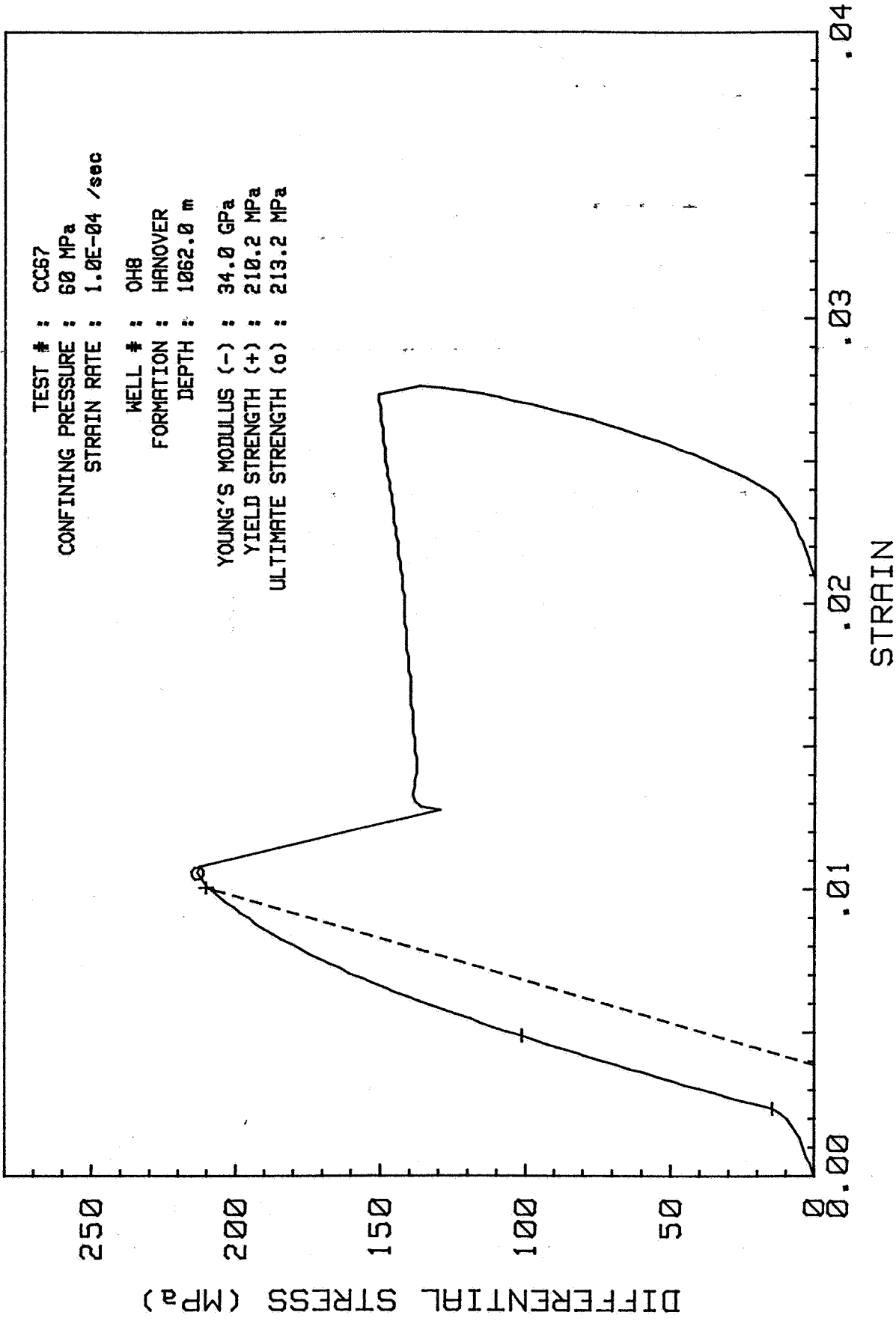
YOUNG'S MODULUS (-) : 33.9 GPa  
YIELD STRENGTH (+) : NA  
ULTIMATE STRENGTH (o) : 154.0 MPa

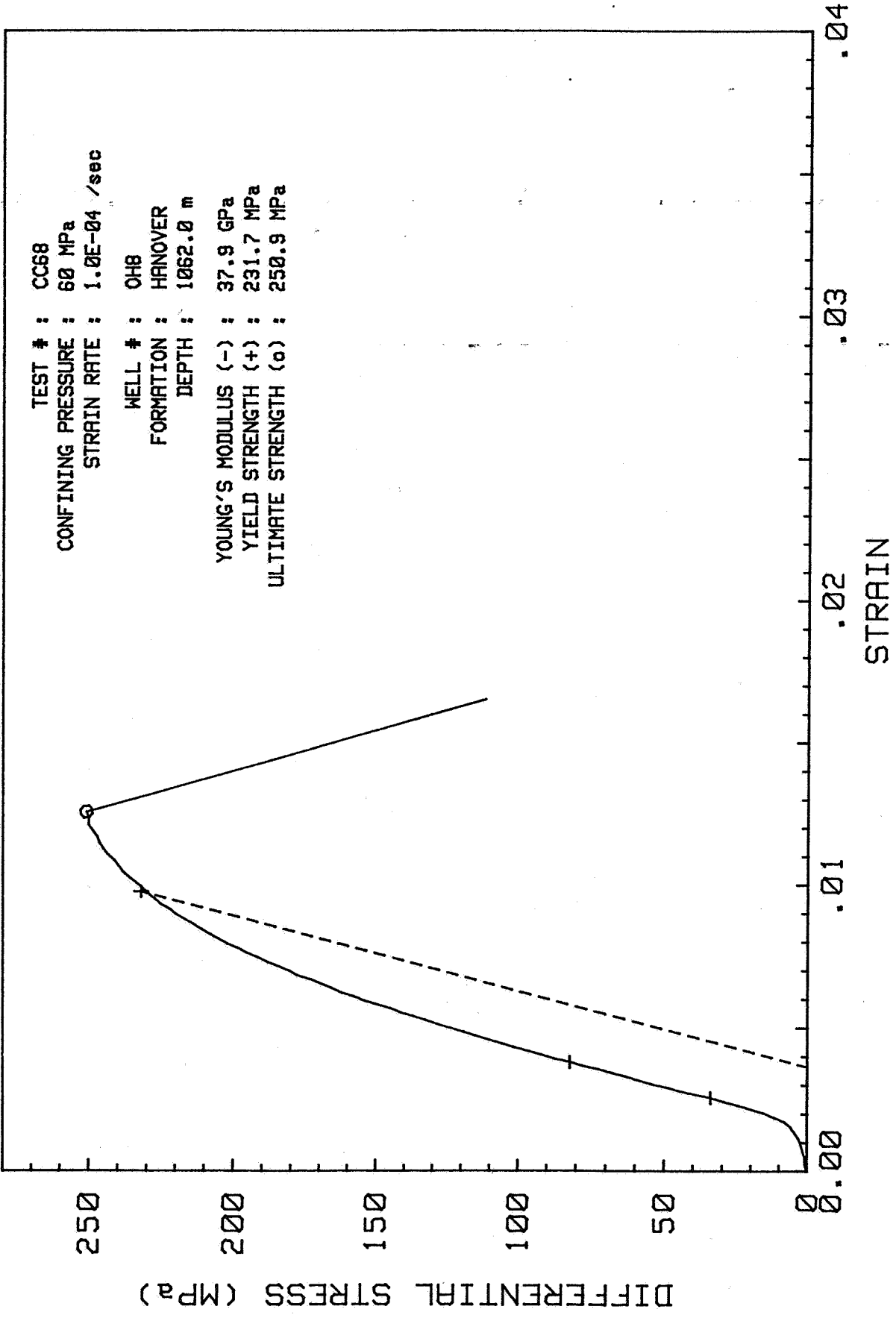








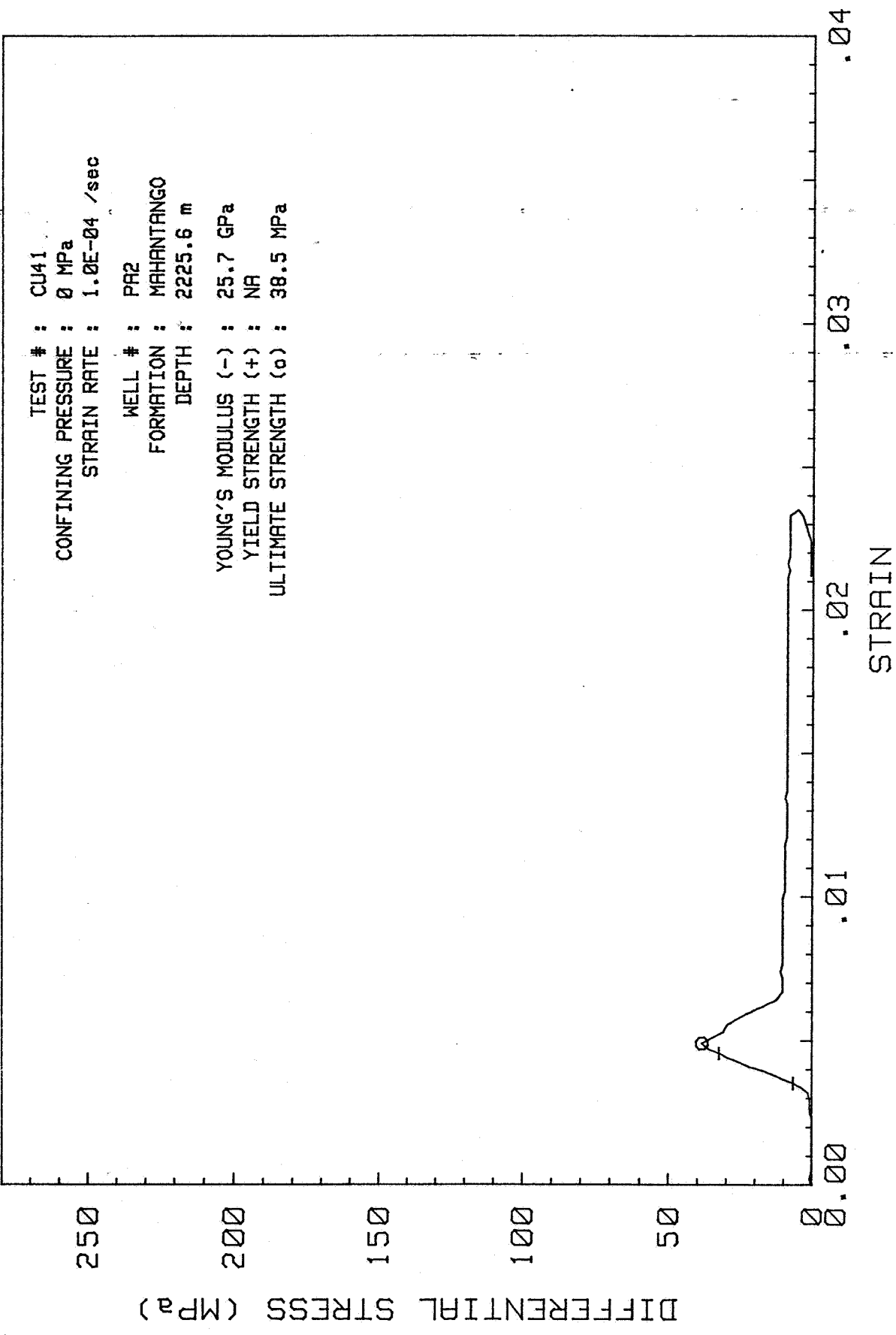


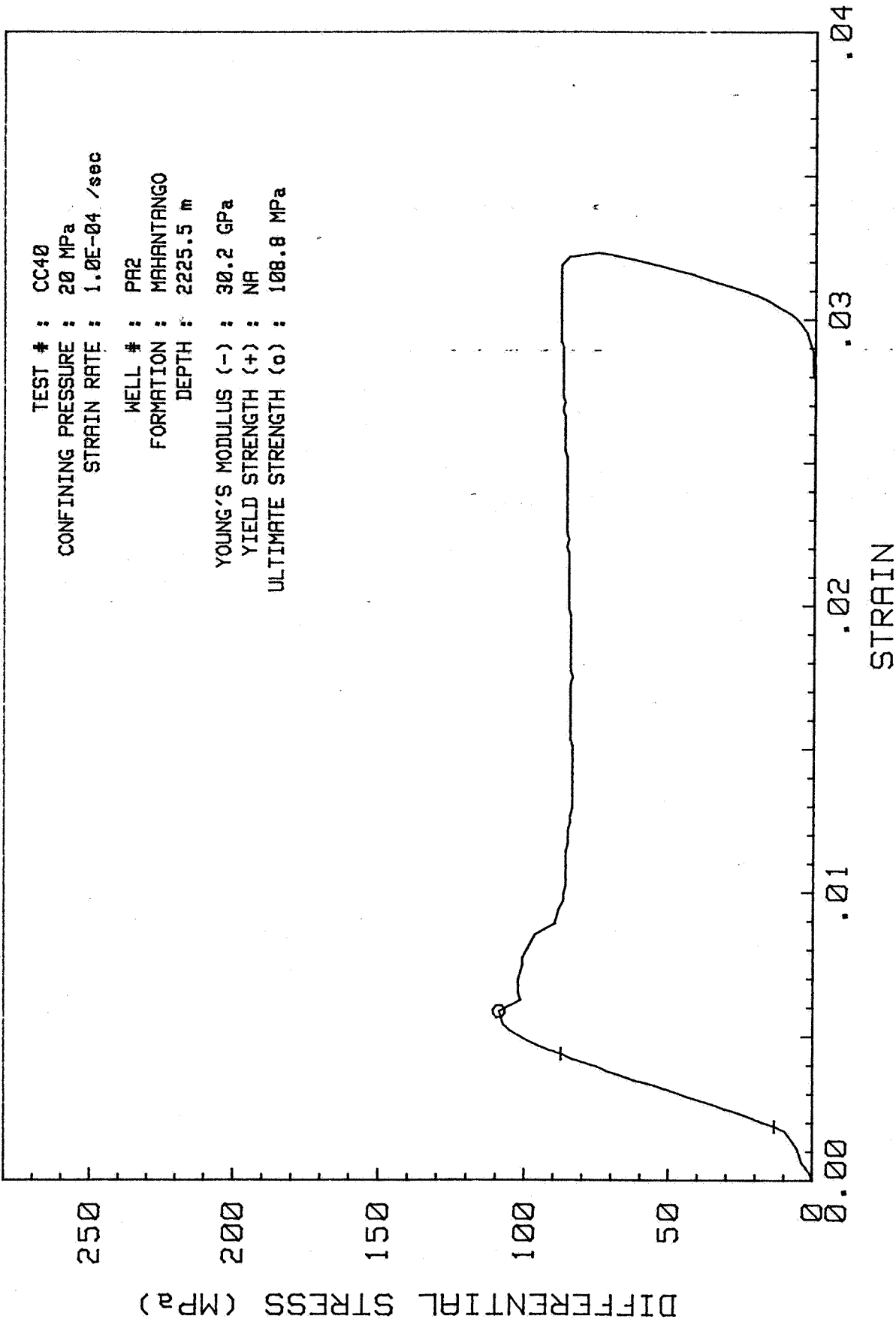


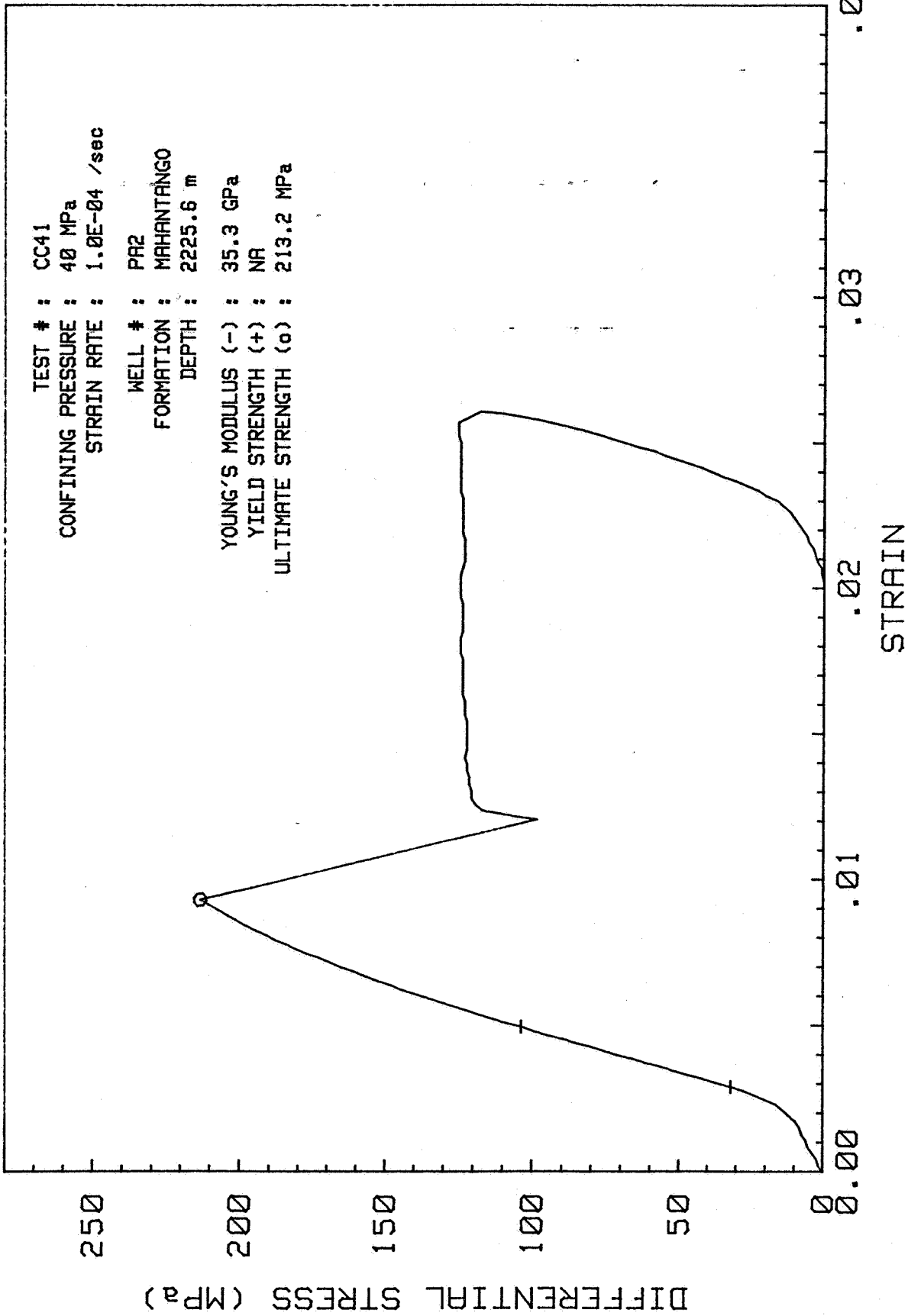
TEST # : CU41  
CONFINING PRESSURE : 0 MPa  
STRAIN RATE : 1.0E-04 /sec

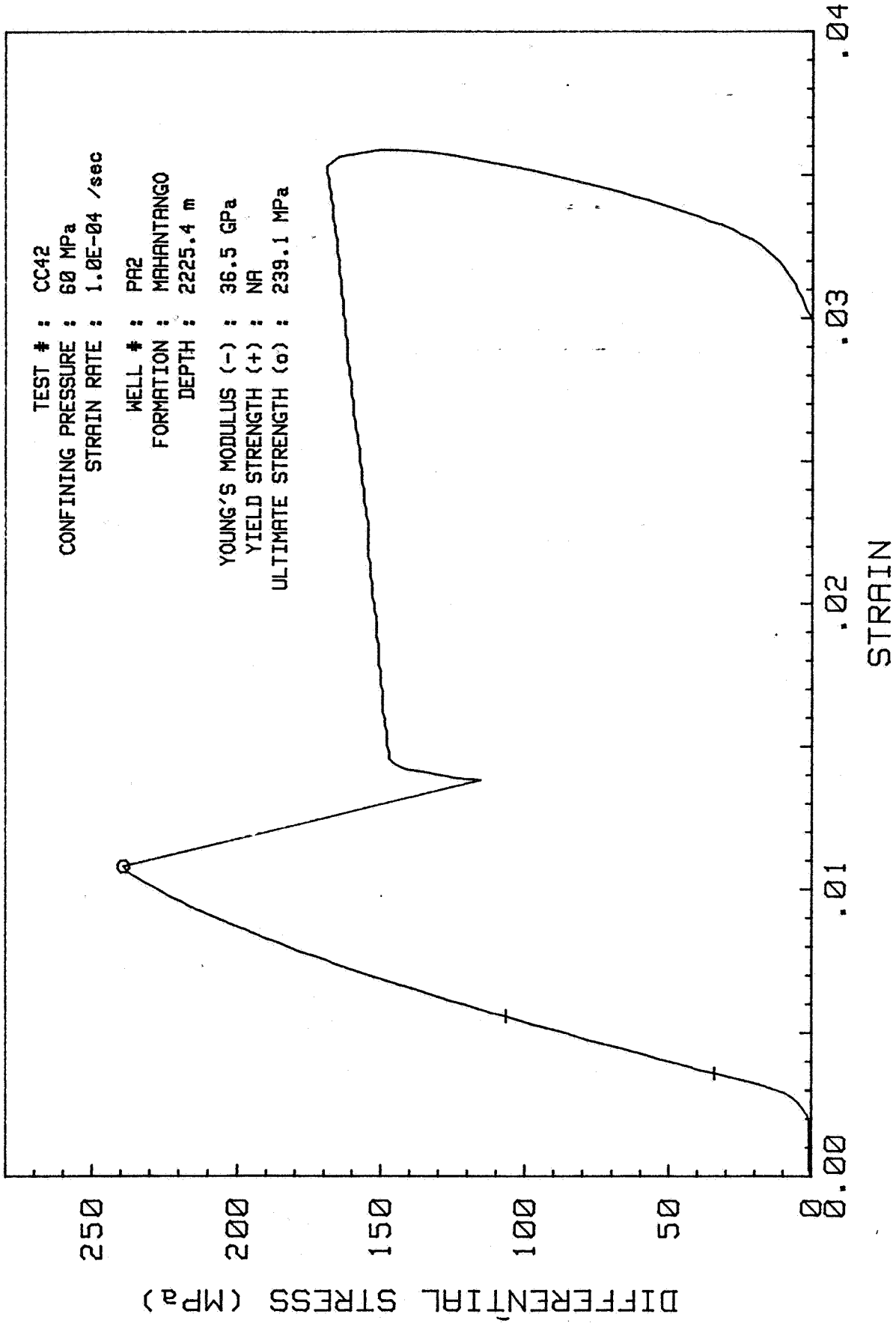
WELL # : PA2  
FORMATION : MAHANTANGO  
DEPTH : 2225.6 m

YOUNG'S MODULUS (-) : 25.7 GPa  
YIELD STRENGTH (+) : NA  
ULTIMATE STRENGTH (o) : 38.5 MPa









**APPENDIX B:**

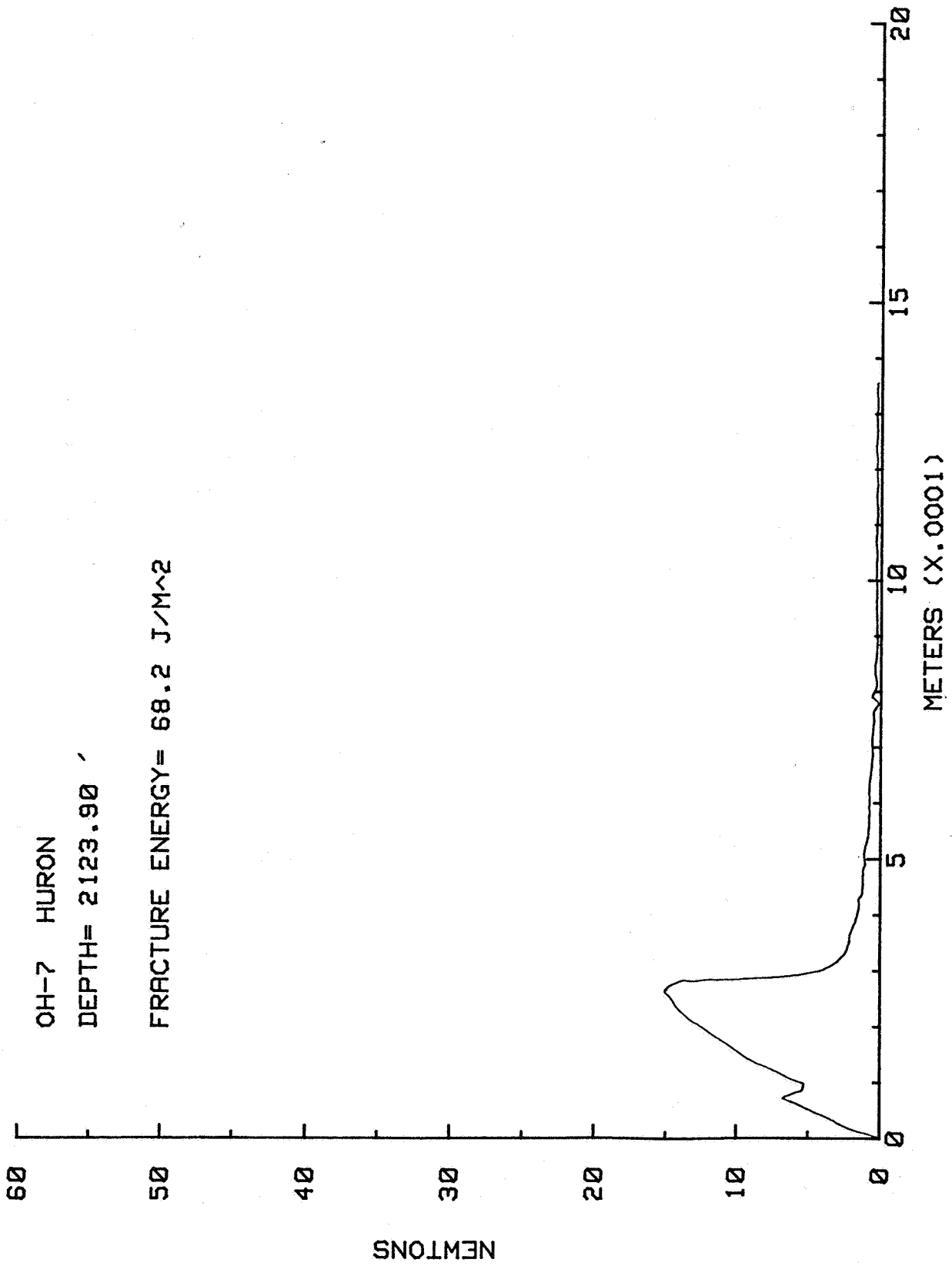
**Load-Displacement Curves for Fracture Energy Tests**

TEST # 9

OH-7 HURON

DEPTH= 2123.90 '

FRACTURE ENERGY= 68.2 J/M<sup>2</sup>

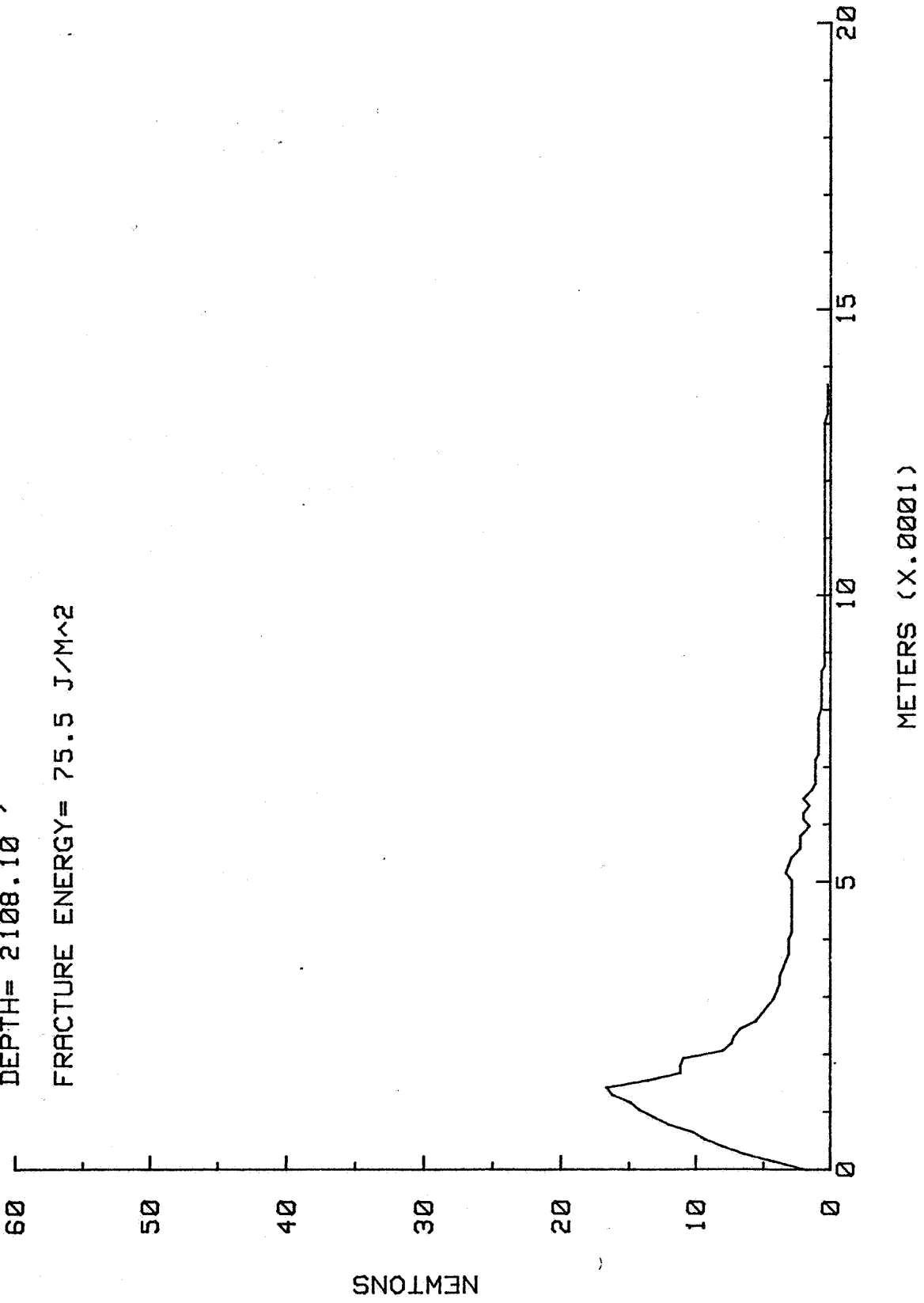


TEST # 10

OH-7 HURON

DEPTH= 2108.10 '

FRACTURE ENERGY= 75.5 J/M<sup>2</sup>

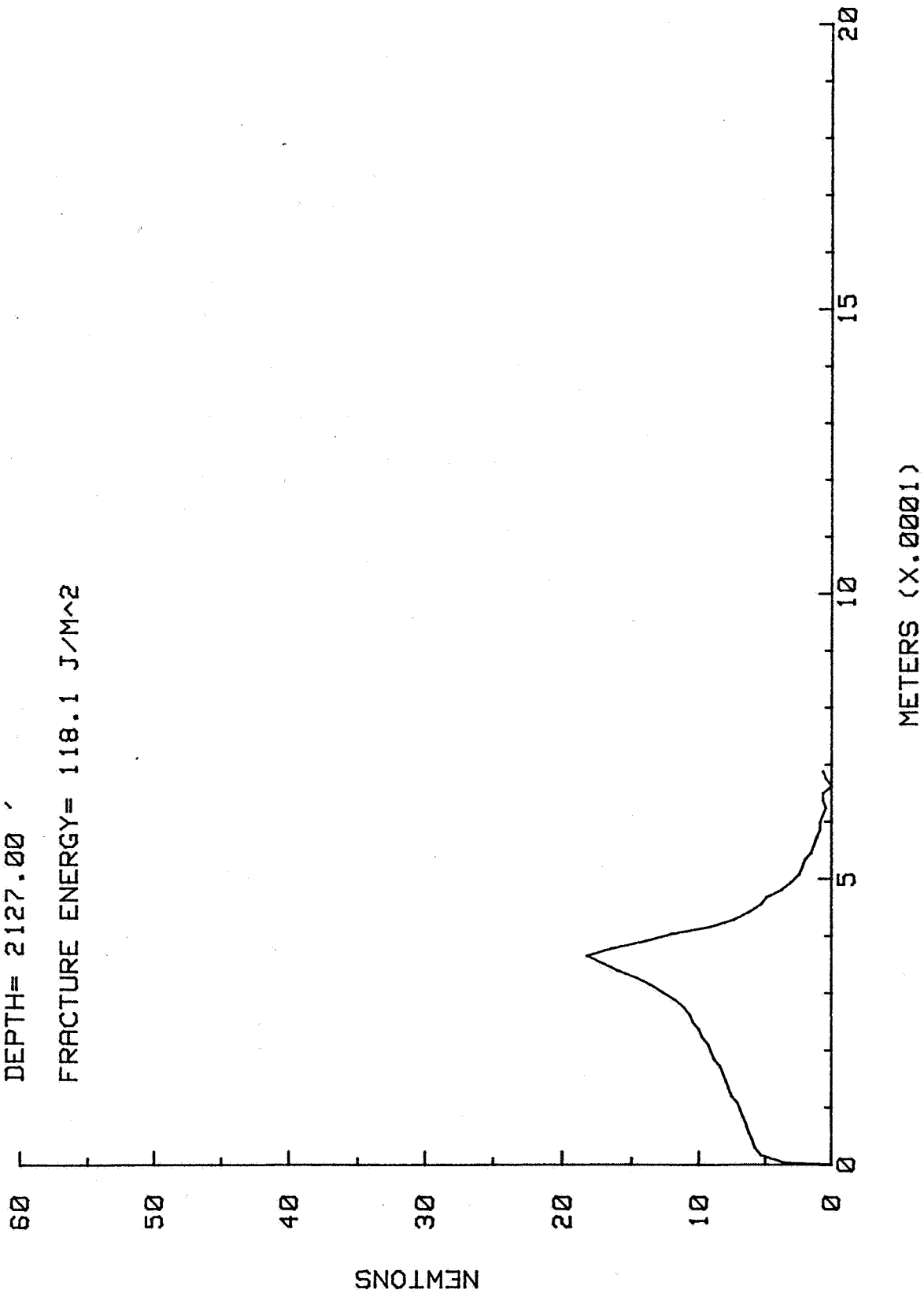


TEST # 13

OH-7 HURON

DEPTH= 2127.00

FRACTURE ENERGY= 118.1 J/M<sup>2</sup>

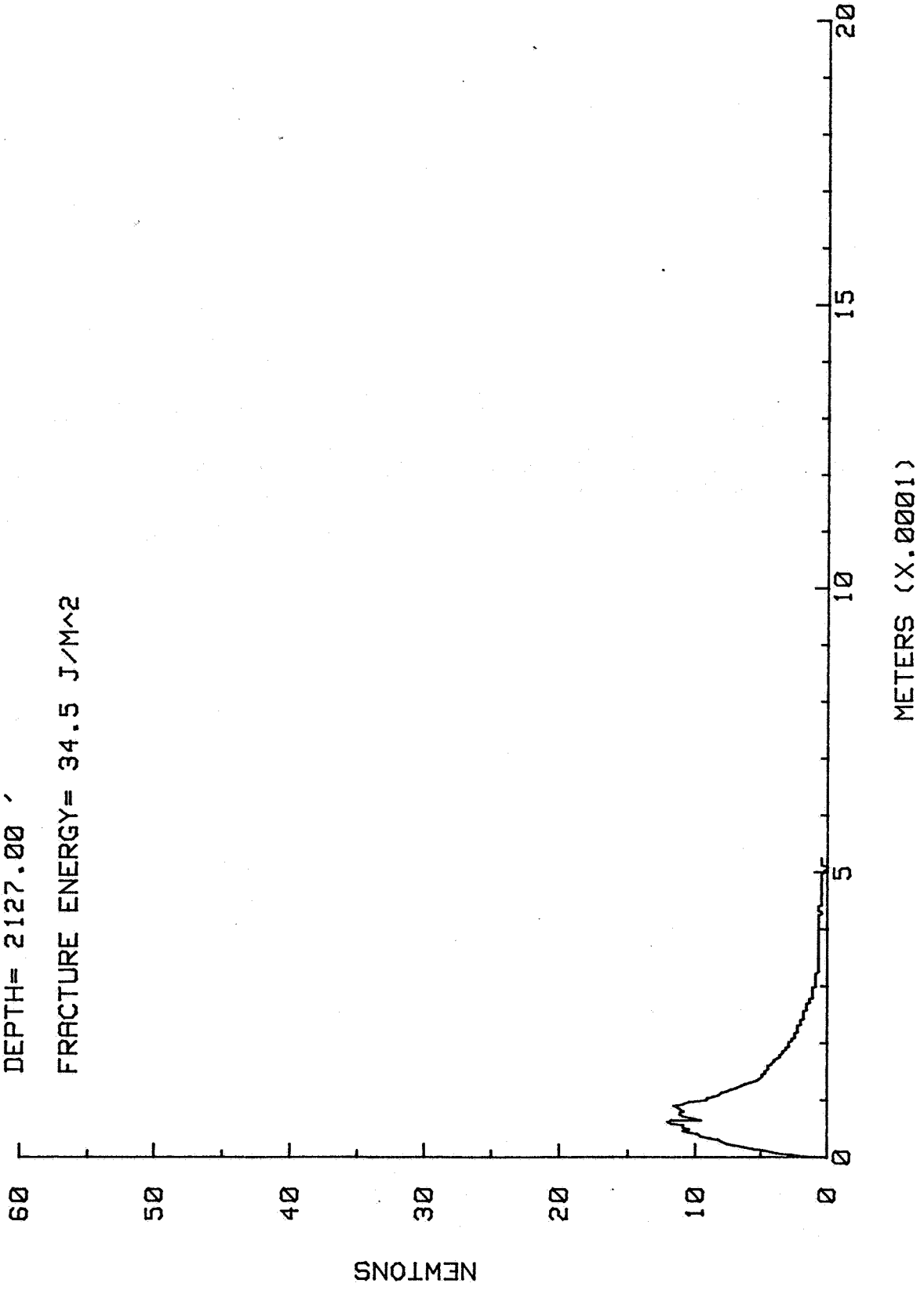


TEST # 15

OH-7 HURON

DEPTH= 2127.00 '

FRACTURE ENERGY= 34.5 J/M<sup>2</sup>

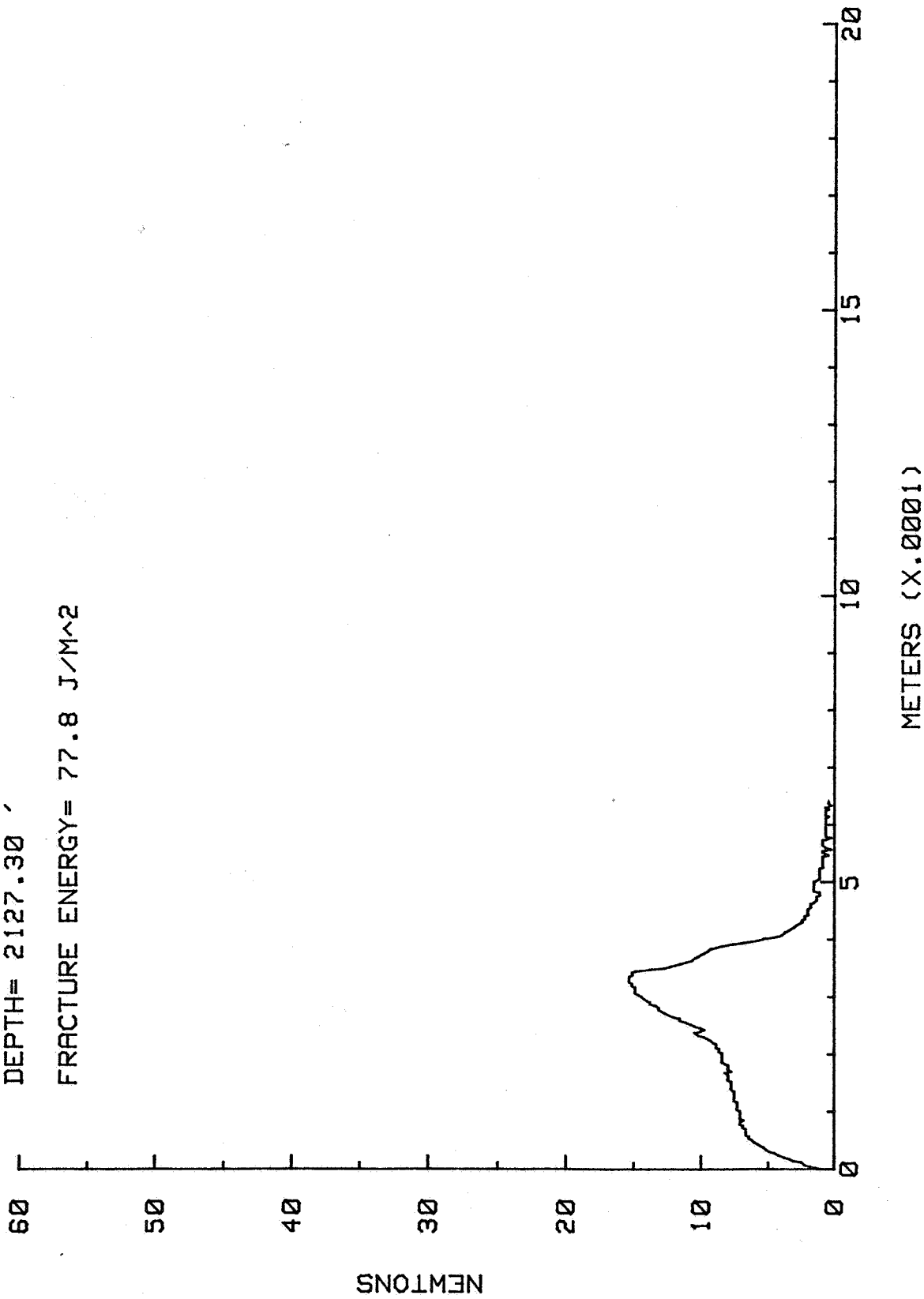


TEST # 16

OH-7 HURON

DEPTH= 2127.30 '

FRACTURE ENERGY= 77.8 J/M<sup>2</sup>

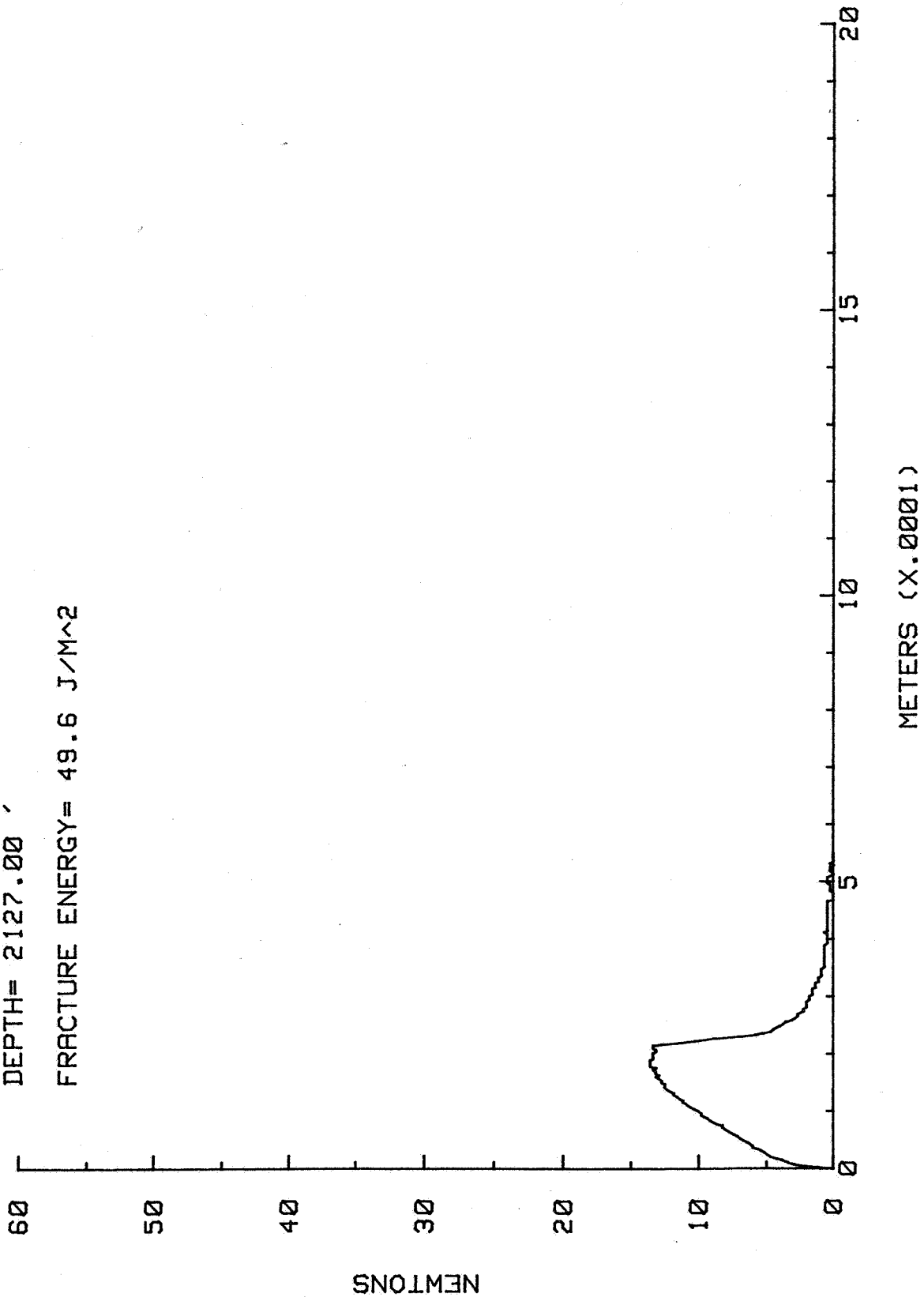


TEST # 17

OH-7 HURON

DEPTH= 2127.00

FRACTURE ENERGY= 49.6 J/M<sup>2</sup>

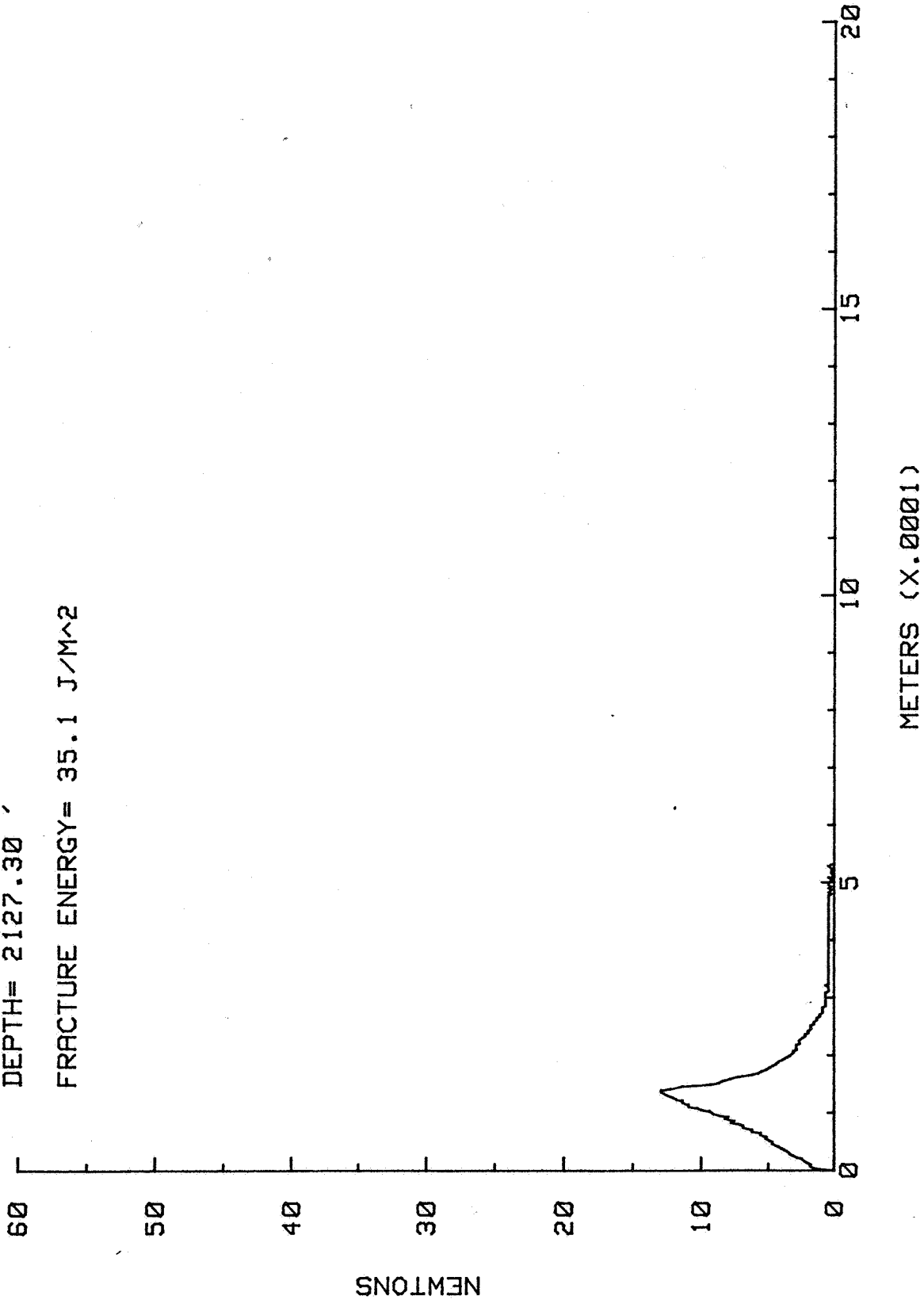


TEST # 18

OH-7 HURON

DEPTH= 2127.30

FRACTURE ENERGY= 35.1 J/M<sup>2</sup>

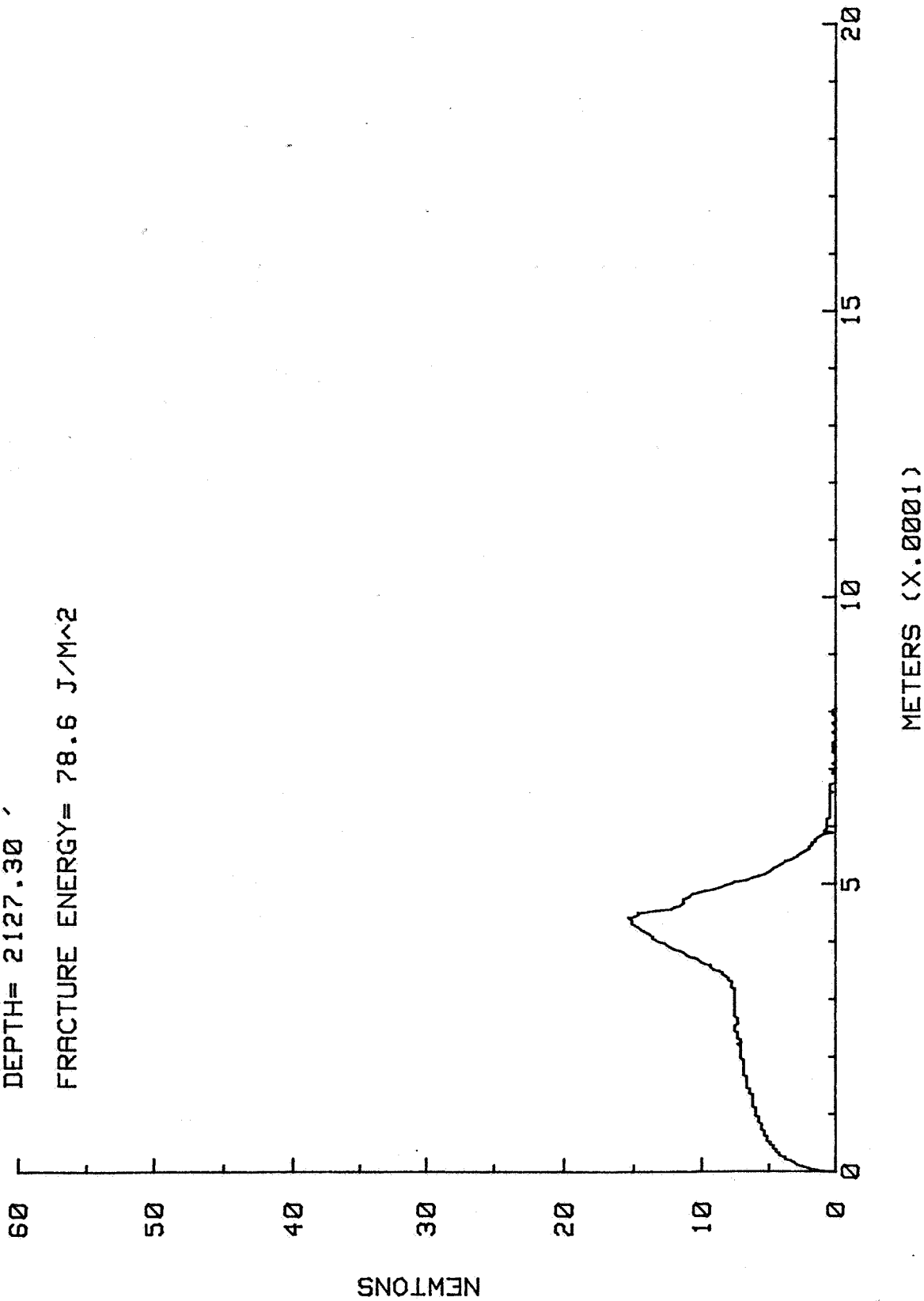


TEST # 19

OH-7 HURON

DEPTH= 2127.30

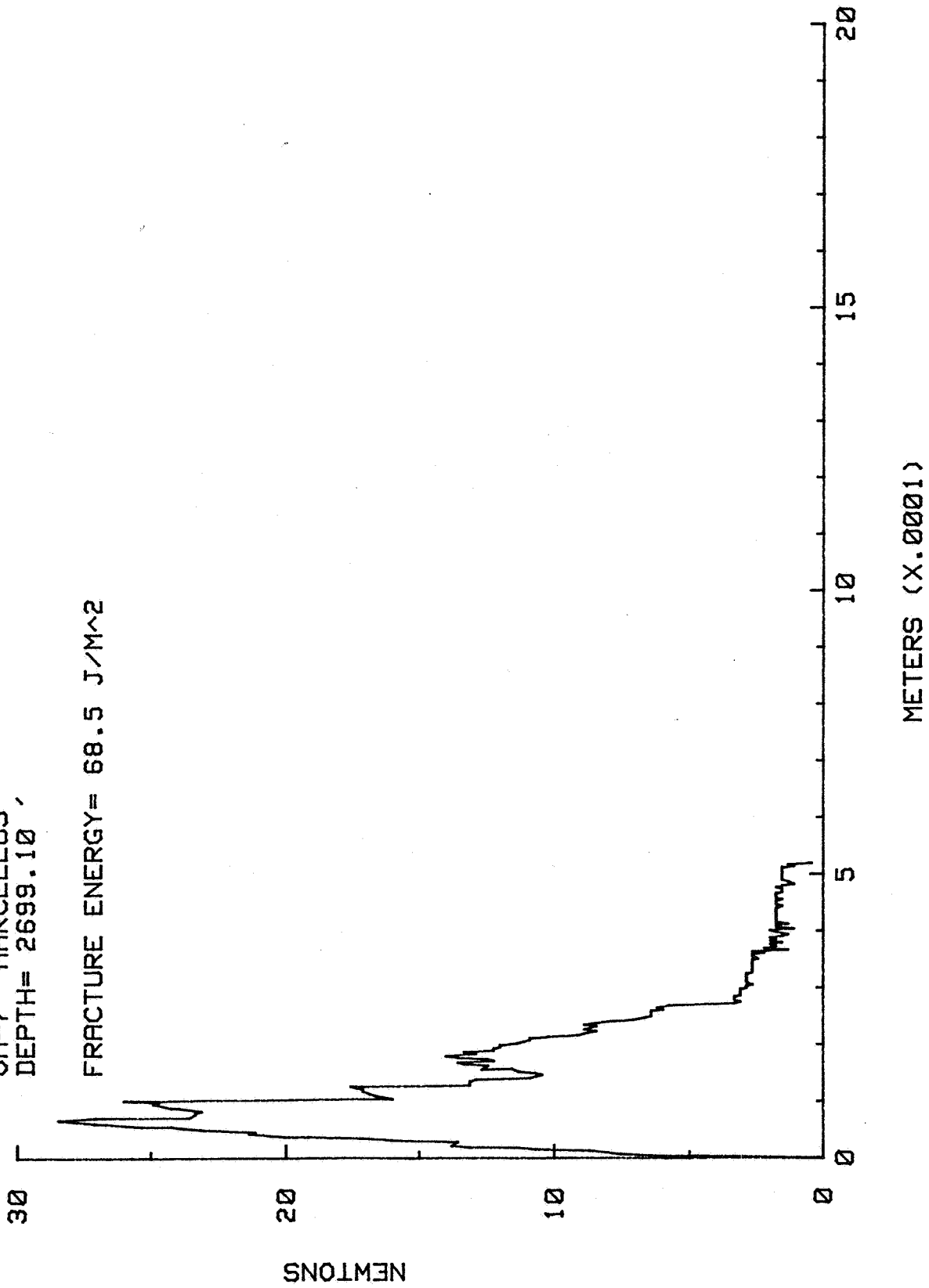
FRACTURE ENERGY= 78.6 J/M<sup>2</sup>



TEST # 28

OH-7 MARCELLUS  
DEPTH= 2699.10

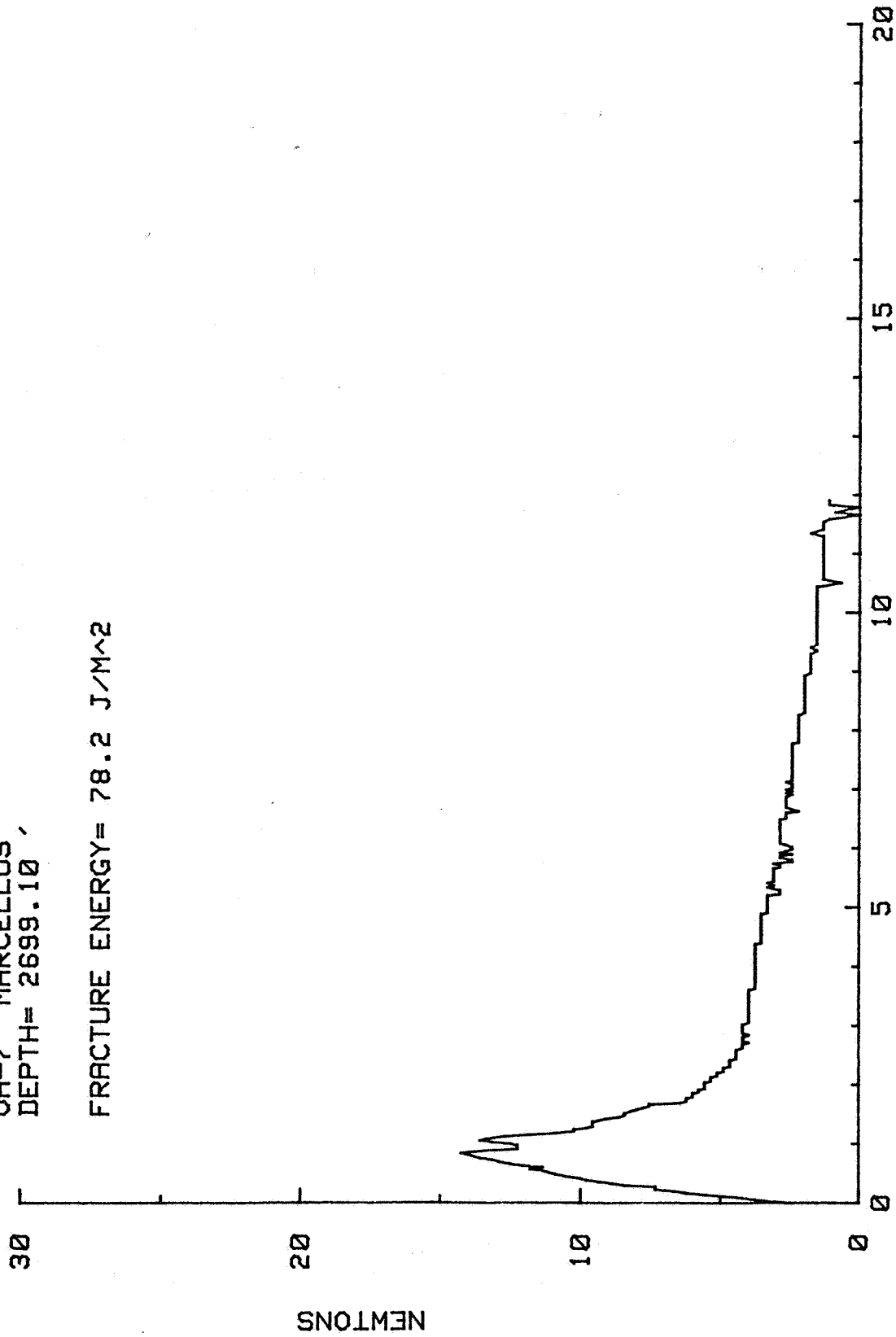
FRACTURE ENERGY= 68.5 J/M<sup>2</sup>



TEST # 29

OH-7 MARCELLUS  
DEPTH= 2699.10'

FRACTURE ENERGY= 78.2 J/M<sup>2</sup>

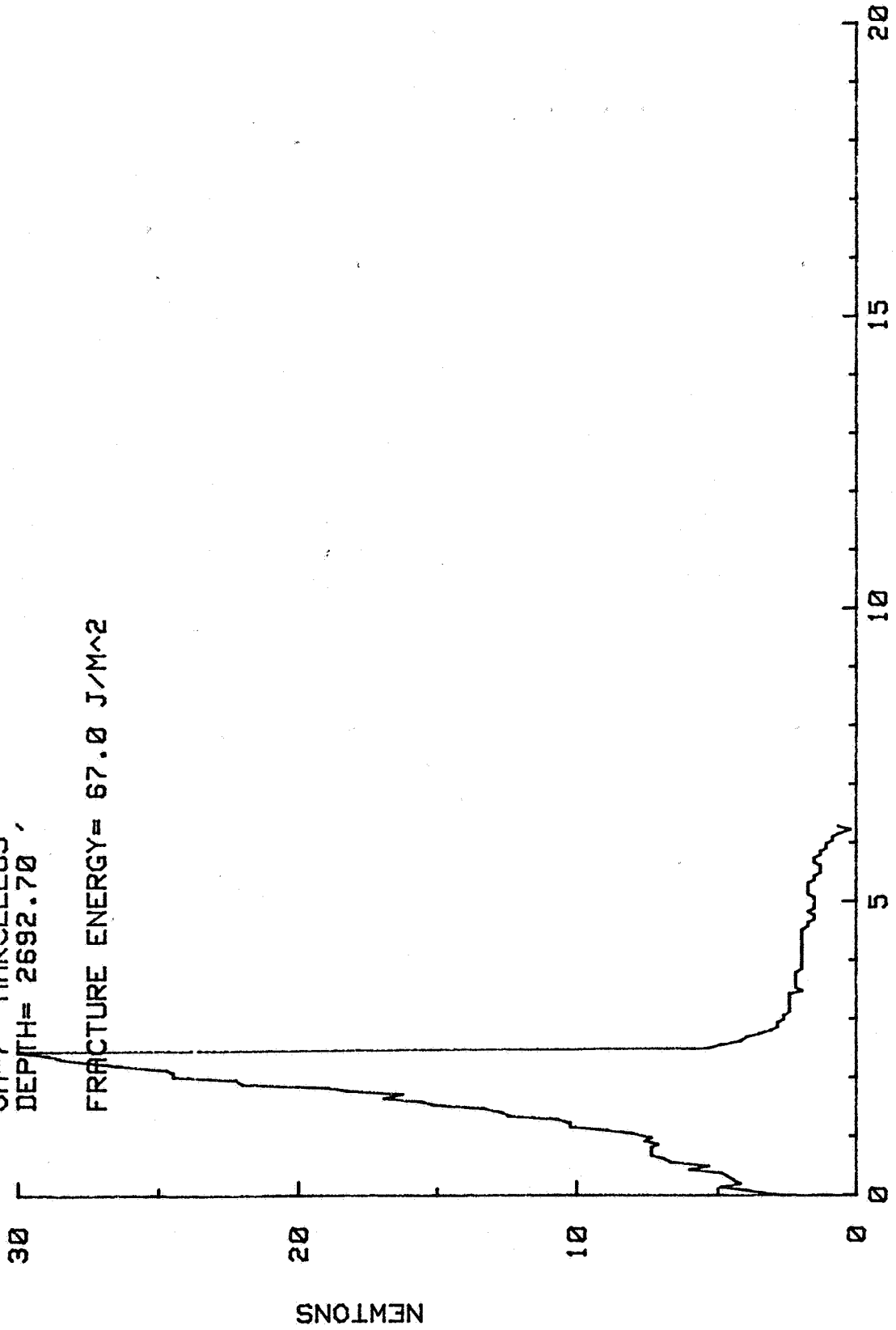


METERS (X.0001)

TEST # 55

OH-7 MARCELLUS  
DEPTH= 2692.70

FRACTURE ENERGY= 67.0 J/M<sup>2</sup>

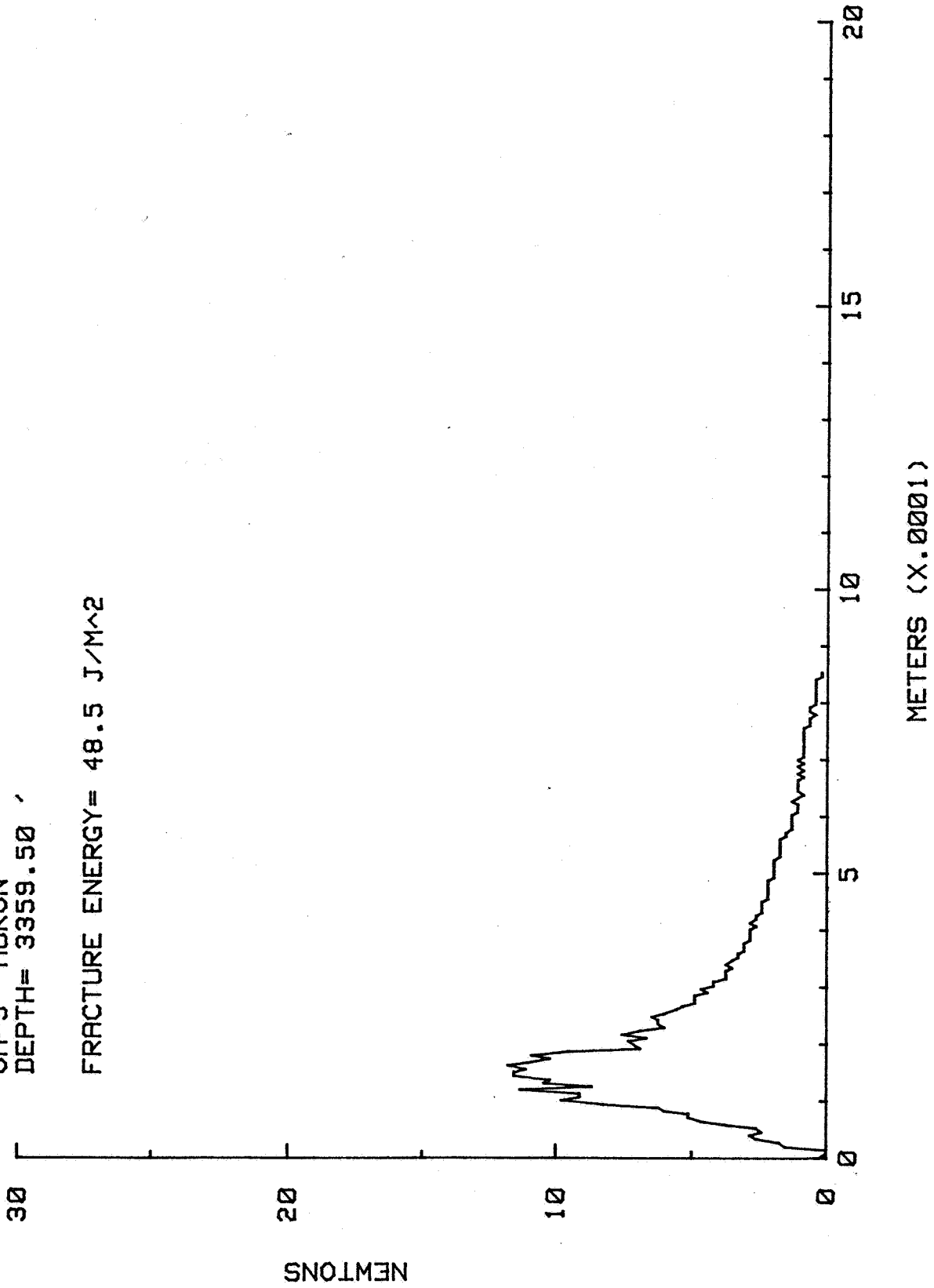


METERS (X.0001)

TEST # 62

OH-9 HURON  
DEPTH= 3359.50

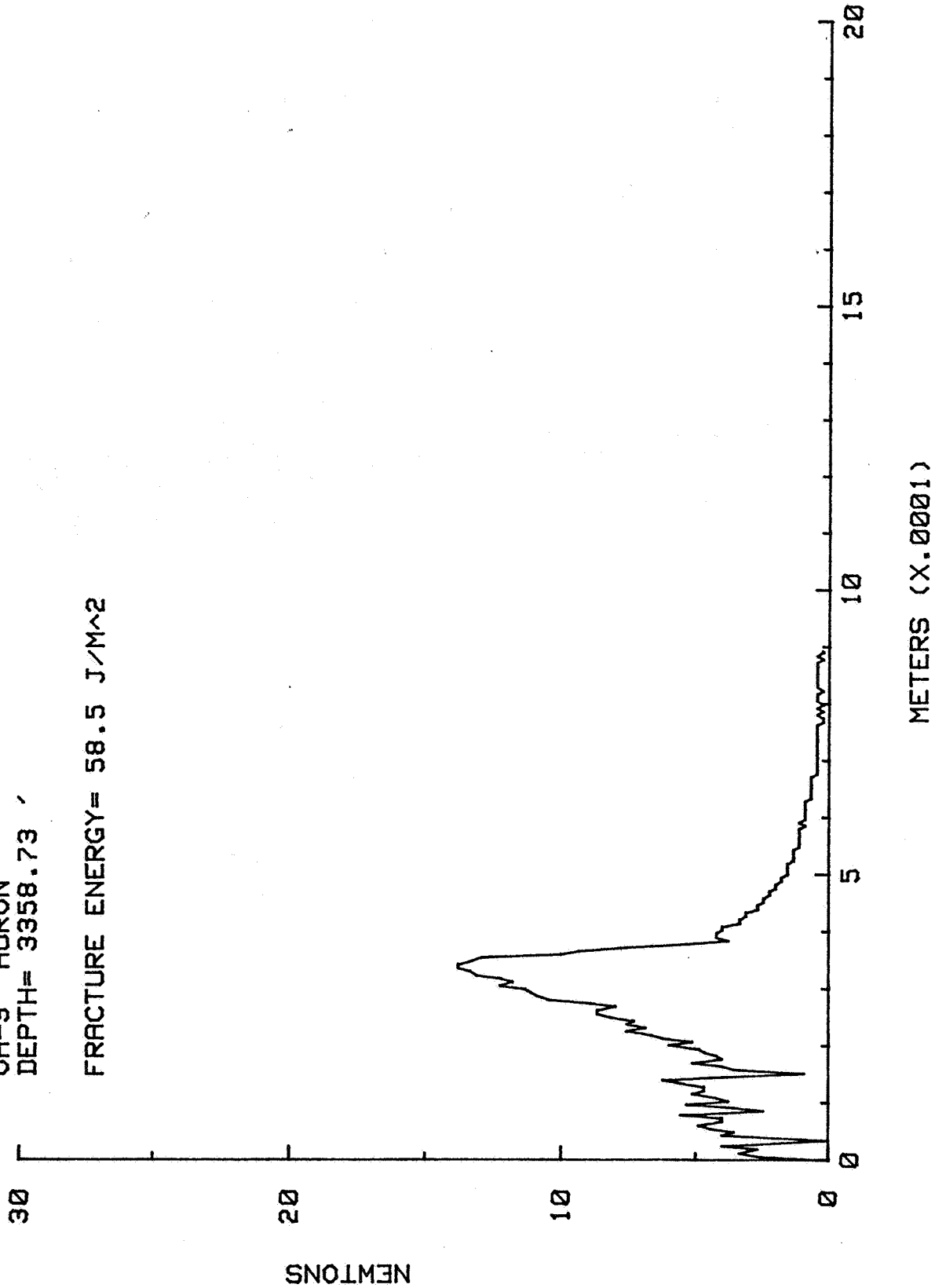
FRACTURE ENERGY= 48.5 J/M<sup>2</sup>



TEST # 63

OH-9 HURON  
DEPTH= 3358.73

FRACTURE ENERGY= 58.5 J/M<sup>2</sup>

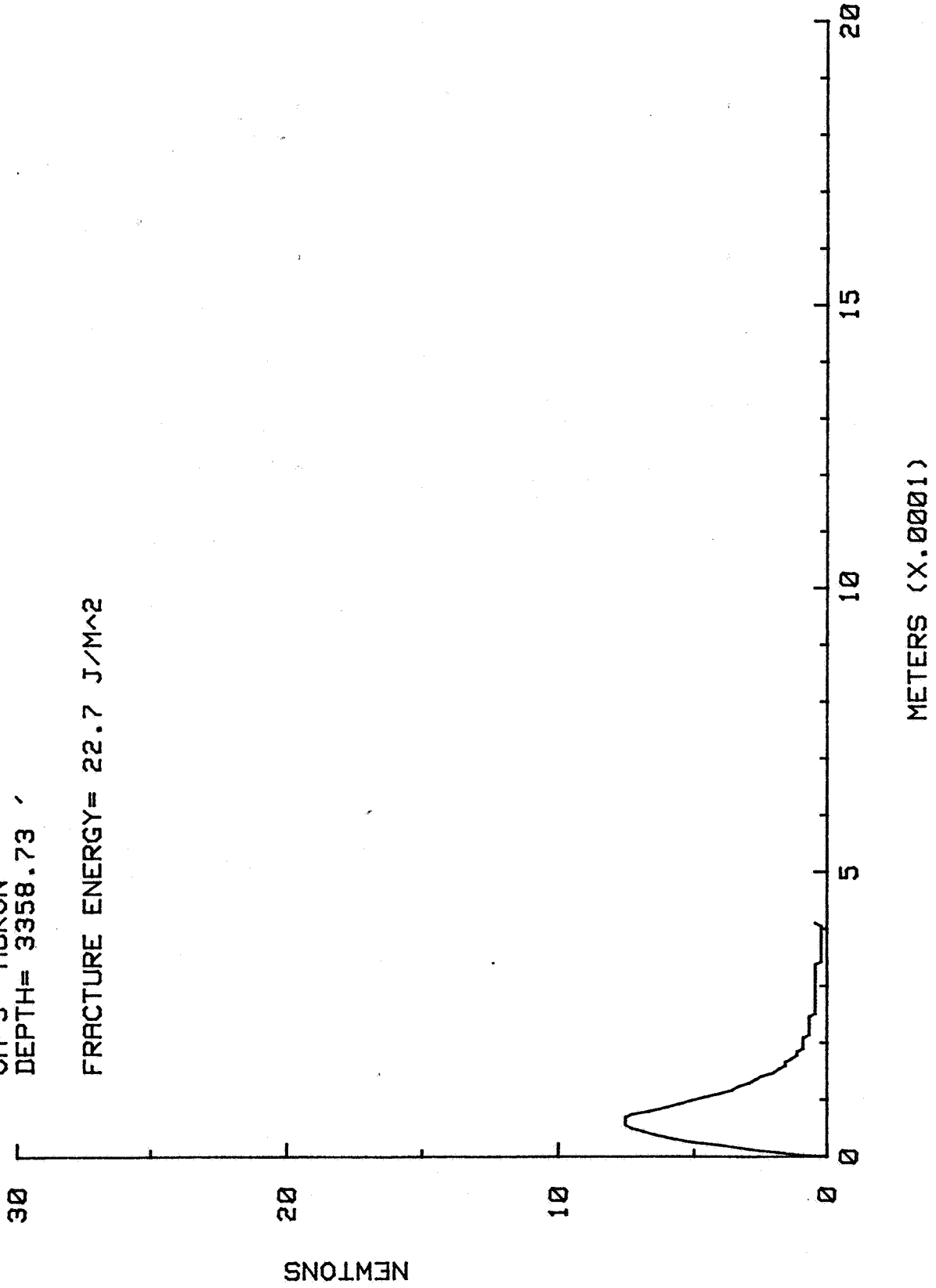


TEST # 64

OH-9 HURON

DEPTH= 3358.73

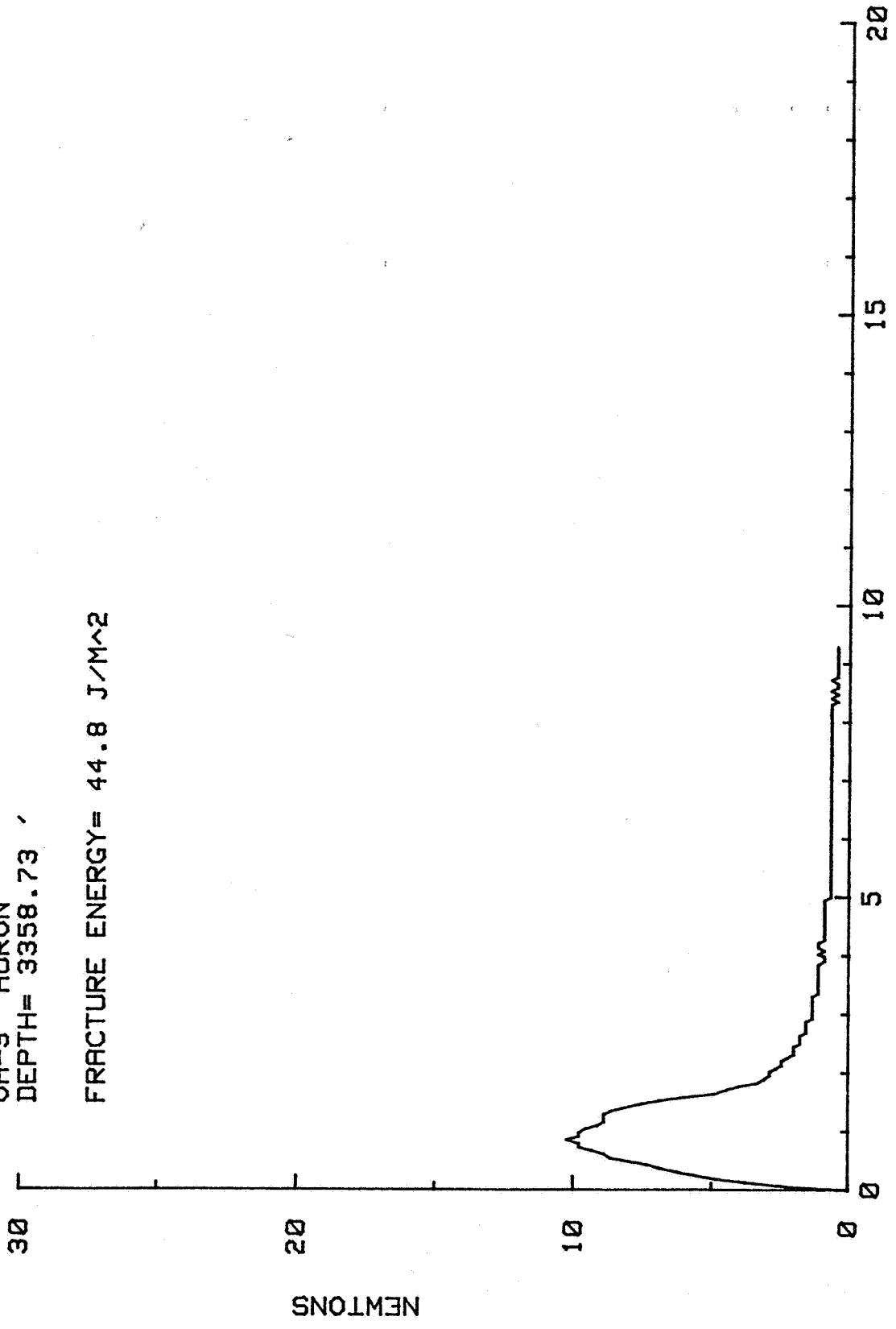
FRACTURE ENERGY= 22.7 J/M<sup>2</sup>



TEST # 65

OH-8 HURON  
DEPTH= 3358.73 '

FRACTURE ENERGY= 44.8 J/M<sup>2</sup>

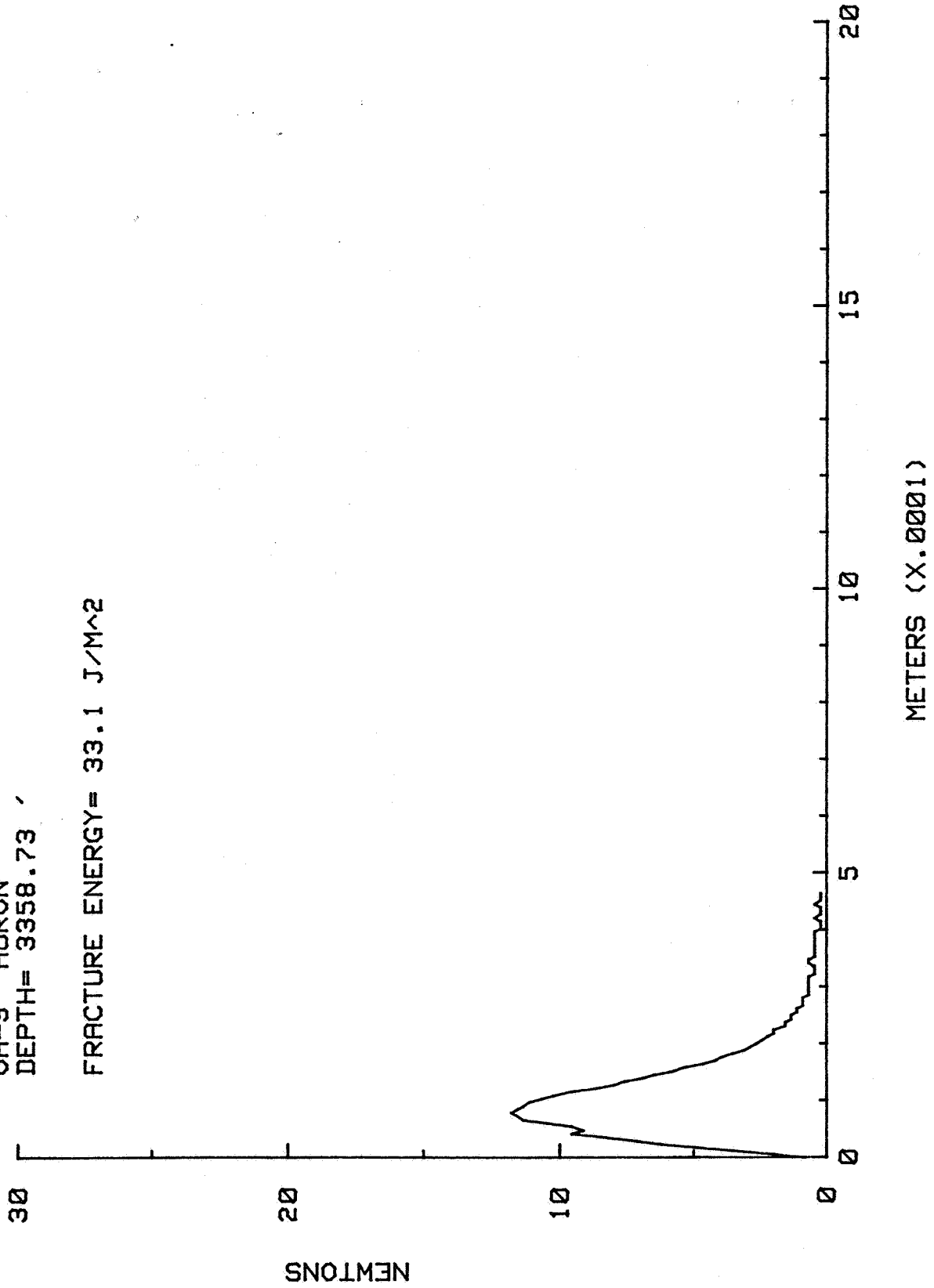


METERS (X.0001)

TEST # 66

OH-9 HURON  
DEPTH= 3358.73

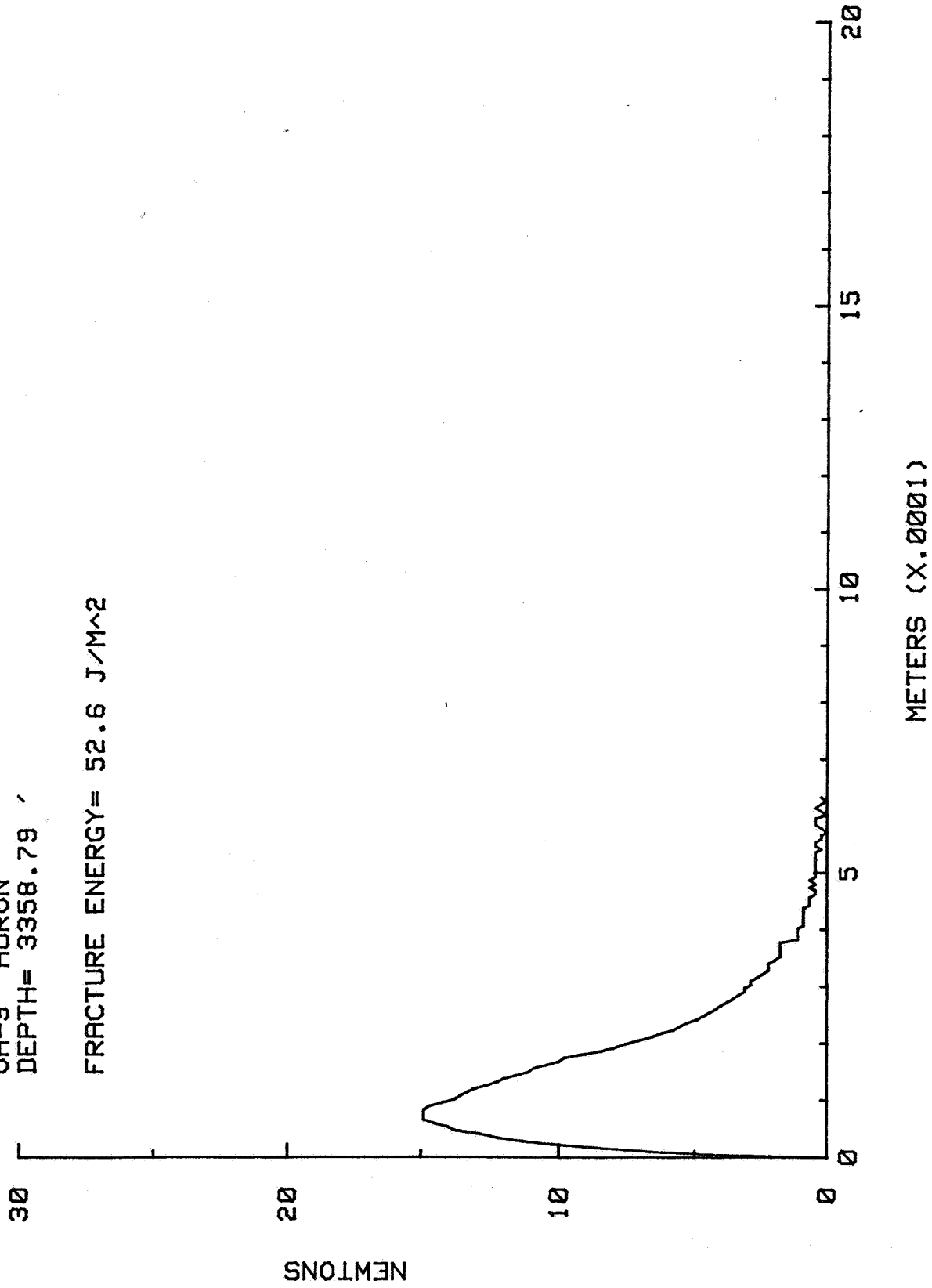
FRACTURE ENERGY= 33.1 J/M<sup>2</sup>



TEST # 68

OH-9 HURON  
DEPTH= 3358.79

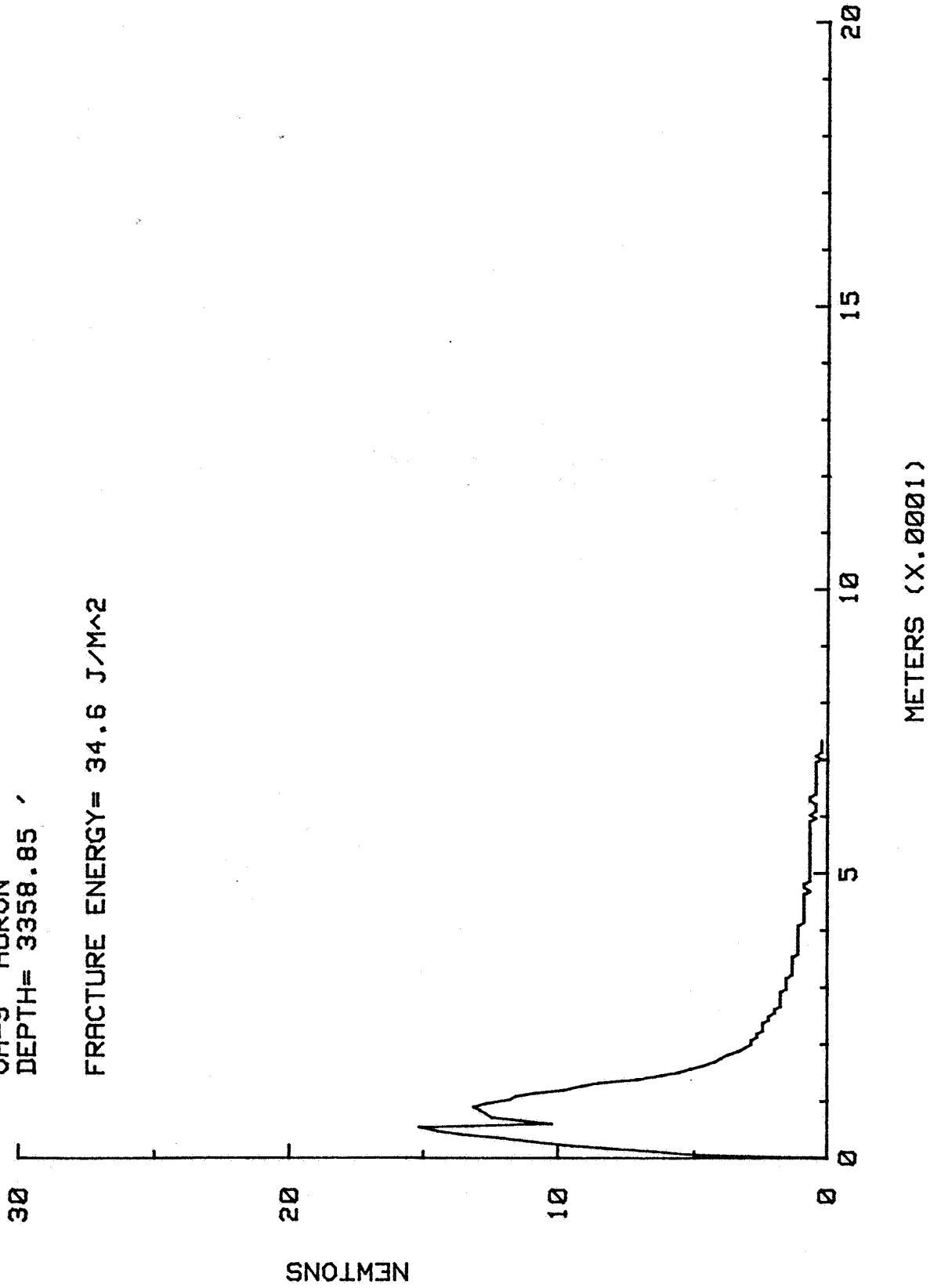
FRACTURE ENERGY= 52.6 J/M<sup>2</sup>



TEST # 69

OH-9 HURON  
DEPTH= 3358.85 '

FRACTURE ENERGY= 34.6 J/M<sup>2</sup>

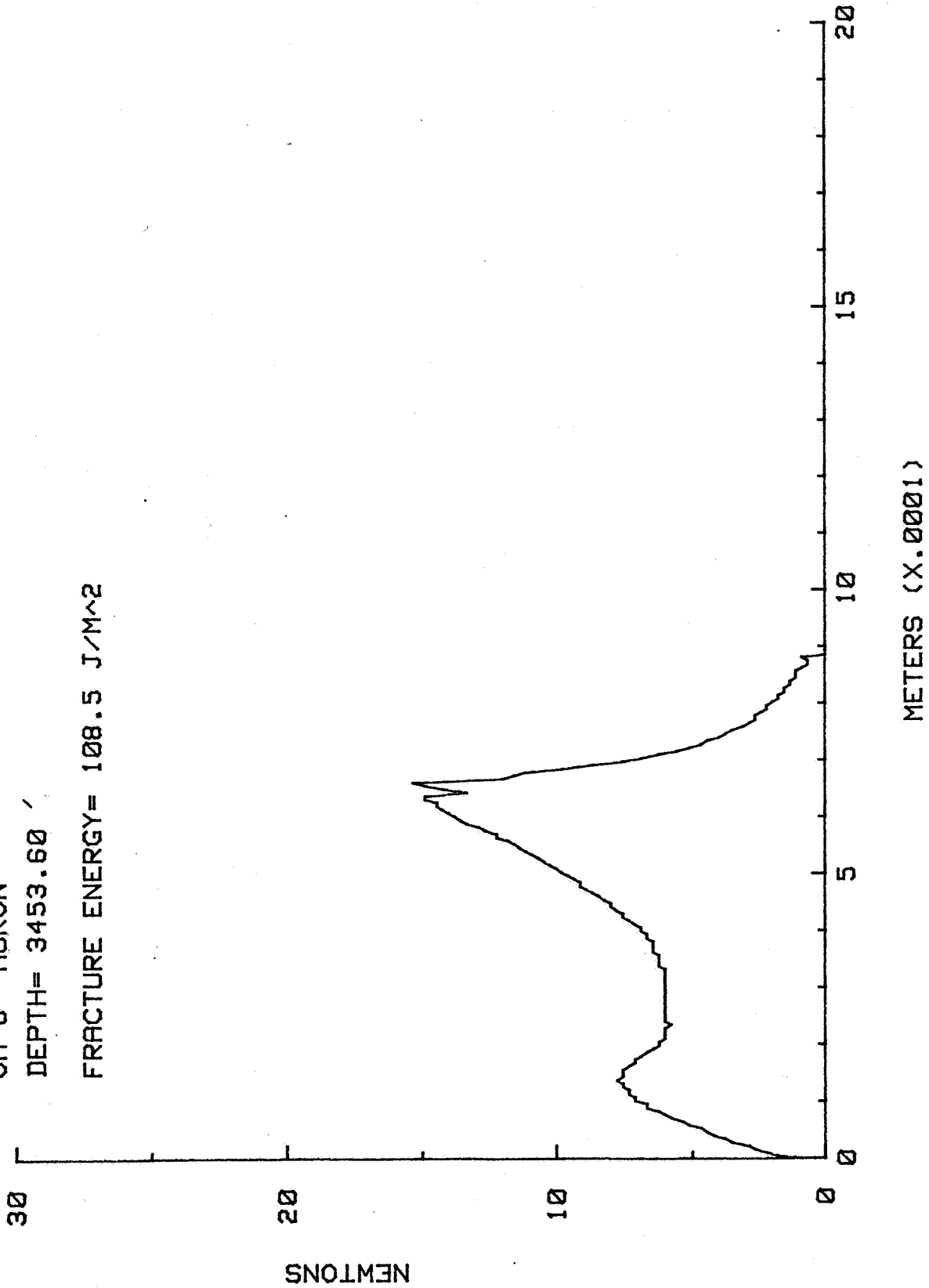


TEST # 44

OH-8 HURON

DEPTH= 3453.60 '

FRACTURE ENERGY= 108.5 J/M<sup>2</sup>

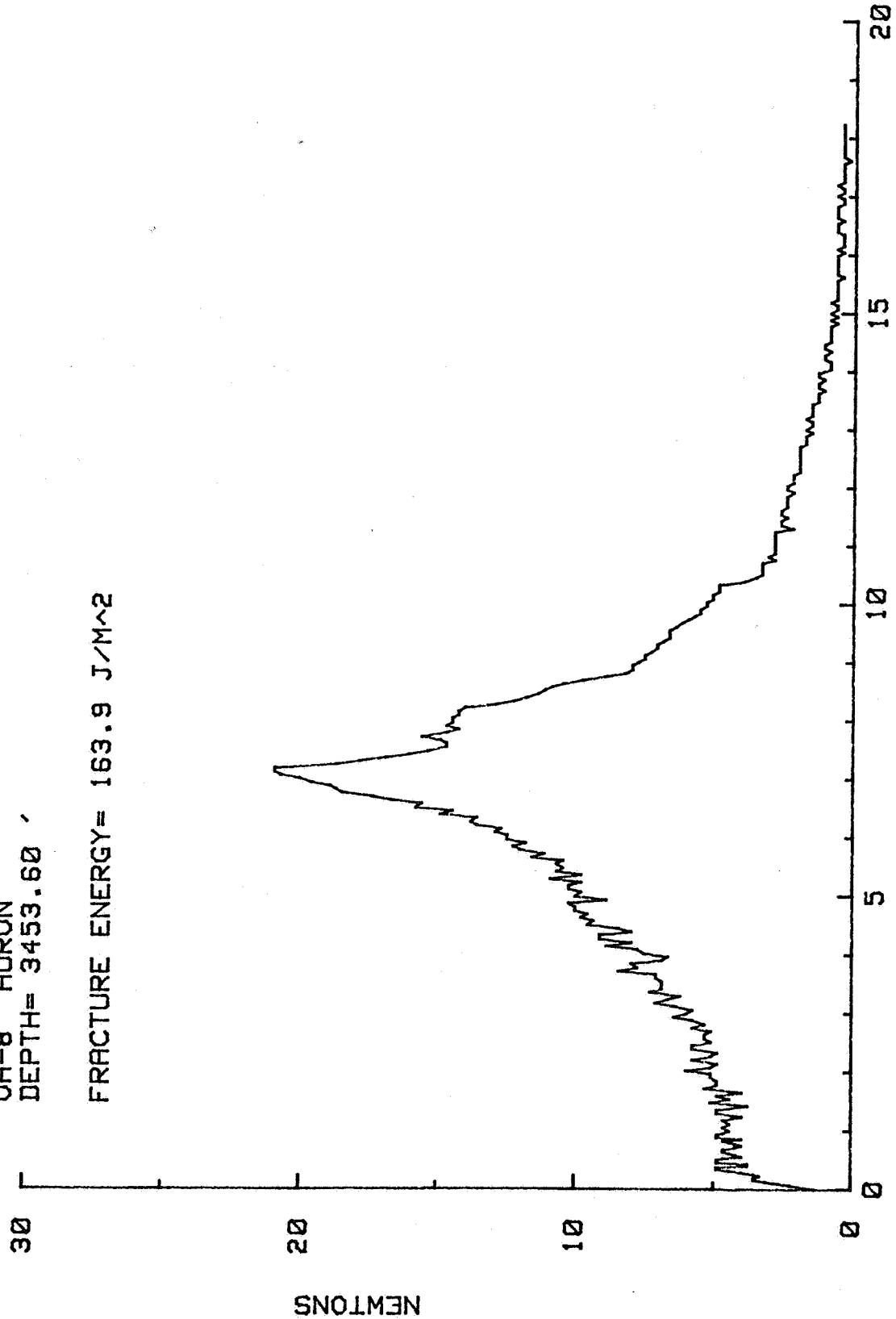


TEST # 45

OH-8 HURON

DEPTH= 3453.60

FRACTURE ENERGY= 163.9 J/M<sup>2</sup>



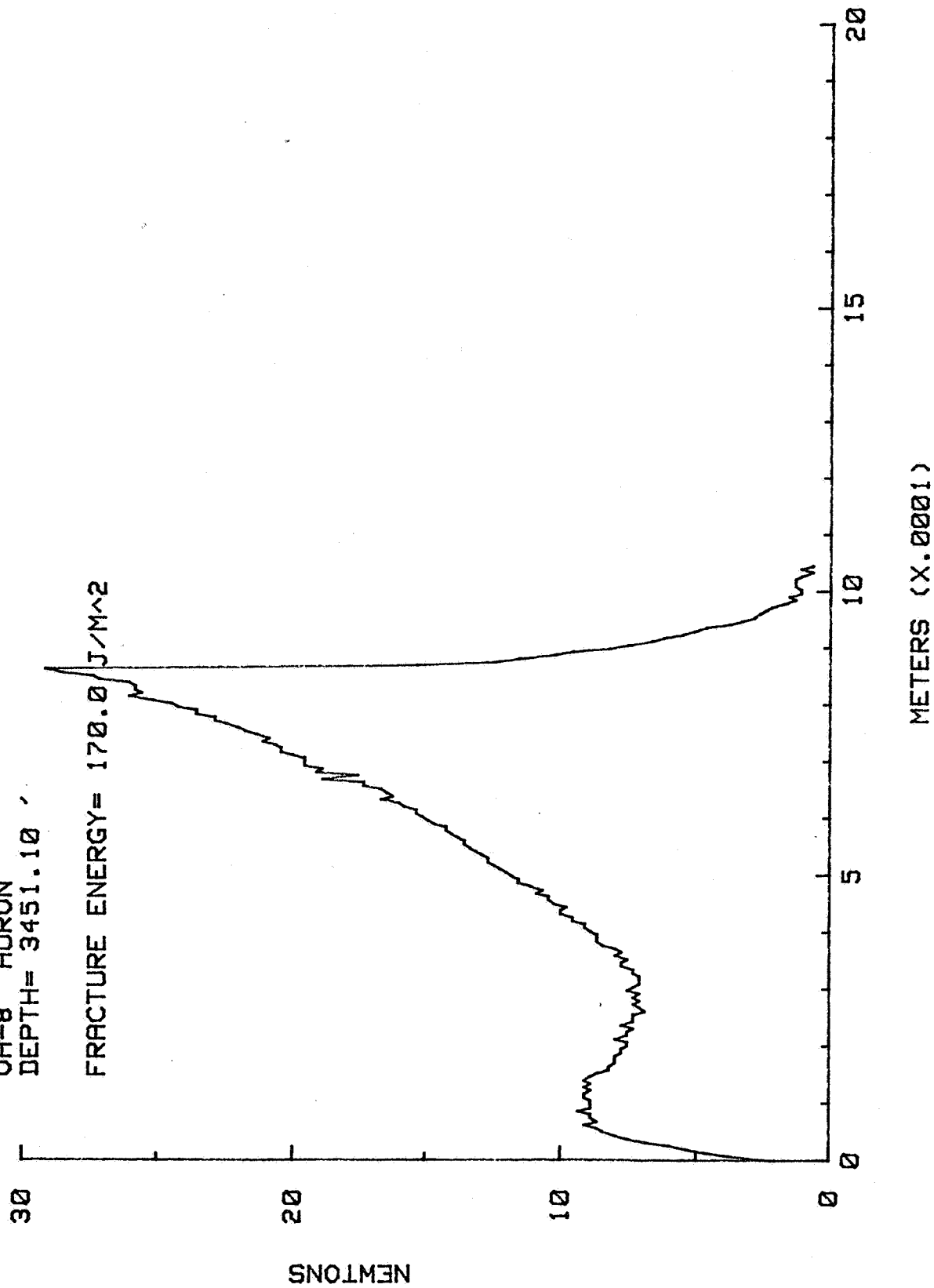
METERS (X.0001)

TEST # 46

OH-8 HURON

DEPTH= 3451.10

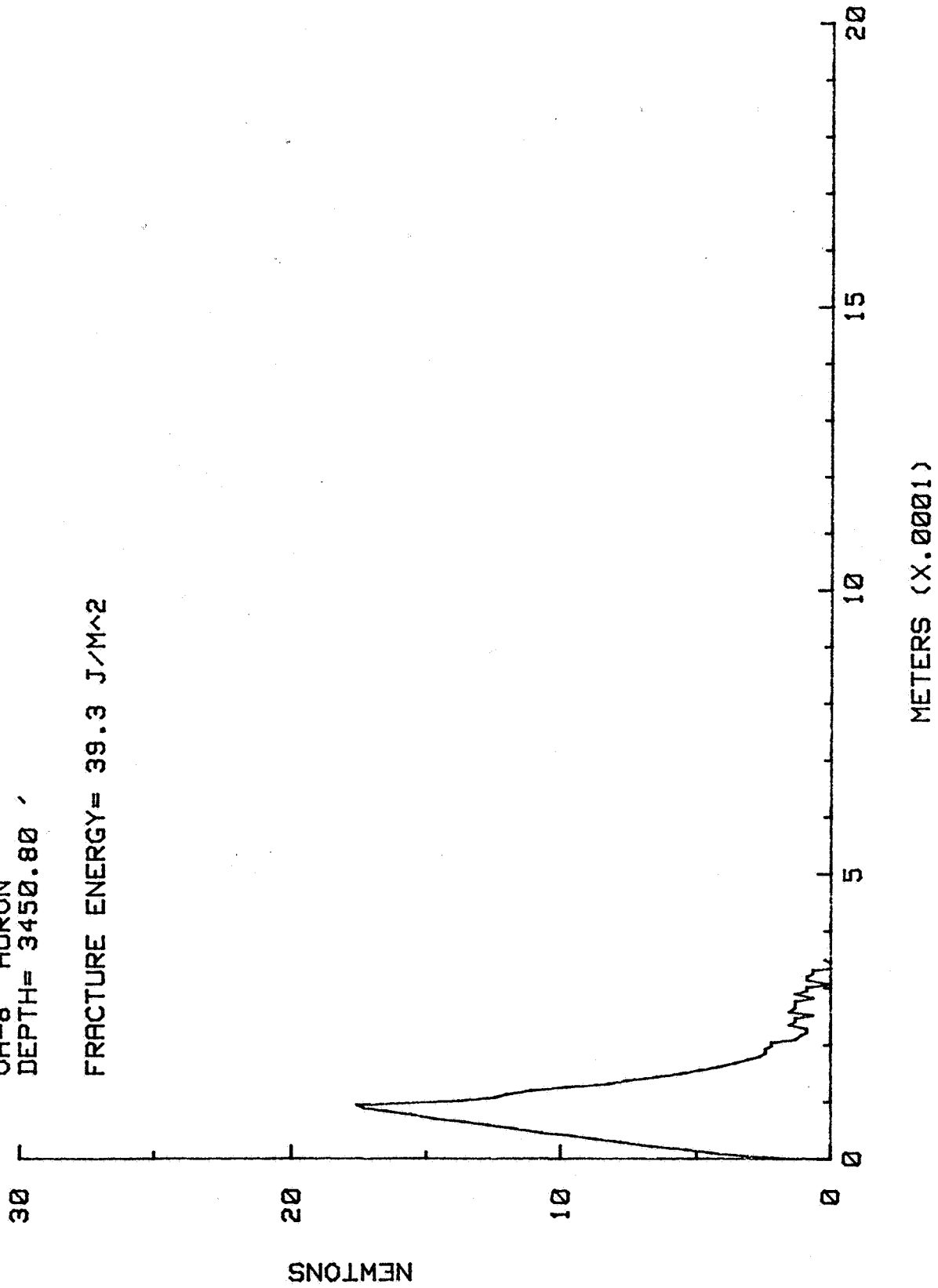
FRACTURE ENERGY= 170.0 J/M<sup>2</sup>



TEST # 47

OH-8 HURON  
DEPTH= 3450.80

FRACTURE ENERGY= 39.3 J/M<sup>2</sup>

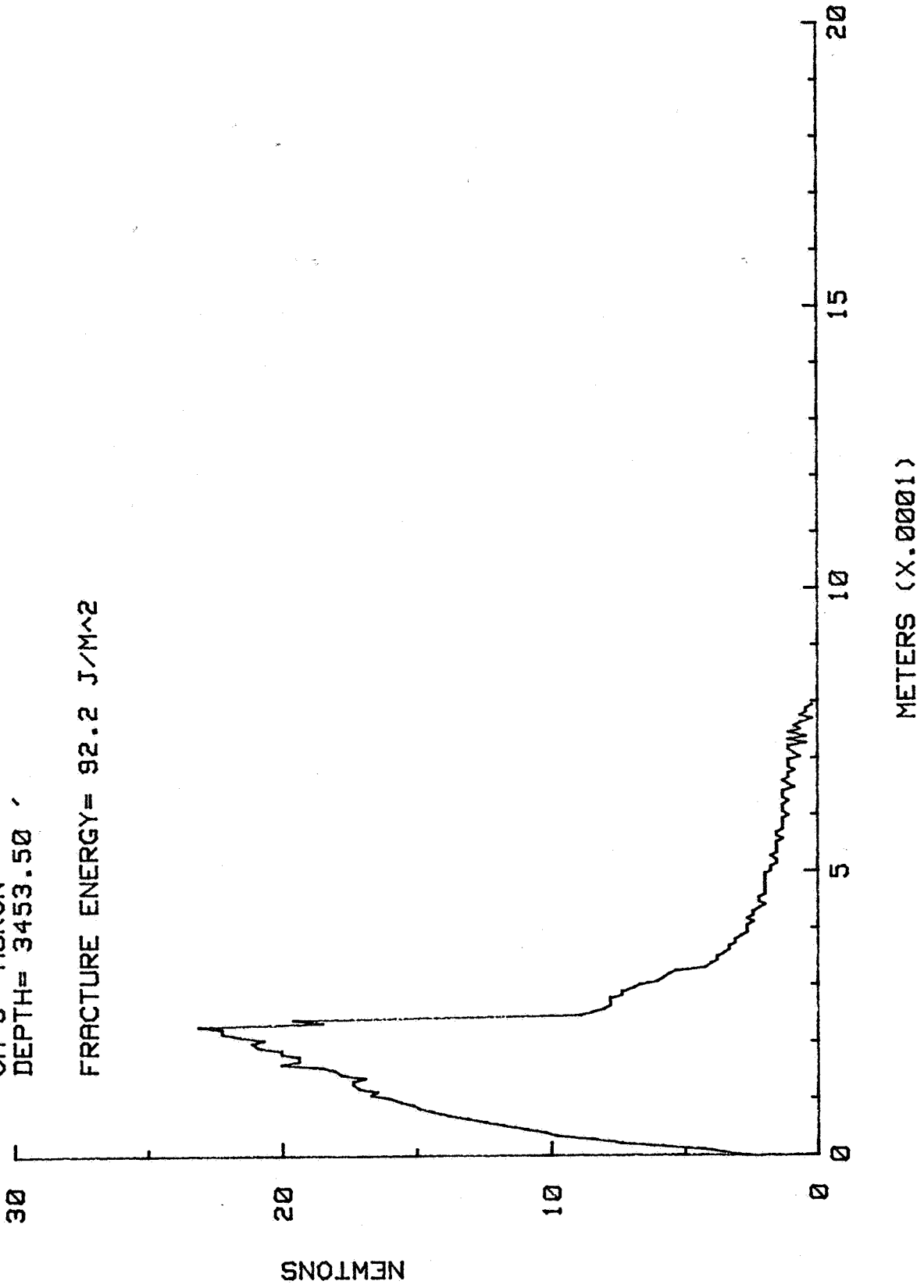


TEST # 48

OH-8 HURON

DEPTH= 3453.50

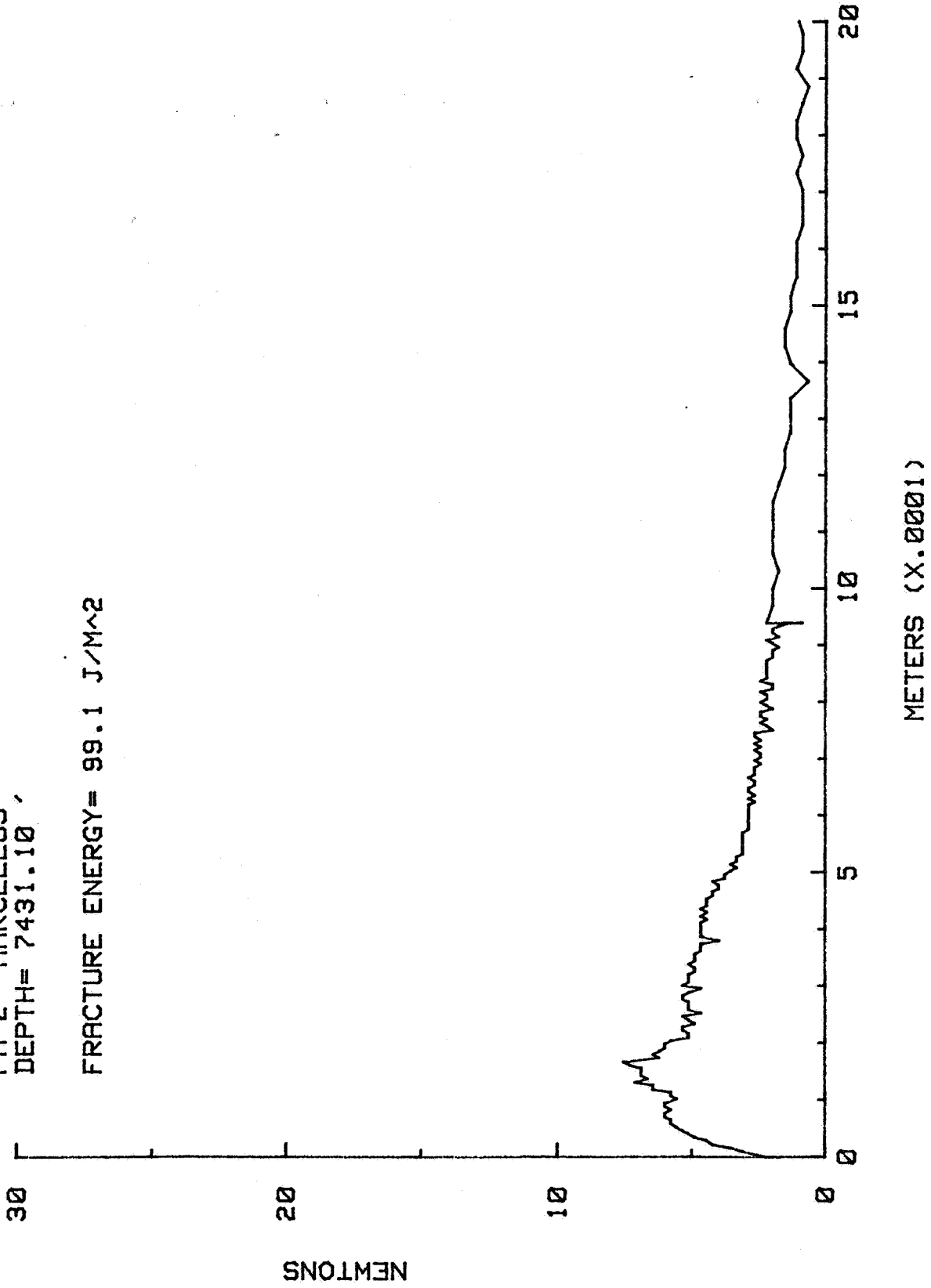
FRACTURE ENERGY= 92.2 J/M<sup>2</sup>



TEST # 56

PA-2 MARCELLUS  
DEPTH= 7431.10'

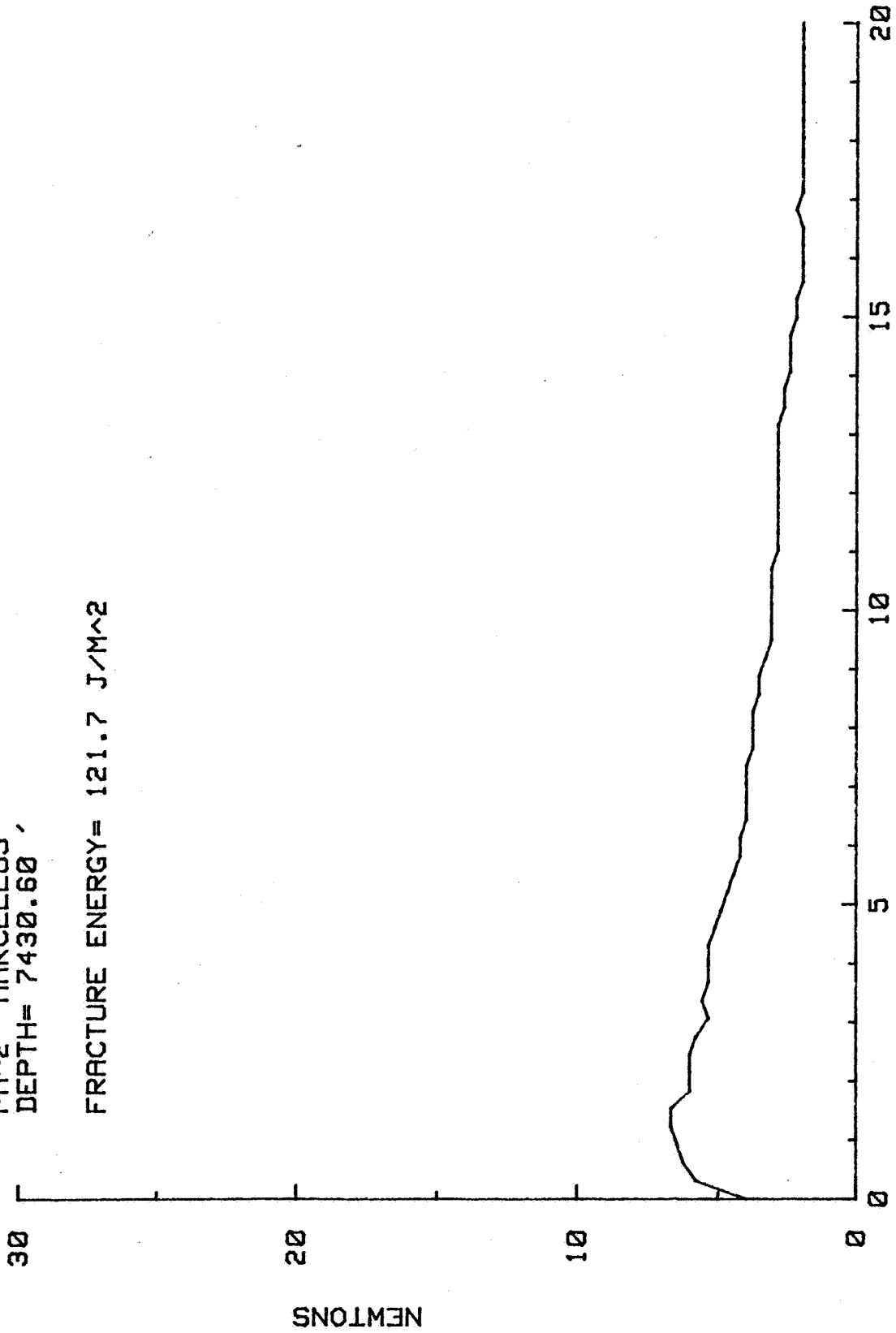
FRACTURE ENERGY= 99.1 J/M<sup>2</sup>



TEST # 57

PA-2 MARCELLUS  
DEPTH= 7430.60

FRACTURE ENERGY= 121.7 J/M<sup>2</sup>

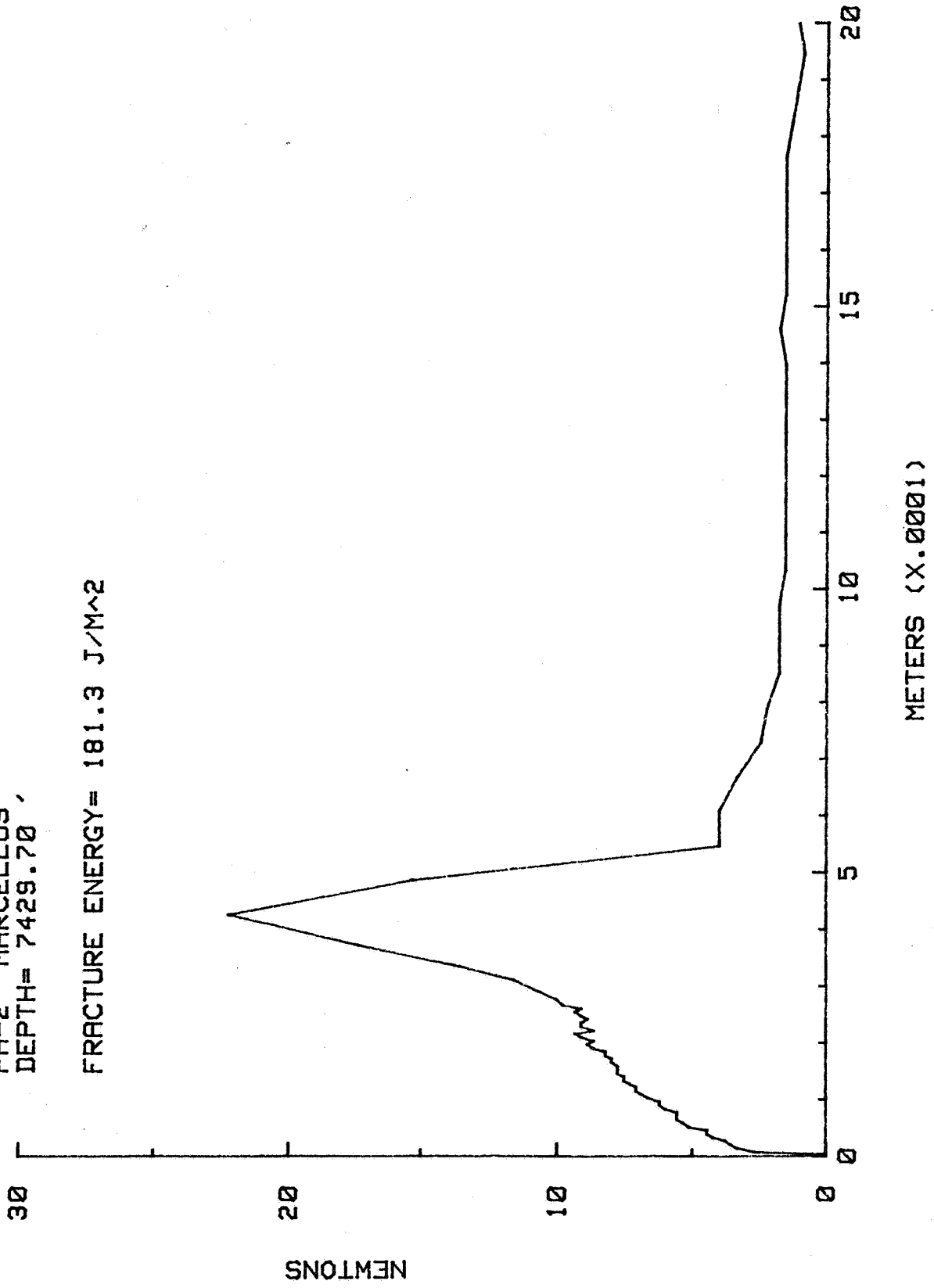


METERS (X.0001)

TEST # 58

PA-2 MARCELLUS  
DEPTH= 7429.70'

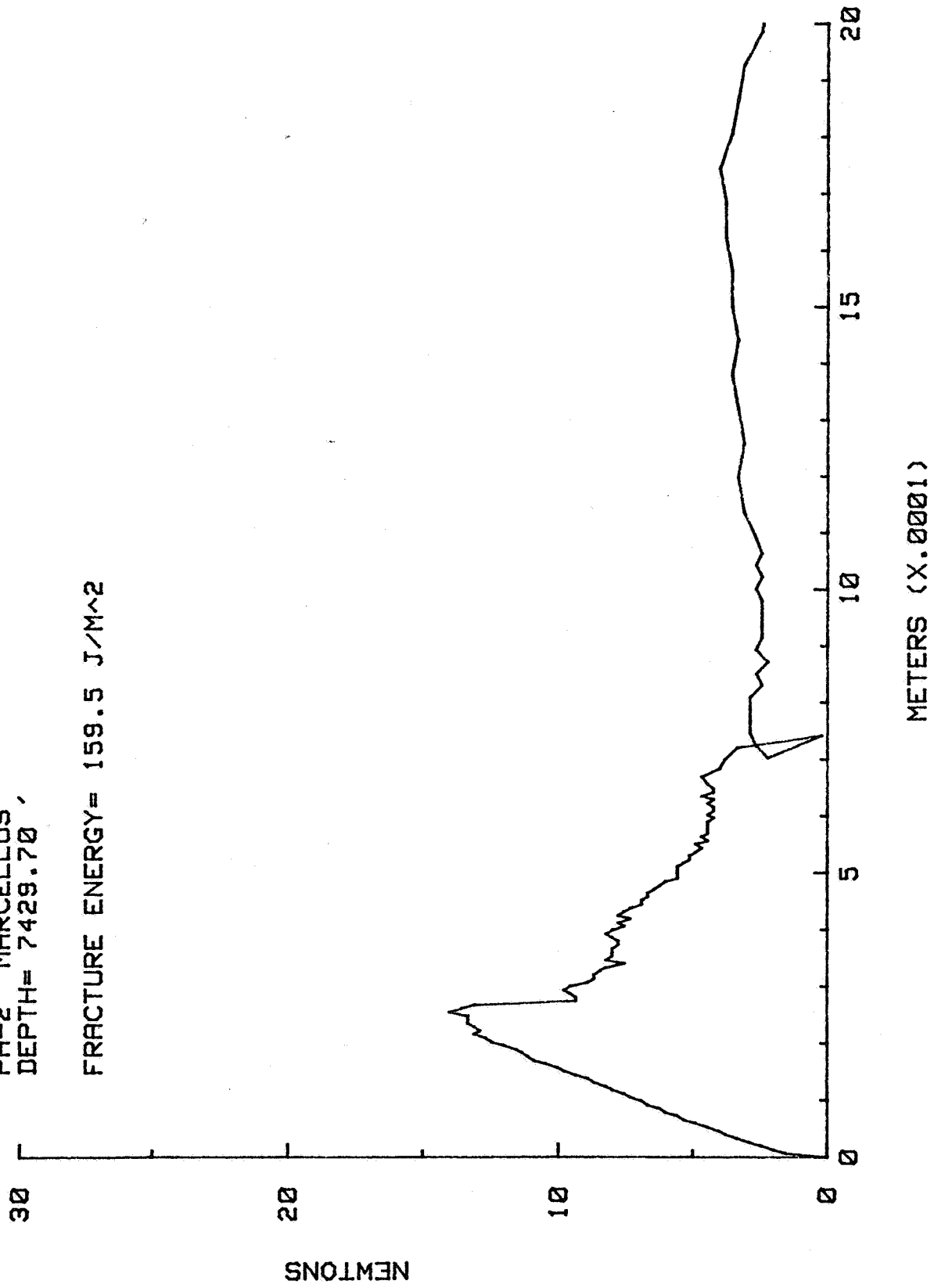
FRACTURE ENERGY= 181.3 J/M<sup>2</sup>



TEST # 59

PA-2 MARCELLUS  
DEPTH= 7429.70

FRACTURE ENERGY= 159.5 J/M<sup>2</sup>

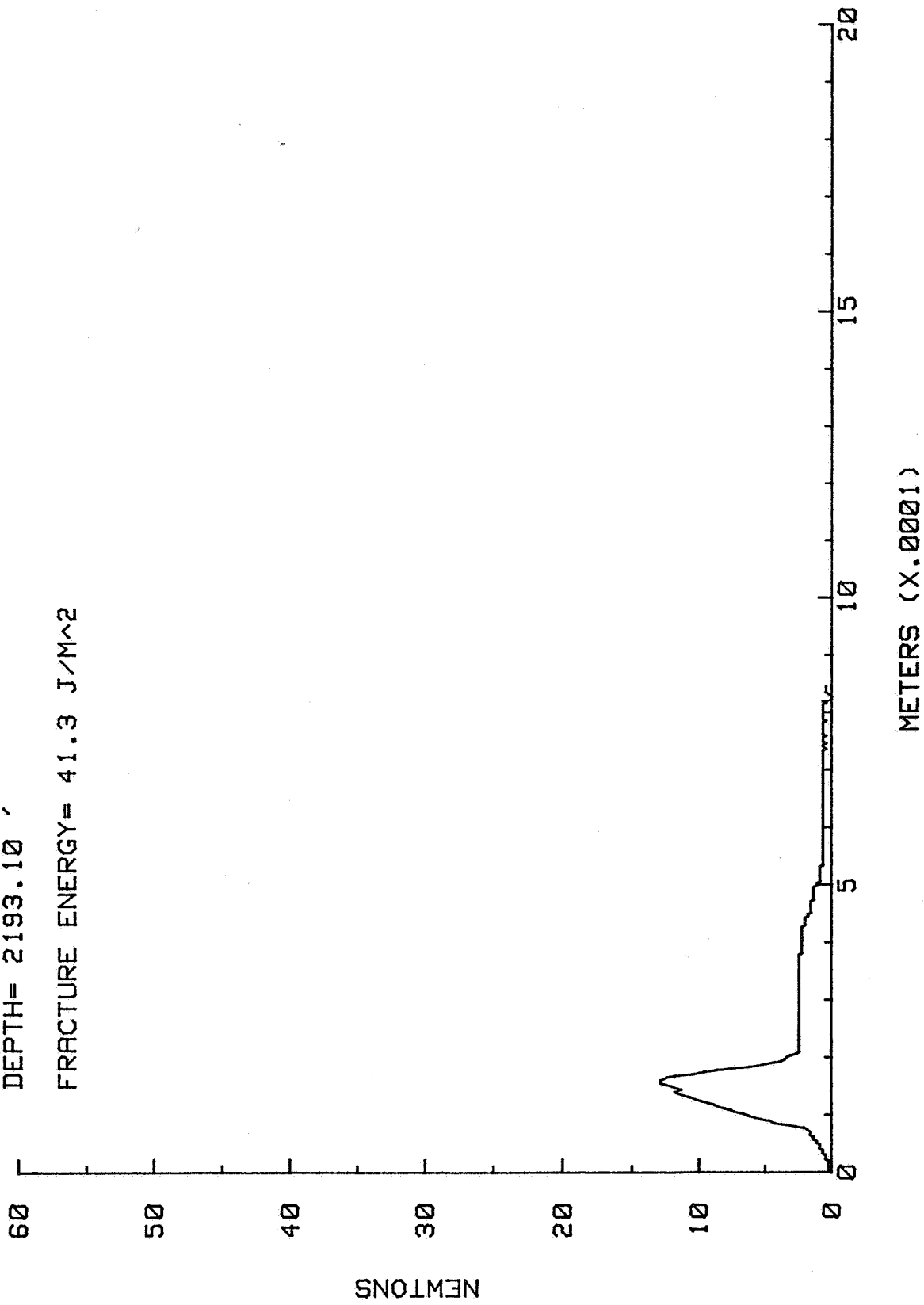


TEST # 20

OH-7 HANOVER

DEPTH= 2193.10 '

FRACTURE ENERGY= 41.3 J/M<sup>2</sup>

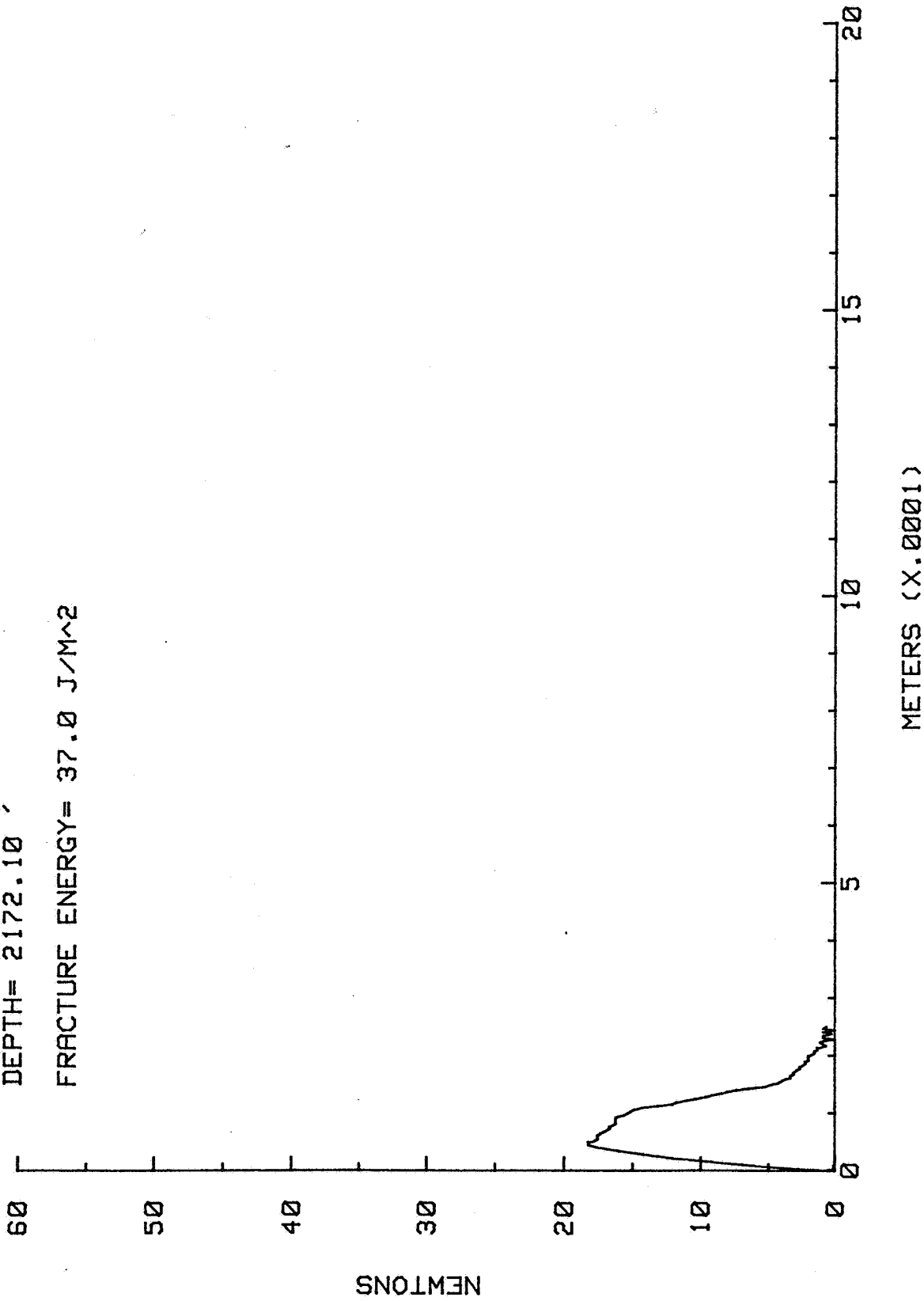


TEST # 21

OH-7 HANOVER

DEPTH= 2172.10

FRACTURE ENERGY= 37.0 J/M<sup>2</sup>

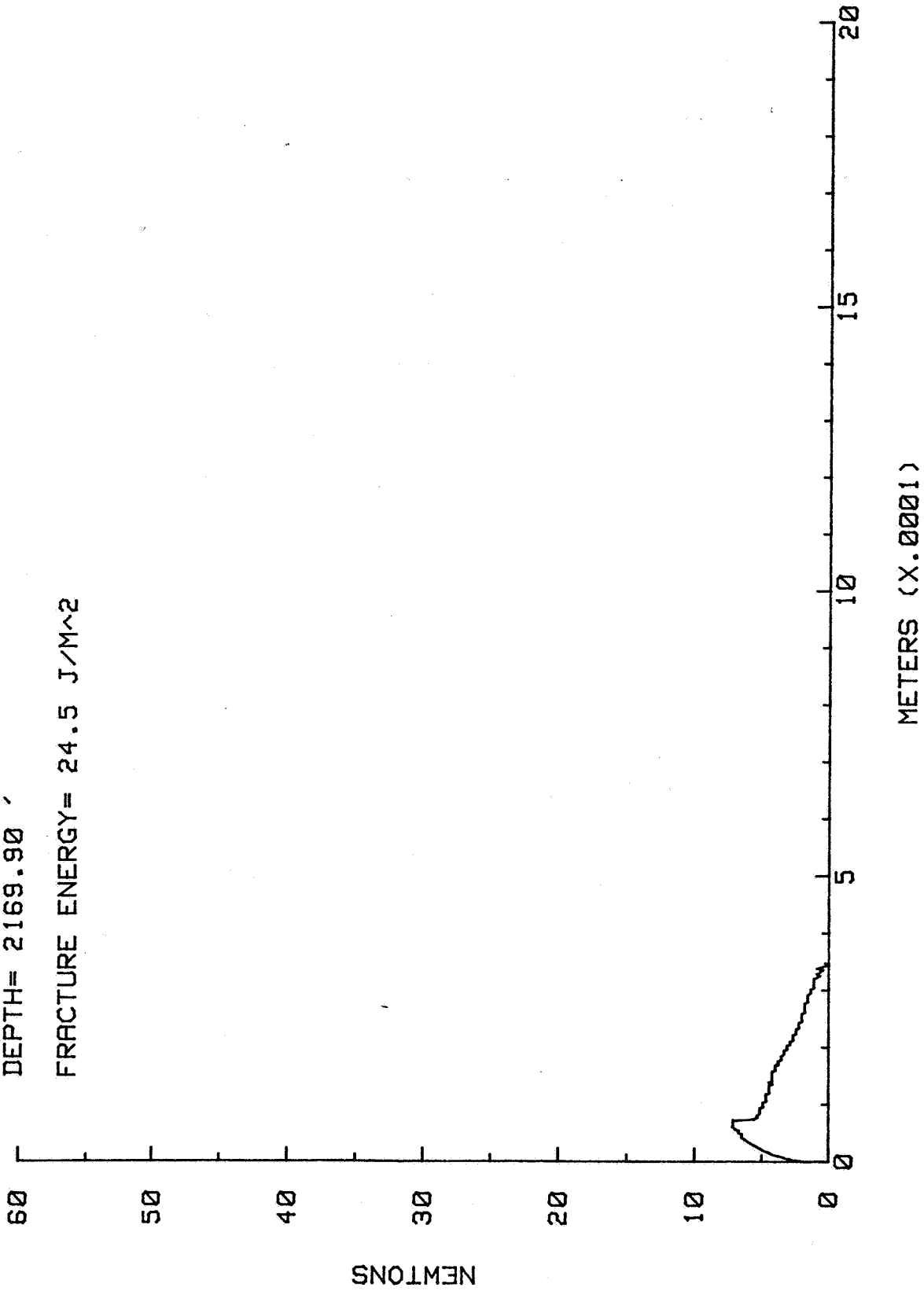


TEST # 22

OH-7 HANOVER

DEPTH= 2169.90

FRACTURE ENERGY= 24.5 J/M<sup>2</sup>

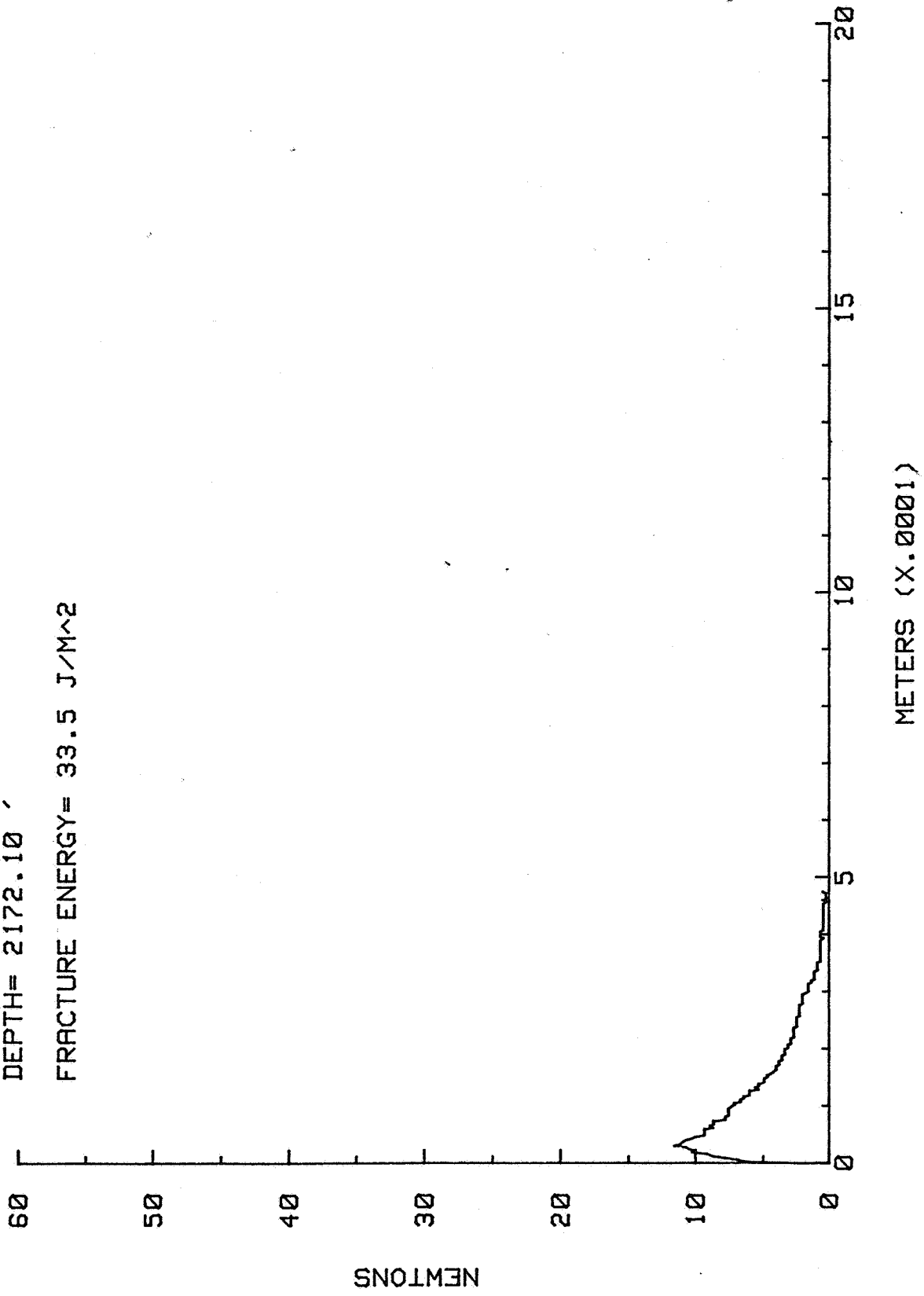


TEST # 23

OH-7 HANOVER

DEPTH= 2172.10

FRACTURE ENERGY= 33.5 J/M<sup>2</sup>

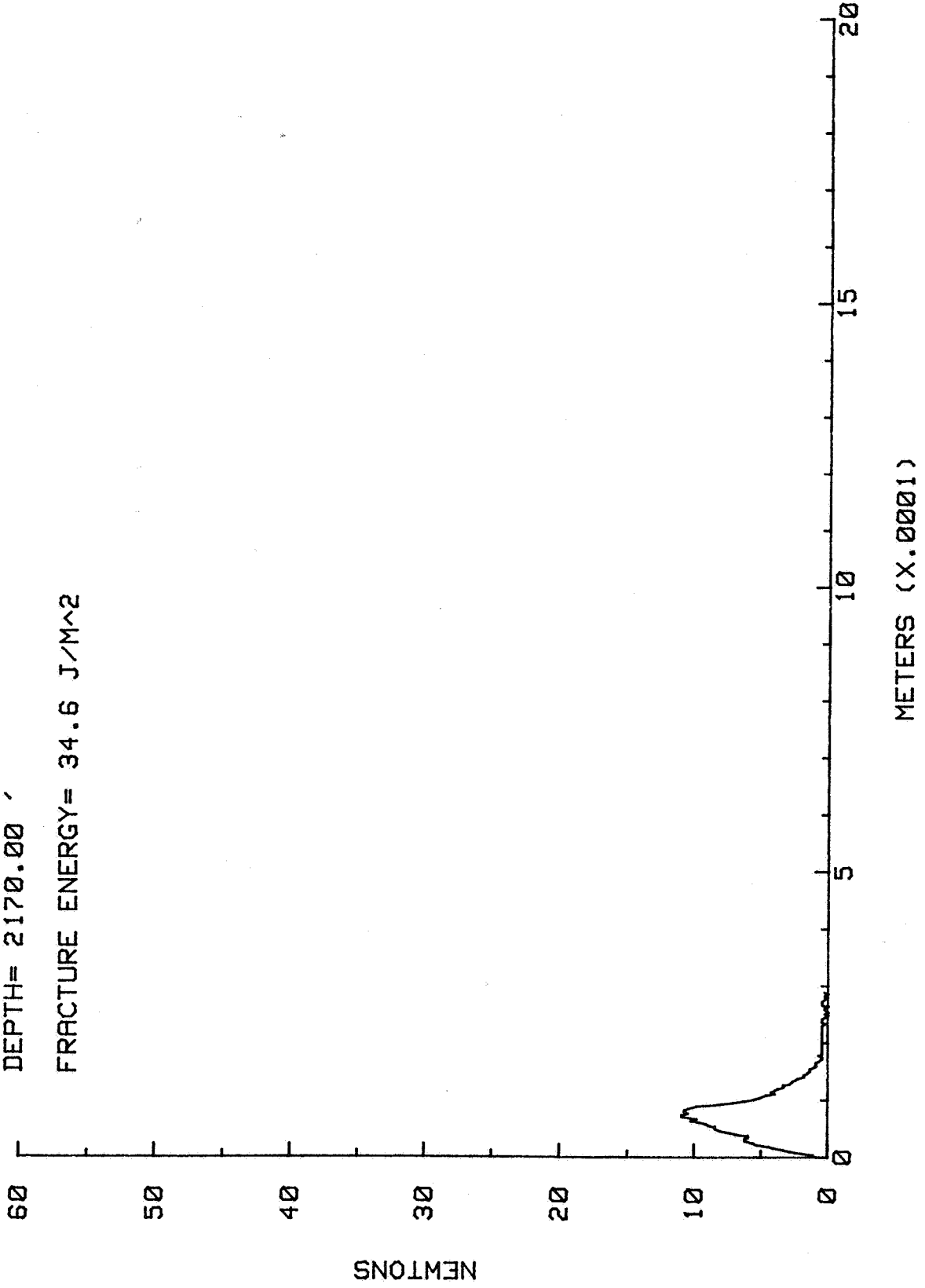


TEST # 25

OH-7 HANOVER

DEPTH= 2170.00

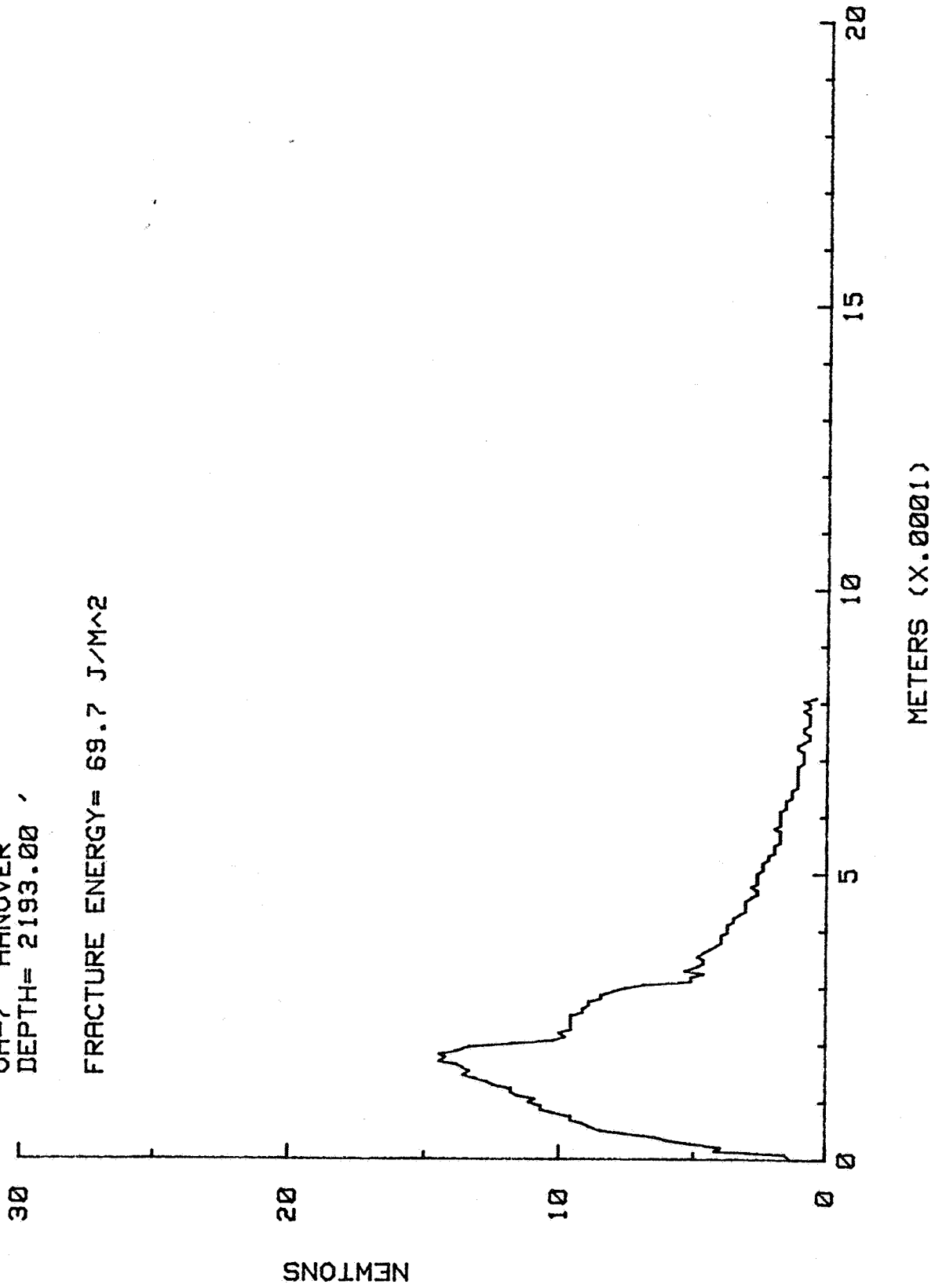
FRACTURE ENERGY= 34.6 J/M<sup>2</sup>



TEST # 54

OH-7 HANOVER  
DEPTH= 2193.00

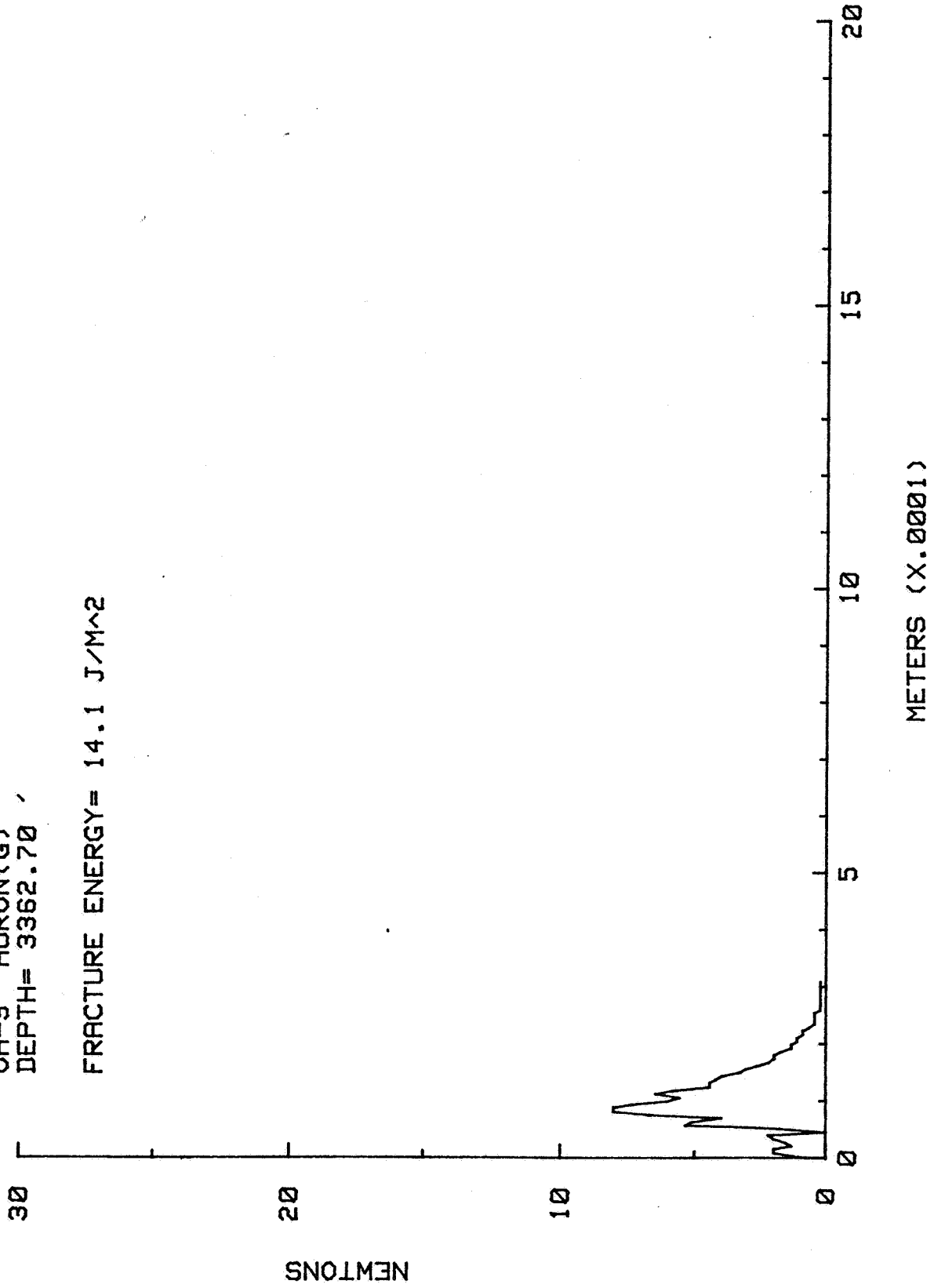
FRACTURE ENERGY= 69.7 J/M<sup>2</sup>



TEST # 72

OH-9 HURON(G)  
DEPTH= 3362.70

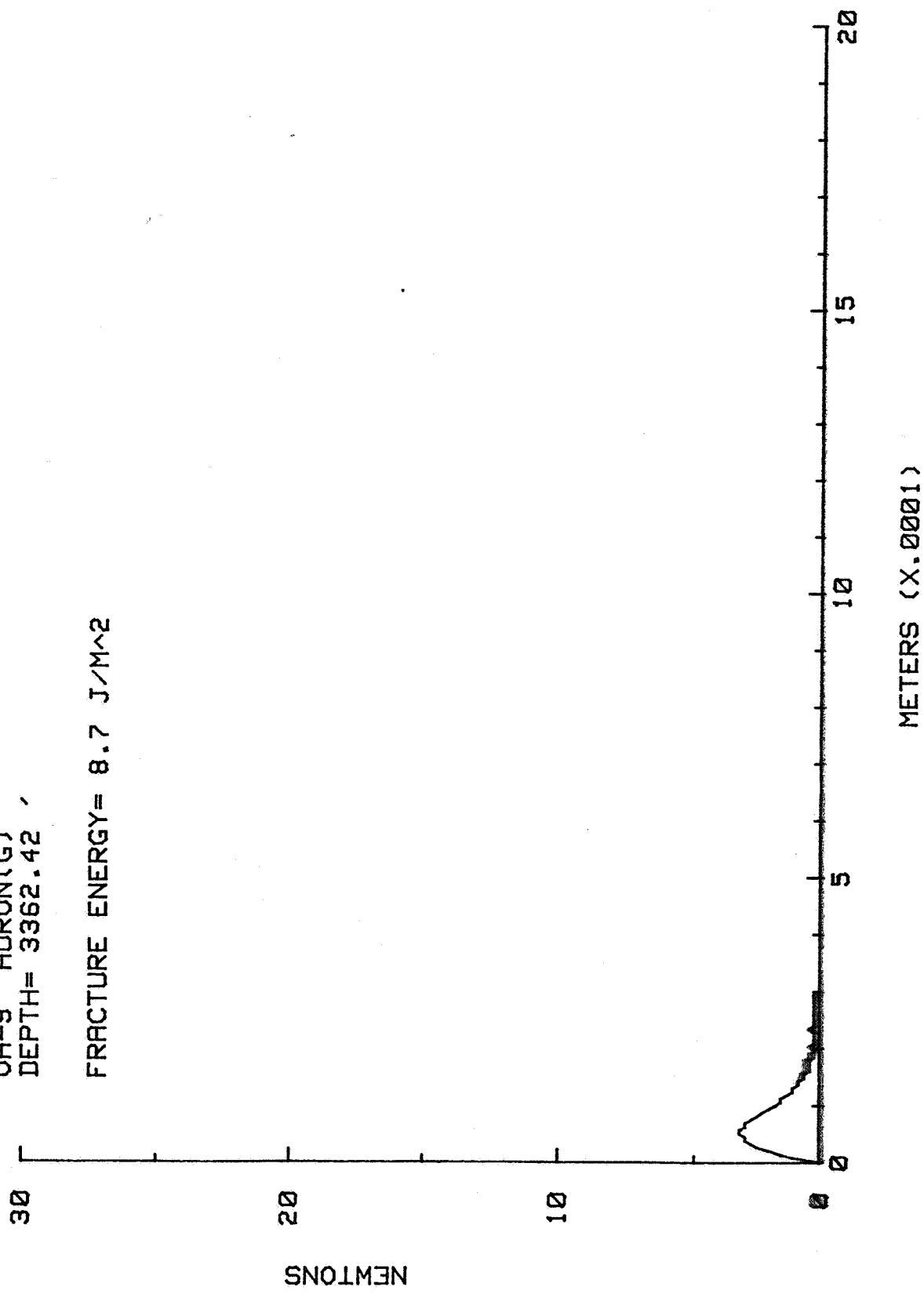
FRACTURE ENERGY= 14.1 J/M<sup>2</sup>



TEST # 73

OH-9 HURON(G)  
DEPTH= 3362.42

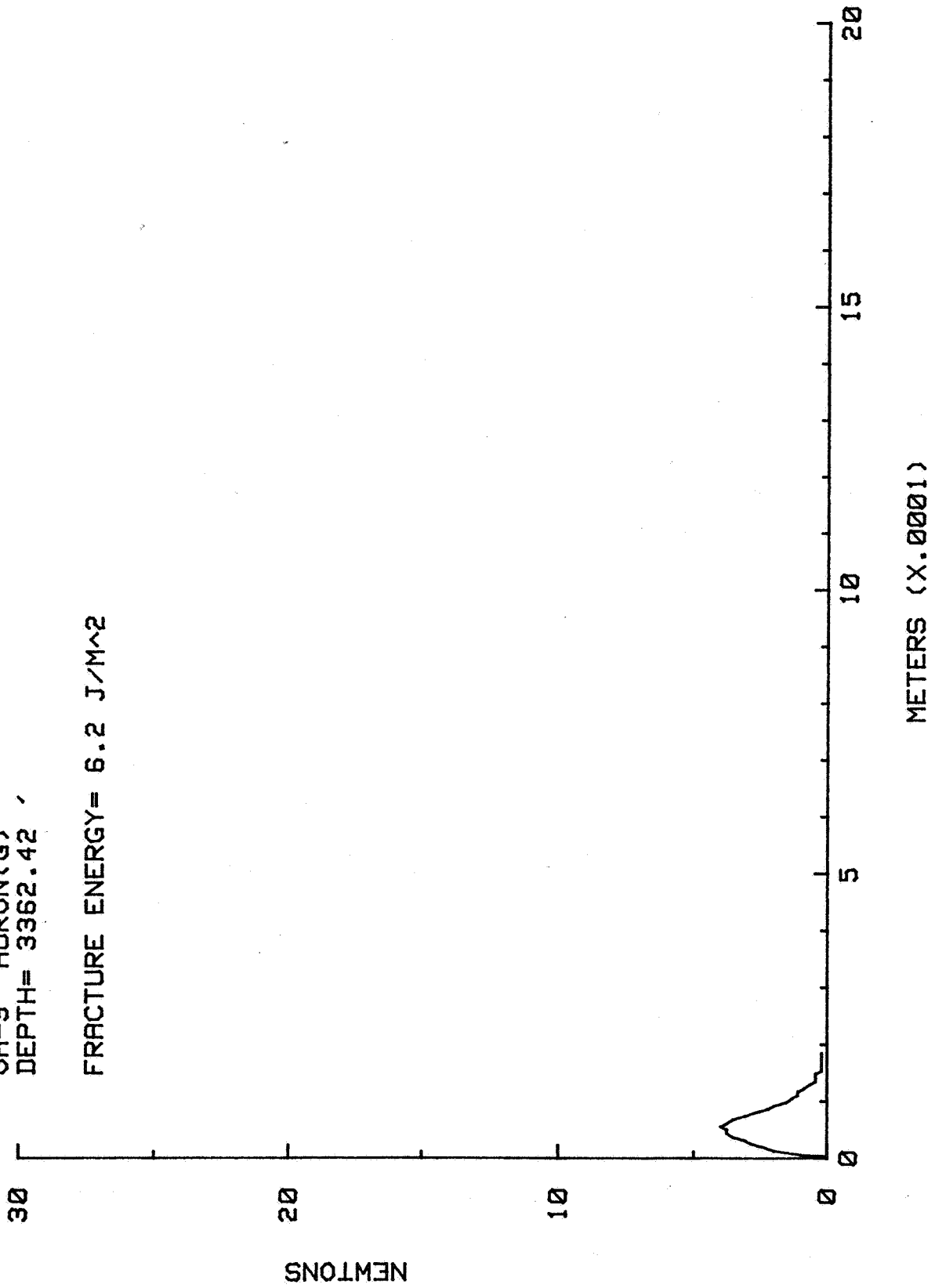
FRACTURE ENERGY= 8.7 J/M^2



TEST # 74

OH-9 HURON(G)  
DEPTH= 3362.42

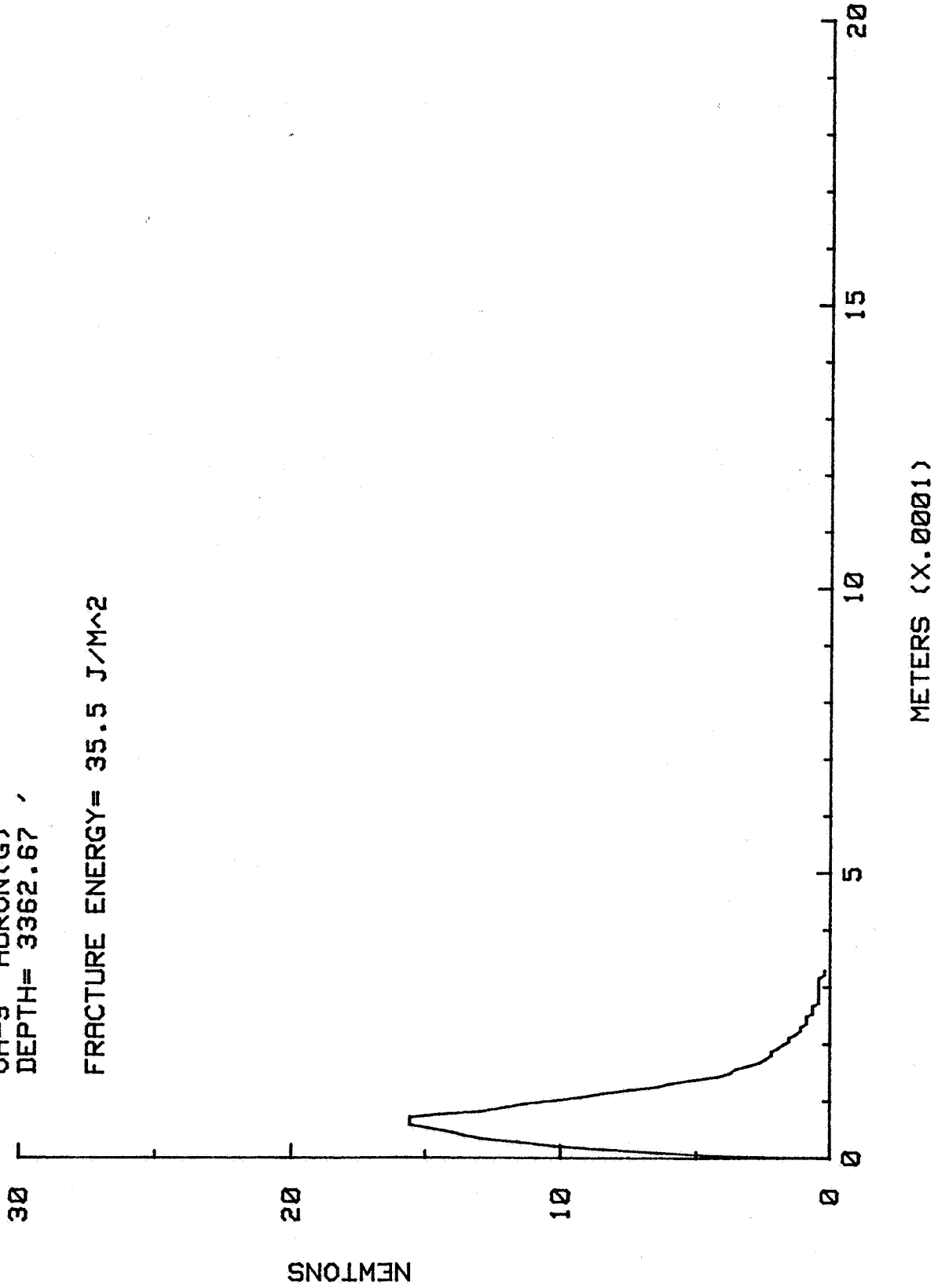
FRACTURE ENERGY= 6.2 J/M^2



TEST # 76

OH-9 HURON(G)  
DEPTH= 3362.67

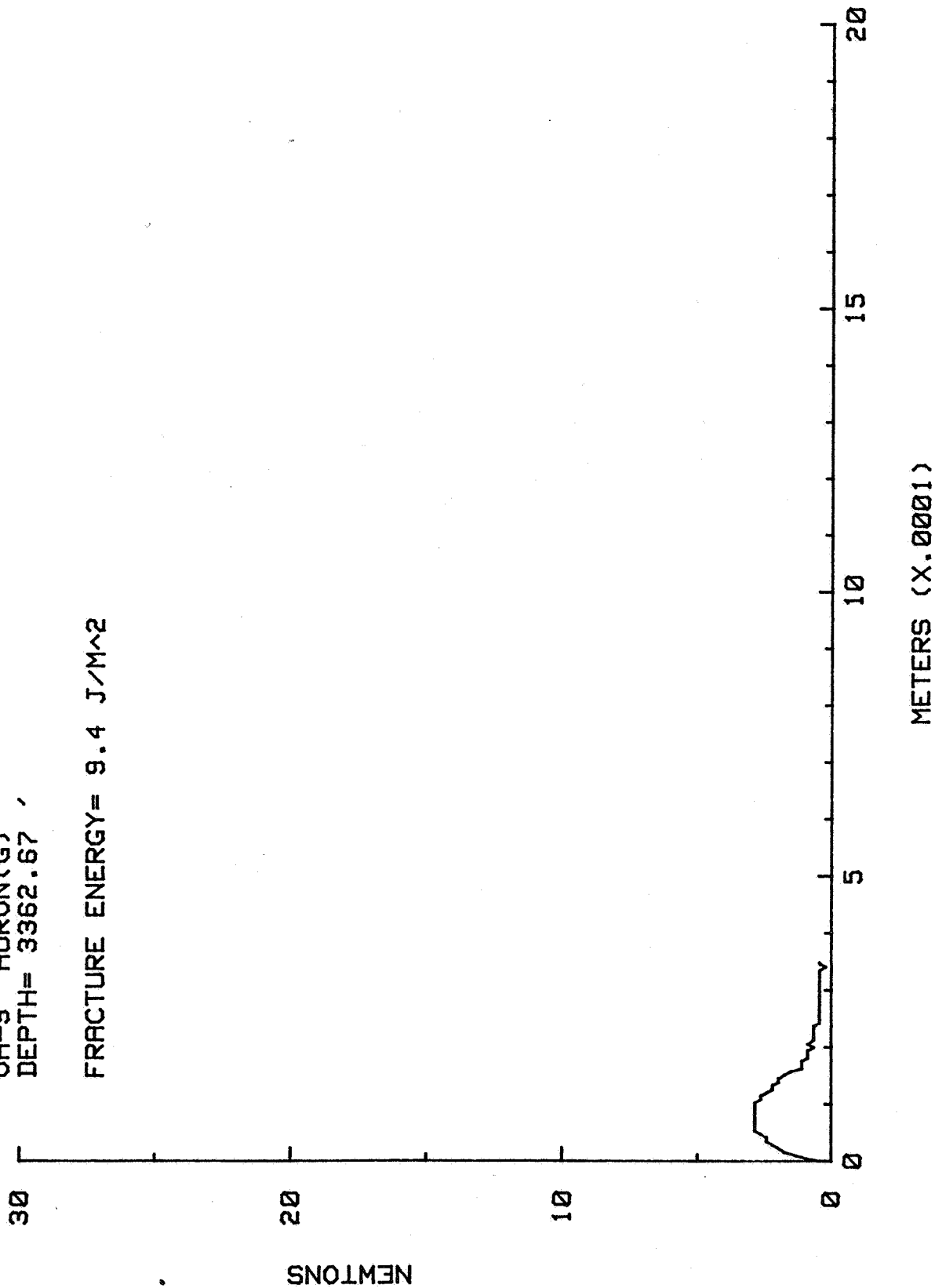
FRACTURE ENERGY= 35.5 J/M<sup>2</sup>



TEST # 77

OH-9 HURON(G)  
DEPTH= 3362.67

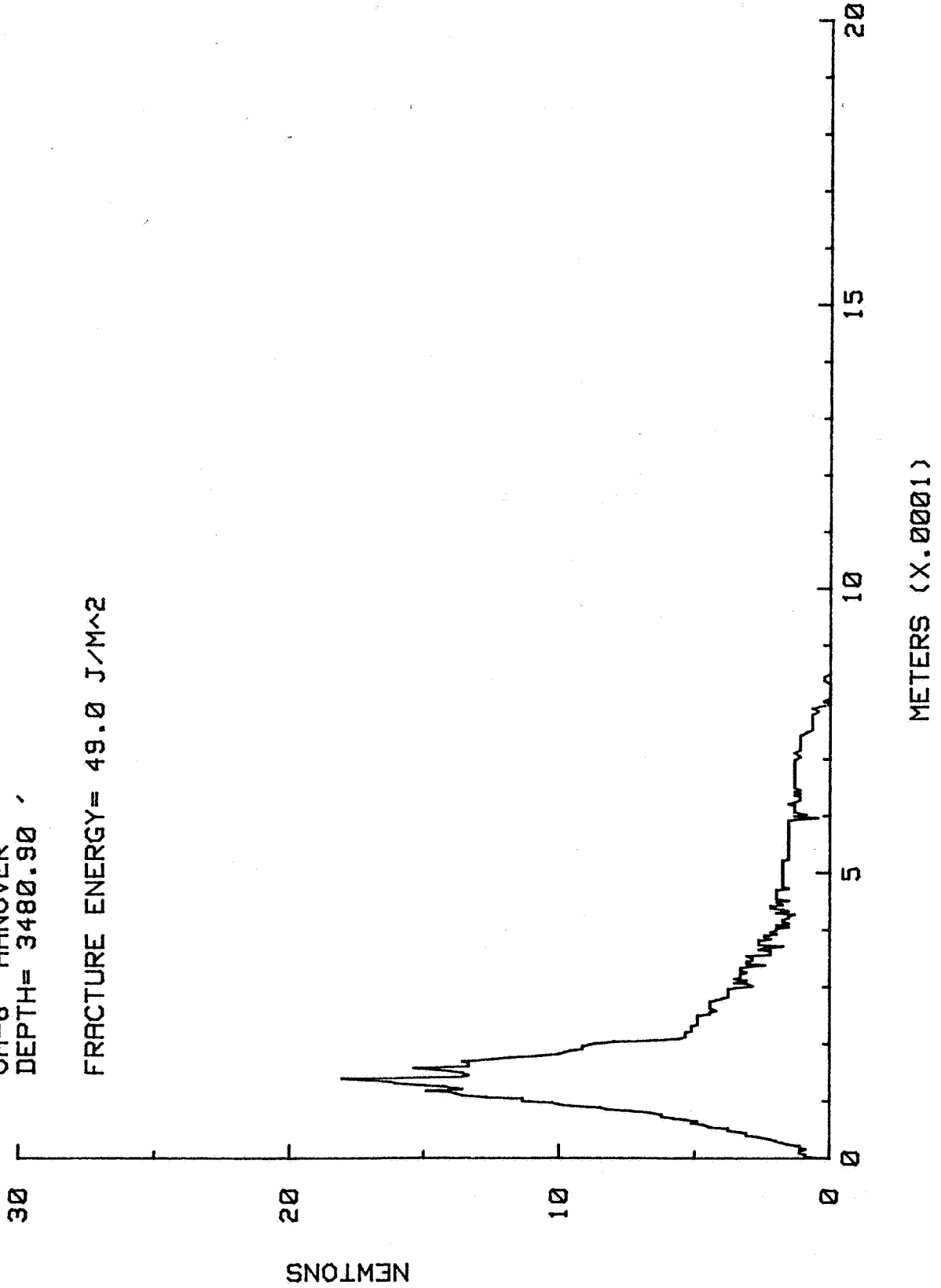
FRACTURE ENERGY= 9.4 J/M<sup>2</sup>



TEST # 35

OH-8 HANOVER  
DEPTH= 3480.90

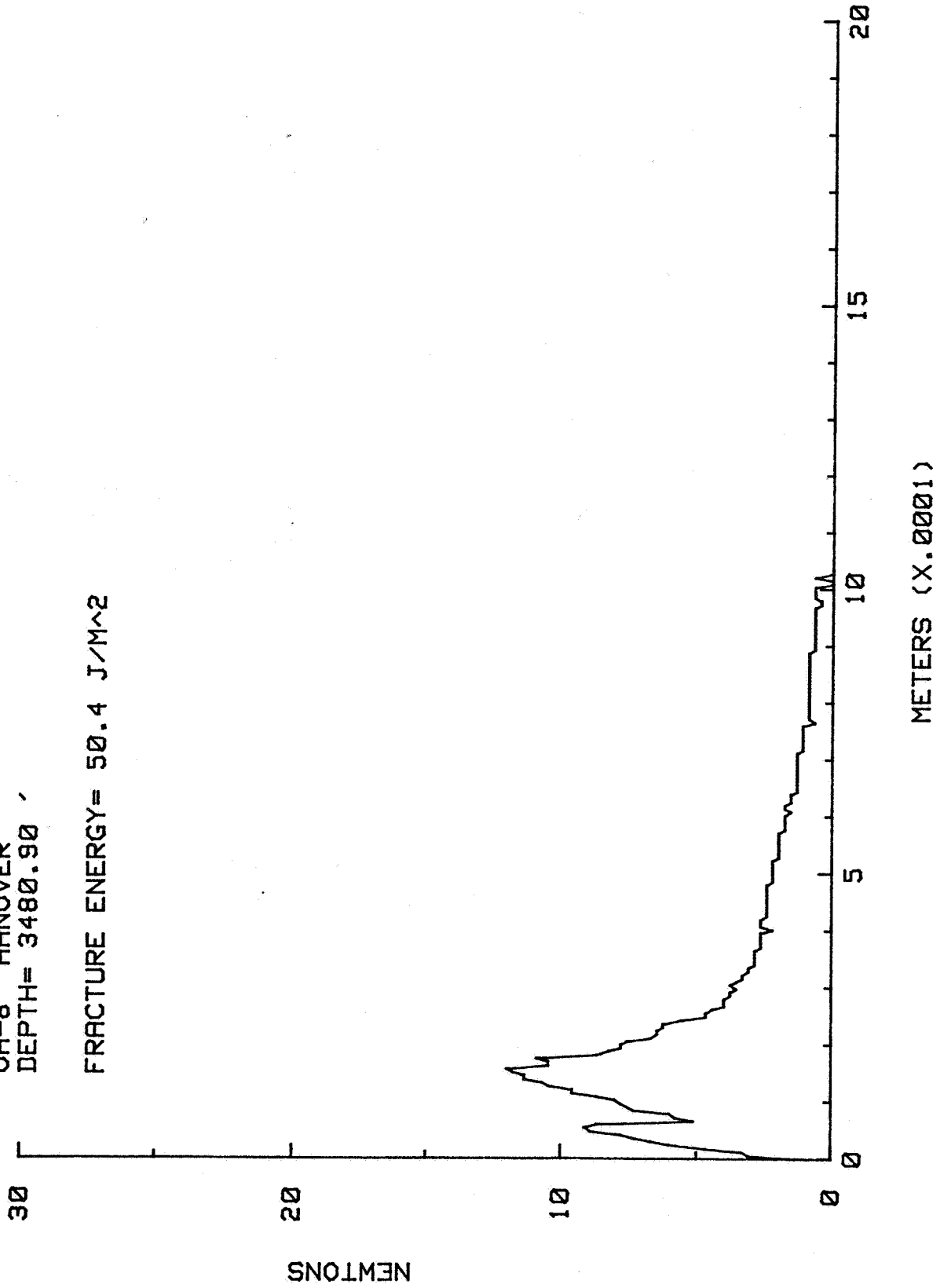
FRACTURE ENERGY= 49.0 J/M^2



TEST # 36

OH-8 HANOVER  
DEPTH= 3480.90

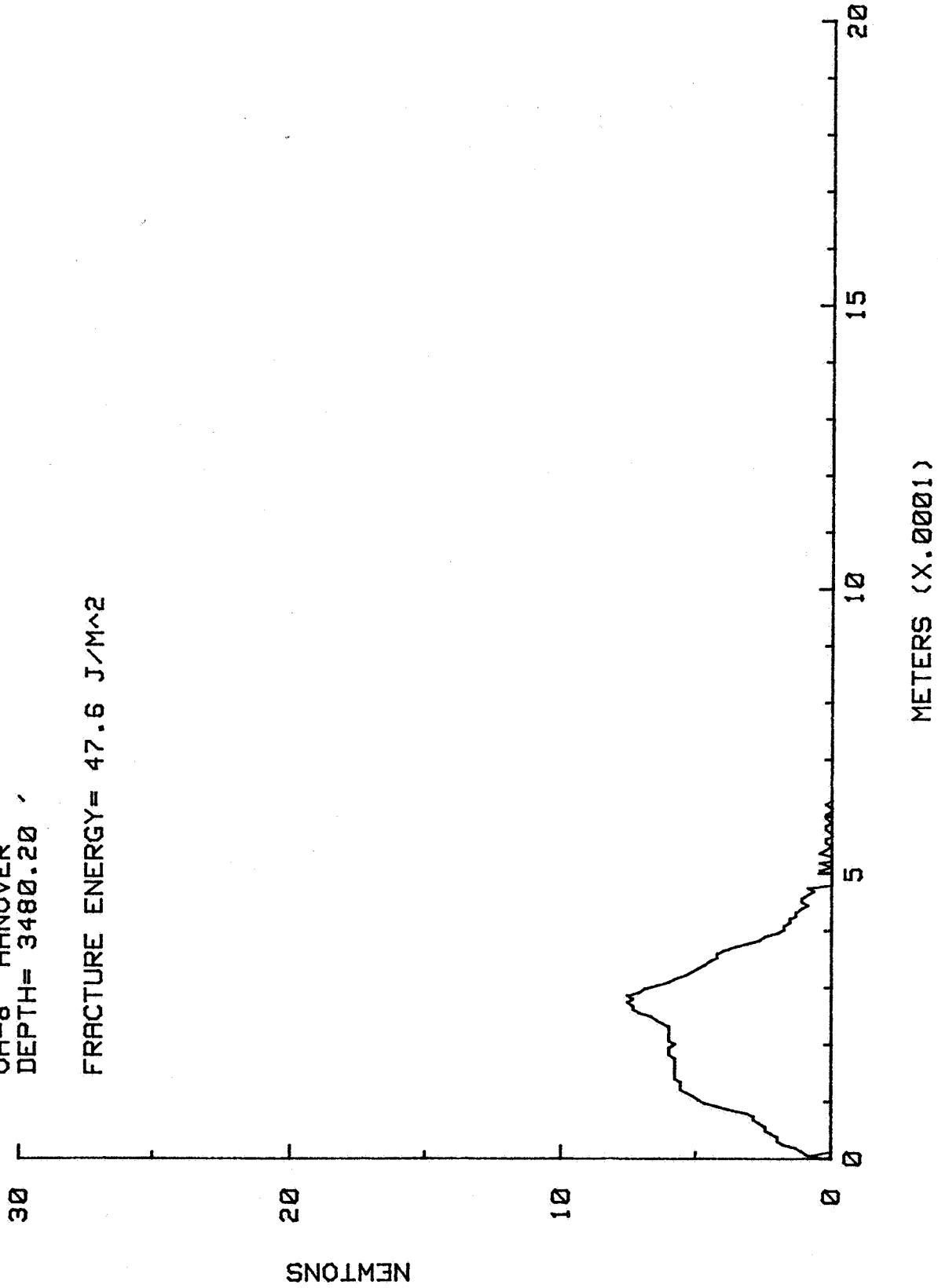
FRACTURE ENERGY= 50.4 J/M<sup>2</sup>



TEST # 38

OH-8 HANOVER  
DEPTH= 3480.20

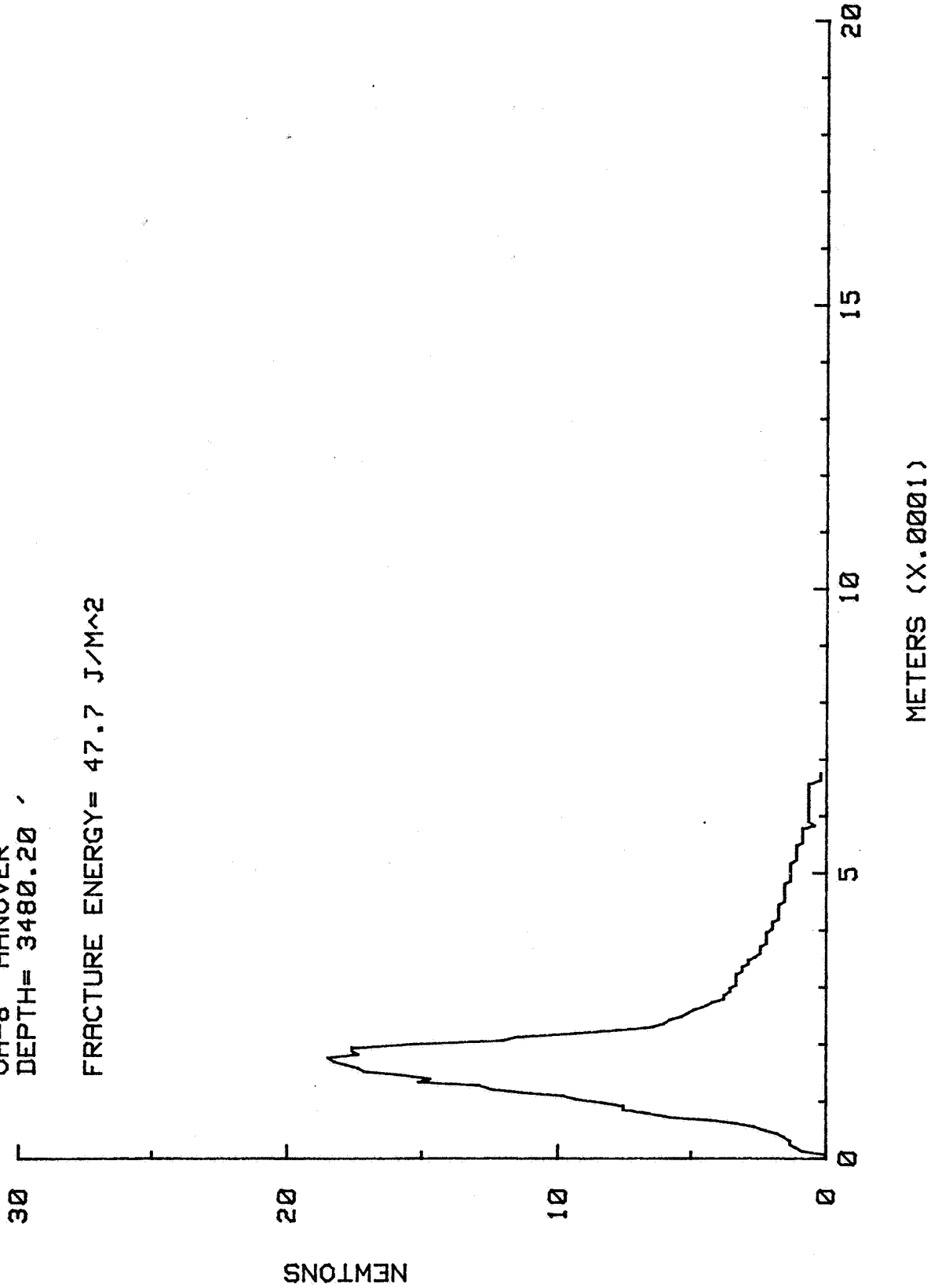
FRACTURE ENERGY= 47.6 J/M<sup>2</sup>



TEST # 39

OH-8 HANOVER  
DEPTH= 3480.20

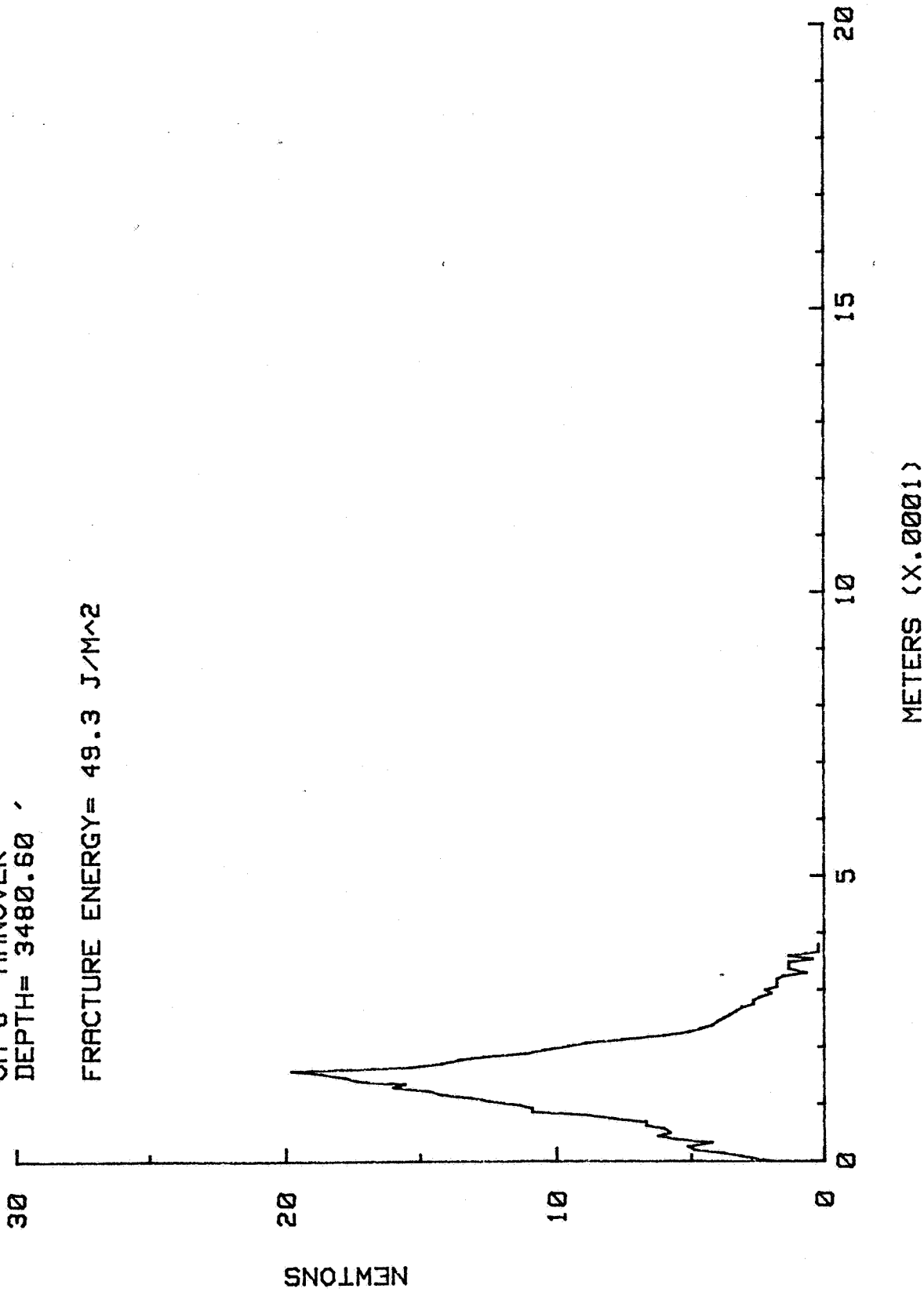
FRACTURE ENERGY= 47.7 J/M<sup>2</sup>



TEST # 51

OH-8 HANOVER  
DEPTH= 3480.60

FRACTURE ENERGY= 49.3 J/M<sup>2</sup>

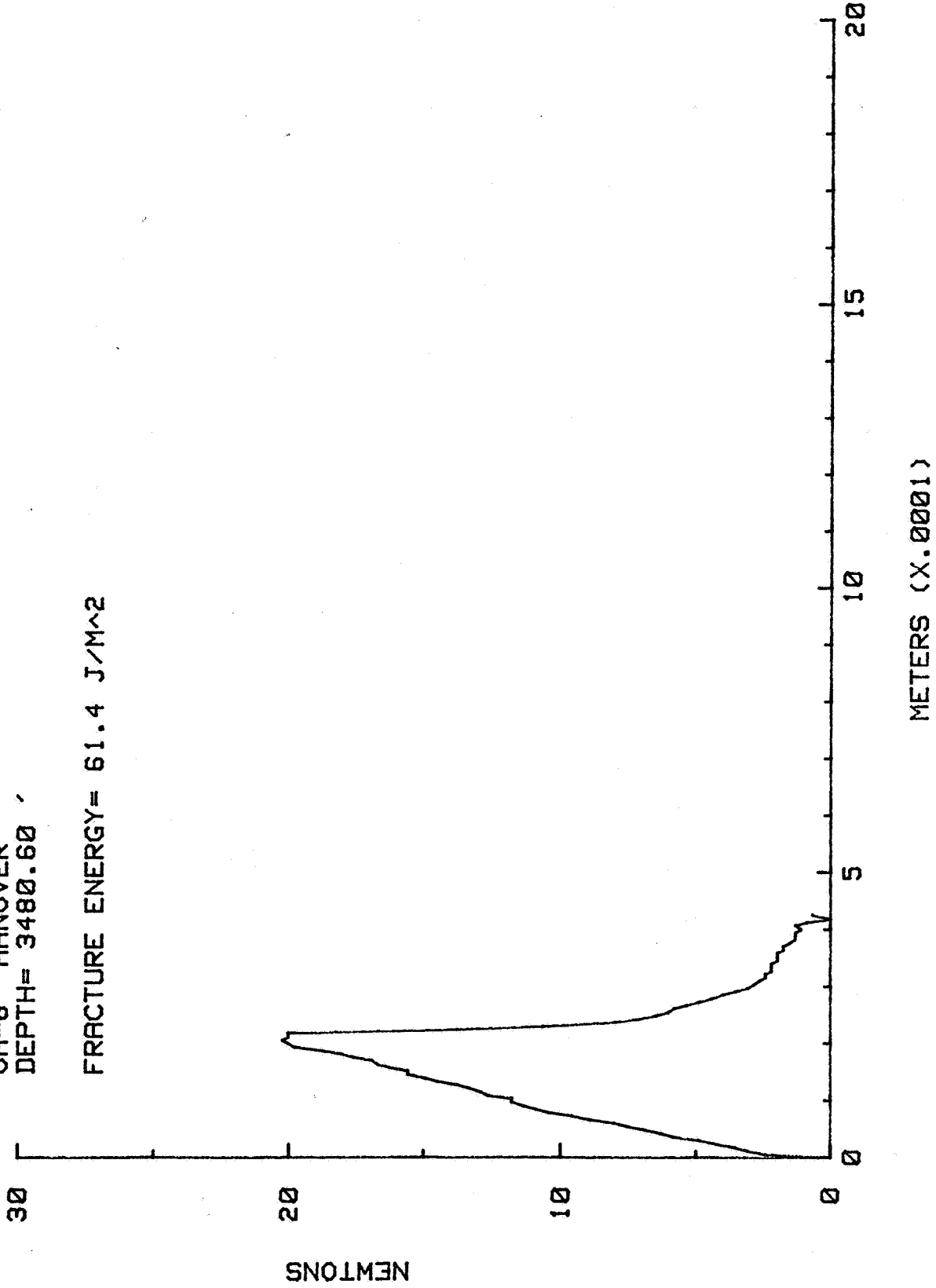


TEST # 53

OH-8 HANOVER

DEPTH= 3480.60

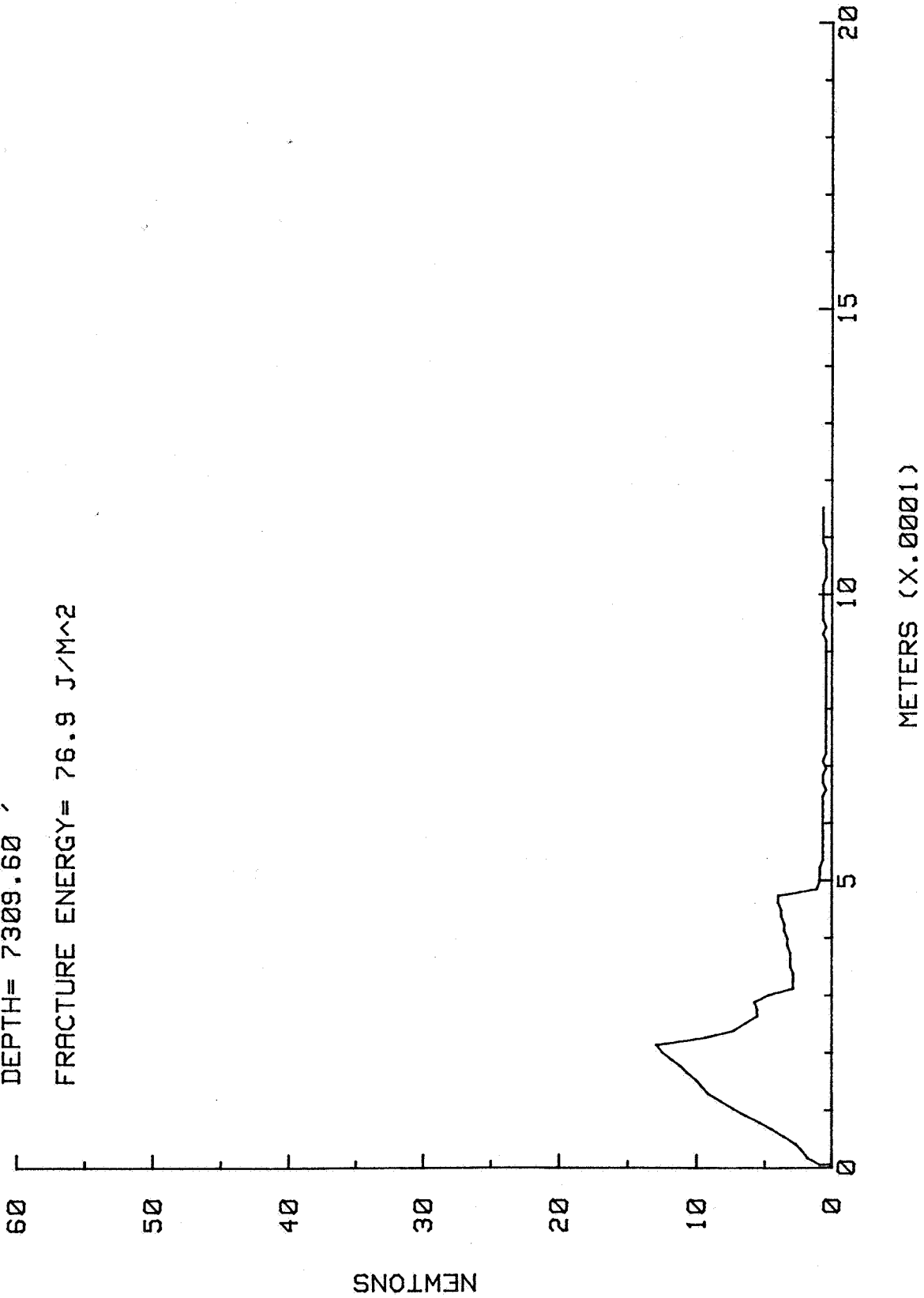
FRACTURE ENERGY= 61.4 J/M<sup>2</sup>



TEST # 2

PA-2 MAHANTANGO  
DEPTH= 7309.60'

FRACTURE ENERGY= 76.9 J/M<sup>2</sup>



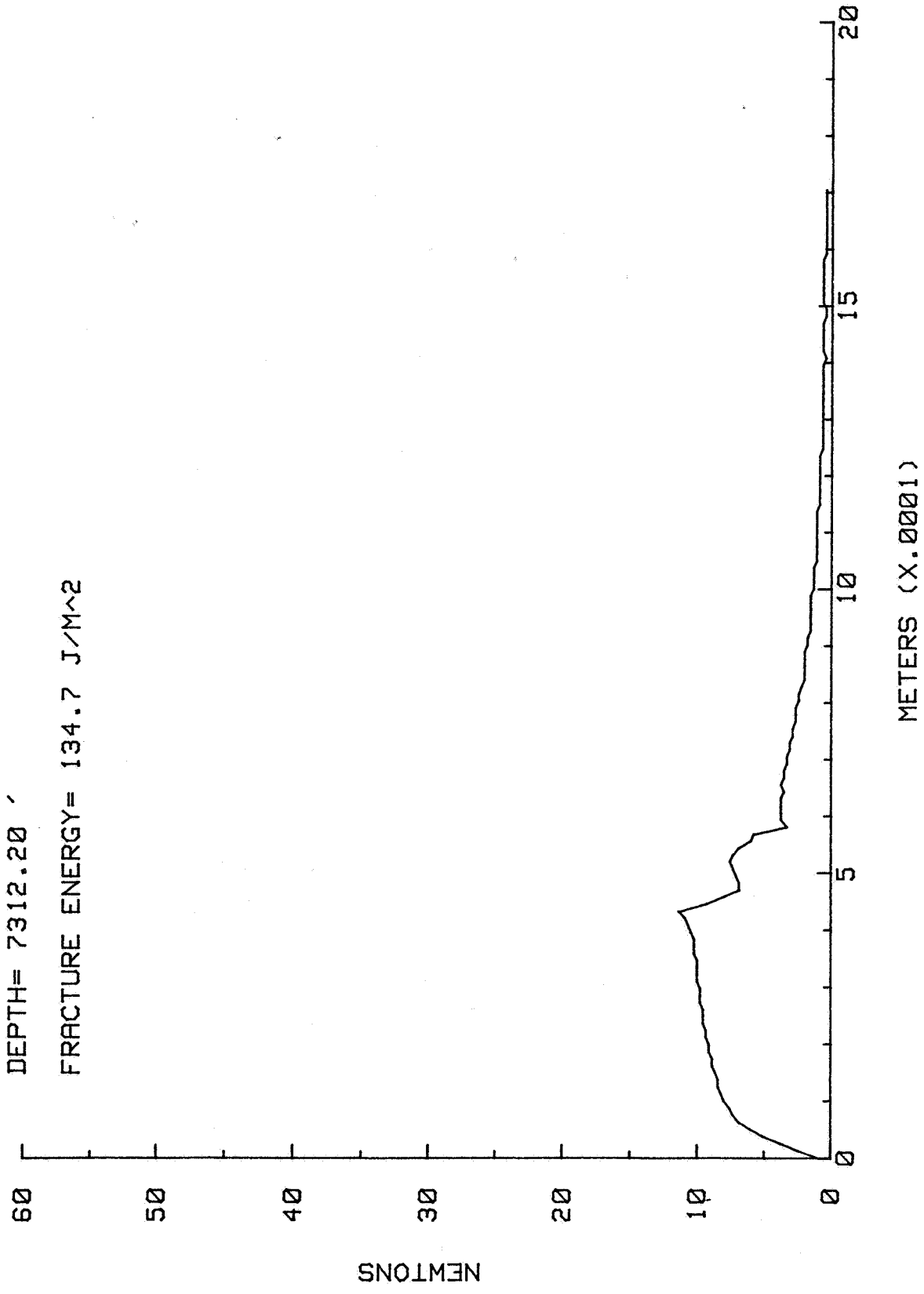
NEWTONS

METERS (X.0001)

TEST # 4

PA-2 MAHANTANGO  
DEPTH= 7312.20'

FRACTURE ENERGY= 134.7 J/M<sup>2</sup>



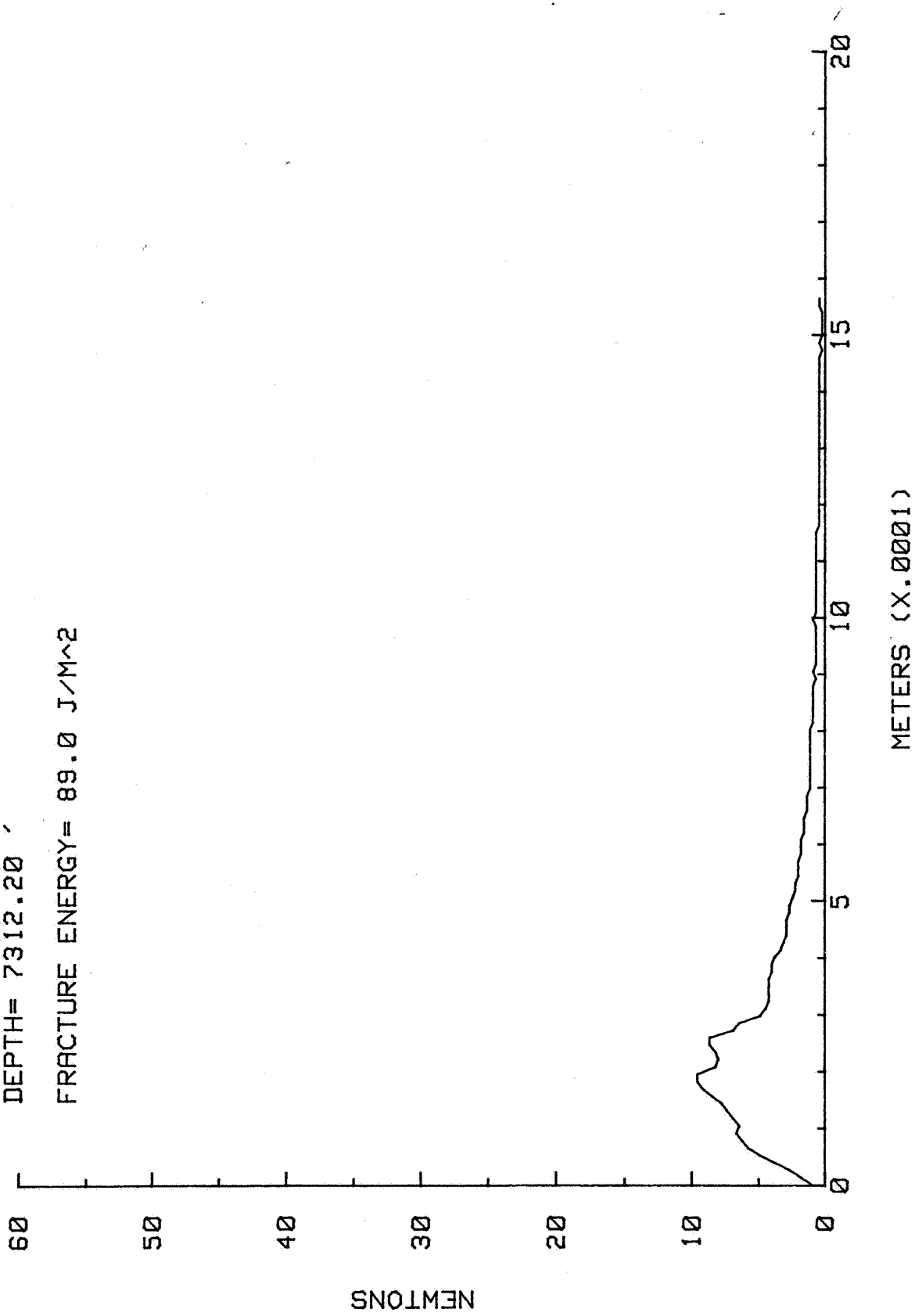
NEWTONS

METERS (X.0001)

TEST # 5

PA-2 MAHANTANGO  
DEPTH= 7312.20'

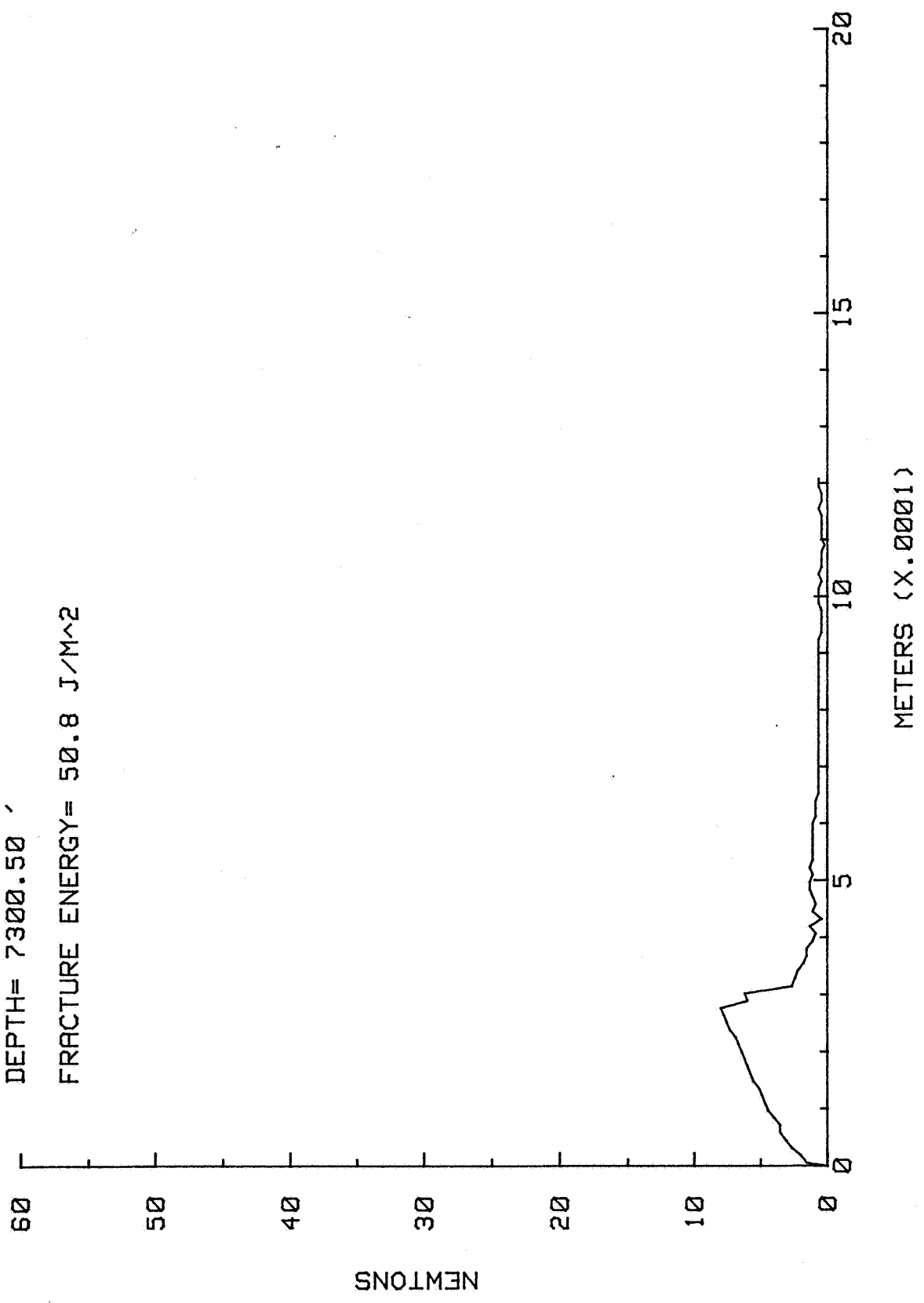
FRACTURE ENERGY= 89.0 J/M<sup>2</sup>



TEST # 6

PA-2 MAHANTANGO  
DEPTH= 7300.50 ;

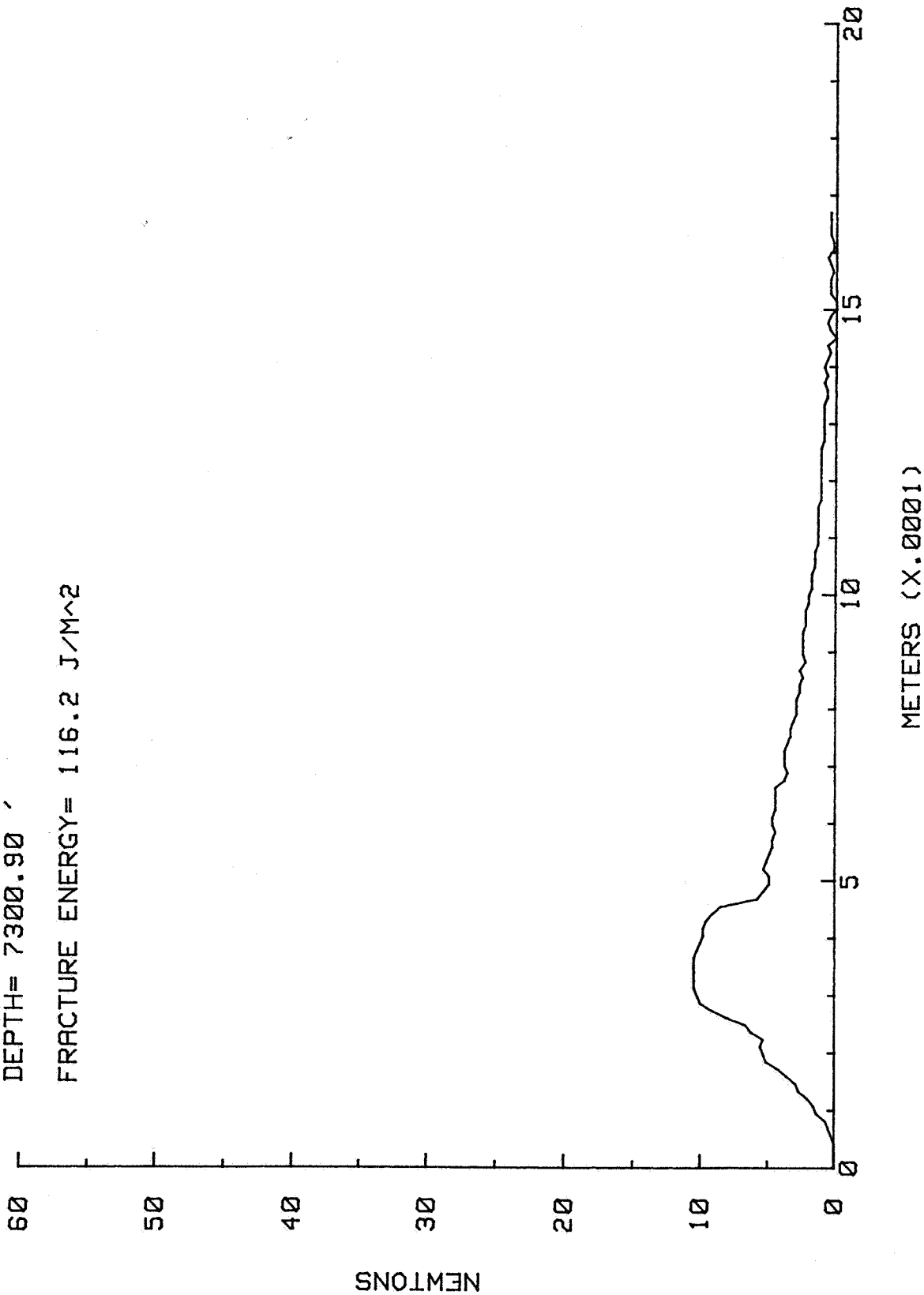
FRACTURE ENERGY= 50.8 J/M<sup>2</sup>



TEST # 7

PA-2 MAHANTANGO  
DEPTH= 7300.90'

FRACTURE ENERGY= 116.2 J/M<sup>2</sup>



TEST # 8

PA-2 MAHANTANGO  
DEPTH= 7300.90'

FRACTURE ENERGY= 41.6 J/M<sup>2</sup>

